SEISMIC PERFORMANCE OF REINFORCED CONCRETE FRAMES WITH NOMINAL DUCTILITY

By

KHALED AHMED HAMDY, B.Sc., M.Sc.

A Thesis

Submitted to the School of Graduate Studies

in Partial Fulfilment of the Requirements

for the Degree of

Doctor of Philosophy

McMaster University

June 1992

SEISMIC PERFORMANCE OF REINFORCED CONCRETE FRAMES WITH NOMINAL DUCTILITY

For My Wife Maha

DOCTOR OF PHILOSOPHY (1992)
(Civil Engineering and Engineering Mechanics)

McMASTER UNIVERSITY
Hamilton, Ontario

TITLE: Seismic Performance of Reinforced Concrete Frames with Nominal Ductility

AUTHOR: Khaled Ahmed Hamdy, B.Sc.(Ain Shams University, Cairo, Egypt)
M.Sc.(Ain Shams University, Cairo, Egypt)

SUPERVISORS: Professor W.K. Tso and
Professor A. Ghobarah

NUMBER OF PAGES: xxiii, 237

ABSTRACT

According to the current Canadian practice, the designer has two options for the design of reinforced concrete frames in seismic regions : a nominally ductile frame or a ductile frame. Frames designed based on the ordinary design practice have a limited amount of ductility and are referred to as "nominally ductile moment resisting frames" (NDMRFs). To further increase the ductility of a nominally ductile frames, a special design philosophy and special detailing requirements need to be adopted. The end product is a frame with higher ductility and is referred to as a "ductile moment resisting frame" (DMRF). The seismic performance of ductile moment resisting frames received extensive attention in both experimental and analytical studies. On the other hand, there is only limited research reported on the seismic performance of nominally ductile frames despite the fact that there are more nominally ductile frames designed and constructed than ductile frames. Therefore, an analytical and experimental study is undertaken in this thesis to evaluate the seismic performance of Nominally Ductile Moment Resisting Frames (NDMRFs) designed to conform to the current Canadian provisions.

Buildings of different heights and typical configurations are considered. The frames of such buildings are designed as nominally ductile frames for the combined gravity and seismic loading in accordance with the National Building Code of Canada, NBCC 1990. The frame members are proportioned and detailed to satisfy the clauses of the Canadian concrete design Code (CAN3-A23.3-M84) applicable to nominally ductile frames. The designed frames are then analyzed statically under monotonically increasing static lateral loading to study their force-deformation

characteristics and order of hinge formation among members. Following the static analysis, the frames are analyzed dynamically under earthquake excitation. The response parameters of interest are the overall displacements, drifts and ductility demands, the flexural ductility demands and the shear demands in beams and columns.

Several deficiencies are observed in the seismic performance of NDMRFs designed strictly following the minimum Code requirements. First, the interstorey drifts are substantial which implies excessive non-structural damage. Second, the beam ductility demands are much larger than what is implied in the Code. Third, the beam shear demands can exceed the capacity of the provided stirrups. With cracking more extensive than anticipated, it is debatable that the concrete contribution to shear resistance should be relied upon, as currently permitted in the Code. Beam shear failure may occur in some cases if the concrete shear resistance was indeed unreliable.

An experimental investigation is carried out to evaluate the reliability of the concrete shear resistance when the beams are subjected to ductility demands similar to those obtained in the dynamic analysis. Two beam specimens are constructed and tested under reversed cyclic loading. The specimens are a half scale model of the beams of the frames considered in this study. The experimental investigation showed that the concrete contribution to the beam shear resistance diminishes rapidly if the beams are subjected to a ductility level similar to that obtained in the analysis. Therefore, it may be prudent in the design code to disallow the concrete contribution to the beam shear resistance.

To ensure no beam shear failure in this type of frame, a procedure is proposed to modify the factored design shears in the beams of NDMRFs to be more reflective of the demand shears. The modified design shears calculated based on the proposed procedure are shown to be in good agreement with the response values. Therefore, shear failure in the beams of NDMRFs can be avoided if the capacity of the provided stirrups is based on the modified design shears with the concrete contribution to the beam shear resistance neglected.

Finally, an alternative design procedure, based partially on the capacity design philosophy, is proposed for the design of gravity-dominated frames in seismic regions. Reinforced concrete frame design using the proposed procedure can avoid many of the deficiencies observed in the seismic performance of NDMRFs designed strictly following the minimum Code requirements, and is therefore a preferred design procedure to enhance seismic performance.

ACKNOWLEDGEMENTS

I would like to express my sincere gratitude to my supervisors Dr. W.K. Tso and Dr. A. Ghobarah for their guidance, advice and encouragement during the course of this study.

Special thanks are due to Dr. R.M. Korol and Dr. M. El-Bestawi, members of my supervisory committee, for their valuable comments and suggestions.

Particular acknowledgement is due to the Canadian International Development Agency (CIDA), the Natural Sciences and Engineering Research Council of Canada (NSERC) and McMaster University for providing the financial support for the research work.

TABLE OF CONTENTS

TABLE OF CONTENTS (continued) PAGE

TABLE OF CONTENTS (continued) PAGE

TABLE OF CONTENTS (continued) PAGE

TABLE OF CONTENTS (continued) PAGE

LIST OF TABLES

LIST OF FIGURES

LIST OF FIGURES (continued)

LIST OF FIGURES (continued)

LIST OF FIGURES (continued)

LIST OF FIGURES (continued)

LIST OF FIGURES (continued)

LIST OF FIGURES (continued)

LIST OF SYMBOLS

a_1, a_2	proportionality factors relating damping matrix to the mass and stiffness matrices respectively
A_v	area of transverse reinforcement
b	beam section width
c	distance from extreme compression fibre to neutral axis
C	Damping matrix.
C_m	factor relating the actual moment diagram to an equivalent uniform moment diagram.
d	beam section effective depth
d'	distance from extreme compression fibre to the centriod of compression steel
D	dead load
D_i	energy dissipation index (Darwin and Nmai, 1986)
E_c	concrete modulus of elasticity
f_c'	concrete compressive strength
$f_{ji}, f_{ij}, f_{ji}, f_{jj}$	flexibility influence coefficients.
f_y	yield strength of the longitudinal steel
f_{yv}	yield strength of transverse reinforcement
f_u	ultimate strength of reinforcing bars
F	foundation factor in NBCC base shear calculations
F_t	portion of base shear to be concentrated at the top floor in addition to F_N
F_x	lateral load at level x
G_c	concrete shear modulus
h_c	column clear height
h_x	height of level x above ground
i	storey level number
I	importance factor in NBCC base shear calculations
I_c, I_b	moment of inertia of column and beam
I_{ext}, I_{int}	moment of inertia of the exterior and interior span beams
I_g	gross moment of inertia of the column section neglecting steel
k	effective length factor
k_i, k_j	stiffness of the non-linear flexural springs at ends i and j of the single component element.
K_o	initial loading stiffness
K_G	geometric stiffness matrix.
K_T	Stiffness matrix of the structure in its current state.
K_u	unloading stiffness
l_c, l_b	clear length of column and beam
l_u	unsupported length of column
l'	length of beam section between the hinging zone and point of load application.

LIST OF SYMBOLS (continued)

L	live load
L_{ext}, L_{int}	clear length of the exterior and interior span beams
m_i	lumped mass at the i^{th} floor level.
M	Mass matrix.
M_b^+	positive moment resistance of the beam
M_b^-	negative moment resistance of the beam
M_b^{ext}	positive beam moment at the face of the interior columns.
M_{max}	maximum moment attained in the beam
M_{nb}	nominal moment resistance of the beam
M_{nc}	nominal moment resistance of the column
M_p	crack closing moment
M_{pb}^-	negative probable moment resistance of the beam section at the exterior column
$M_{pc_b}^a$	probable strength of the column section above the joint
M_{pc}	probable strength of the column section below the joint
M_{rb}	factored moment resistance of the beam
M_{rc}	factored moment resistance of the column
M_x	moment at unloading point
M_x	moment at point towards which reloading branch is aiming
M_y	yield moment
N	total number of storeys in the building
N_c	total number of experimental cycles
p	ratio of strain hardening stiffness to initial stiffness
$P^+_{e,i}$	Force obtained from experiment at the positive peak displacement of the i^{th} cycle.
$P^-_{e,i}$	Force obtained from experiment at the negative peak displacement of the i^{th} cycle.
P_f	factored axial load in the column
$P^+_{m,i}$	Force calculated from model at the positive peak displacement of the i^{th} cycle.
$P^-_{m,i}$	Force calculated from model at the negative peak displacement of the i^{th} cycle.
Q	seismic load
R	force modification factor in NBCC base shear calculations
s	spacing between stirrups
s_{min}	specified spacing for minimum stirrups = d/4
S	seismic response factor in NBCC base shear calculations
T	fundamental natural period
T_m	undamped period of the m^{th} mode
$\mathbf{u}$	velocity at the beginning of the new time step.
v	zonal velocity ratio
V	seismic base shear
V_c	concrete shear resistance
V_{col}	column shear force
V_{Code}	code base shear
V_{demand}	maximum response shear force

LIST OF SYMBOLS (continued)

V_D	shear force due to dead load
V_e	elastic demand seismic base shear
V_f	factored design shear force
V'_f	modified factored design shear force
V_j	joint design shear force
V_L	shear force due to live load
V_Q	shear force due to seismic lateral loads
V'_Q	magnified shear force due to seismic lateral loads
V_s	stirrups shear resistance
V_{supply}	shear resistance of a beam
$(V_s)_{min}$	resistance of minimum stirrups
W	total building weight
W_x	portion of W assigned to level x
Z_a	acceleration seismic zone
Z_v	velocity seismic zone
α	input parameter to govern pinching in the hysteresis model
β	input parameter to govern strength deterioration in the hysteresis model
δ	error factor in calibrating new hysteretic model
δ_b	column moment amplification factor for slenderness effects
δ_{max}	maximum roof displacement
δ_y	roof displacement at general yielding of the frame.
Δ	beam tip displacement
Δ_y	beam yield displacement
ΔF_c	damping corrective force
Δ_1	Deflection due to flexural rotation within the plastic hinge zone.
Δ_2	Deflection due to shear strain within the plastic hinge zone.
Δ_3	Deflection due flexural deformations outside the plastic hinge zone.
Δ_4	Deflection due shear deformations outside the plastic hinge zone.
ΔK	change in the tangent stiffness matrix during Δt.
Δt	time increment
Δu	finite increment of displacement.
Δu	finite increment of velocity.
$\Delta \ddot{u}$	finite increment of acceleration.
$\Delta \ddot{u}_g$	finite increment of ground acceleration.
ϵ_u	ultimate strain of reinforcing bars
θ_p	crack closing rotation
θ_r	rotation at load reversal
θ_x	rotation at unloading point
θ_x	rotation at point towards which reloading branch is aiming
θ_y	yield rotation
θ_3	shear strain angle in plastic hinge zone
θ_4	angle of flexural rotation in plastic hinge zone

LIST OF SYMBOLS (continued)

μ_a	available ductility factor (Park, 1989)
μ_δ	global displacement ductility factor
μ_ϕ	curvature ductility
ξ_m	damping ratio of the m^{th} mode
ρ	longitudinal reinforcement ratio
σ	standard deviation
ϕ_c	concrete resistance factor = 0.6
ϕ_m	member resistance factor (=0.65).
ϕ_{max}	maximum curvature
ϕ_o	overstrength factor
ϕ_s	steel resistance factor = 0.85
ϕ_y	yield curvature
ψ	ratio of sum of column stiffness to beam stiffness at a joint
ψ_{avg}	average of two ψ values at two ends of a column

CHAPTER 1

INTRODUCTION

1.1 BACK GROUND AND MOTIVATION

Moment Resisting Frames (MRFs) are commonly used as lateral load resisting systems in multi-storey buildings located in seismically active regions. For the design of conventional building structures, the seismic design forces adopted are usually smaller than those required if the buildings were to remain elastic during strong ground shaking for economic reasons. As a result, MRFs will be expected to deform in the inelastic range when subjected to strong seismic shaking. In order to survive a strong earthquake without collapse, the frames must possess some ductility (i.e. to withstand large inelastic deformations without a significant loss of strength).

MRFs in seismic regions may be classified into two broad classes. One is called Ductile Moment Resisting Frame (DMRF) and the other may be called Nominally Ductile Moment Resisting Frame (NDMRF). One major difference between the two classes is the seismic force level for which the frame is required to be designed. DMRFs are designed for lower strength than NDMRFs. As a result, the members of DMRFs need to be designed and detailed to have a high ductility

capacity. To outlast the earthquake without collapse, DMRFs rely on energy dissipation achieved by flexural hinging in the beams. Columns are provided with sufficient strength to ensure that hinging will be limited to the beams (strong column-weak beam). In order to ensure that the beam energy dissipation mechanisms are maintained, brittle failures (such as shear and joint failures) must be avoided. This is achieved by calculating the design shear forces based on the probable strength of potential plastic hinges. The design concepts described above are termed "Capacity design procedures" and were developed by Park and Paulay (1975).

Since NDMRFs are designed for higher strength than DMRFs, capacity design procedures need not be adopted in their design. Traditionally used design techniques can be applied with only minor modifications. Also, the detailing requirements in the members of NDMRFs are less stringent than those employed in DMRFs.

Because DMRFs are based on a new concept and subjected to a number of strict design rules, they received considerable attention in research in the recent years in order to examine the validity of the design rules and to ensure that the whole design concept leads to appropriate seismic performance. On the other hand, NDMRFs received far less attention despite the fact that they constitute the majority of reinforced concrete frames constructed in most countries. One reason may be that since there are no innovative concepts for the design of NDMRFs, there is no need to check their seismic performance. Another reason is that due to the lack of strict design rules, NDMRFs comprise a wide variety of frames and each frame type leads

to a different seismic performance. As a result, it is more difficult to arrive at a general assessment of the seismic performance of NDMRFs as a whole.

According to the current Canadian practice, the designer is given two options for the design of MRFs in seismic zones: DMRF or NDMRF. DMRFs are designed for a lower strength level and are to be designed following the capacity design procedures outlined in chapter 21 of the concrete design Code (CSA, 1984). NDMRFs are designed to resist twice the seismic lateral loading as that specified for DMRFs. However, all design actions (moment, shear and axial forces) are obtained from elastic static analysis under the prescribed factored loads and loading combinations. The frame members are designed using the conventional design procedures given in chapters 1 through 20 of the Code. Some special detailing requirements are specified to provide some ductility potential for the frame members.

By giving the designer the choice between DMRFs and NDMRFs, it is implied that both classes are equally suitable for seismically active areas. The performance of DMRFs designed according to the current Canadian Codes has been evaluated by different researchers (e.g. Zhu, 1989 and Paultre and Mitchell, 1991). They found that the seismic performance of DMRFs designed based on Canadian practice measures to expectations. Although the seismic performance of DMRFs is excellent, they have not been widely used as lateral load resisting systems for two main reasons: 1) stringent detailing requirements can create congestions of reinforcing steel

making construction difficult, and 2) the capacity design philosophy is not suitable for gravity dominated situations because of the unrealistic column overdesign resulting from the strong column-weak beam requirement. Gravity load dominance occurs in low-rise frames in all seismic zones and most frames in moderate seismic zones. The population centres in Canada are mainly concentrated in moderate seismic zones and in such zones NDMRFs would be more commonly used than DMRFs.

It should be mentioned here that other design codes also allow the use of NDMRFs for buildings in seismically active regions. The American Concrete Institute design code (ACI 318-89) labels this class of frames as "frames in moderate seismic zones". The New Zealand concrete design code (NZS 3101) labels this class as "frames of limited ductility". All three codes have similar design philosophies and procedures for NDMRFs except in the specification of design shears. Both the ACI and NZS code specify some amplification of the shear forces obtained from elastic static analysis for design. On the other hand, no amplification is required using the Canadian code. In view of such a difference, the performance of NDMRFs designed to satisfy the minimum code requirements in Canada, needs to be thoroughly evaluated.

The research performed on MRFs in the past three decades involved designing the frames according to the codes and then subjecting them to appropriate earthquake input. The main emphasis was on the distribution of plastic hinges and the ductility demands attained in those hinges. As a result very few researchers

reported the shear demands in their studies. It was usually assumed that there is sufficient shear resistance in the designed members such that shear failures can not occur. This is probably justified for DMRFs. In such frames, the provided shear capacity is based on the probable strength of the beam plastic hinges and thus the shear demands are guaranteed not to exceed the shear capacity. For NDMRFs, this is not necessarily true since the shear capacity is based on the shear forces obtained from the loading combinations using static analysis.

Clough et al (1965) developed a model for the inelastic dynamic analysis of multistorey reinforced concrete frames. The moment-rotation relationship of the proposed model was of the bilinear type. Such a model can only represent reinforced concrete members that are well detailed such that they will not show stiffness and strength deterioration or pinching in the hysteresis loops. The model was used by Clough et al to analyze a number of DMRFs. In their analysis the researchers did not monitor the shear stresses attained in the frame members during the inelastic response.

Bertero and Popov (1975) studied the effect of shear stresses on the behaviour of particular subassemblages of DMRFs. In the inelastic dynamic analysis, no comparison was made between the design and response shear forces in the different frame members. Thus, it was assumed that the provided shear reinforcement would have been adequate to resist the applied shear forces.

Roufaiel and Meyer (1987) and Chung et al. (1989) reported the inelastic

dynamic analysis on DMRFs and once again it was implicitly assumed that shear failures can not occur in the beams, as the shear demands attained in the beams during earthquake response of the frames were not reported.

Zhu et al (1991) reported the results of static and dynamic analysis on DMRFs of different heights designed according to the current Canadian practice. The response parameters investigated were the storey drifts and the ductility demands. The shear stresses attained during the response were not investigated. They used a bilinear hysteresis model to represent the member behaviour implying that good detailing of the frame members has been carried out.

Paultre and Mitchell (1991) designed three six-storey reinforced concrete MRFs with different levels of ductility according to the current Canadian practice. One of the frames was designed and detailed as a NDMRF. The columns of the NDMRF were overdesigned to ensure good performance of the frame. This resulted in a design very similar to DMRF. However, no guidelines as to the extent to which the columns should be overdesigned were provided. The NDMRF was then analyzed under ground motion records of different characteristics. The response shear forces in the frame members were monitored. It was found that the response shear forces exceeded the design values obtained from the loading combinations based on elastic static analysis. However, the minimum beam stirrups requirements specified in the concrete design code (No. 10 @ d/4 spacing) were found to be sufficient to resist the seismic shear forces during earthquake excitation for this particular frame. As a

result, Paultre and Mitchell concluded that the design and detailing requirements of the Canadian Codes are adequate to ensure the good seismic performance of the NDMRF.

This conclusion can not be generalized to all nominally ductile frames for two reasons. First, the frame analyzed by Paultre and Mitchell (1991) is not necessarily representative of a typical NDMRF because its columns were overdesigned beyond the minimum Code requirements. Second, the minimum stirrups may not always be adequate to resist the maximum induced shear forces. For example, a frame sustaining larger loads will experience larger shear forces while the minimum stirrups will remain the same.

Some researchers were interested in the effect of shear failure on the energy dissipation capacities of the beams when subjected to inelastic cyclic loading. Most of the experimental research showed that beam shear failures reduce energy dissipation capacity. To avoid beam shear failure, the stirrups capacity must be larger than the maximum applied shear forces in order to ensure adequate performance under inelastic reversed cyclic loading.

Gosain et al (1977) compiled the test results of various experiments performed on reinforced concrete beams. Their discussions indicated that for a beam to behave adequately under reversed bending and shear, the capacity of the stirrups should be at least equal to (if not greater than) the maximum applied shear. Nevertheless, Gosain et al. did not elaborate on the behaviour of the specimens when the applied

shear exceeded the stirrups capacity.

Scribner and Wight (1978, 1980) reported the results of 12 tests on exterior beam-column subassemblages. Their results showed that the larger the ratio of the stirrups capacity-to-the applied shear, V_s/V_m, the better the performance of the specimens. Nevertheless, none of the specimens they tested had a V_s/V_m ratio less than 0.98. Moreover, they indicated that in order to improve the behaviour of beams under large reversed shear stresses, intermediate longitudinal reinforcement may be added. They did not provide a rational approach for designing the longitudinal reinforcement.

Viwathanatepa et al (1979) tested half scale models of an exterior beam column joint. The prototype frame was designed as DMRF and consequently the provided shear reinforcement was adequate to resist the maximum applied shear forces in the specimens. Thus, their specimens could only represent beams in which V_s/V_m is greater than unity. Therefore, their results may not be representative of beams in NDMRFs.

Hwang (1982) reported the results of 11 tests on beams with different shear stress levels and different loading histories. Four of the specimens had a V_s/V_m less than unity while the other seven specimens had a V_s/V_m ratio greater than unity. Once again, it was concluded that specimens with V_s/V_m less than unity perform poorly under cyclic loading and should be avoided in MRFs in seismic zones.

Darwin and Nmai (1986) analyzed the energy dissipation capacities of specimens tested by various researchers. Their results showed that the behaviour of specimens with a V_s/V_m ratio less than unity was unfavourable.

Paultre et al (1989) performed some experiments on beam column subassemblages from DMRFs and NDMRFs detailed according to the current Canadian practice. The current Canadian concrete design code specifies the use of stirrups spaced at 1/4 the member depth, placed in the member end zones. The specimen tested by Paultre et al (1989) was subjected to a shear force smaller than the capacity of the minimum stirrups specified by the Code. Their results showed that the nominally ductile specimen behaved in a favourable manner and did not show any distress due to shear. They concluded that the beam shear design and detailing requirements of NDMRFs are adequate.

From the preceding discussions and literature survey, it can be seen that the attention received by NDMRFs is limited and does not commensurate to the number of NDMRFs constructed in practice. Therefore, a more detailed investigation of the seismic performance of NDMRFs is needed.

Gravity loads dominate the design in the case of a long span-low rise frame in all seismic zones or in most frames in moderate seismic zones. In such a case the strength of the beams will normally be governed by the gravity load moments rather than the seismic lateral loading. Designing such a frame as a DMRF, which requires the columns to be stronger than the beams by following capacity procedures, will

result in an unrealistic overdesign of the columns. Designing such a frame as a NDMRF may result in excessive seismic responses, and hence damage. Therefore, there appears to be a need for an alternative design approach for such frames.

1.2 OBJECTIVES AND SCOPE

The objectives of this study are :

1) To evaluate the seismic performance of nominally ductile reinforced concrete frames designed according to the National Building Code of Canada (NBCC 1990) and the Canadian concrete design code (CAN3-A23.3-M84). In the course of this thesis, they will be referred to as the Code or Codes for convenience.

2) To suggest design modifications to improve the seismic performance of nominally ductile frames designed according to the current Codes.

3) To propose an alternative design approach to modify the design procedure of nominal ductility for gravity-dominated reinforced concrete frames.

To achieve these objectives, buildings of different heights (four, six and ten storeys) were designed and detailed as nominally ductile frames and satisfied the

minimum requirements according to NBCC 1990 and CAN3-A23.3-M84. The designed frames were then analyzed statically under monotonically increasing loading to study their force-deformation characteristics. Then, the seismic behaviour of the designed frames was obtained by means of dynamic analysis under earthquake excitation using the computer code DRAIN-2D (Kanaan and Powell, 1973). Fifteen normalized ground motion records were used as input. The performance of each frame is evaluated based on a statistical analysis of the responses to each individual ground motion record. In this way, one avoids the dependence of the obtained results on the characteristics of any single record. The response parameters investigated in the dynamic analysis were the frame deflection, storey drifts and overall ductility demands, the local (member) ductility demands and the beam and column shear demands. An experimental investigation was performed in order to evaluate the validity of including the concrete contribution to the shear resistance in the design of beams in NDMRFs. The results of the analytical and experimental investigations are then used to develop the new design approach for low-rise frames.

1.3 ORGANIZATION OF THE THESIS

The current practice for the seismic design of reinforced concrete frames is described in chapter 1. A brief literature survey on the experimental and analytical research on reinforced concrete frames is presented. This presentation provided the

research background and allowed the formulation of the objectives of the present study.

The dimensions of the six storey reinforced concrete office building reported by Paultre and Mitchell (1991) are adopted for the building frames studied in chapter 2. The building is redesigned once to conform to the minimum requirements for NDMRFs according to the Codes and another time to conform to the strong column-weak beam requirement of DMRFs. The design procedures are explained followed by a detailed description of the procedures employed in the static and dynamic analyses of the frames. The results of the static and dynamic analysis of these frames are reported and compared with those designed by Paultre and Mitchell in order to provide a broad view on the performance of different types of NDMRFs designed based on the current Codes.

In chapter 3, a six-storey building with 8.0 metre frame spacing is considered. The building is designed as a NDMRF according to the minimum Code requirements. The designed frame is analyzed statically under monotonically increasing loading and dynamically under earthquake excitation to show that while many inelastic demands of the NDMRFs considered in chapter 2 are typical of NDMRFs designed according to the Canadian practice, the relationship between beam shear demands and shear capacity of chapter 2 NDMRFs is not typical. This points to the need for special provisions for beam shear design in NDMRFs if beam shear failures are to be avoided.

Chapter 4 includes the procedures and results of the experimental investigation on beams of nominally ductile frames. The chapter starts with a detailed description of the test specimens and the test setup. The instrumentation and data acquisition system are described followed by a description of the loading history used in the experiments. The test results presented included the force-deformation loops, the crack propagation, the stirrups strains, the flexural and shear deformations in the plastic hinge zone and the energy dissipation capacities.

The procedure proposed for the calculation of design shears in the beams of NDMRFs is described in chapter 5. The proposed procedure is used to calculate the design shear forces in the beams of the six-storey buildings described in chapters 2 and 3 to show that the modified design shears are comparable to the demand shears obtained from the dynamic analysis of these frames. To further check the validity of the proposed formula, two additional NDMRFs, one four-storey and one ten-storey, are designed and analyzed dynamically under earthquake excitation.

An alternative approach is proposed in chapter 6 for the design of low-rise reinforced concrete frames in seismic regions. A full description of the proposed approach is followed by an application of the proposed design approach to the six-storey building described in chapter 2. The seismic performance of the frame designed using the proposed approach is compared to the responses of the frames reported in chapter 2 to illustrate the advantage of the proposed design approach.

Finally, chapter 7 presents a summary and the significant conclusions of this study. Recommendations for future research are also presented.

CHAPTER 2

DESIGN AND ANALYSIS OF A SIX STOREY BUILDING WITH 6.0 METRE FRAME SPACING

2.1 INTRODUCTION

In the design of nominally ductile moment resisting frames (NDMRF) in seismically active regions, columns are designed to resist the factored moments and axial forces obtained from the elastic static analysis. One may choose to design the columns strictly following the minimum code requirements. A more experienced designer may choose to overdesign the columns beyond minimum code requirements so that yielding occurs mainly in the beams in order to enhance the performance of the frame when subjected to strong ground shaking. The amount of overdesign would be based mainly on the designer's engineering judgement since there are no definite design rules regarding the relationship between beam and column strengths. The six-storey NDMRFs reported by Paultre and Mitchell (1991) are examples of such a case. The columns of their frame were overdesigned to enhance its seismic performance. Unfortunately, no guidelines are provided on the increase of column sizes and reinforcement over and beyond minimum code requirements.

In this chapter, the six storey building considered by Paultre and Mitchell will be redesigned twice in order to bracket the practical range of nominally ductile frames that can be conceived in the design process. The first design strictly follows the minimum code requirements for nominally ductile frames to provide a lower bound. The second design uses the seismic base shear appropriate for NDMRFs, but follows the strong column-weak beam requirement of ductile frames as prescribed by clause 21 of the concrete Code. In practice, this second design is the design for a ductile moment resisting frame and NBCC 90 allows it to be designed for a base shear that is only half that appropriate for NDMRFs. Therefore, this second design can be considered as an upper bound in terms of member sizes and reinforcement requirements for NDMRFs. The static and dynamic responses of these frames are then compared to those of the frames designed by Paultre and Mitchell (PM frames). Such a comparison will show the level of overdesign of the PM frames and also contrast the seismic performances between the PM frames and a frame that satisfies the minimum code requirement. This comparison leads to a better appreciation of the implication of the term "nominally ductile R/C frame" as used in the current Canadian codes (NBCC 1990 and CAN3-A23.3-M84).

A description of the building reported by Paultre and Mitchell is first given, followed by a detailed description of the design of the "lower bound" and "upper bound" NDMRFs. After a description of the procedures used in the inelastic dynamic analysis, the results of the analysis will be presented, compared and discussed.

2.2 DESCRIPTION OF BUILDING

The six storey building reported by Paultre and Mitchell has seven 6.0 metre bays in the N-S direction and three bays in the E-W direction as shown in figure (2.1). The E-W bays consist of two 9.0 metre external office bays and an internal 6.0 metre corridor bay. The first storey is 4.85 metres high while all remaining storeys are 3.65 metres high. The one way slab is 110 mm thick and the secondary beams are all 300 mm wide by 350 mm deep. The building is assumed to be located in Montreal and was designed accordingly. The concrete compressive strength is 30 MPa and the steel yield strength is 400 MPa.

Paultre and Mitchell reported the design of two nominally ductile frames. One of the frames had smaller columns than the other one. The small columns frame will be denoted 6SPM while the large columns frame will be denoted 6-PM. The numeral 6 in the frame designation stands for six storeys, the letters PM stand for Paultre and Mitchell while the letter S stands for the smaller column sizes. The member dimensions of these two frames are shown in figure (2.2) while figure (2.3) shows the reinforcement ratios. Although they concluded that the seismic performance of 6SPM is less than desirable, it will still be included in this chapter since it represents one of the many possible designs of nominally ductile frames that satisfies the Code requirements.

2.3 DESIGN OF THE SIX STOREY BUILDING TO MINIMUM CODE REQUIREMENTS FOR NOMINALLY DUCTILE FRAMES

To evaluate the performance of nominally ductile frames designed according to the current Canadian practice, the six storey building described in section 2.2 will be redesigned strictly following the minimum code requirements for NDMRFs. The factored forces and moments obtained directly from elastic static analysis will be used to obtain the flexural and shear reinforcement in the beams and columns. Two frames will be designed. The first frame, denoted 6SND, will have the same member dimensions as those of 6SPM shown in figure (2.2a). The second frame, denoted 6-ND, will have the same member dimensions as those of 6-PM shown in figure (2.2b). The letters ND in the frame designation stand for nominally ductile frames.

2.3.1 DESIGN LOADING

The frames will be designed for the critical combinations of gravity and seismic loading as given by the National Building Code of Canada (NBCC 1990). The loads are taken identical to those used by Paultre and Mitchell in the design of 6SPM and 6-PM.

2.3.1.1 Gravity Loading

The design dead load includes the self weight of the structural components, the partitions loading and the mechanical services loading. The live load is taken as that suggested by NBCC 1990 for an ordinary office building with double live load on the 6 metre corridor bay. The roof live loads include snow loads plus mechanical

services loading over the central 6 metre bay. The gravity loads are distributed to the different elements using the tributary area. Table (2.1) gives a summary of the gravity loads used in the design of the frames.

2.3.1.2 Seismic Loading

The seismic loading calculation follows strictly the NBCC 1990 provisions. The weight of the building, W, is based on the dead loads plus 25 percent of the roof snow loads. The weights are assumed to be lumped at the floor levels. The total seismic base shear, V, is calculated using the following equations:

$$V = (V_e/R)\ U \tag{2.1}$$

and

$$V_e = vSIFW \tag{2.2}$$

where

V_e = elastic demand base shear
v = zonal velocity ratio
S = seismic response factor
I = importance factor
F = foundation factor
R = force modification factor
U = 0.6

The building is assumed to be located in Montreal where the zonal velocity ratio is equal to 0.1 and $Z_a > Z_v$. The importance and foundation factors are both taken as unity. The seismic response factor is a function of the fundamental period of vibration of the designed structure. Figure (2.4) provides a graphical presentation of the seismic response factor, S, for a region in which $Z_a > Z_v$ according to NBCC 1990. The fundamental period, T, is estimated using the following formula for regular moment resisting frames, namely

$$T = 0.1\,N \tag{2.3}$$

where N is the total number of storeys in the building.

The force modification factor, R, is intended to reflect the energy dissipation capacities of the designed structure (Rainer, 1987). NBCC 1990 recommends a value of R = 2.0 for nominally ductile reinforced concrete frames.

Based on the above discussions, the total seismic base shear for this building was found to be

$$V = 0.058\,W \tag{2.4}$$

This total base shear is to be distributed through the building height using the following formula :

$$F_x = \frac{(V - F_t)\,W_x h_x}{\sum_{i=1}^{N} W_i h_i} \tag{2.5}$$

where
W_i, W_x = portion of W assigned to levels i or x respectively
h_i, h_x = heights of level i or x above ground
N = total number of storeys in the building
F_x = lateral load at level x
F_t = portion of V to be concentrated at the top floor in addition to F_N

F_t is intended to account for higher mode effects and can be calculated from the following equation

$$F_t = \begin{cases} 0.07\,TV & \leq 0.25\,V \\ 0 & \text{if } T \leq 0.7 \text{ sec} \end{cases} \tag{2.6}$$

For the frames designed here, $T = 0.6$ seconds < 0.7, and F_t is equal to zero. The lateral load acting at each floor level is resisted by eight identical frames in the E-W direction. Therefore, the load on each frame will be taken as one eighth of the total lateral load acting on the building as it is assumed by Paultre and Mitchell (1991).

2.3.1.3 Loading Combinations

In accordance with NBCC 1990, the following loading combinations are used in the design of the frame members

$$\begin{aligned}
&1.25\,D + 1.5\,L \\
&1.25\,D + 1.0\,Q \\
&1.25\,D - 1.0\,Q \\
&1.25\,D + 0.7\,(1.5\,L + 1.0\,Q) \\
&1.25\,D + 0.7\,(1.5\,L - 1.0\,Q) \\
&0.85\,D + 1.0\,Q \\
&0.85\,D - 1.0\,Q
\end{aligned} \qquad (2.7)$$

where D is the dead load, L is the live load due to occupancy and Q is the seismic loading. Pattern live loading and live load reduction factors were taken into consideration in the design process.

2.3.2 EFFECTS OF GEOMETRIC NONLINEARITY

The effects of geometric nonlinearities can be separated into two types (Lai and McGregor, 1983). The first type is the lateral drift effect (P-Δ effect) and the second is the member slenderness effect. The Canadian concrete design code provides separate provisions for these two types of geometric nonlinearities (clauses

10.11.6and 10.11.7).

The lateral drift, P-Δ, effect can be evaluated through a second order static analysis involving an iterative procedure. However, a linearized procedure will be employed herein to account for the P-Δ effects in the design process. In this procedure (WiHxon and Habibullah, 1987), a geometric stiffness matrix is evaluated based on the column axial force due to gravity loading. This geometric stiffness matrix is subtracted from the element stiffness matrix and the solution is obtained directly without iteration. The member slenderness effects will be considered in the design of the columns as described in section 2.3.3.2.

2.3.3 MEMBER DESIGN

In this study, longitudinal and transverse reinforcements in the beams and the columns are calculated. All design forces and moments are obtained from the elastic static analysis under the prescribed loading combinations. The SUPERETAB computer program (Wilson et al. 1975) is used in the elastic static analysis of the frames. The design procedures described in the following sections were programmed as separate subroutines and combined with SUPERETAB such that the whole design process was automated. In the static analysis, the gross moment of inertia of the beams is first calculated based on a T-shape section to allow for the slab contributions. The effective flange width is calculated according to the recommendation given in Code clause 8.10.2.For cc :putation purposes, the effective moment of inertia of the beams is taken as 60 percent of the gross moment of inertia

to account for cracking. The effective moment of inertia of the columns is assumed as 80 percent of the gross moment of inertia. Rigid end zones are considered for the beams and columns to account for the finite size of the beam-column joints. The beam design moments are obtained at the column faces and the column design moments are obtained at the beam faces. The obtained column moments are further amplified to account for slenderness effects.

2.3.3.1 Beam Design for Flexure

Although it is possible to redistribute beam moments due to gravity and seismic loading, only gravity load moments were redistributed within the limits provided by code clause 8.4. Such a decision is consistent with the procedure used by Paultre and Mitchell.

In determining the flexural strength for the beams, the slab bars within three times the slab thickness on each side of the beam were assumed to contribute to the negative moment resistance of the beam. A lower bound is imposed in determining the positive reinforcement at the beam end sections. This lower bound is intended to recognize the cyclic nature of the seismic loading and also to provide some confinement for the compressed concrete in the plastic hinge zones. Clause 21.9.2.1.1 of the Code suggests this lower bound as

$$M_b^+ = \frac{|M_b^-|}{3} \tag{2.8}$$

where M_b^+,M_b^- are the positive and negative moment resistances at the support section respectively.

Moreover, the beam reinforcement ratios are bound by the following lower and upper bounds for flexural members

$$\begin{aligned} &\textit{lowerbound} && \rho \geq \frac{1.4}{f_y} \\ &\textit{upperbound} && \frac{c}{d} \leq \frac{600}{600+f_y} \end{aligned} \qquad (2.9)$$

where
f_y = yield strength of the longitudinal steel
c = distance from extreme compression fibre to neutral axis
d = beam effective depth

2.3.3.2 Column Design for Flexure

The column design moments are obtained directly from the results of the elastic static analysis of the frames under the factored loads and taking P-Δ effects into consideration. These design moments are further amplified to account for the slenderness effects. The amplification factor, δ_b, is given by

$$\delta_b = \frac{C_m}{1 - \frac{P_f}{\phi_m P_c}} \geq 1.0 \qquad (2.10)$$

where

$$P_c = \frac{\pi^2 EI}{(kl_u)^2}$$

P_f = factored axial load in the column
C_m = factor relating the actual moment diagram to an equivalent uniform moment diagram.
ϕ_m = member resistance factor (=0.65).
EI = $0.25\, E_c I_g$
E_c = concrete modulus of elasticity
I_g = gross moment of inertia of the column section neglecting steel
l_u = unsupported length of column
k = effective length factor

The effective length factor is determined based on the rotational restraints at the top and bottom of the column. A measure of this restraint can be given as

$$\psi = \frac{\sum (EI_c/l_c)}{\sum (EI_b/l_b)} \qquad (2.11)$$

where I is the effective moment of inertia of the member and l is the clear span of the member. The subscripts b and c denote beam and column respectively. The summation is carried out for all beams and columns framing into the joint. The effective length factor can be determined from equation (2.12) as suggested by Furlong (1971)

$$k = \begin{cases} \dfrac{20 - \psi_{avg}}{20}\sqrt{1 + \psi_{avg}} & \psi_{avg} \le 2 \\ 0.9\sqrt{1 + \psi_{avg}} & \psi_{avg} > 2 \end{cases} \qquad (2.12)$$

where ψ_{avg} is the average of the two ψ values calculated at the top and bottom of the column.

The column design charts provided by the Canadian Portland Cement Association (1985) are used to determine the column reinforcement ratios based on the amplified design moments and the corresponding axial forces from the different loading combinations.

2.3.3.3 Beam Shear Design

The target for shear design of beams in seismic design is to prevent beam shear failure by providing shear resistance, V_{supply}, greater than the shear demand V_{demand}. At the design stage, V_{demand} is unknown, thus the designer tries to provide V_{supply} greater than the factored design shears, V_f, which is an estimate of V_{demand} provided by the design Codes. In the beams of nominally ductile frames, V_f is obtained from the results of elastic static analysis. V_{supply} is assumed to consist of the factored concrete shear resistance, $\phi_c V_c$ and the stirrups resistance $\phi_s V_s$ which are calculated by the following formulae according to the Code;

$$V_c = 0.2\sqrt{f'_c}\, b_w d \qquad (2.13)$$

$$V_s = \frac{A_v f_{yv} d}{s} \qquad (2.14)$$

where

ϕ_c = concrete resistance factor = 0.6
ϕ_s = steel resistance factor = 0.85
f_c' = concrete compressive strength
b_w = beam width
d = effective depth
f_{yv} = yield strength of stirrups steel
A_v = area of stirrups
s = spacing between stirrups

Since the beam size is already known, then V_c is known. The designer will have to provide stirrups such that

$$\phi_s (V_s)_{req} \geq V_f - \phi_c V_c \qquad (2.15)$$

from which the stirrups area and spacing can be determined using equation (2.14). However, the code specifies the use of minimum stirrups to provide confinement for concrete and steel (clause 21.9.2.1.2). The minimum stirrups are No. 10 at a spacing equal to 1/4 of the beam effective depth. If the stirrups spacing required for shear resistance is larger than d/4, the stirrups should be placed at d/4 spacing. For the design of the frames considered here it was found that the maximum V_f = 209 kN. For the given beam size, $\phi_c V_c$ = 136 kN. Thus, $(V_s)_{req}$ = (209 - 136)/ϕ_s = 86 kN. Using 2 legged No. 10 stirrups (A_v = 200 mm^2), the required spacing will be 480 mm. Since the minimum requirement specifies a d/4 spacing, the 2-legged No. 10 stirrups will be spaced at 1/4 the member depth giving a stirrups resistance $(V_s)_{min}$ = 320 kN as calculated from equation 2.16 below.

$$(V_s)_{min} = \frac{A_{vmin} f_{yv} d}{s_{min}} = \frac{A_{vmin} f_{yv} d}{d/4} = 4 A_{vmin} f_{yv} = 320\ kN \qquad (2.16)$$

where
A_{vmin} = area of 2 legged No. 10 stirrups = 200 mm^2
s_{min} = specified spacing for minimum stirrups = d/4
f_{yv} = 400 MPa.

The effective shear capacity in the beam, V^*_{supply}, will be

$$V^*_{supply} = V_c + (V_s)_{min} \qquad (2.17)$$

It should be noted that the nominal resistance of the minimum stirrups, $(V_s)_{min}$, is independent of beam size and that V^*_{supply}, is based on the assumption that V_c can be relied upon. This in turn implies that upon yielding, the ductility demand is small and the concrete is not extensively cracked. If the beam undergoes large ductility demands, V_c is likely to decrease rapidly and the shear resistance will be limited to $(V_s)_{min}$. If one follows the Code recommendation to provide shear resistance, the following questions need to be addressed: a) what are the ductility demands in the beams of nominally ductile frames designed according to the current Canadian practice? b) can V_c be relied upon at those ductility demands? c) is the factored design shear, V_f, based on static analysis a realistic estimate of shear demand, V_{demand}, on the beams during earthquakes? and d) in case that V_c is not reliable, will $(V_s)_{min}$ as given in equation (2.16) be larger than the shear demand V_{demand}, such that shear failure will not occur for beams of different sizes? These questions will be addressed in this study.

2.3.3.4 Column Design for Shear

The column design shear forces are obtained from the elastic static analysis under the prescribed loading combinations. The concrete is assumed to contribute to the column shear resistance according to Code clause 11.3.4.3.It is found that only minimum ties are required for all columns. For the columns of the 6-ND frame, the 4-legged No. 10 ties will be spaced at 150 mm in the end zones (500 mm at each end of the column) and 300 mm in the remainder of the column height (Code clauses 21.9.3.1and 7.6.5).For the columns of the 6SND frame, the ties will be spaced at 125 mm in the end zones and 250 mm in the remainder of the column height.

2.3.4 FINAL DESIGN RESULTS

The reinforcement ratios of the two frames 6SND and 6-ND are shown in figure (2.5). The numbers placed at the right of the exterior and interior columns depict the flexural reinforcement ratios for the exterior and interior columns respectively. The numbers placed above and below the beams depict the top and bottom reinforcement ratios of the beams. Since minimum stirrups are used in the beams, 2 legged No. 10 stirrups are placed at 130 mm spacing for the first three floors and at 115 mm for the top three floors. Also, only minimum ties are required for the columns. For the large columns frame, 4-legged No. 10 ties are spaced at 150 mm for the end regions and 300 mm for the rest of the column. For the small columns frame, the ties are spaced at 125 and 250 mm for the end and central regions respectively.

2.4 DESIGN OF THE SIX STOREY BUILDING USING STRONG COLUMN WEAK BEAM REQUIREMENT

The six storey building described in section 2.2 will be redesigned once more to conform to the strong column weak beam requirement prescribed for ductile frames in clause 21.4.2.2of the concrete design code. In practice, since the ductile moment resisting frame (DMRF) design procedure is followed, the force modification factor, R in the seismic base shear formula (equation 2.1) can be taken equal to 4.0. As a result, NBCC 1990 allows these DMRF to be designed using half the seismic loads as those on the NDMRFs. However, for comparison purposes in the present study the design seismic base shear will be taken the same as that used in designing 6SND and 6-ND. Two frames will be designed. Frame 6SD will have the same member dimensions as 6SPM while frame 6-D will have the same member dimensions as 6-PM. The letter D in the frame designation stands for ductile frames. It is recognized that the 6SD and the 6-D frames are in fact overdesigned frames. They are included in this study to provide an upper bound reference for nominally ductile frame design.

The procedures for designing the beams for flexure are identical to those of nominally ductile frames. However, the column design and the beam shear design procedures are different from those used in nominally ductile frame design as will be explained in sections 2.4.1 and 2.4.2.

2.4.1 COLUMN DESIGN FOR FLEXURE

After the flexural reinforcing steel for the beams is obtained, the nominal moment resistance of the beams can be calculated. At any joint the column design moments are obtained such that

$$\sum M_{rc} \geq 1.1 \sum M_{nb} \tag{2.18}$$

where

ΣM_{nb} = sum of the nominal moment resistance of the beams framing into the joint ($\phi_c = \phi_s = 1.0$)

ΣM_{rc} = sum of the factored moment resistance of the columns framing into the joint

ΣM_{rc} can be distributed to the columns above and below the joint according to their relative stiffness to obtain the column design moments. The design axial forces are obtained directly from elastic static analysis and the columns are designed for the different combinations of moments and axial forces.

2.4.2 BEAM SHEAR DESIGN

The factored design shear forces, V_f, are obtained based on the probable strength of the plastic hinges at the beam ends in addition to the factored gravity loading. In this case V_f is found to be greater than the values calculated from the elastic static analysis. However, if V_c is considered reliable and used in the design, the same minimum stirrups as those in 6SND and 6-ND are also sufficient for beams in 6SD and 6-D.

2.4.3 COLUMN SHEAR DESIGN

The column design shear forces are obtained by assuming that the potential plastic hinges in the beams develop their probable strengths (Code clause 21.7.2.2). These design shears were found to be almost twice those obtained for the columns of 6SND and 6-ND. However, the columns still require only minimum ties due to the contribution of concrete to the column shear resistance. The ties provided for the columns of 6SD and 6-D are identical to those provided in 6SND and 6-ND.

2.4.4 FINAL DESIGN RESULTS

The reinforcement ratios of the two frames 6SD and 6-D are shown in figure (2.6). It should be mentioned here that the upper bound for the column reinforcement ratio ($\rho < 6$ %) was ignored in designing 6SD in order to be able to design a frame with strong columns-weak beams and the same member dimensions as 6SPM. The transverse reinforcement provided in the beams and columns of both frames are identical to those provided in 6SND and 6-ND.

2.5 COMPARISON OF THE FINAL DESIGN RESULTS OF THE DIFFERENT FRAMES

In this chapter a total of six frames are considered. Three frames had 400x400 mm exterior columns and 450x450 mm interior columns. The three other frames had 500x500 mm exterior and interior columns. The frames with the larger columns were considered to be a improvement to the frames of the smaller columns. The frames

with smaller columns were denoted 6SND for the frame designed to meet minimum code requirements for nominally ductile frames, 6SPM for the frame designed by Paultre and Mitchell and 6SD for the frame designed to meet strong column-weak beam requirements of code clause 21.4.2.2.The frames with larger columns were denoted 6-ND, 6-PM and 6-D for the frame designed to meet minimum code requirements for nominally ductile frames, for the frame designed by Paultre and Mitchell and for the frame designed to meet strong column-weak beam requirements respectively. The frames considered here cover a wide range of frames that are designed using an R factor equal to 2.0 in the seismic base shear formula and satisfy the Code requirements.

The reinforcement ratios in the beams and columns of 6SPM and 6-PM are significantly larger than those of 6SND and 6-ND respectively. It appears therefore that the frames reported by Paultre and Mitchell (1991) have been overdesigned**. The columns of 6SD and 6-D include more steel than those of the ND and PM frames as a result of the strong column-weak beam requirement employed in their design. However, the reinforcement ratios in the columns of 6-D are not significantly larger than those in 6-PM. Thus, in terms of reinforcement ratios, the large columns frame designed by Paultre and Mitchell is not much different from the ductile frame design.

** See Appendix A

2.6 LATERAL STRENGTH OF THE FRAMES

To evaluate the lateral strengths of the frames, they were analyzed under a montonically increasing static loading. A modified version of DRAIN-2D was used in the incremental static analysis (Zhu, 1989). The static loads were distributed over the frame height according to the distribution formula of NBCC 1990 (equations 2.5 and 2.6). The results of the incremental static analysis will be discussed in two parts, the first for the small column frames and the second for the large column frames.

2.6.1 SMALL COLUMN FRAMES

Figure (2.7) shows the base shear-top displacement curves of the frames 6SND, 6SPM and 6SD. The ultimate strength of the frames was determined at a displacement equal to R/0.6 = 3.3 times the displacement at code level loading. The overstrength factors, ϕ_o, (ultimate strength/code base shear) are also shown in figure (2.7). As expected, the three frames have the same initial stiffness but their post yielding behaviour differs from one to the other. The overstrength factor of 6SD is much larger than that of 6SND and 6SPM. However, frame 6SPM is still 20 percent stronger than 6SND. Nevertheless, Paultre and Mitchell still considered the behaviour of 6SPM undesirable because of the large drift experienced under dynamic loading. The seismic performance of the 6SND frame is likely to be less satisfactory than the 6SPM frame.

The inelastic static analysis has also provided an estimation of the overall yield displacements, δ_y, of the frames. These values of δ_y will be used to calculate the

global ductility demands of the frame under earthquake excitations. The overall yield displacement is estimated as the roof displacement value at the intersection of the elastic and inelastic branches of the load displacement-curves. Table (2.2) gives the values of the global yield displacement, δ_y, for the three small column frames.

Figure (2.8) shows the sequence of plastic hinge formation in the three frames. Both 6SND and 6SPM have formed a storey side-sway mechanism at the first floor quite early in the loading process. Frame 6SD did not form a storey side-sway mechanism despite the occurrence of some plastic hinges in the interior columns. The loads at which the first column and beam hinges formed for each of the frames are shown in the figure. The first hinge occurs in a column for all three frames.

2.6.2 LARGE COLUMN FRAMES

Figure (2.9) shows the base shear-top displacement curves of 6-ND, 6-PM and 6-D. The 6-PM frame is much stronger than 6-ND. In fact, the post-yielding responses of 6-PM and 6-D are similar. In view of the similarity between the 6-PM and 6-D force-displacement curves, it is not surprising that the 6-PM frame behaves well under strong seismic shaking as reported by Paultre and Mitchell.

Figure (2.10) shows the sequence of plastic hinge formation in the three frames, 6-ND, 6-PM and 6-D. Only 6-ND formed a storey side sway mechanism. Frame 6-PM formed hinges in the different columns but a storey side-sway mechanism was prevented due to the stronger columns. Frame 6-D formed an almost ideal beam side-sway mechanism. The base shear which corresponds to formation of

the first beam and column hinges is shown in the same figure. The yield displacements of the three large columns-frames were determined from the force-displacement curves and are given in table (2.3).

2.6.3 OVERVIEW OF THE STATIC BEHAVIOUR OF FRAMES

Under montonically increasing static loading, hinges will form eventually at both the beams and columns of the frames. In all except the 6-D frame, column hinging occurs before beam hinging. Of more importance in evaluating the seismic performance is the potential of forming a storey side-sway mechanism. Such a mechanism is formed in frames 6SND, 6-ND and 6SPM. Formation of such a mechanism usually implies large storey drifts at the mechanism level, causing extensive and sometimes non-repairable damage. On the other hand, no such storey side-sway mechanism is formed in frames 6-PM, 6SD and 6-D. It is not surprising that the storey side-sway mechanism does not form in frames 6SD and 6-D since these frames are designed based on the strong column-weak beam concept. Although, the 6-PM frame was not designed strictly according to the strong column-weak beam requirement, the columns of this frame were deliberately overdesigned. The end result is that it behaves similar to the 6-D frame.

The following observations can be made based on the lateral behaviour of the six frames : 1) Frames that adhere to the minimum Code requirements for NDMRF design exhibit a storey side-sway mechanism in the post-elastic range (e.g. 6SND, 6-ND), 2) storey side-sway mechanism does not form in frames designed using the

strong column-weak beam requirement of the Code (6SD, 6-D). 3) Frames that follow the NDMRF design procedure, but having their columns somewhat strengthened, may (6SPM) and may not (6-PM) exhibit the storey side-sway mechanism.

2.7 DYNAMIC ANALYSIS PROCEDURES

The inelastic dynamic analysis of the frames was performed using the DRAIN-2D computer program (Kanaan and Powell, 1973). The gravity loads (dead + 50 % live) were applied to the frames prior to the earthquake loading. This section summarizes the important aspects of the non-linear dynamic analysis performed in this study. The section begins with a description of the basic assumptions used in the analysis. The solution procedures and the evaluation of the dynamic matrices are then explained followed by a description of the hysteretic models available in DRAIN-2D. The section closes with a description of the response parameters used to evaluate the dynamic response.

2.7.1 BASIC ASSUMPTIONS

The following basic assumptions are made in order to simplify the analysis of the buildings considered in this study;

1) Coupling between different parallel frames through the floor system is neglected. Therefore, it is assumed that the response of a typical interior E-W frame is representative of the response of the whole building in the E-W direction.

2) Only planar response of the frames in the E-W direction is considered. No vertical ground motion components are applied to the frames. The frames are assumed to be totally fixed at their supports and all supports are assumed to move in phase.

3) The floor diaphragms are assumed to be infinitely rigid in their own plane. Thus, the nodes of each storey level are constrained to have the same horizontal displacement.

4) The masses are assumed to be lumped at the floor levels. The storey masses are assumed to have lateral inertia only and the vertical and rotational inertia effects are neglected.

5) Only small deformations are considered and equilibrium is based on the initial configuration of the frame.

6) It is assumed that the beam column joints are designed such that no yielding will occur in the joints. In the dynamic analysis, the joints are treated as rigid elements.

2.7.2 EQUATIONS OF MOTION AND SOLUTION PROCEDURE

The dynamic incremental equations of equilibrium for a structural system responding non-linearly to earthquake excitation can be written for a finite time step, Δt, as :

$$M\Delta\ddot{u} + C\Delta\dot{u} + K_T\Delta u = -M\Delta\ddot{u}_g \qquad (2.19)$$

where

Δu = finite increment of displacement.
$\Delta \dot{u}$ = finite increment of velocity.
$\Delta \ddot{u}$ = finite increment of acceleration.
$\Delta \ddot{u}_g$ = finite increment of ground acceleration.
M = Mass matrix.
C = Damping matrix.
K_T = Stiffness matrix of the structure in its current state.

The Newmark-beta method (Newmark, 1962) with beta= 1/4 is used for the numerical integration of the equations of motion. In this method, the acceleration is assumed to be constant over a user specified time step, Δt. This method was found to be unstable for systems responding non-linearly if a relatively large time step is used (Adeli et al., 1978). Therefore, a time step equal to approximately one tenth of the smallest natural period of the analyzed structures was used to avoid the problem of numerical divergence of the solution.

In the numerical integration, the tangent stiffness matrix at the beginning of the time step is assumed to be constant during the time step. Out-of-balance forces resulting from any changes in stiffness during the time step are added to the load vector in the subsequent time step.

2.7.3 DYNAMIC MATRICES

This section describes the evaluation of the mass matrix, the damping matrix and the instantaneous stiffness matrix. The assumptions made in the evaluation are clearly defined and justified.

2.7.3.1 Mass Matrix

In a real structure, the mass is distributed over all the structural elements. For analysis purposes, it is customary to assume that the mass is concentrated in the floor slabs. In this study vertical and rotational inertia forces are ignored and only lateral (horizontal) inertia forces are considered. Assuming rigid floor diaphragm, all the nodes at a floor level are constrained to have the same lateral displacement. Therefore, the mass matrix is reduced to the following diagonal matrix with zero off-diagonal terms.

$$M = \begin{bmatrix} m_1 & 0 & 0 & . & . \\ 0 & m_2 & 0 & . & . \\ . & & . & & \\ . & & & . & 0 \\ . & . & & 0 & m_N \end{bmatrix} \qquad (2.20)$$

where
m_i = lumped mass at the i^{th} floor level.
N = Total number of storeys in the building.

2.7.3.2 Damping Matrix

The viscous damping matrix is assumed to be of the Rayleigh type, i.e., can be presented by a linear combination of the mass and stiffness matrices as follows;

$$C = a_1 M + a_2 K_T \qquad (2.21)$$

where a_1 and a_2 are proportionality factors which can be determined from the modal damping ratios of any two modes using the following equations;

$$a_1 = \frac{4\pi(T_m\xi_m - T_n\xi_n)}{T_m^2 - T_n^2} \tag{2.22a}$$

$$a_2 = \frac{T_m T_n(T_m\xi_n - T_n\xi_m)}{\pi(T_m^2 - T_n^2)} \tag{2.22b}$$

where
T_m, T_n = undamped period of the m^{th} and n^{th} modes.
ξ_m, ξ_n = damping ratio of the m^{th} and n^{th} modes.

For this study, the first and second modes are used to determine the proportionality factors a_1 and a_2. The damping ratios for these two modes are assumed as 5 percent of critical. This value is considered to be appropriate for cracked reinforced concrete structures (Newmark and Hall, 1982).

Since stiffness dependent damping is assumed, the damping matrix may change suddenly between time steps due to the change in the yield state of the structural elements. This introduces equilibrium unbalance at the beginning of the new time step. In DRAIN-2D, this unbalance is eliminated by applying corrective forces equal and opposite to the change in the damping forces as follows;

$$\Delta F_c = -a_2 \Delta K \dot{u} \tag{2.23}$$

where
ΔF_c = corrective force.
ΔK = change in the tangent stiffness matrix during Δt.
$\dot{u}$ = velocity at the beginning of the new time step.

2.7.3.3 Tangent Stiffness Matrix

The structure stiffness matrix is assembled from the stiffness matrices of the different elements. The element degrees of freedom are related to the global degrees of freedom such that the element stiffness matrices will be placed in their appropriate position in the global stiffness matrix. Two different types of elements are used in this study, the dual component element and the single component element. The following sections describe the calculation of the stiffness matrices of the two elements.

i) Dual component element

This element was used to model the columns of the frames analyzed in this study. The element possesses both flexural and axial stiffness. Effects of variable cross section, shear deformations and rigid links can be taken into account.

The element is idealized as an elastic member acting in parallel with an elasto-plastic element as shown in figure (2.11)(Clough et al., 1965). Yielding may take place only in concentrated plastic hinges at the ends of the elasto-plastic component. The hinges in the elasto-plastic component yield under constant moment while the moment in the elastic component may continue to increase, thus simulating strain hardening effect.

To determine if yield occurs in the element, an idealized axial load-moment interaction diagram is used (figure (2.12)). For each column section, the interaction diagram is constructed using the nominal material properties. During yielding, internal forces are constrained to remain on the interaction curve. Yielding is assumed to only affect the flexural stiffness of the element while the axial stiffness remains unchanged. Because of the formulation of the element, only bilinear hysteretic response can be reproduced.

ii) <u>Single component element</u>

This element possesses both flexural and axial stiffness. Shear deformations and effects of eccentric connections and varying cross section can be taken into account.

The element consists of an elastic beam element in series with two inelastic springs at its ends as shown in figure (2.13). The flexibility matrix of the element is formed by adding the flexibility matrix of the elastic beam element to the current flexibilities of the rotational springs as follows;

$$f = \begin{bmatrix} f_{ii}+\frac{1}{k_i} & f_{ij} \\ f_{ji} & f_{jj}+\frac{1}{k_j} \end{bmatrix} \qquad (2.24)$$

where
$f_{ii}, f_{ij}, f_{ji}, f_{jj}$ = flexibility influence coefficients.
k_i, k_j = stiffness of the non-linear flexural springs at ends i and j.

The resulting flexibility matrix is then inverted to the current element stiffness matrix k_T. Before yielding the springs are assumed to be infinitely rigid, thus not affecting the element stiffness matrix. No interaction between axial load and moment is considered in determining yielding, which can only take place at the element ends. All plastic deformations are introduced by means of the moment-rotation relationships of the inelastic springs whose yield moment is based on the nominal material properties. The single component element can adopt any shape of the moment rotation hysteretic models.

iii) Geometric stiffness

The axial forces in the columns result in secondary moments which may increase the inelastic deformations. In this study, the following linear approximation of the geometric stiffness is used (Wilson and Habibullah, 1987).

$$K_G = \frac{P}{H}\begin{bmatrix} 1 & -1 \\ -1 & 1 \end{bmatrix} \tag{2.25}$$

where
K_G = geometric stiffness matrix.
P = axial load in the column.
H = column height.

The geometric stiffness matrix is expanded into a 6x6 matrix by adding zero-rows and columns and then subtracted from the element stiffness matrix to determine the element stiffness including geometric stiffness effects.

2.7.4 HYSTERETIC MODELS IN DRAIN-2D

In the original version of DRAIN-2D, two hysteresis models are available, the bilinear model and the stiffness degrading model. The bilinear hysteretic model is used in the column elements which are idealized by the dual component elements. The virgin curve is bilinear and no stiffness or strength degradation are simulated. The stiffness degrading hysteretic model is used for the plastic hinges at the ends of the single component element described in section 2.7.3.3(ii).The hysteresis model used in DRAIN-2D is a modified version of the Takeda model (1970). The main rules governing the behaviour are explained by Powell (1975). The general moment-rotation relationship of this model is shown in figure (2.14). In this study, the stiffness degrading model will be used to model the beams of the analyzed frames.

2.7.5 DESCRIPTION OF THE DYNAMIC RESPONSE PARAMETERS

In order to be able to estimate the amount of damage a structure will sustain during seismic response, several response parameters need to be defined. Some parameters are related to the overall response of the structure, while others are associated with the localized member responses. In this study, both types of response parameters will be used to compare the seismic response of the different frames.

2.7.5.1 Overall Displacements, Ductility Demands and Drift Indices

The maximum displacement at each storey level is recorded and plotted to form the envelope of lateral displacements. The global displacement ductility is calculated as

$$\mu_\delta = \frac{\delta_{max}}{\delta_y} \qquad (2.26)$$

where δ_{max} is the maximum roof displacement and δ_y is the roof displacement at general yielding of the frame obtained from an inelastic static analysis of the frame under monotonically increasing loading as discussed in section 2.6. The drift index is defined as the ratio of the maximum interstorey drift to the storey height. This ratio is a good measure of the damage potential to the non-structural elements such as windows and partitions.

2.7.5.2 Member Ductility Demands

The curvature ductility demands are used to represent the inelastic deformations in the beams and columns of the frames analyzed in this study. The advantage of using curvature ductility over rotational ductility is that the calculation of curvature ductility does not require the assumption that the member is bent in double curvature as the case of rotational ductility. The curvature ductility, μ_ϕ, is defined as the ratio of maximum curvature, ϕ_{max}, to the yield curvature ϕ_y.

$$\mu_\phi = \frac{\phi_{max}}{\phi_y} \qquad (2.27)$$

For a bi-linear moment-curvature relationship, the curvature ductility is obtained by

$$\mu_\phi = 1 + \frac{M_{max} - M_y}{pM_y} \tag{2.28}$$

where
M_y, M_{max} = the yield and maximum moment of the section
p = ratio of the strain hardening stiffness to the initial elastic stiffness

It should be noted that equation (2.28) is only valid for beams where the axial force has a negligible effect on the yield moment of the beam. For columns two values of μ_ϕ may be considered. One value, μ_ϕ^t, is associated with the yield moment, M_y^t which corresponds to the axial force in the column, P^t, at the time instant at which M_{max} occurs. The other value, μ_ϕ^g, is associated with the yield moment, M_y^g, which corresponds to the axial force caused by gravity loads, P^g. In this study, μ_ϕ^t is used to represent the curvature ductility demands in the columns.

$$\mu_\phi^t = 1 + \frac{M_{max} - M_y^t}{pM_y^t} \tag{2.29}$$

2.7.5.3 Beam and Column Shear Demands

The maximum shear forces attained in the beams and columns during the response are recorded and plotted to form the envelope of shear demands. The resulting shear demand envelopes are compared to the member shear capacity as calculated from the member section to evaluate the potential for shear failure in the beams and columns.

2.7.6 GROUND MOTION INPUT

To avoid dependence on the characteristics of a single record, a total of fifteen earthquake records are used as the ground motion input for this study. All the chosen records were in the high a/v (peak ground acceleration-to-velocity ratio) range (> 1.2 g/m/s) to reflect the seismic zoning at Montreal ($Z_a > Z_v$). Table (2.4) gives a complete description of the fifteen records. For the analysis reported in this chapter, all the records were normalized to the design zonal velocity of the Montreal region which is equal to 0.097 m/s. According to the National Building Code of Canada (1990), this velocity value has a 10 percent probability of exceedance in 50 years. Figure (2.15) shows a comparison between the mean and mean plus one standard deviation (mean+σ) response spectra of the fifteen ground motion records and the elastic design spectrum (NBCC 1990). Also shown on the same figure is the inelastic design spectrum calculated by implementing the factors R and U in the elastic design spectrum (NBCC 1990). The dynamic analysis results discussed in this study are based on a statistical analysis of the individual frame responses to each record.

2.8 COMPARISON OF THE DYNAMIC RESPONSES OF THE DIFFERENT FRAMES

The first three natural periods of the 6Sxx frames are 1.26, 0.42 and 0.23 seconds while those of the 6-xx frames are 1.22, 0.40 and 0.22 seconds. The first

natural periods of these frames are marked in figure (2.15) to indicate the appropriate level of actual excitation as far as these frames are concerned.

The responses of the different frames are compared to arrive at a better understanding of the performance of nominally ductile frames. The response parameters used in the comparison are the overall displacements, drift indices and ductility demands of the frames plus the member ductility and shear demands.

2.8.1 OVERALL DISPLACEMENTS, DRIFT INDICES AND DUCTILITY DEMANDS

Figure (2.16) shows the envelopes of mean lateral displacements and mean drift indices for the three frames 6SND, 6SPM and 6SD. As expected, the 6SND frame has larger responses than the 6SPM frame, which in turn has larger responses than the 6SD frame. The displacements of 6SPM are 25 percent smaller than those of 6SND. This is due to the column overdesign in 6SPM which resulted in a larger overstrength of the whole frame. Paultre and Mitchell (1991) considered the performance of 6SPM to be unacceptable based on the large drift values of 0.7 percent. The global ductility demands of the three frames are given in table 2.5.The global ductility demand of the 6SND frame is in the order of 2.0 which is in the expected range. The drift index for the 6SND frame is in the order of 1.0 % which is excessive.

Figure (2.17) shows the mean lateral displacements and mean drift indices for 6-ND, 6-PM and 6-D. The displacements and drift indices of 6-PM are very close to

those of 6-D. This confirms that the performance of 6-PM is very similar to that of 6-D as indicated from the inelastic static analysis. Both the 6-PM and the 6-D frames have 30 percent less deformations than 6-ND which was designed to minimum code requirements. The drift index of 6-ND is reduced from the corresponding small column frame 6SND to a value of 0.7 percent. However, this value can still be considered excessive. The overall ductility demands of the three frames are given in table 2.6. The 6-PM frame behaves almost elastically under the design level earthquake.

Comparing figures (2.16) and (2.17), it can be seen that the frames with larger column sizes have a 25 percent decrease in deformations. This improvement is due to the increase in the overall stiffness of the frame. However, this does not reflect an equal improvement in the overall ductility demands as shown by tables 2.5 and 2.6. The reason is that the overall yield displacement also decreases with the increase of the column sizes resulting that the ductility demand (maximum deformation/yield displacement) does not change significantly.

2.8.2 MEMBER DUCTILITY DEMANDS

The mean and mean+σ ductility demands in the beams of the small column frames are depicted in figure (2.18) while figure (2.19) shows the mean and mean+σ column ductility demands for the same three frames. The ductility demands in the beams and columns of 6SND are much larger than those in the members of 6SPM and 6SD. For example, the mean and mean plus one standard deviation beam

ductility at the first floor of 6SND reach values of 3.0 and 4.0 respectively. It is questionable that under such high values of ductility demand, the shear capacity provided by concrete, V_c, can be relied upon to resist the shear demands on those beams. Another concern is the curvature ductility demands at the base of the first storey columns. It is doubtful that the detailing requirements of nominally ductile frames can promote such ductile behaviour.

The lower ductility demand in the members of 6SPM or 6SD is due to the fact that the columns of 6SPM and 6SD were provided with more reinforcement than what was required from the elastic loading combinations resulting in a large overstrength for the whole frame.

Figure (2.20) shows the mean and mean+σ ductility demands in the beams of 6-ND, 6-PM and 6-D while the mean and mean+σ column ductility demands are depicted in figure (2.21). The ductility demands in the beams and columns of 6-PM and 6-D are in the order of 1.0 due to the large overstrength possessed by these two frames as indicated from the inelastic static analysis. The ductility demands in the beams of 6-ND are in the order of 2.5 to 3.0. Although these values are approximately 25 percent smaller than those attained in the beams of 6SND, they are still large and extensive cracking can be anticipated. The column ductility demands in 6-ND are also 25 percent smaller than those in 6SND. However, they may still be excessive for the level of detailing required for NDMRFs.

2.8.3 BEAM SHEAR DEMANDS vs BEAM SHEAR CAPACITY

As discussed earlier, the beam shear capacity in nominally ductile frames is calculated as the sum of the concrete shear resistance and the stirrups resistance. The concrete shear resistance can be relied upon only if the beam ductility demands are small so that cracking is not extensive. The inelastic dynamic analysis of the frames designed to meet the minimum code requirements has shown that the beams undergo ductility demands in the order of 3 or 4. In such a case, the concrete shear resistance would diminish rapidly and the shear capacity would be composed only of the resistance of the minimum stirrups. Figures (2.22) and (2.23) show a comparison between the beam shear demands, the factored design shears and the capacity of the minimum stirrups in the beams of the small columns and large columns frames respectively. The shear demands exceed the factored shears by 30 percent. However, the resistance of the minimum stirrups exceeded the demand shears in all cases. Therefore, the requirement of $(V_s)_{min}$ from the Code would prevent shear failure, even if the concrete shear resistance were non existent and the shear demand exceeds the factored design shears for this set of six storey frames.

2.8.4 COLUMN SHEAR DEMANDS vs COLUMN SHEAR CAPACITY

Figures (2.24) to (2.27) show a comparison between the column shear demands, the factored design shears and the column shear capacities for the six storey frames considered here. The column shear capacities are determined using the Code equations and the tie spacing for the central portion of the column. In

determining the column shear capacity, the column axial forces corresponding to 85 percent of the dead load are considered. The shear demands exceeded the design shears for all frames except for the 6SD and 6-D frames in which the design shears were calculated based on the probable strengths of the beams. However, for all frames the column shear capacities always exceeded the shear demands by a large margin. This would prevent column shear failures in these frames.

The large ductility demands on the columns of 6SND and 6-ND do not necessarily imply that the concrete contribution to column shear resistance is unreliable. The axial compression on the columns minimizes cracking and can maintain the concrete shear resistance even under such large ductility demands (Park and Paulay, 1975).

Comparing the shear in the columns of the large and small frames, it can be seen that the safety margin against shear failure (difference between shear capacity and shear demands) is larger in the case of the large column frames. This presents another advantage of increasing the column sizes.

2.9 DISCUSSIONS

Two sets of six storey frames are designed. One set of frames has smaller columns and are designated as 6SND, 6SPM and 6SD. The second set with larger columns are designated 6-ND, 6-PM and 6-D. All these frames met or exceeded the minimum Code requirements for nominally ductile moment resisting frames. These

frames were subjected to monotonically increasing static lateral loading, and also subjected to base motions as represented by a set of fifteen earthquake records.

Reviewing the seismic responses of the frames designed to meet minimum Code requirements for NDMRF shows two concerns that need to be addressed.

First, a shear failure may occur in some beams of such frames. Shown in figures (2.22) and (2.23) are the mean earthquake beam shear demands on frames 6SND and 6-ND. In both instances, the beam shear demand exceeds the factored design shear, V_f. However, shear failure does not occur in the beams of either frame because the minimum stirrup requirement specified by the Code for NDMRFs provides a shear resistance which exceeds the shear demand in these frames. However, $(V_s)_{min}$ does not depend on the size of the beam and therefore is insensitive to the bay sizes and/or loading on the NDMRF. It is conceivable that a building having different frame spacing and loadings will experience seismic beam shear demands that exceed $(V_s)_{min}$. Examination of the beam ductility demands of the 6SND and 6-ND frames (figures 2.18 and 2.20 respectively), show that they reach a value of 3 to 4. Subjected to this level of ductility demands, extensive cracking will occur and the concrete shear resistance can not be relied upon. It is under such circumstances that shear failure may occur in beams of NDMRFs designed to satisfy minimum Code requirements.

In chapter 3, a six storey NDMRF with 8.0 metre bay size is studied to show that it is not uncommon to find that seismic shear demand is larger than $(V_s)_{min}$. In

chapter 4, an experimental study is carried out to show that when a beam member is deformed to a ductility level of 3, extensive cracking did occur and the concrete shear resistance, V_c, decreased drastically. As a result, one expects the possibility of shear failure in the NDMRF considered in chapter 3.

The second concern is the large drift experienced by NDMRFs designed to minimum Code requirements. The drift of the 6SND frame is over 0.8 percent. This drift is reduced to 0.7 percent for increasing the column sizes as shown by the 6-ND frame. This is still a large drift and substantial nonstructural damage can be expected when drift reaches such large values. This large drift may be caused by the development of the storey side-sway mechanism during the dynamic response of these frames. Frames that do not exhibit the storey-side sway mechanism under static loading (frames 6SD, 6-PM and 6-D) all show drifts about half of those experienced by 6SND or 6-ND. In order to reduce the large drift, some modifications such as those carried out by Paultre and Mitchell are required. Unfortunately, no guideline was provided by Paultre and Mitchell to modify NDMRF design in general to achieve the level of performance shown by the 6-PM frame.

Finally, the seismic performance of the frames designed by Paultre and Mitchell was distinctly better than that of the frames designed to meet the minimum code requirements. In particular, the performance of the one frame designed by Paultre and Mitchell (6-PM) was similar to that of the frame designed for strong column-weak beam (6-D). In one sense, Paultre and Mitchell provided an excellent

design for a nominally ductile frame that gives desirable seismic responses. However, the frame designed by Paultre and Mitchell is not representative of typical nominally ductile frames since its members are overdesigned beyond the minimum Code requirements. Therefore, their conclusion on nominally ductile frames (Paultre and Mitchell, 1991) can be misleading as it can not be extended to all nominally ductile frames that satisfy the Canadian code provisions.

Table (2.1) Design Gravity Loads

	Dead	Live
Floors	Self weight of concrete Partition loads 1 kPa Mechanical services 0.5 kPa	Office bays 2.4 kPa Corridor bay 4.8 kPa
Roof	Self weight of concrete Roof insulation 0.5 kPa	Snow load 2.2 kPa Mechanical on central bay 1.6 kPa

Table (2.2) Yield displacements of the small column frames

Frame	6SND	6SPM	6SD
δ_y (mm)	89	108	129

Table (2.3) Yield displacements of the large column frames

Frame	6-ND	6-PM	6-D
δ_y (mm)	80	97	109

Table (2.4) List of the Earthquake Records used in this study

Earthquake	Date	Magn.	Site	Epic. Dist. (km)	Comp	Max Acc A(g)	Max Vel V(m/s)	A/V	Soil Cond
Parkfield California	June 27 1966	5.6	Temblor No. 2	7	N65W	0.269	0.145	1.86	Rock
Parkfield California	June 27 1966	5.6	Cholame, Shandon No. 5	5	N85E	0.434	0.255	1.70	Rock
San Francisco California	Mar. 22 1957	5.25	Golden Gate Park	11	S80E	0.105	0.046	2.28	Stiff Soil
San Francisco California	Mar. 22 1957	5.25	State Bldg., S.F.	17	S09E	0.085	0.051	1.67	Stiff Soil
Helena Montana	Oct. 31 1935	6.0	Carroll College	8	N00E	0.146	0.062	2.03	Rock
Lyttle Creek	Sep 12 1970	5.4	Wrightwood, California	15	S25W	0.198	0.096	2.06	Rock
Oroville California	Aug. 1 1975	5.7	Seismogr. Station Oroville	13	N53W	0.084	0.044	1.91	Rock
San Fernando California	Feb. 9 1971	6.4	Pacoima Dam	4	S74W	1.075	0.577	1.86	Rock
San Fernando California	Feb. 9 1971	6.4	Lake Hughes Station 4	26	S21W	0.146	0.085	1.72	Rock
Nahani, N.W.T., Canada	Dec 23 1985	6.9	Site 1, Iverson	7.5	LONG	1.101	0.462	2.38	Rock
Central Honshu Japan	Feb 26 1971	5.5	Yoneyama Bridge	27	TRAN	0.151	0.059	2.56	Stiff Soil
Near E. Coast of Honshu, Japan	May 11 1972	5.8	Kushiro Central Wharf	33	N00E	0.146	0.060	2.43	Stiff Soil
Honshu Japan	Apr. 5 1966	5.4	Hachinohe-A	4	N00E	0.270	0.111	2.43	Stiff Soil
Monte Negro Yugoslavia	Apr. 9 1979	5.4	Albatros Hotel Ulcinj	12.5	N00E	0.042	0.016	2.63	Rock
Bania Luka Yugoslavia	Aug. 13 1981	6.1	Seism. Station Banja Luka	8.5	N90W	0.074	0.032	2.31	Rock

Table (2.5) Global ductility demands in the small column frames

Frame	6SND	6SPM	6SD
Mean	1.87	1.26	0.93
Mean+σ	2.30	1.56	1.07

Table (2.6) Global ductility demands in the large column frames

Frame	6-ND	6-PM	6-D
Mean	1.68	1.12	0.90
Mean+σ	2.04	1.37	1.03

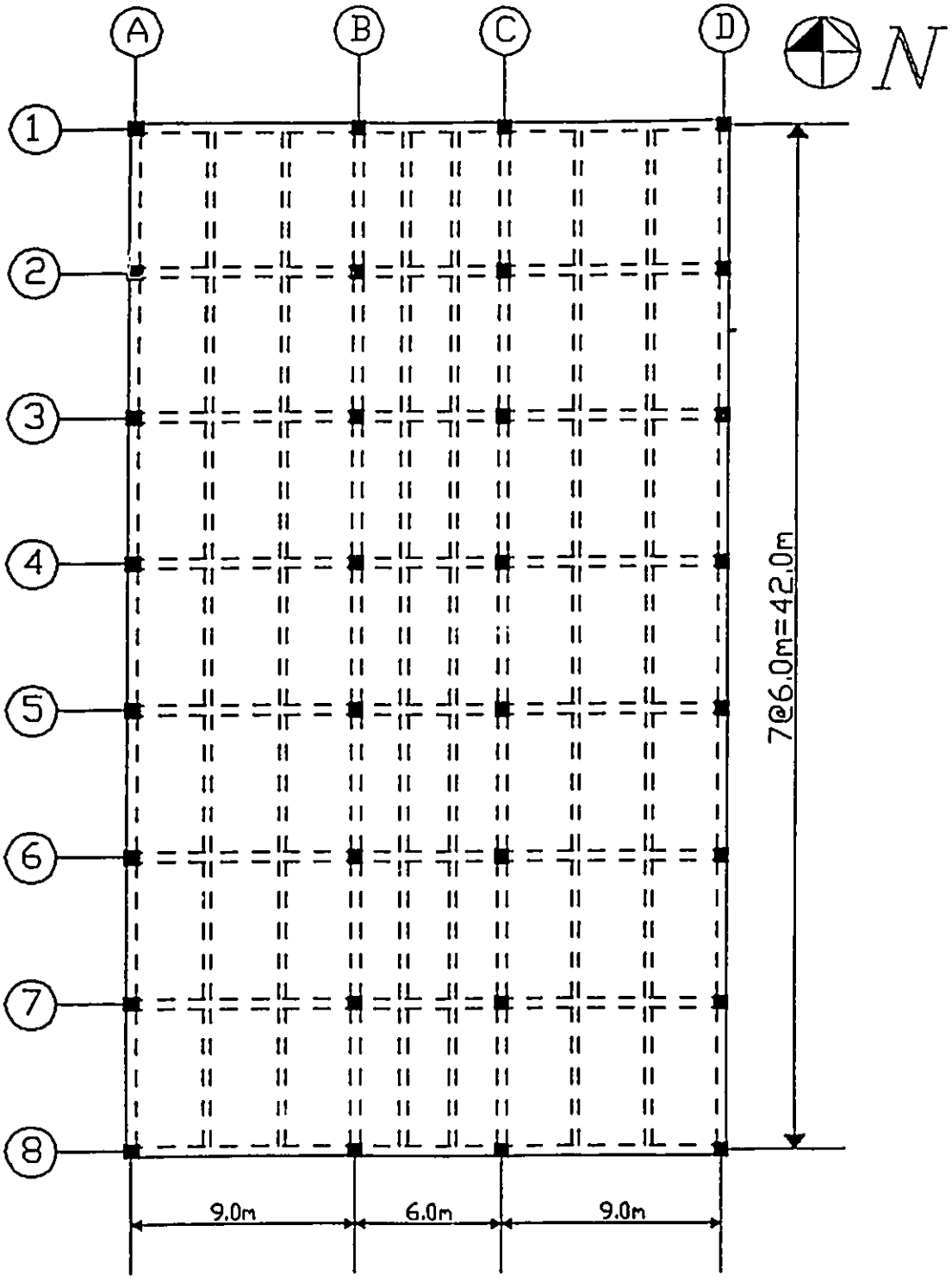

Fig. (2.1) Typical floor plan of the six storey building.

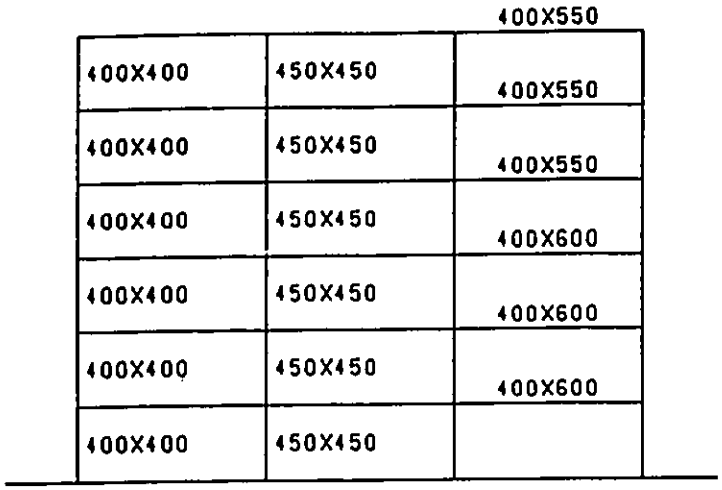

a) 6SPM

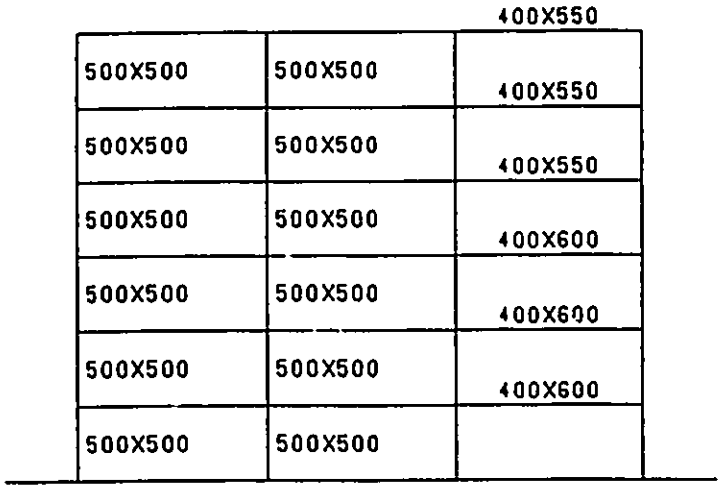

b) 6-PM

Fig. (2.2) Member dimensions of the six storey frames considered in chapter 2.

		1.450
1.900 1.900	1.900 1.900	0.550 1.450
1.900 1.900	1.900 1.900	0.550 1.450
1.900 1.900	1.900 1.900	0.550 1.670
2.400 2.400	3.000 3.000	0.500 1.670
2.400 2.400	3.000 3.000	0.500 1.670
3.000 3.000	3.400 3.400	0.500

a) 6SPM

		1.450
1.400 1.400	1.400 1.400	0.550 1.450
1.400 1.400	1.400 1.400	0.550 1.450
1.400 1.400	1.400 1.400	0.550 1.670
1.400 1.400	1.900 1.900	0.500 1.670
1.400 1.400	1.900 1.900	0.500 1.670
2.400 2.400	3.200 3.200	0.500

b) 6-PM

Fig. (2.3) Reinforcement ratios of the frames designed by Paultre and Mitchell (1991).

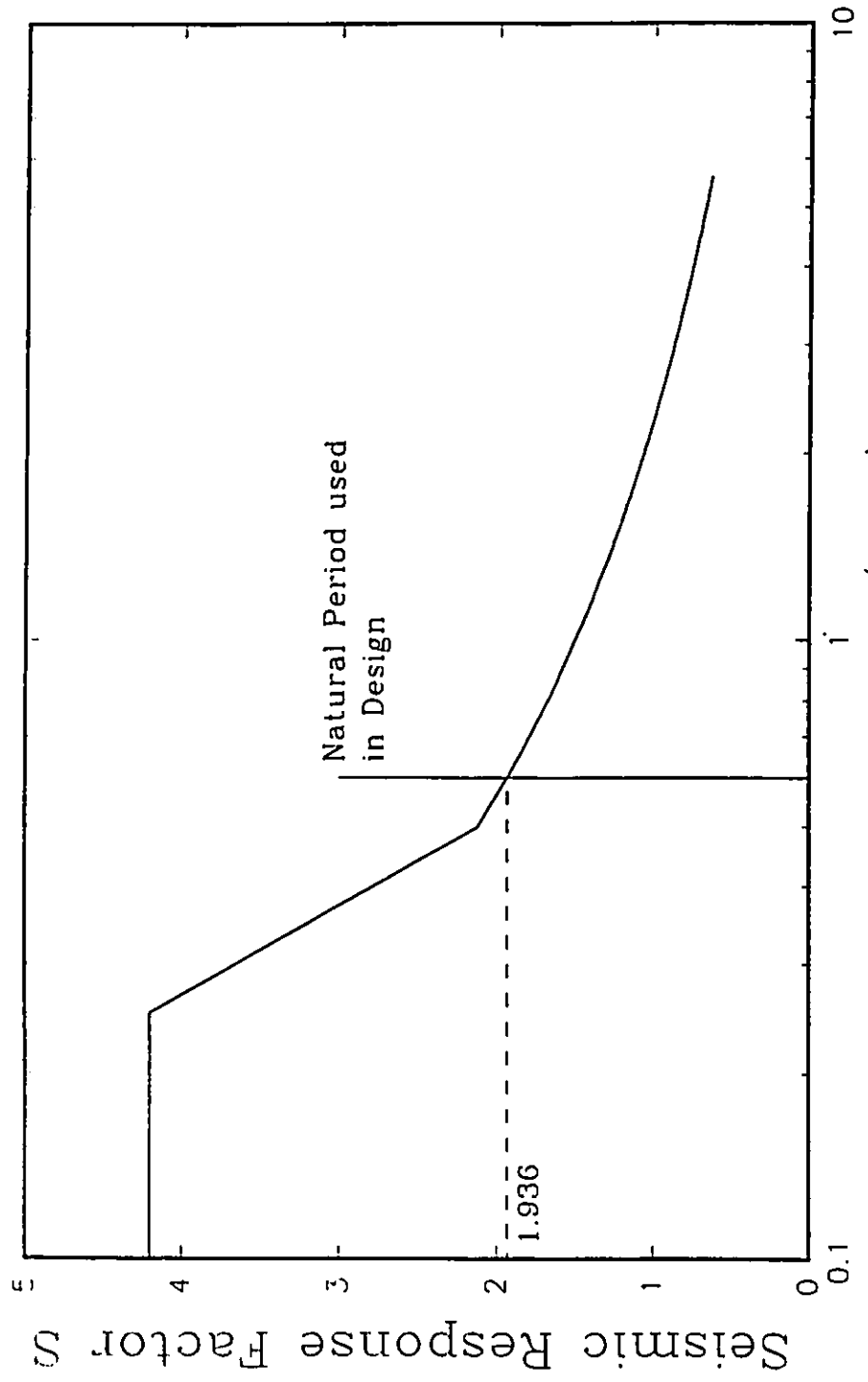

Fig. (2.4) Seismic response factor, S, in regions where $Z_a > Z_v$ (NBCC 1990).

		1.350
1.300 1.300	1.000 1.000	0.460 1.440
1.300 1.300	1.000 1.000	0.510 1.480
1.300 1.300	1.000 1.000	0.530 1.370
1.300 1.300	1.000 1.000	0.450 1.390
1.400 1.400	1.400 1.400	0.480 1.410
1.400 1.600	1.700 2.300	0.500

a) 6SND

		1.340
1.000 1.000	1.000 1.000	0.530 1.420
1.000 1.000	1.000 1.000	0.540 1.510
1.000 1.000	1.000 1.000	0.580 1.340
1.000 1.000	1.000 1.000	0.460 1.390
1.050 1.100	1.300 1.300	0.480 1.400
1.000 1.300	1.600 2.100	0.480

b) 6-ND

Fig. (2.5) Reinforcement ratios of the six storey frames designed to minimum code requirements.

		1.350
6.000	5.900	0.460
3.700	3.100	1.440
3.900	3.400	0.510
4.000	3.500	1.480
4.200	3.600	0.530
4.400	3.700	1.370
4.600	4.500	0.450
4.700	4.700	1.390
5.000	5.600	0.480
6.000	6.500	1.410
6.000	6.500	0.500
1.600	2.300	

a) 6SD

		1.340
2.600	3.000	0.530
1.700	2.100	1.420
1.700	2.100	0.540
1.800	2.300	1.510
1.800	2.300	0.580
1.800	2.600	1.340
1.800	2.600	0.460
1.900	3.000	1.390
1.900	3.000	0.480
2.000	3.700	1.400
2.000	3.700	0.480
1.300	2.100	

b) 6-D

Fig. (2.6) **Reinforcement ratios of the six storey frames designed to strong column-weak beam requirements.**

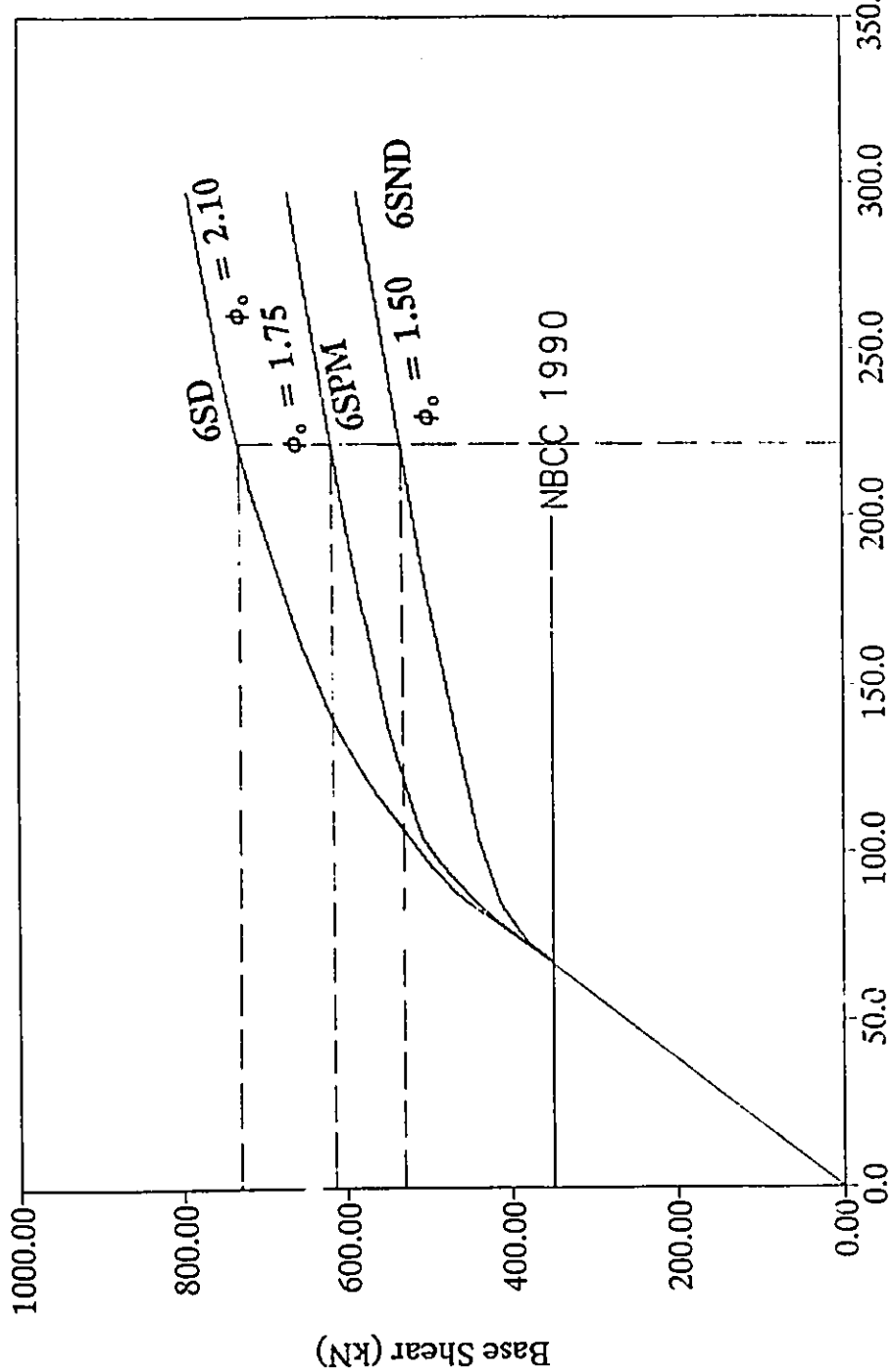

Fig. (2.7) Base shear-top displacement curves of the six storey frames with the small columns.

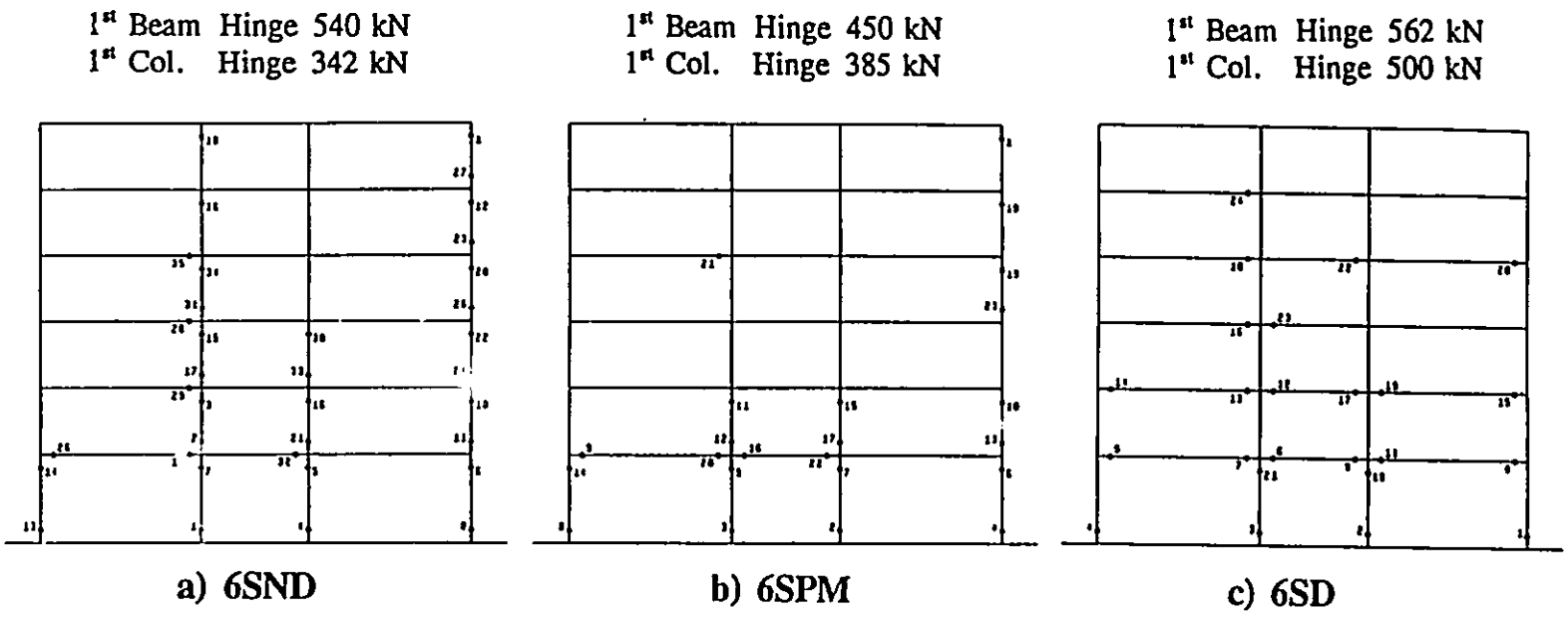

Fig. (2.8) Sequence of plastic hinge formation in the six storey frames with small columns.

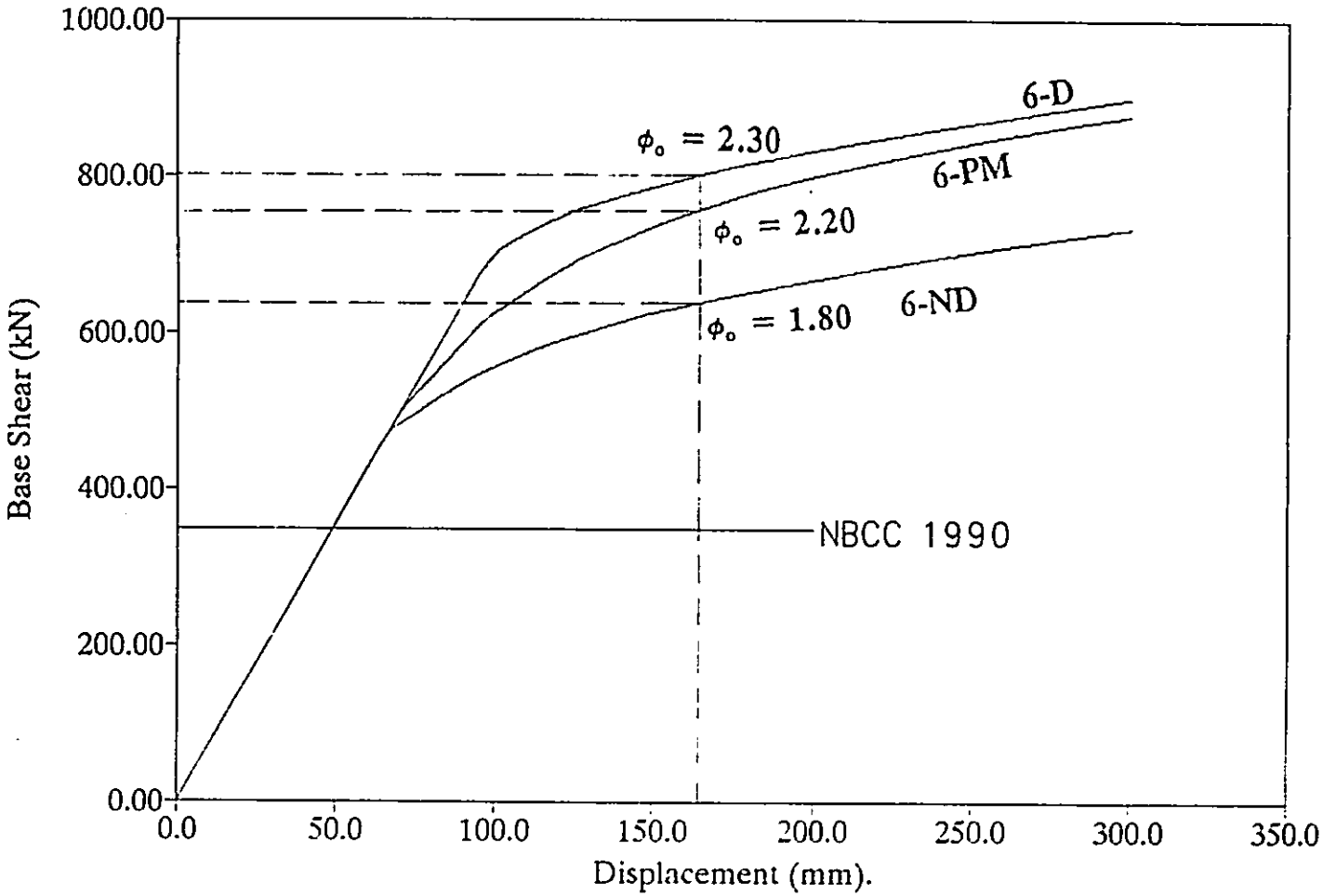

Fig. (2.9) Base shear-top displacement curves of the six storey frames with the large columns.

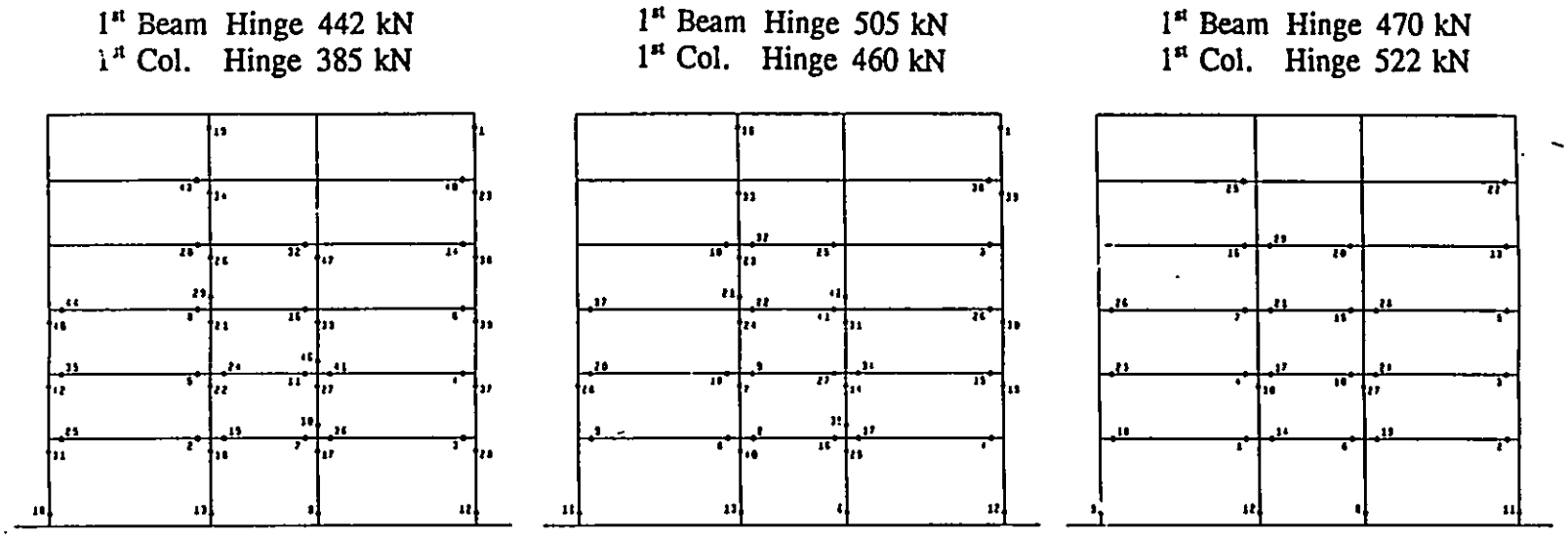

Fig. (2.10) Sequence of plastic hinge formation in the six storey frames with large columns.

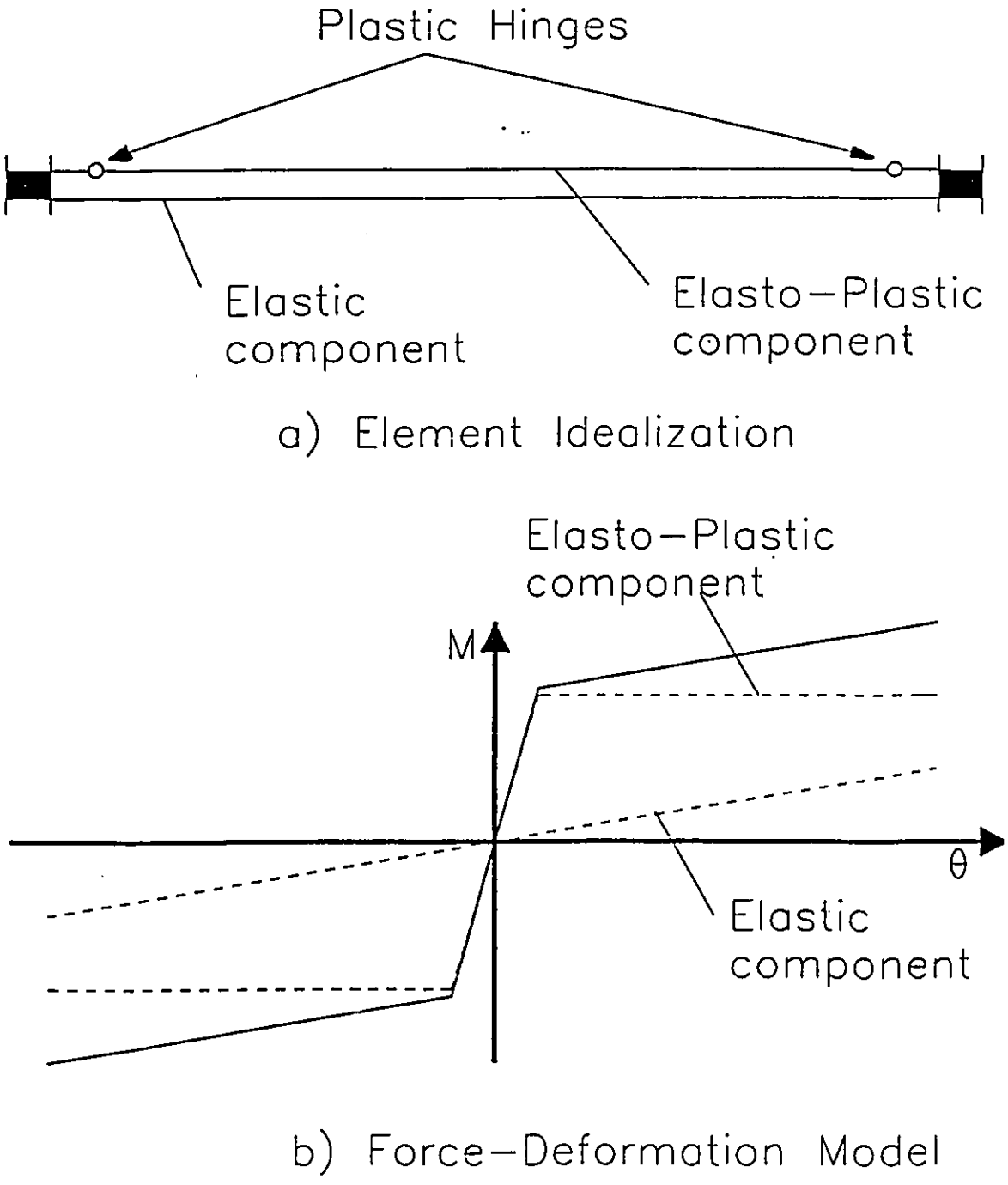

Fig. (2.11) Dual component element.

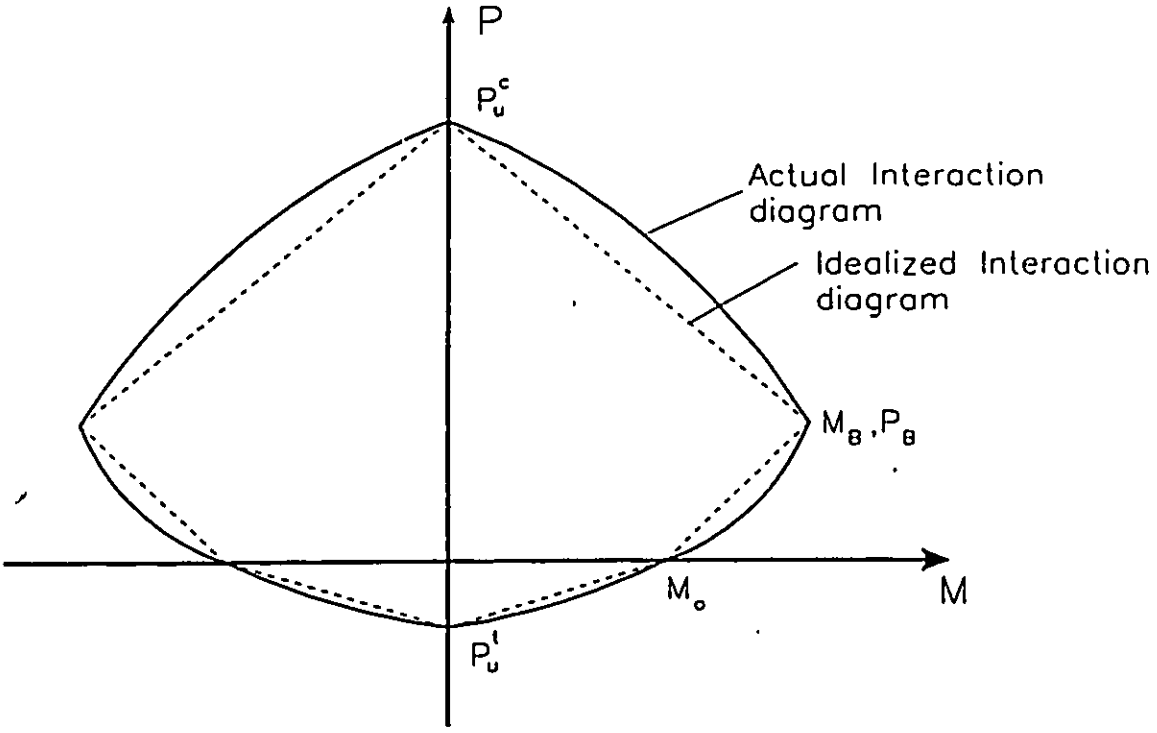

Fig. (2.12) Axial force-moment interaction diagrams for column elements.

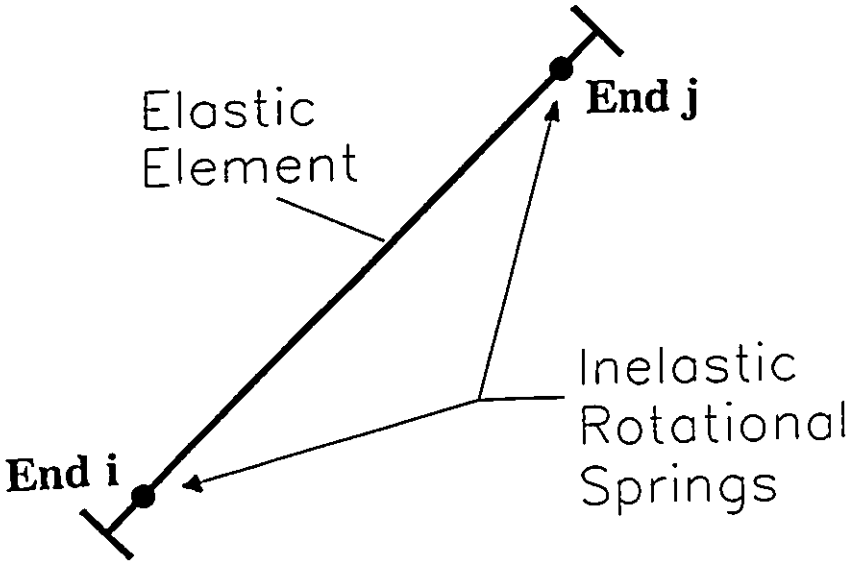

Fig. (2.13) Single component element.

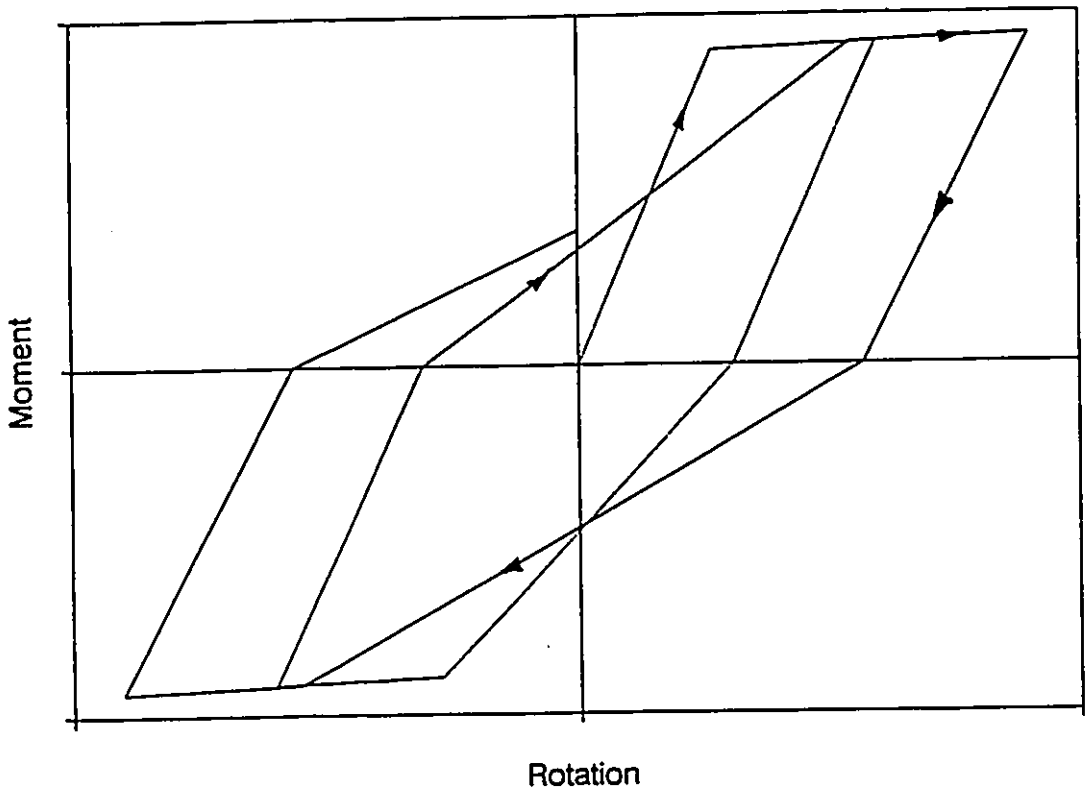

Fig. (2.14) Moment-rotation relationship of the modified Takeda (1971) model used in DRAIN-2D.

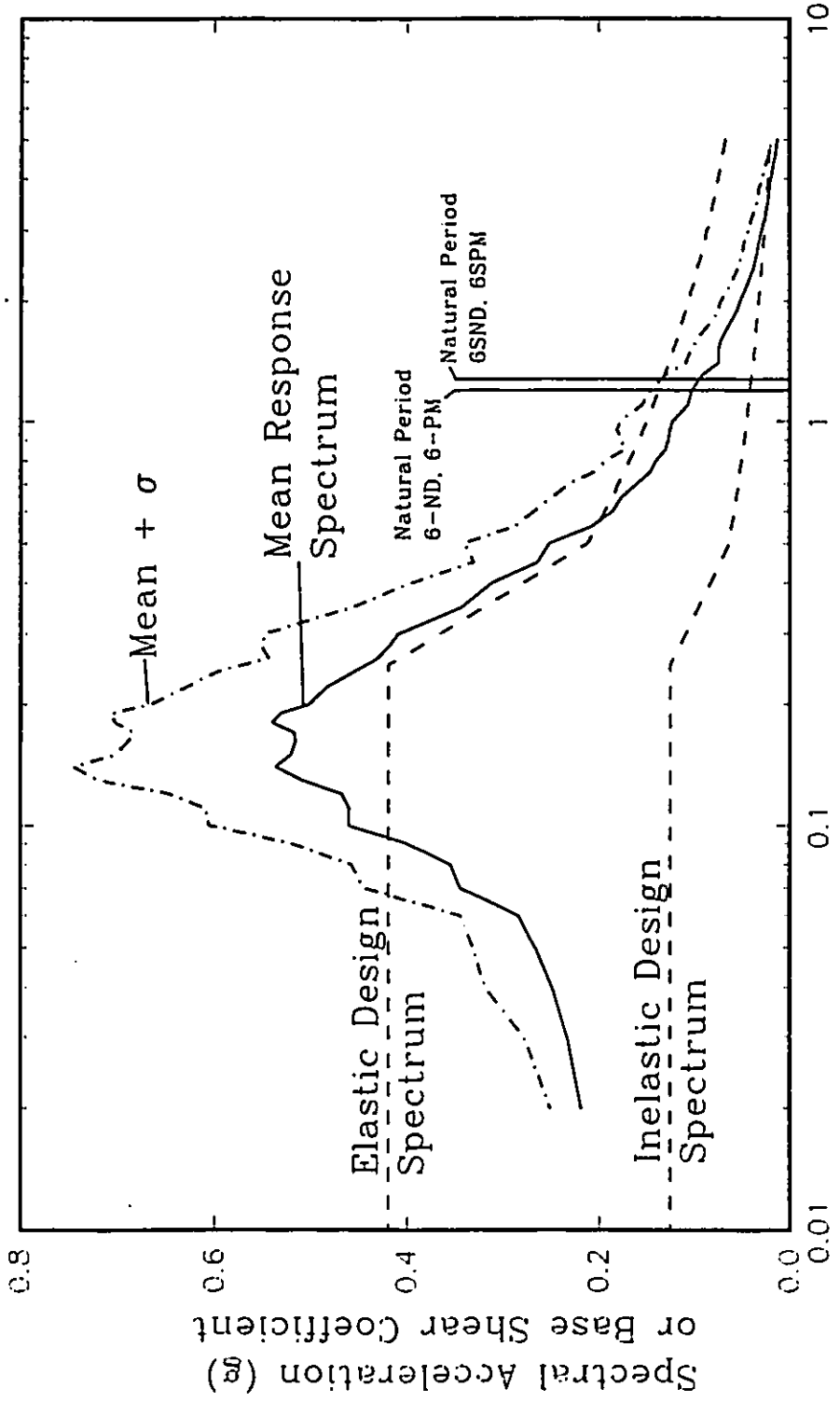

Fig. (2.15) Comparison between the design spectrum and the mean response spectrum of the ground motion records considered in this study.

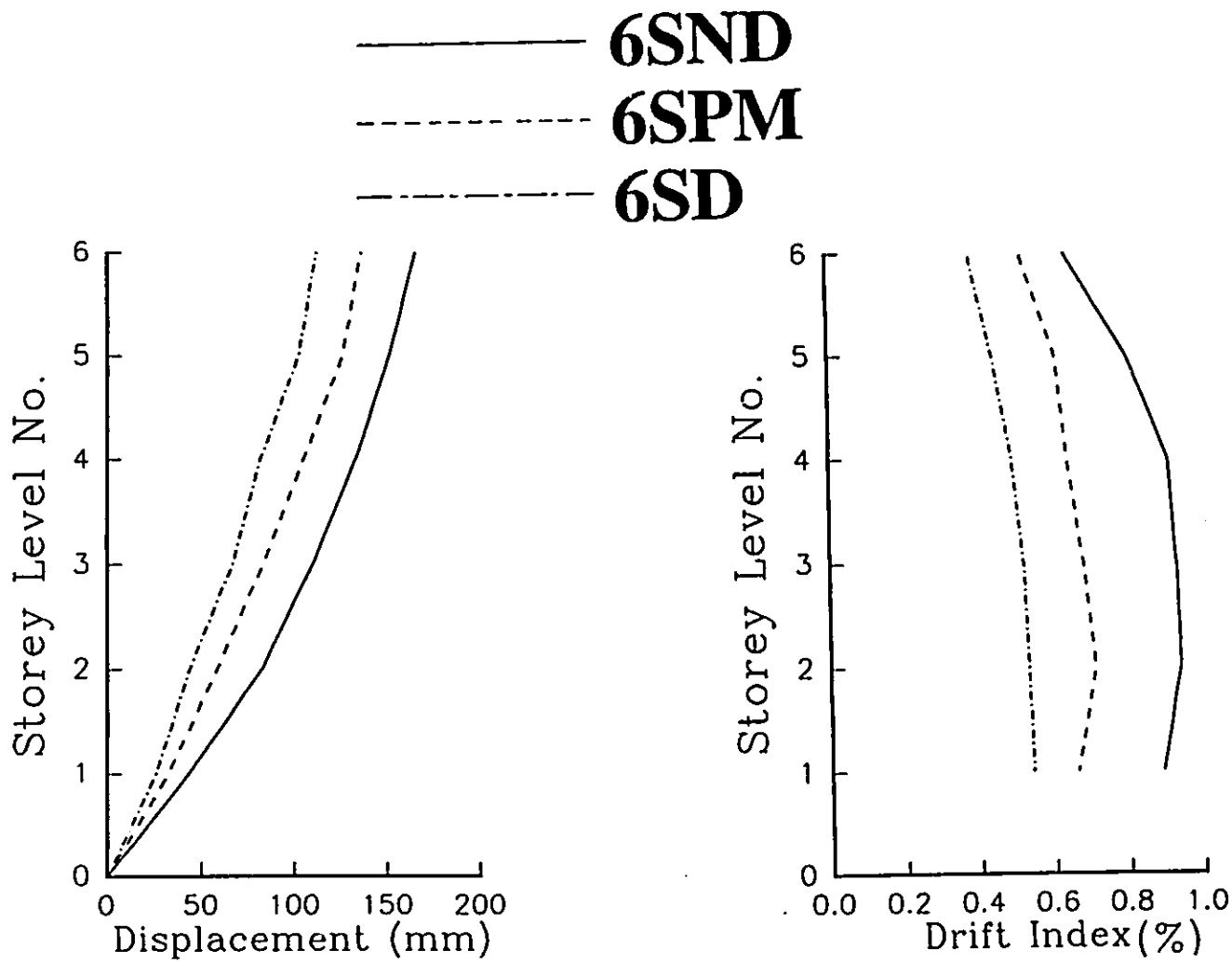

a) Displacements

b) Drift Index

Fig. (2.16) Displacements and interstorey drifts of the six storey frames with small columns.

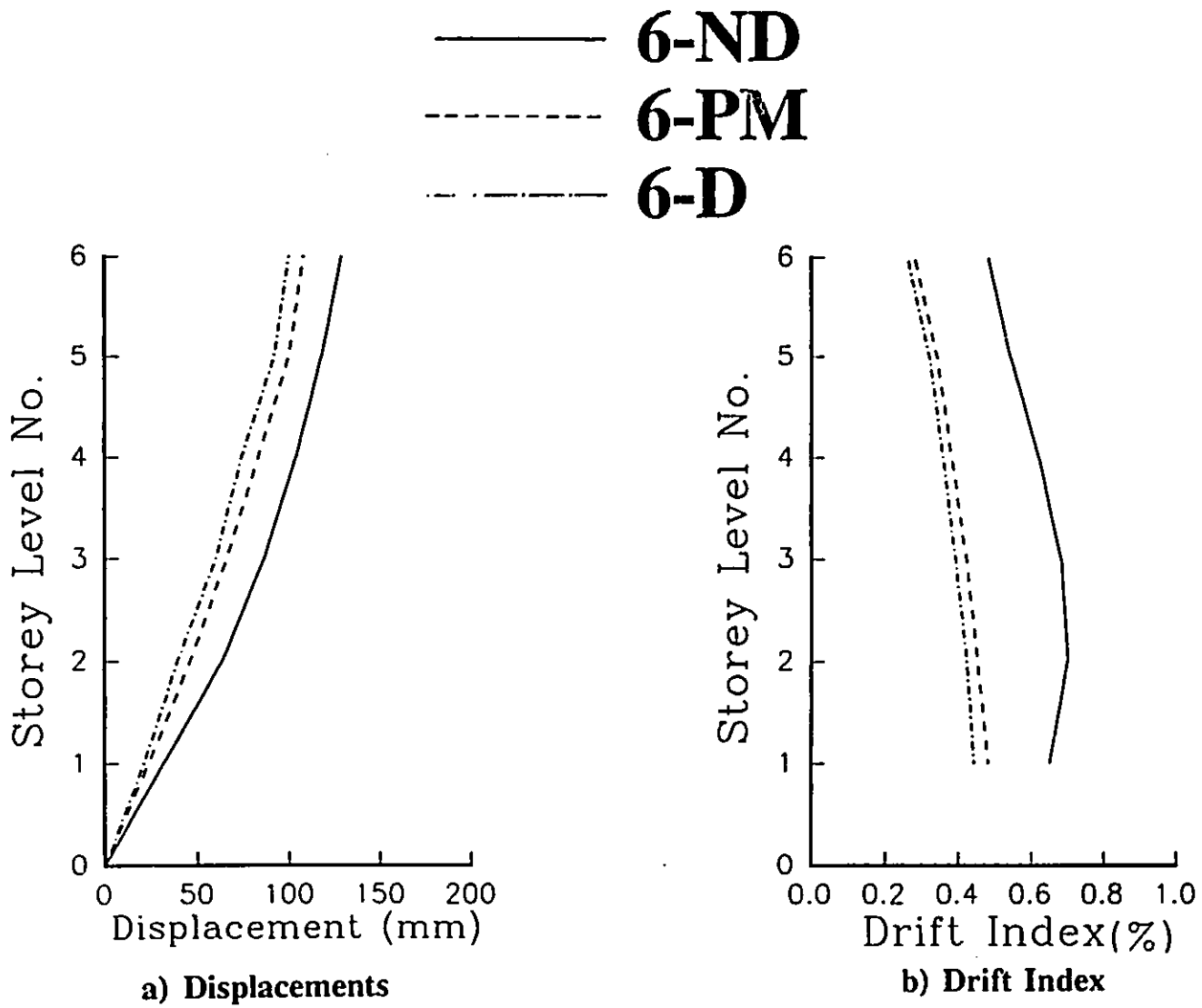

a) Displacements **b) Drift Index**

Fig. (2.17) Displacements and interstorey drifts ot the six storey frames with large columns.

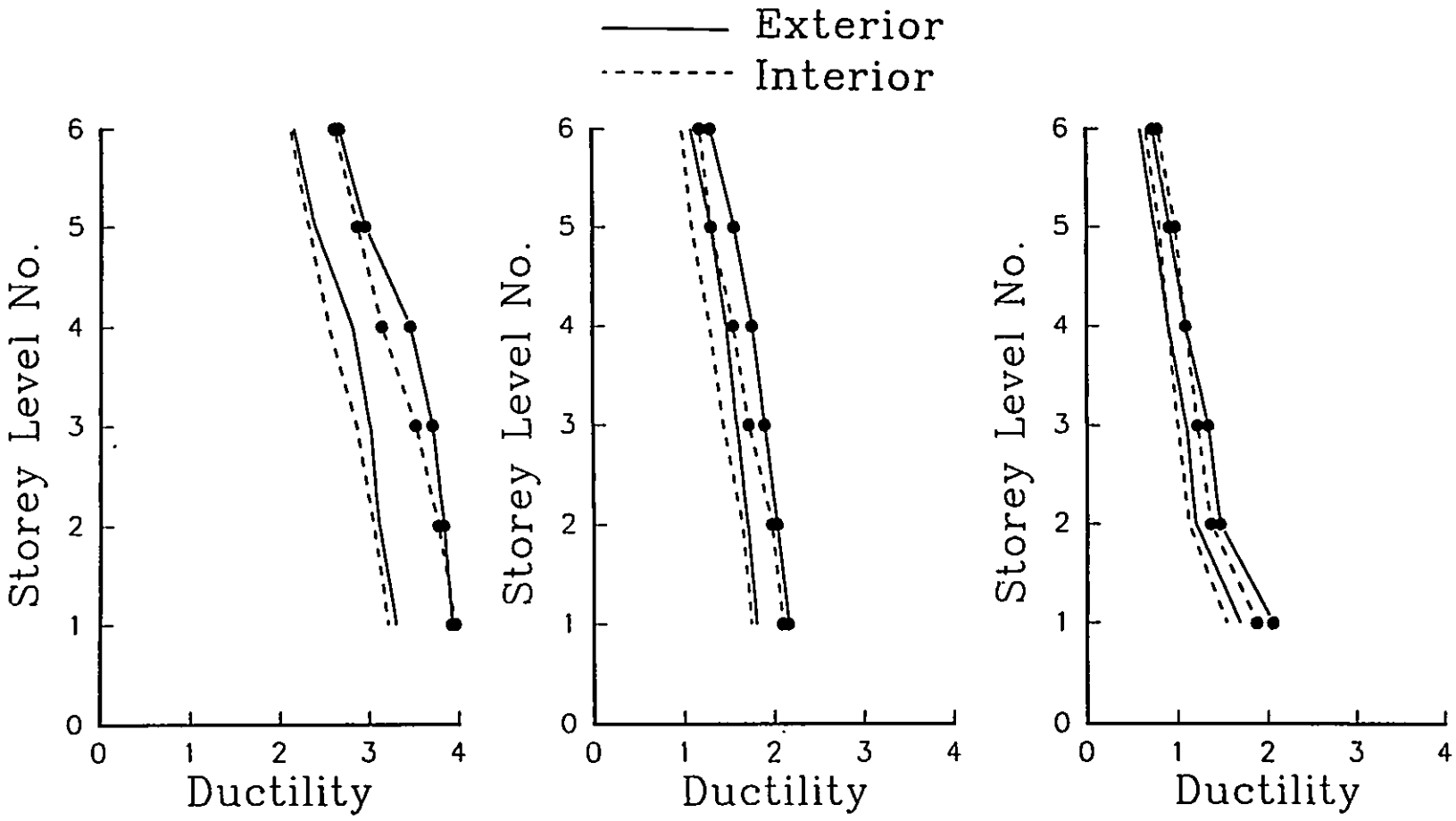

a) 6SND b) 6SPM c) 6SD

Fig. (2.18) Curvature ductility demands in the beams of the six storey frames with the small columns (• = mean + σ).

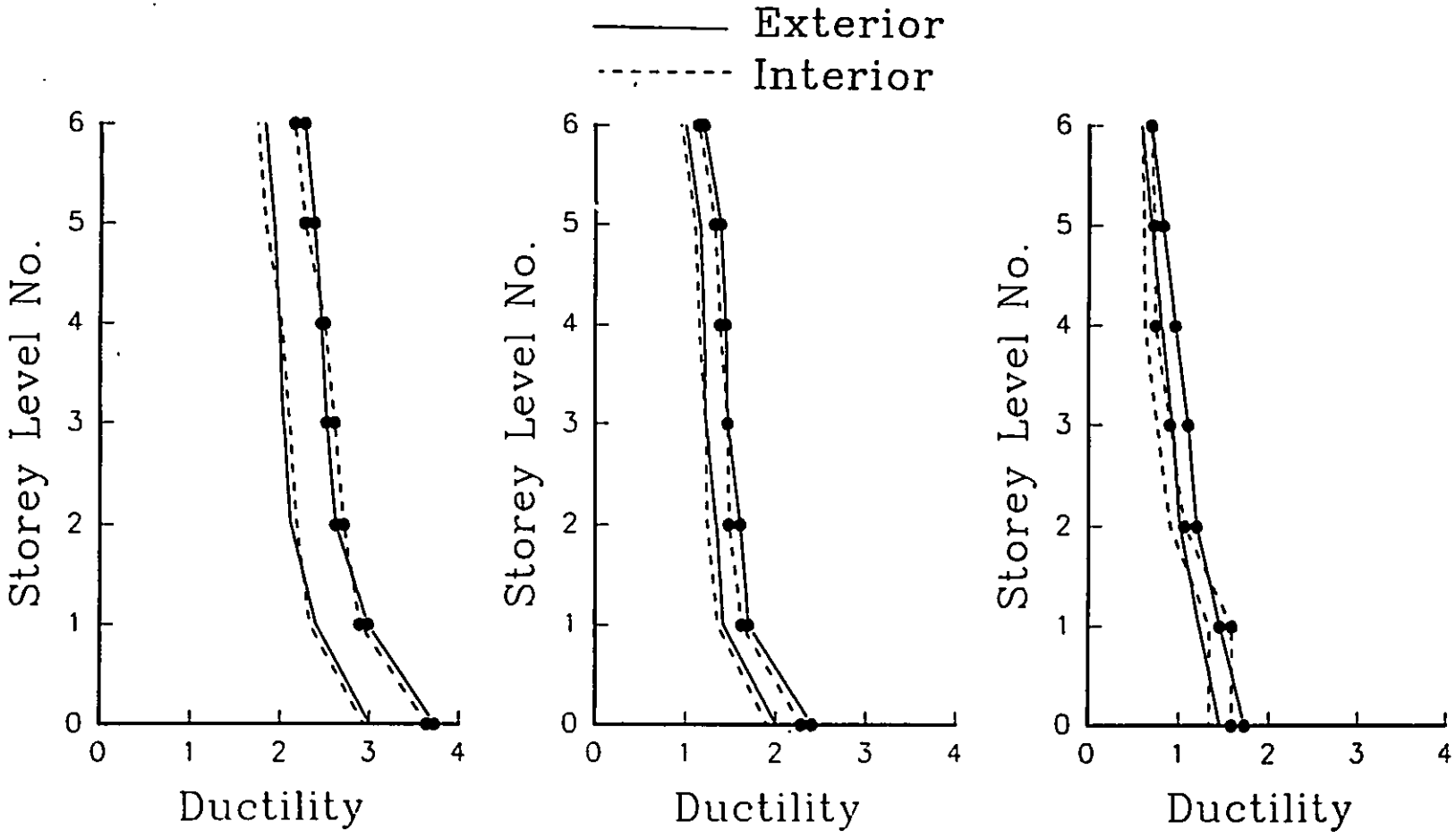

a) 6SND b) 6SPM c) 6SD

Fig. (2.19) Curvature ductility demands in the columns of the six storey frames with the small columns (• = mean + σ).

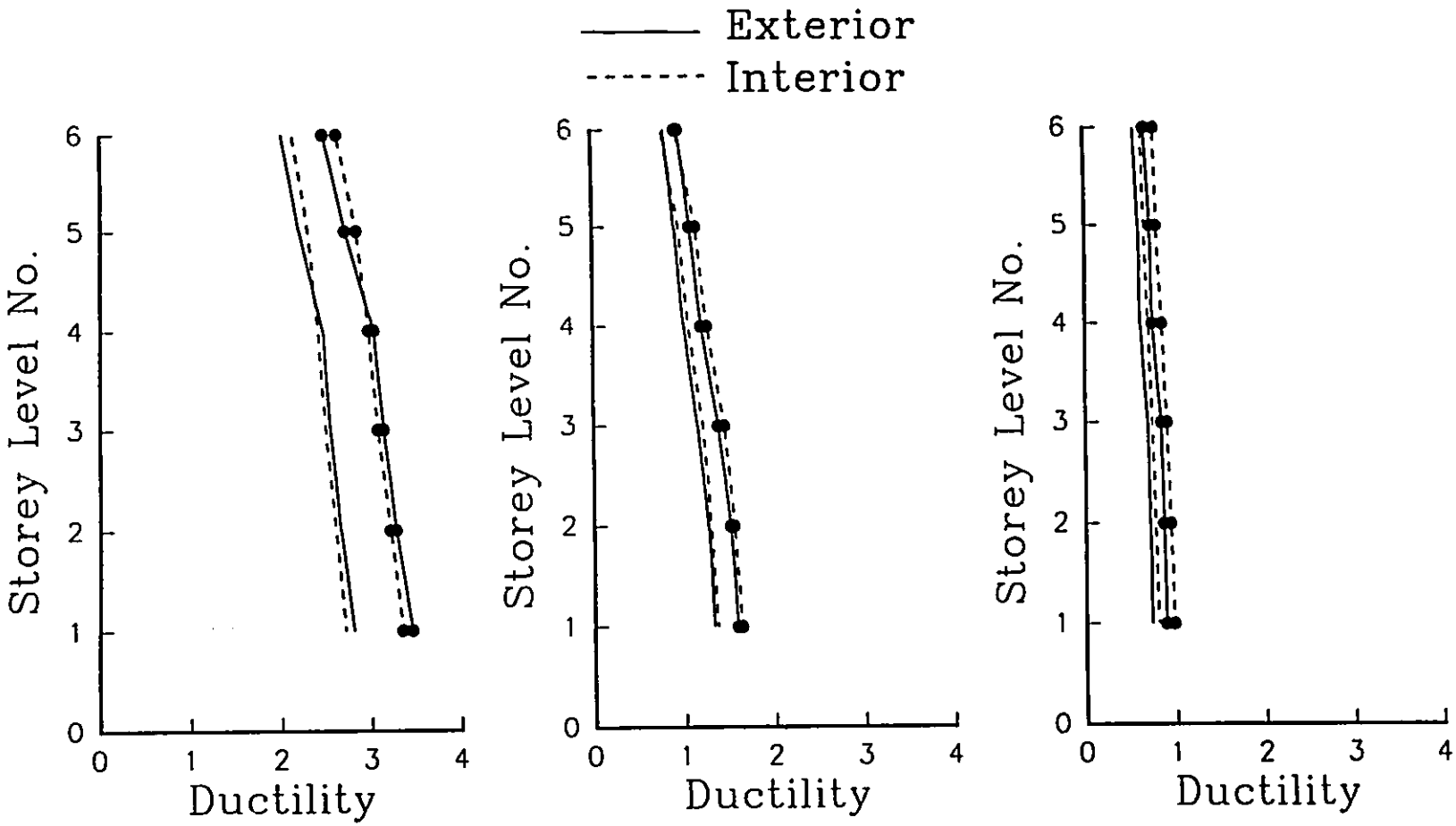

a) 6-ND b) 6-PM c) 6-D

Fig. (2.20) Curvature ductility demands in the beams of the six storey frames with the large columns (• = mean + σ).

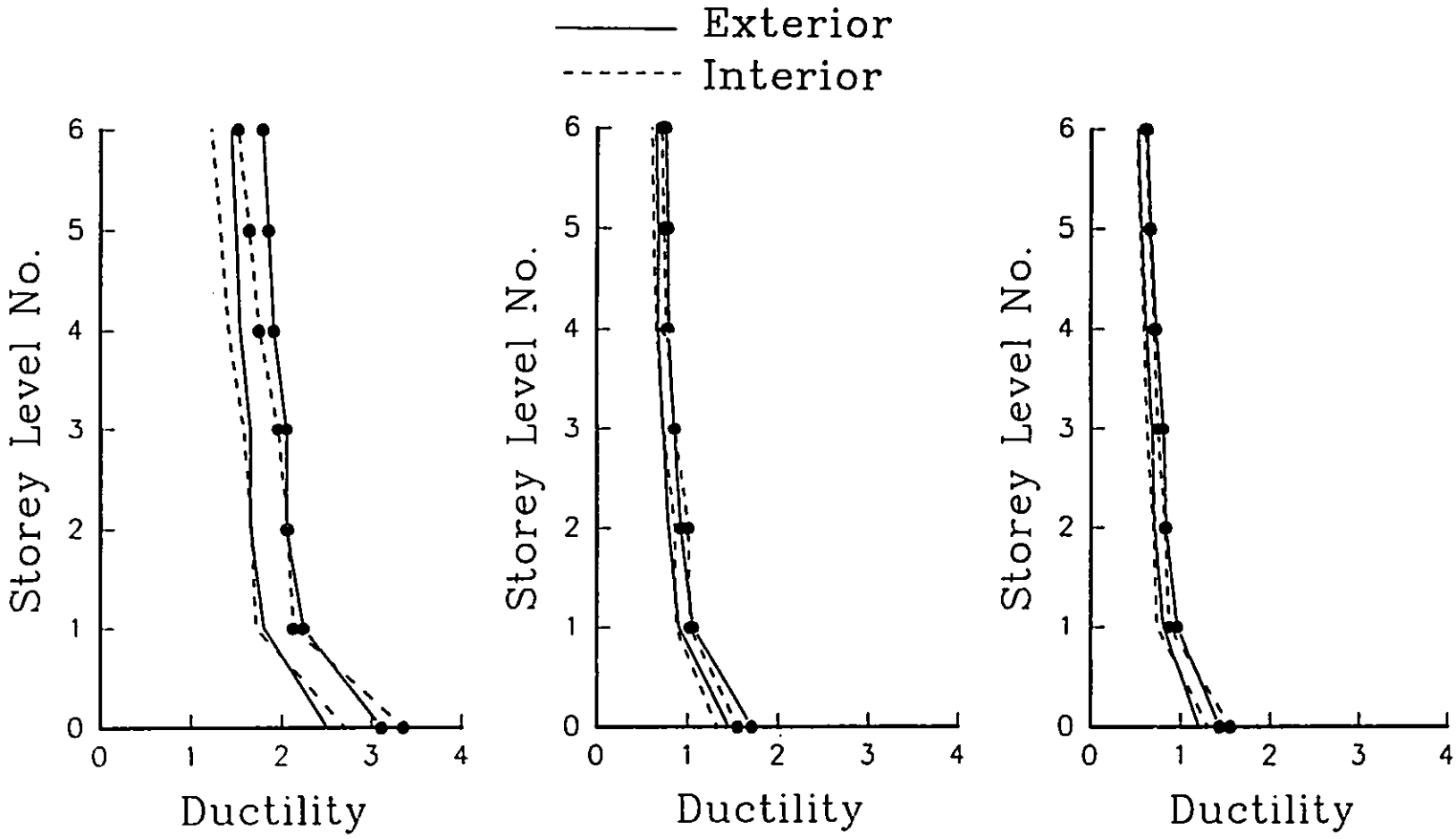

a) 6-ND b) 6-PM c) 6-D

Fig. (2.21) Curvature ductility demands in the columns of the six storey frames with the large columns (• = mean + σ).

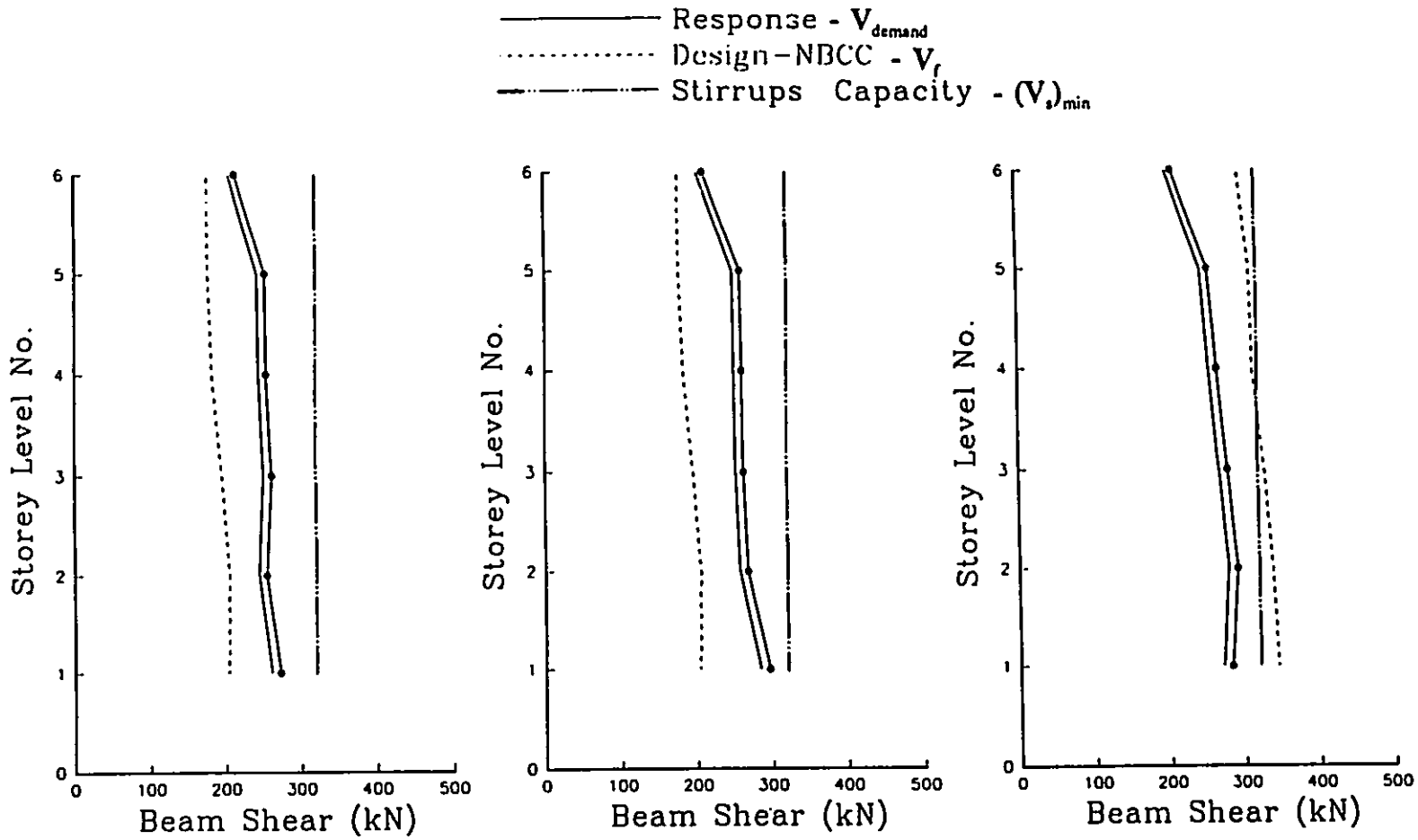

a) 6SND b) 6SPM c) 6SD

Fig. (2.22) Comparison between the shear demands and shear capacities of the beams of the small column frames (• = mean + σ).

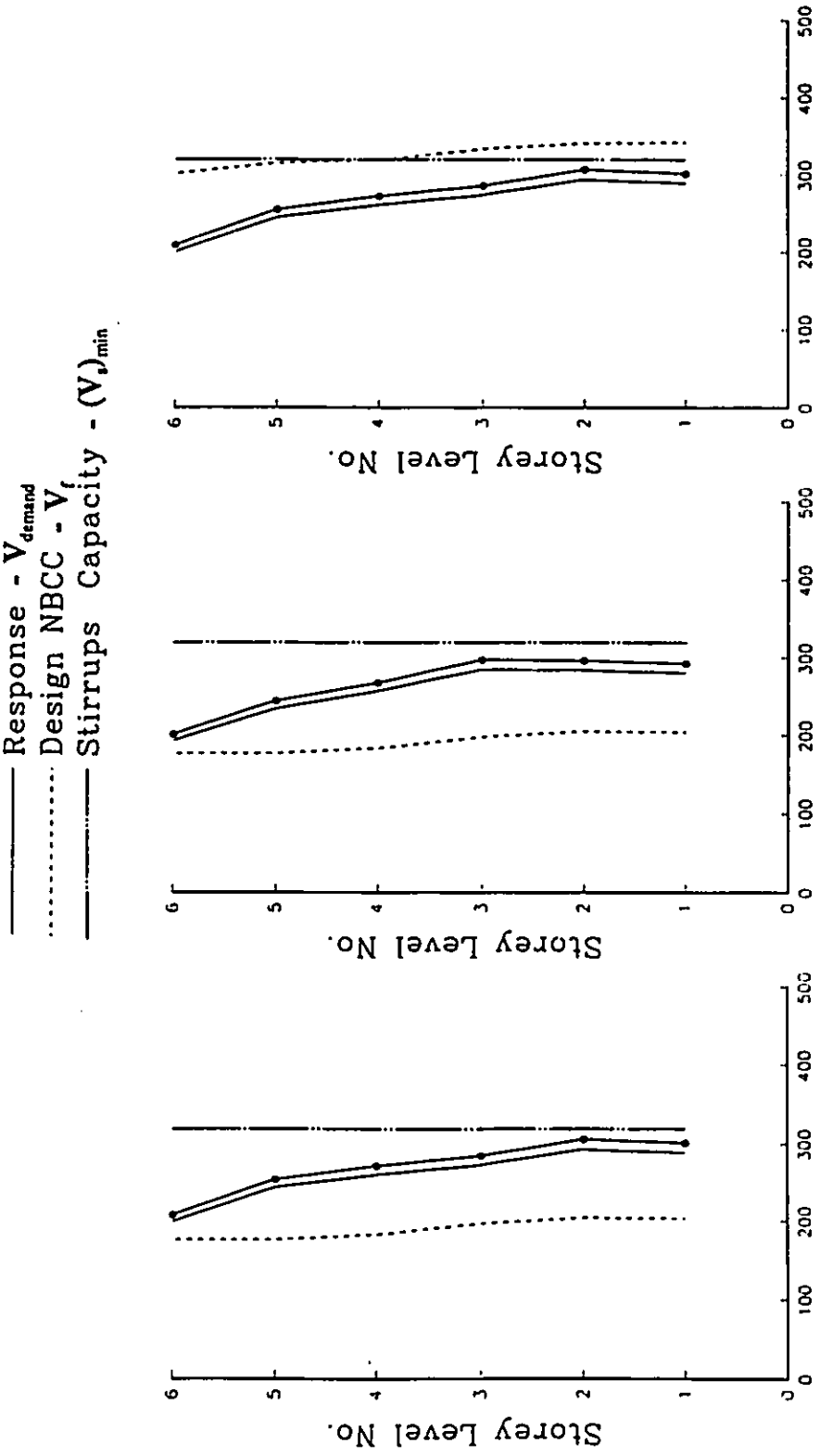

a) 6-ND b) 6-PM c) 6-D

Fig. (2.23) Comparison between the shear demands and shear capacities of the beams of the large column frames (• = mean + σ).

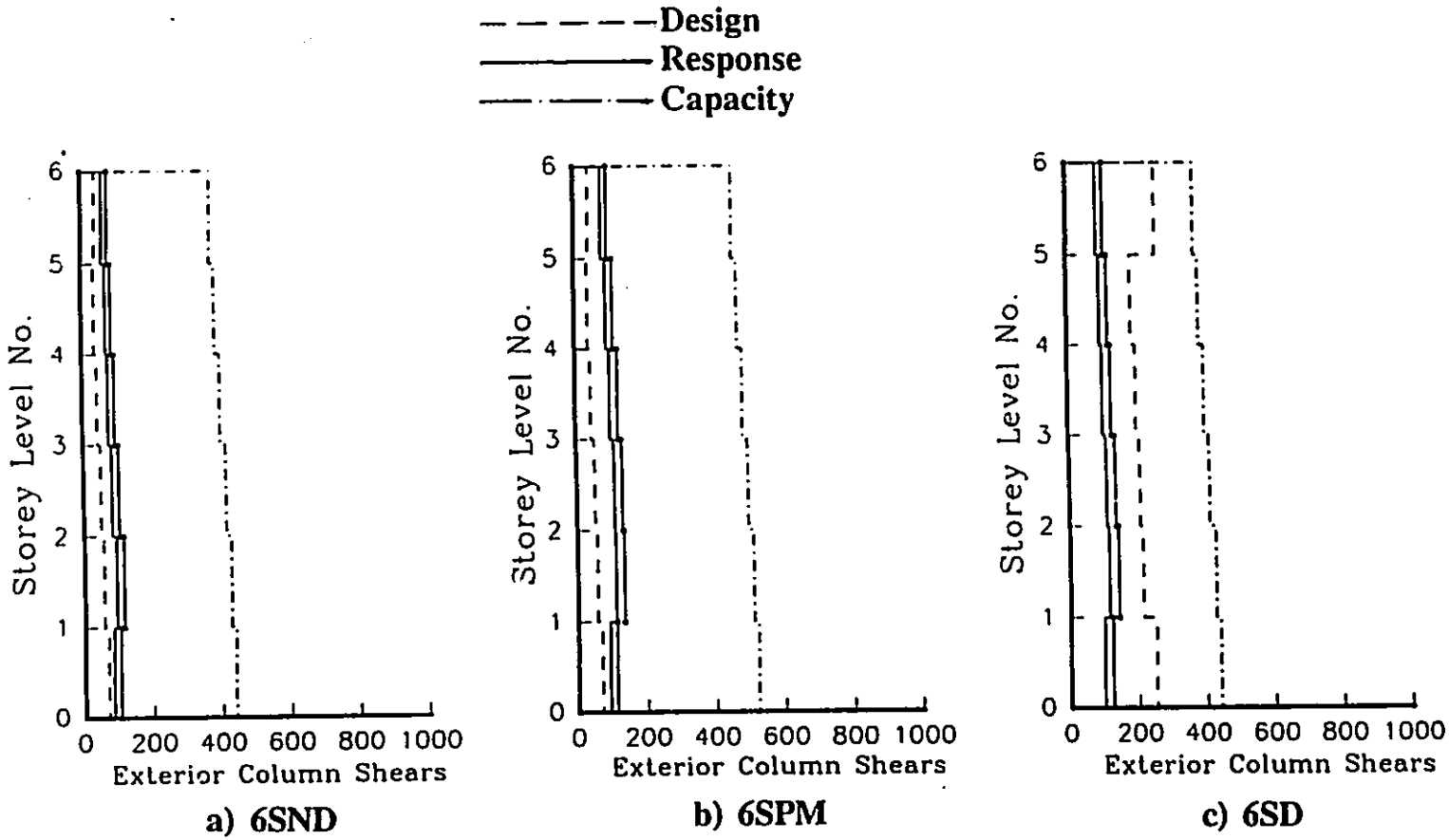

a) 6SND b) 6SPM c) 6SD

Fig. (2.24) Comparison between the shear demands and shear capacities of the exterior columns of the small column frames (• = mean + σ).

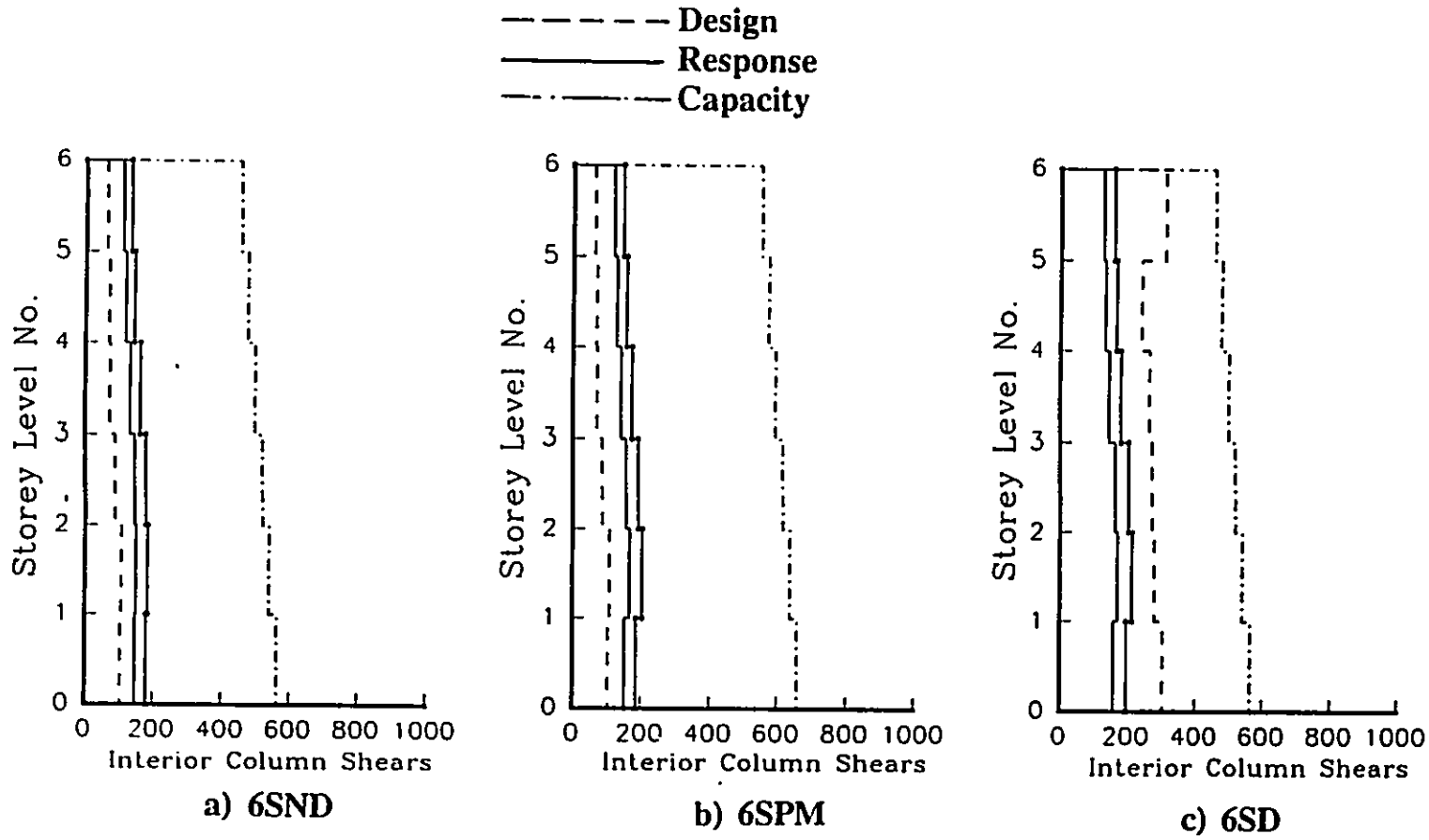

a) 6SND b) 6SPM c) 6SD

Fig. (2.25) Comparison between the shear demands and shear capacities of the interior columns of the small column frames (• = mean + σ).

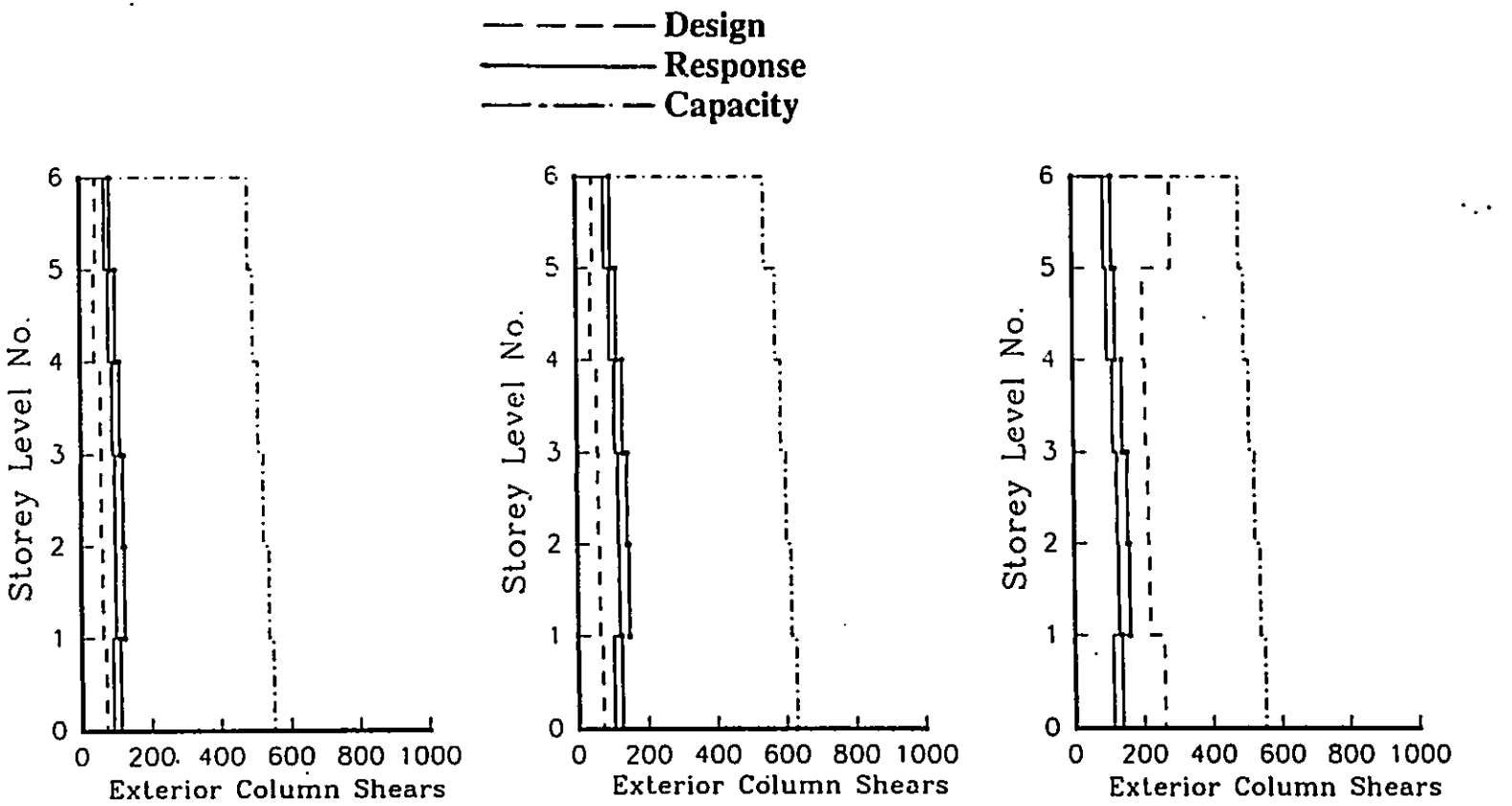

a) 6-ND b) 6-PM c) 6-D

Fig. (2.26) Comparison between the shear demands and shear capacities of the exterior columns of the large column frames (• = mean + σ).

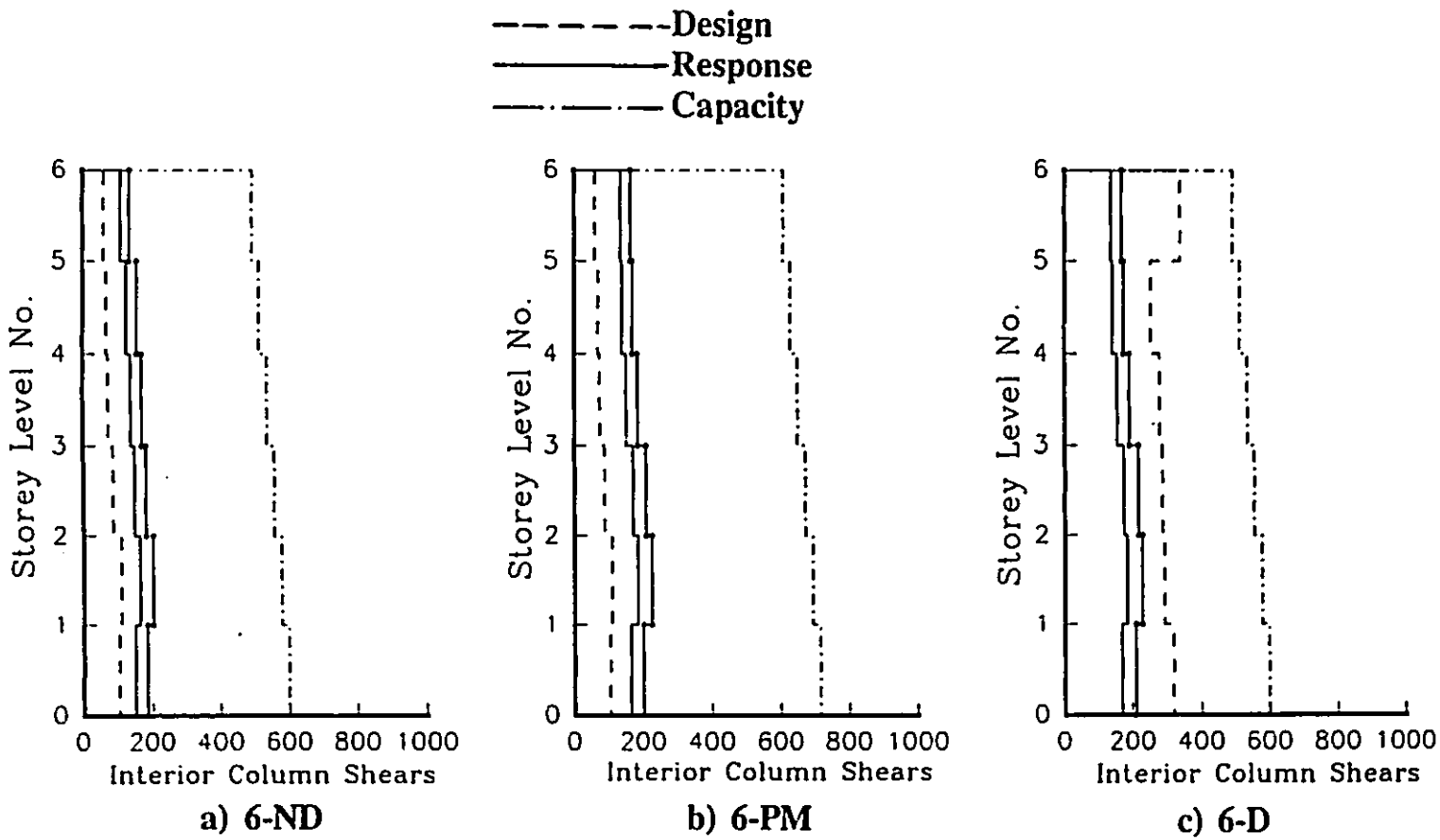

Fig. (2.27) Comparison between the shear demands and shear capacities of the interior columns of the large column frames (• = mean + σ).

CHAPTER 3

SEISMIC RESPONSES OF A SIX STOREY BUILDING WITH 8.0 METRE FRAME SPACING

3.1 INTRODUCTION

As shown in chapter 2, the beams in nominally ductile frames designed to minimum code requirements experience large ductility demands in the order of 3.0 and are subjected to shear demands that exceed the factored design shears by a large margin. However, for the frames considered in chapter 2, the beam shear capacity based on the Code's minimum stirrups requirement alone was found to exceed the beam shear demands. Therefore, the Code's minimum stirrup requirement will prevent any shear failure in the beams irrespective of the concrete contribution to shear resistance. However, the shear capacity provided by the Code's minimum stirrups requirements is independent of the beam size, span or loading. For beams below certain sizes and certain intensity of loading, the shear capacity provided by the minimum stirrups requirement can prove to be a useful "safety net" as exemplified by the beams of the frames considered in chapter 2. As the beam size and/or loading increases, one will arrive at the situation that the shear demands

exceed the shear capacity provided by $(V_s)_{min}$. In this chapter a six-storey building with an eight-metre frame spacing is considered. Due to the larger frame spacing the frames are subjected to larger loads and are expected to undergo larger beam shear demands than those experienced in the frames considered in chapter 2. Of particular interest is the comparison of the beam shear demands to the capacity of the minimum stirrups specified in the concrete design code to show that the "safety net" provided by the minimum stirrups requirement is not universal (i.e. valid for all NDMRFs).

This chapter starts with a description of the building followed by the main features of the building design as a nominally ductile frame structure according to NBCC 1990 and CAN3-A23.3-M84. The designed frame is analyzed under monotonically increasing static loading and then the seismic responses are evaluated. The response parameters investigated are the overall displacements, drift indices and ductility demands plus the member ductility and the beam and column shear demands.

3.2 DESCRIPTION OF BUILDING

The six storey building has three bays in the E-W direction and seven bays in the N-S direction as shown in figure (3.1). The bay widths are 8.0 metres in both directions and the storey height is constant at 3.5 metres. The one way slab spanning in the E-W direction is 120 mm thick and all secondary beams are 300 mm wide by

600 mm deep. The concrete compressive strength is taken as 30 MPa and the steel yield strength is taken as 400 MPa. A typical interior E-W frame is designed and analyzed for seismic actions in the E-W direction. The member dimensions of the typical interior E-W frame are depicted in figure (3.2). The beam and column sections of the frame are chosen to be larger than those of the frames considered in chapter 2 due to the larger bay widths resulting in larger gravity loads and consequently larger forces and moments.

3.3 DESIGN OF THE BUILDING AS A NOMINALLY DUCTILE FRAME STRUCTURE

The building will be designed to meet the minimum code requirements for nominally ductile frames following the same steps as outlined in section 2.3. The designed frame will be designated 6-8ND. The numeral 8 in the frame designation stands for the 8.0 metre bay widths.

The building is designed for the critical combinations of gravity and seismic loading as required by NBCC 1990. The gravity loads used in the design are given in table (3.1). For seismic base shear calculations the building is assumed to be located in Quebec City, Quebec, Canada, having a zonal velocity ratio equal to 0.15 and $Z_a > Z_v$. The force modification factor, R, is taken equal to 2.0 and I=F=1.0 are used in the base shear calculation. The total seismic base shear acting on the building is found to be

$$V = 0.087\,W \tag{3.1}$$

The base shear acting on each frame is taken as one eighth of the total base shear acting on the building. The gravity and seismic loads acting on a typical interior E-W frame are depicted in figure (3.3). Also shown in the same figure are the loads acting on the frames considered in chapter 2. The heavier gravity loading on the current frame is due to the larger frame spacing and member dimensions. The larger seismic loads are due to both the larger masses and the larger zonal velocity ratio of Quebec City (v=0.15) versus that in Montreal (v=0.10).

The forces and moments used in designing the beams and columns of the frame are obtained directly from the results of an elastic static analysis under the prescribed loads. The longitudinal reinforcement ratios of the designed frame are depicted in figure (3.4). The calculation of the beam shear reinforcement is of particular interest here and is described in detail below;

The maximum factored design shear, V_f, is 312 kN. For the given beam size, the factored concrete shear resistance, $\phi_c V_c$, is 189 kN. Thus, the required stirrups resistance, $(V_s)_{req} = (312\text{-}189)/\phi_s = 145$ kN. Using 2-legged No. 10 stirrups, the required spacing would be 397 mm. However, the code requirements specifies that the stirrups spacing should not exceed d/4. Therefore, the 2-legged No. 10 stirrups will be spaced at 180 mm for the first and second floor beams, at 165 mm for the third and fourth floor beams and at 155 mm for the fifth and sixth floor beams. This gives a nominal stirrups capacity $(V_s)_{min} = 320$ kN for these beams. Although the

factored design shears in the beams of this frame are approximately 1.5 times those of the frames designed in chapter 2, the resistance of the provided stirrups in both cases are identical.

Based on the calculated design shears, the columns will require only minimum transverse reinforcement. The 4-legged No. 10 ties will be spaced at 150 mm for the column end zones (600 mm at each end) and 300 mm for the remainder of the column height.

The frequencies and mode shapes of the building were determined from an eigen-value analysis using the cracked values for the moments of inertia. Figure (3.5) shows the first three periods and corresponding mode shapes. The fundamental natural period is 0.72 seconds which is 20 percent higher than the value assumed in the seismic base shear calculation. The fundamental period of the current frame is significantly shorter than that of the frames considered in chapter 2 due to the larger member sizes dictated by the larger gravity and seismic loading.

3.4 LATERAL STRENGTH OF THE FRAME

The frame was first analyzed under monotonically increasing static loading to study its force-deformation characteristics. Figure (3.6) shows the base shear-top displacement curve of the frame. Also shown on the curve is the overstrength factor, ϕ_o = 1.79 (ultimate strength/code base shear) of the designed frame. The ultimate strength is taken as the strength of the frame at a displacement equal to R/0.6 = 3.3

times the displacement at code level loading. The overstrength factor for this frame is in the same order as the values obtained for the nominally ductile frames, 6SND and 6-ND considered in chapter 2. The U factor used in NBCC base shear calculations can be considered as some measure of the overstrength of buildings designed according to NBCC 1990 and the relevant material codes. It has been suggested (Tso, 1991) that 1/U can be interpreted as the overstrength factor. Using this interpretation, an overstrength factor of 1.67 can be expected for all types of structures according to the Code. The overstrength factor of this frame is in the same order as the value assumed in the Code. The overall yield displacement of the frame is determined from the force-deformation curve and was found to be 61 mm.

Figure (3.7) shows the sequence of plastic hinge formation under static loading. Also shown in the same figure are the plastic hinging sequences of the nominally ductile frames 6SND and 6-ND. The current frame developed column hinge before beam hinging and eventually developed a storey side-sway mechanism. Therefore, the inelastic static behaviour of the present frame is similar to those of 6SND and 6-ND.

3.5 DYNAMIC ANALYSIS RESULTS

The same dynamic analysis procedures described in section 2.7 were used in the dynamic analysis of the frame. The fifteen ground motion records listed in table (2.4) are used as the ground motion input, and were normalized to a common

maximum velocity equal to the design ground velocity of Quebec City (0.14 m/sec.). The results discussed below are based on a statistical analysis of the individual frame responses to each record.

3.5.1 DISPLACEMENTS, DRIFTS AND DUCTILITY DEMANDS

Figure (3.8) shows the mean and mean+σ (standard deviation) envelopes of displacements and drift indices. The mean top displacement is 115 mm giving a mean global ductility demand of 1.89. The mean+σ ductility demand was 2.30. The global ductility demand of the current frame are similar to the values obtained for the 6SND, 6-ND frames. The drift indices of the frame considered here are also similar to those observed in 6SND and 6-ND.

Figure (3.9) depicts the mean and mean+σ curvature ductility demands in the beams and columns of the six-storey frame considered in this chapter. The inelastic deformations are distributed over the entire frame (beams and columns). The beam ductility demands are in the order of 3.0 which is similar to those attained in the members of the nominally ductile frames, 6SND and 6-ND, considered in chapter 2.

Table (3.2) shows a comparison of the response parameters discussed above for the current frame and the 6SND and 6-ND frames. For all three frames, the values of ductility demands and drifts are similar. One may infer that the overall and member ductility demands shown in table (3.2) are representative of NDMRFs designed to satisfy the minimum requirements of the Code when exposed to the design level earthquake excitation.

3.5.2 BEAM SHEAR DEMAND vs BEAM SHEAR CAPACITY

Figure (3.10) shows a comparison between the beam shear demands, V_{demand}, the factored design shears, V_f and the capacity of the minimum stirrups $(V_s)_{min}$. Similar to frames 6SND and 6-ND, the shear demands exceed the factored design shears by approximately 40 percent. However due to the larger loads on this frame, the shear demands are not only larger than those in the beams of 6SND and 6-ND, but they also exceeded the capacity of the minimum stirrups specified in the Code. Unless the concrete shear resistance is reliable, the beams of the frame considered here would suffer shear failure. The reliability of the concrete shear resistance under large ductility demands can only be determined through cyclic testing of the beams. Such an investigation was carried out and is reported in chapter 4.

3.5.3 COLUMN SHEAR DEMAND vs COLUMN SHEAR CAPACITY

Figure (3.11) shows a comparison between the shear demands, the factored design shears and the shear capacities of the exterior and interior columns of the considered six storey frame. Although the demand shears exceeded the factored design shears, the column shear capacities were always larger than the shear demands thus preventing column shear failure.

Due to the larger frame spacing and peak ground velocity, the demand shears in the columns of this frame are almost twice those in the columns of the frames spaced at 6.0 metres. However, the column shear capacities are also enhanced due to the larger axial loads in the columns, thus maintaining the same safety margin as

that observed in chapter 2. In other words, the heavier loading will not cause a shear problem in columns similar to that observed in the beams.

3.6 SUMMARY

The seismic responses of a six-storey reinforced concrete office building with 8.0 metre frame spacing designed as a nominally ductile frame structure was presented in this chapter. The designed frame was analyzed statically under monotonically increasing loading and dynamically under earthquake excitation. The drifts and global and local ductility demands were similar to those observed in the nominally ductile frames, 6SND and 6-ND considered in chapter 2. This confirms that the seismic performances of the 6SND and 6-ND frames are typical of NDMRFs that satisfy minimum Code requirements in terms of drifts and ductility demands. However, the beam shear demands and shear resistance of 6SND and 6-ND are not typical of all NDMRFs. A building with larger bay widths such as the 6-8ND frame will be subjected to larger beam shear demands that exceed the capacity of the minimum stirrups. Examining the beam ductility demands of the current frame shows that they reach values of 3.0 to 4.0. Subjected to this level of ductility demands, extensive cracking will occur and the concrete shear resistance will diminish (as it will be shown in chapter 4). Under such conditions, shear failure may occur in the beams of the frame considered here.

Disallowing the concrete contribution to the beam shear resistance because of extensive cracking, there is no guarantee that the "safety net" provided by the minimum stirrups requirement will be sufficient to prevent shear failure in beams of NDMRFs. This leads to the necessity of increasing the factored design shear forces to be more reflective of the actual seismic shear demands, as will be discussed in chapter 5.

Table (3.1) Design Gravity Loads

	Dead	Live
Floors	Self weight of concrete Partition loads 1 kPa Mechanical services 0.5 kPa	2.4 kPa
Roof	Self weight of concrete Roof insulation 0.5 kPa	Snow load

Table (3.2) Comparison of the response parameters for the nominally ductile frames considered in chapters 2 and 3.

Frame		μ_Δ	Drift(%)	Max. Beam Ductility	Max. Column Ductility
6-8ND	Mean	1.89	0.74	3.15	3.00
Chapter 3	Mean+σ	2.30	0.88	3.84	3.69
6SND	Mean	1.87	0.92	3.22	3.00
Chapter 2	Mean+σ	2.31	1.12	4.00	3.72
6-ND	Mean	1.68	0.70	2.80	2.70
Chapter 2	Mean+σ	2.04	0.85	3.50	3.35

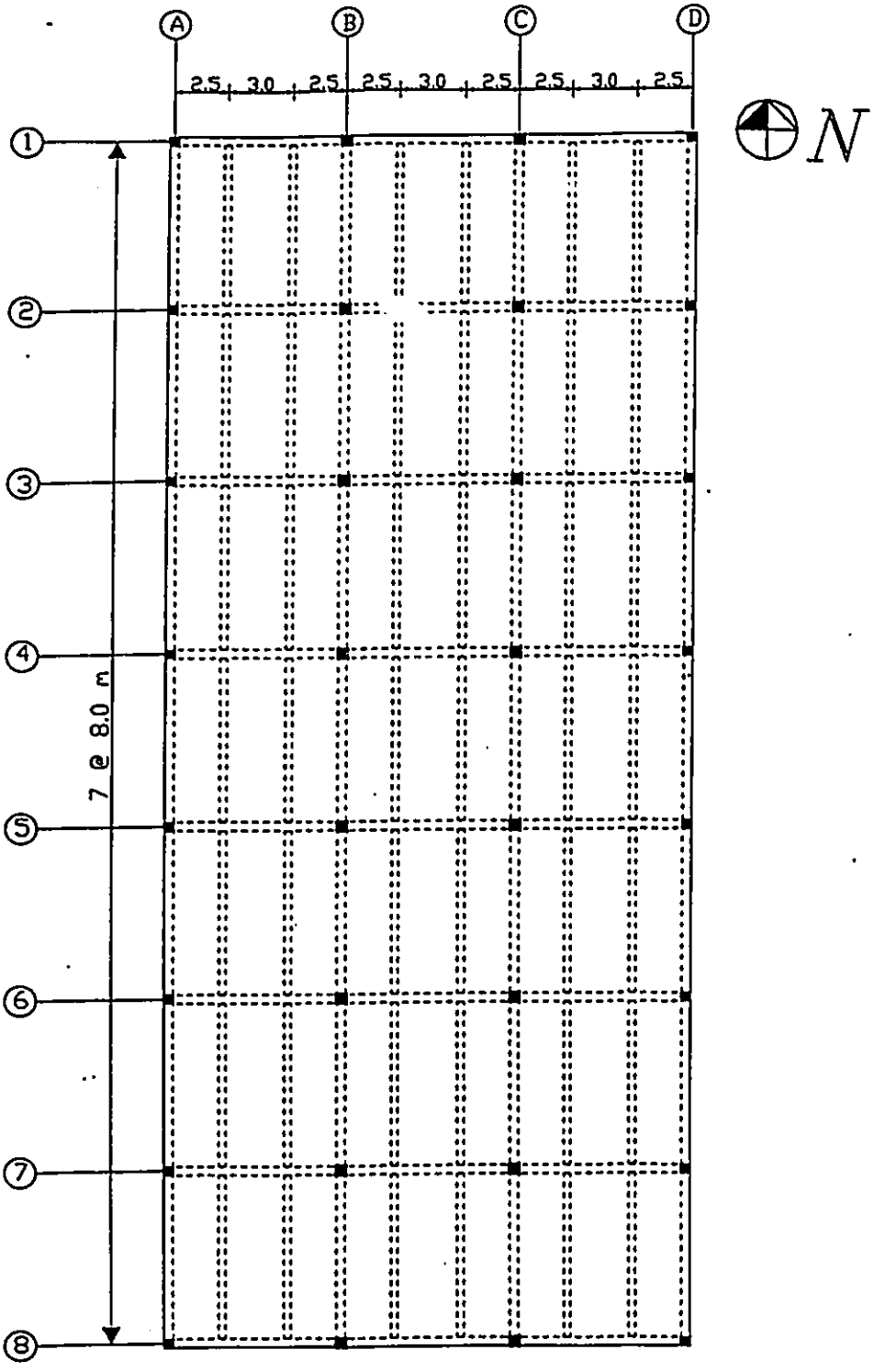

Fig. (3.1) Typical floor plan of the six storey building considered in chapter 3.

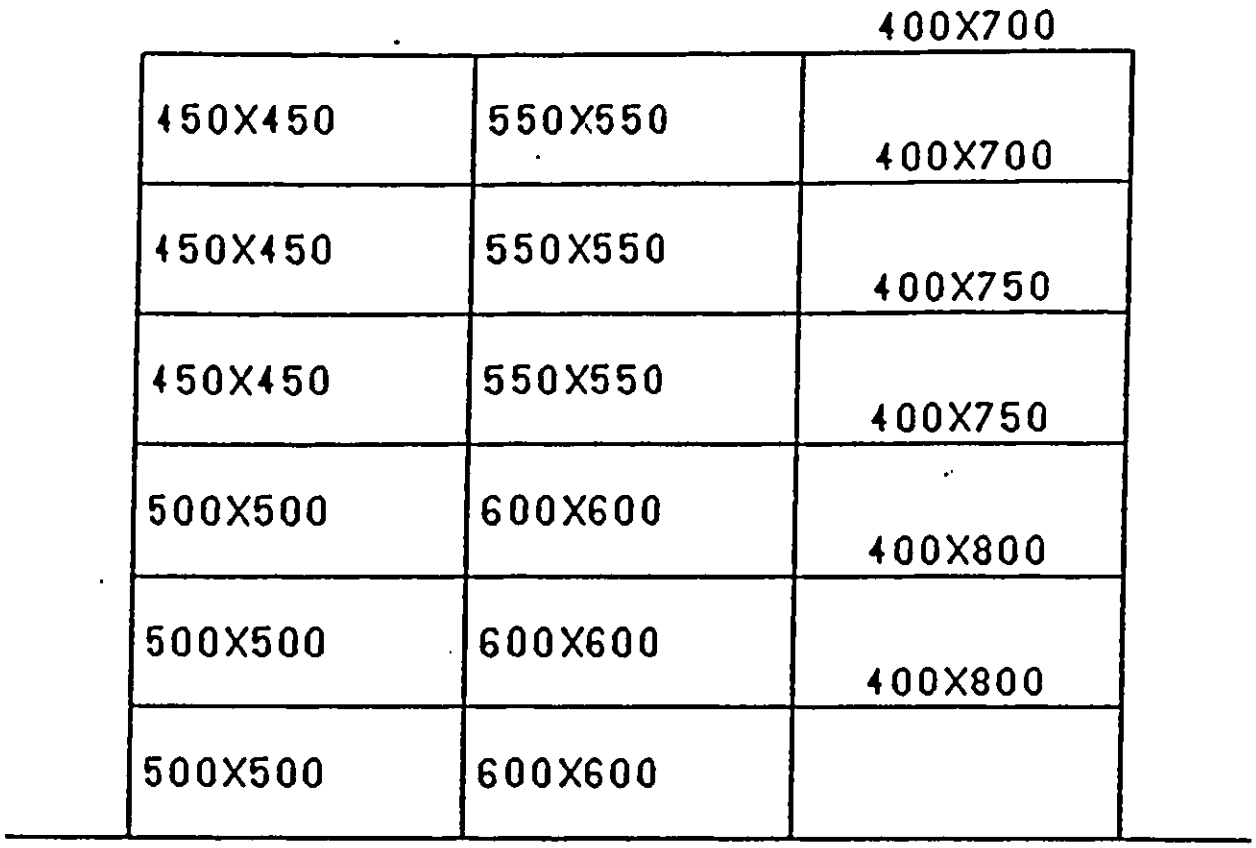

Fig. (3.2) Member dimensions of the six storey frame considered in chapter 3.

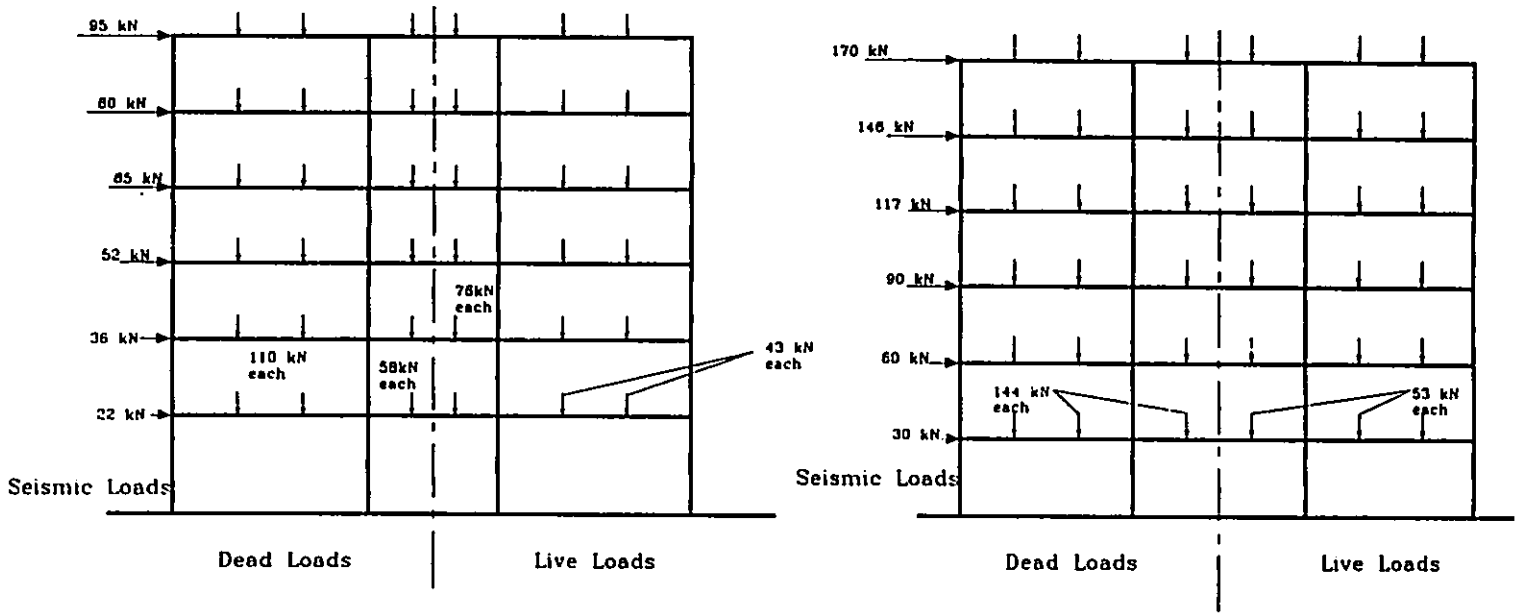

a) Frame considered in chapter 2.

b) Current frame

Fig. (3.3) Comparison of design loads on the current frame and those on the frames considered in chapter 2.

		1.086
1.387 1.244	1.000 1.000	0.456 1.199
1.244 1.388	1.000 1.000	0.487 1.192
1.388 1.335	1.000 1.190	0.481 1.234
1.082 1.070	1.000 1.000	0.507 1.225
1.070 1.147	1.000 1.000	0.501 1.243
1.147 1.087	1.000 1.291	0.512

Fig. (3.4) Longitudinal reinforcement ratios of the six storey frame considered in chapter 3. (percent)

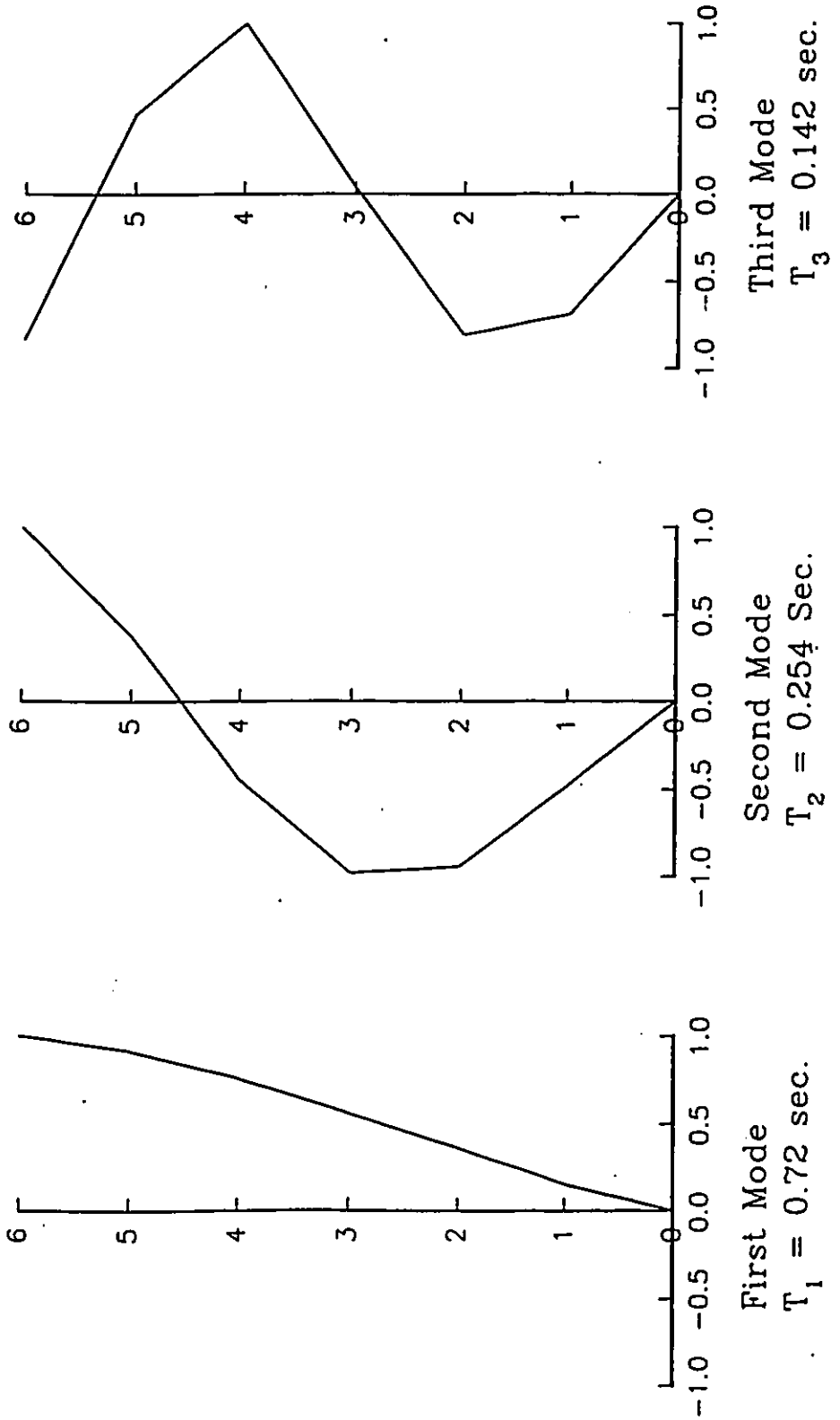

Fig. (3.5) Frequencies and mode shapes of the six storey building considered in chapter 3.

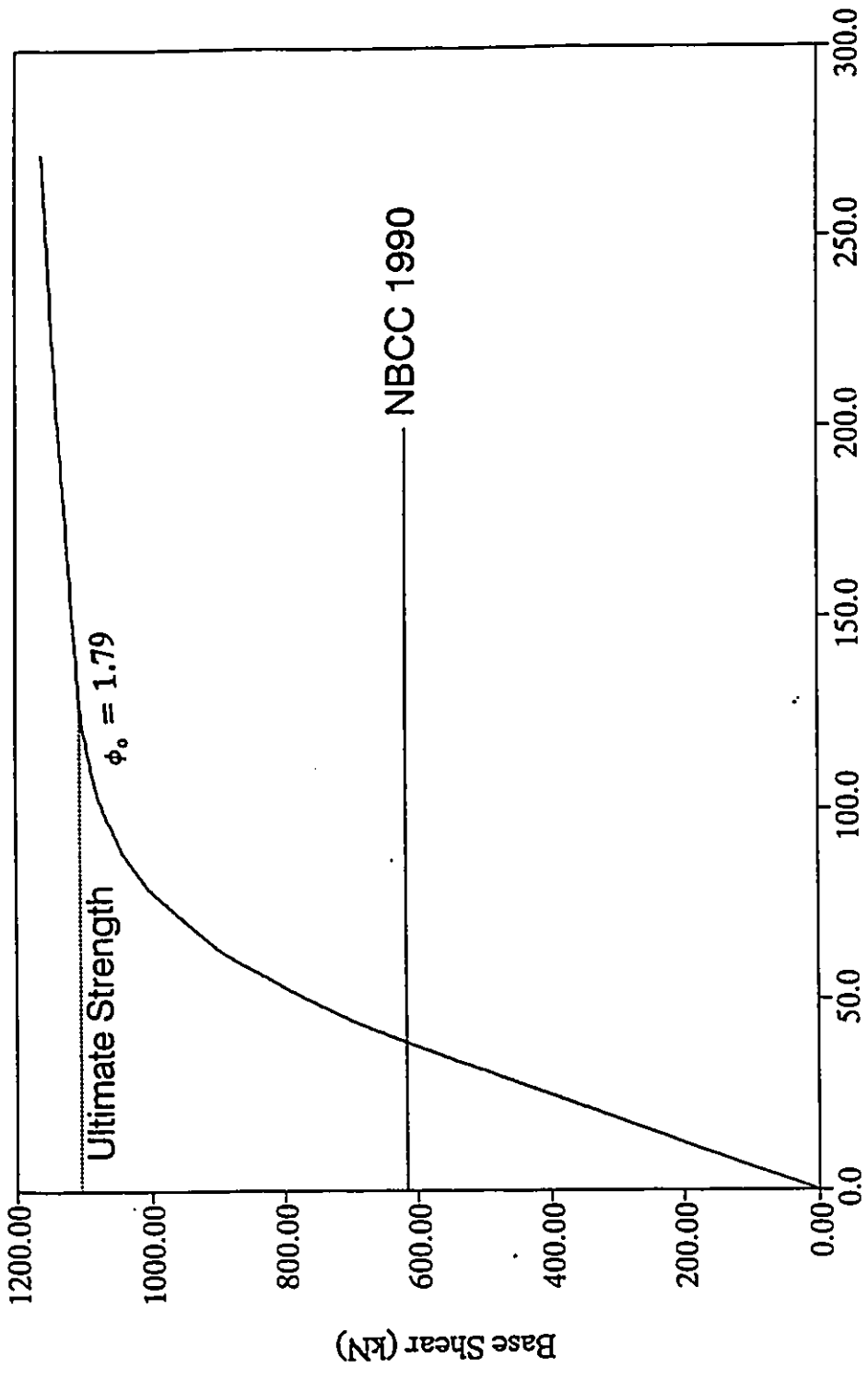

Fig. (3.6) Base shear-top displacement curve of the six storey frame considered in chapter 3.

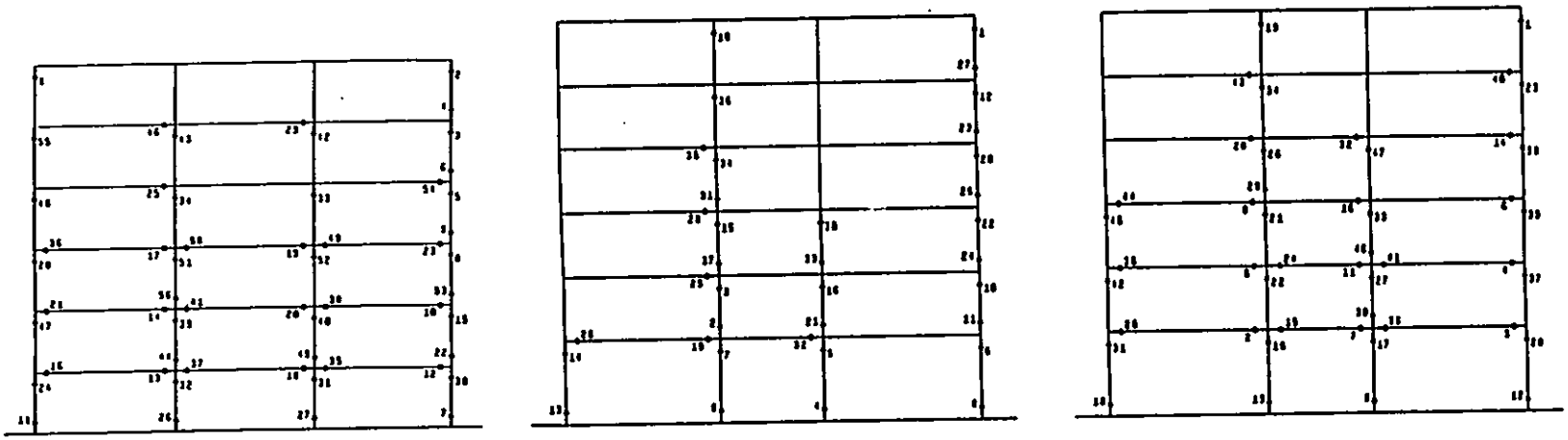

a) Current frame b) 6SND c) 6-ND

Fig. (3.7) Sequence of plastic hinge formation in the six storey frame considered in chapter 3 and the 6SND and 6-ND frames considered in chapter 2.

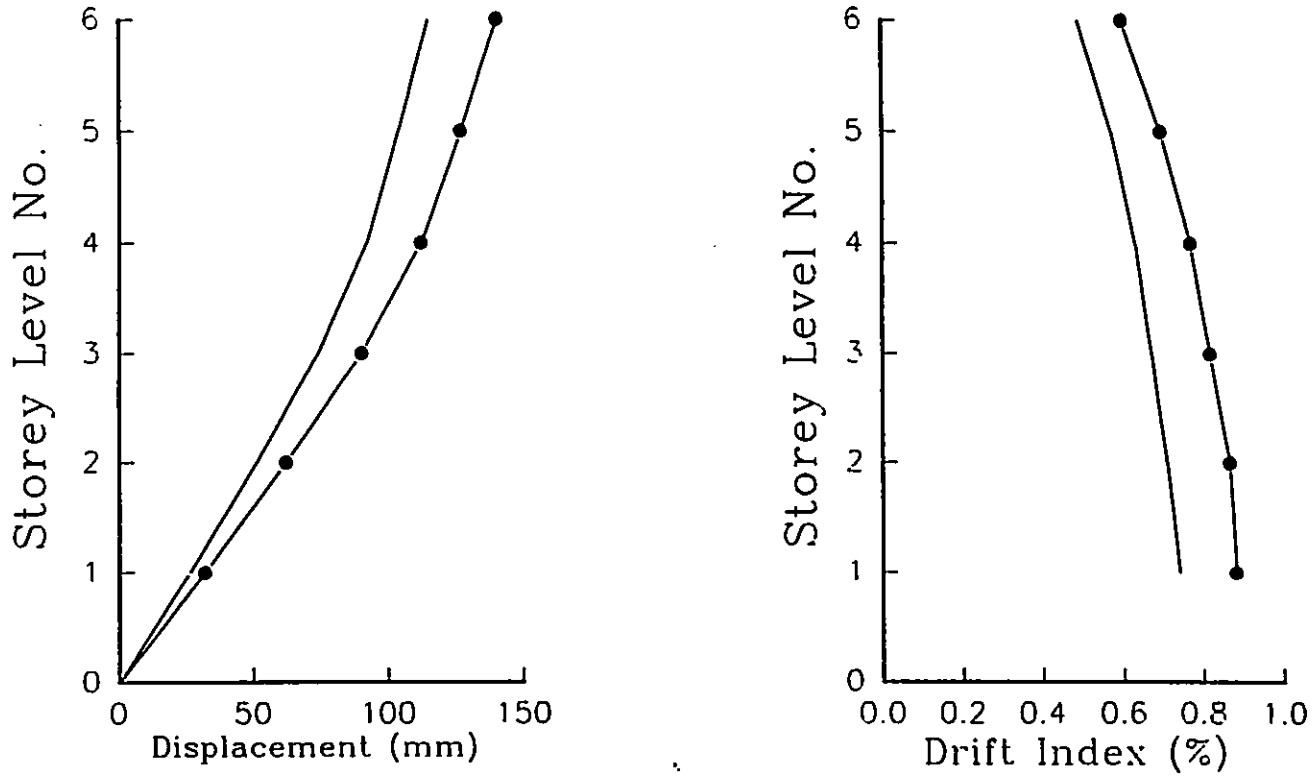

a) Displacements

b) Drift Indices

Fig. (3.8) **Lateral displacement and drift indices envelopes of the six storey frame considered in chapter 3 (• = mean + σ).**

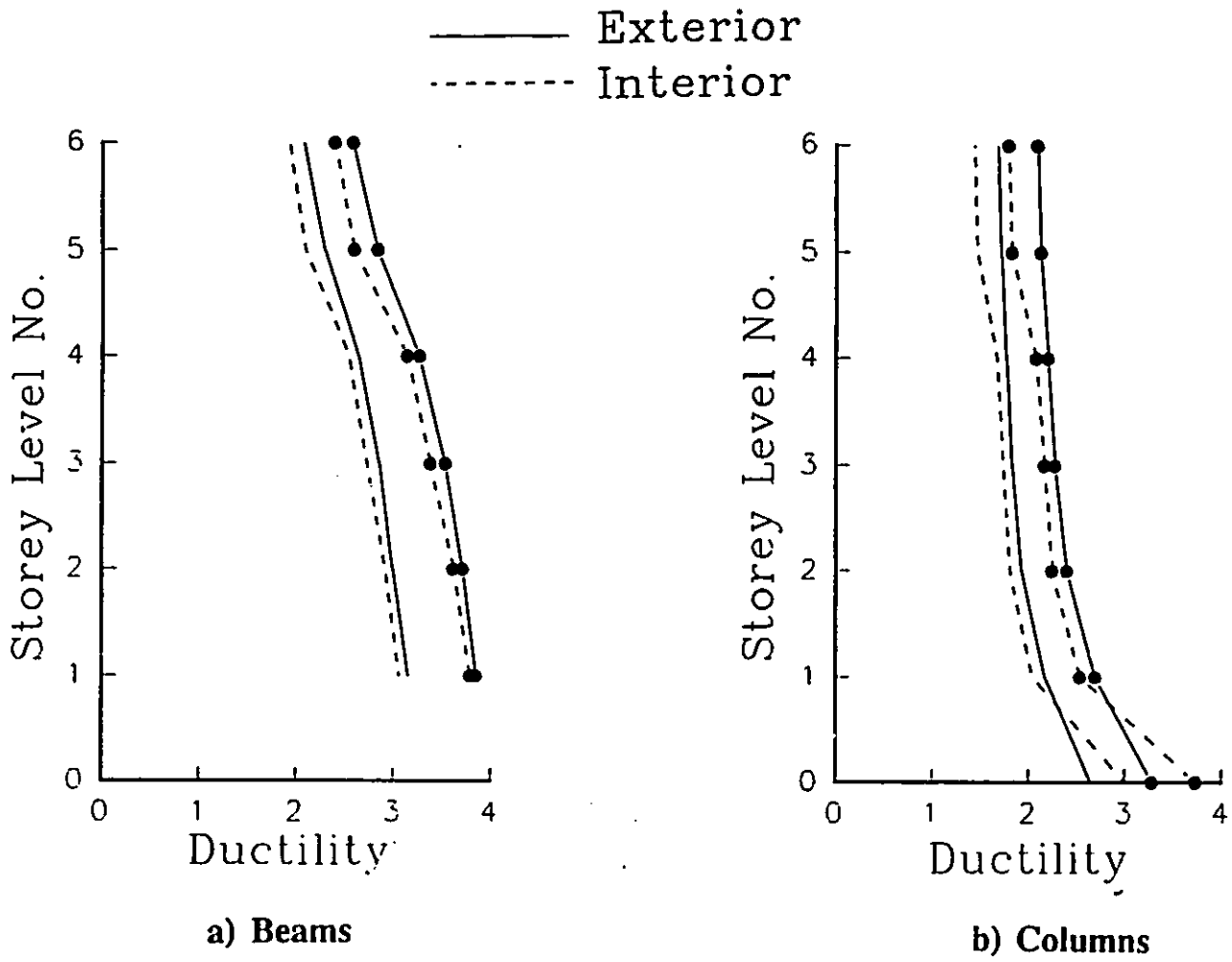

Fig. (3.9) **Curvature ductility demands in the beams and columns of the six storey frame considered in chapter 3 (• = mean + σ).**

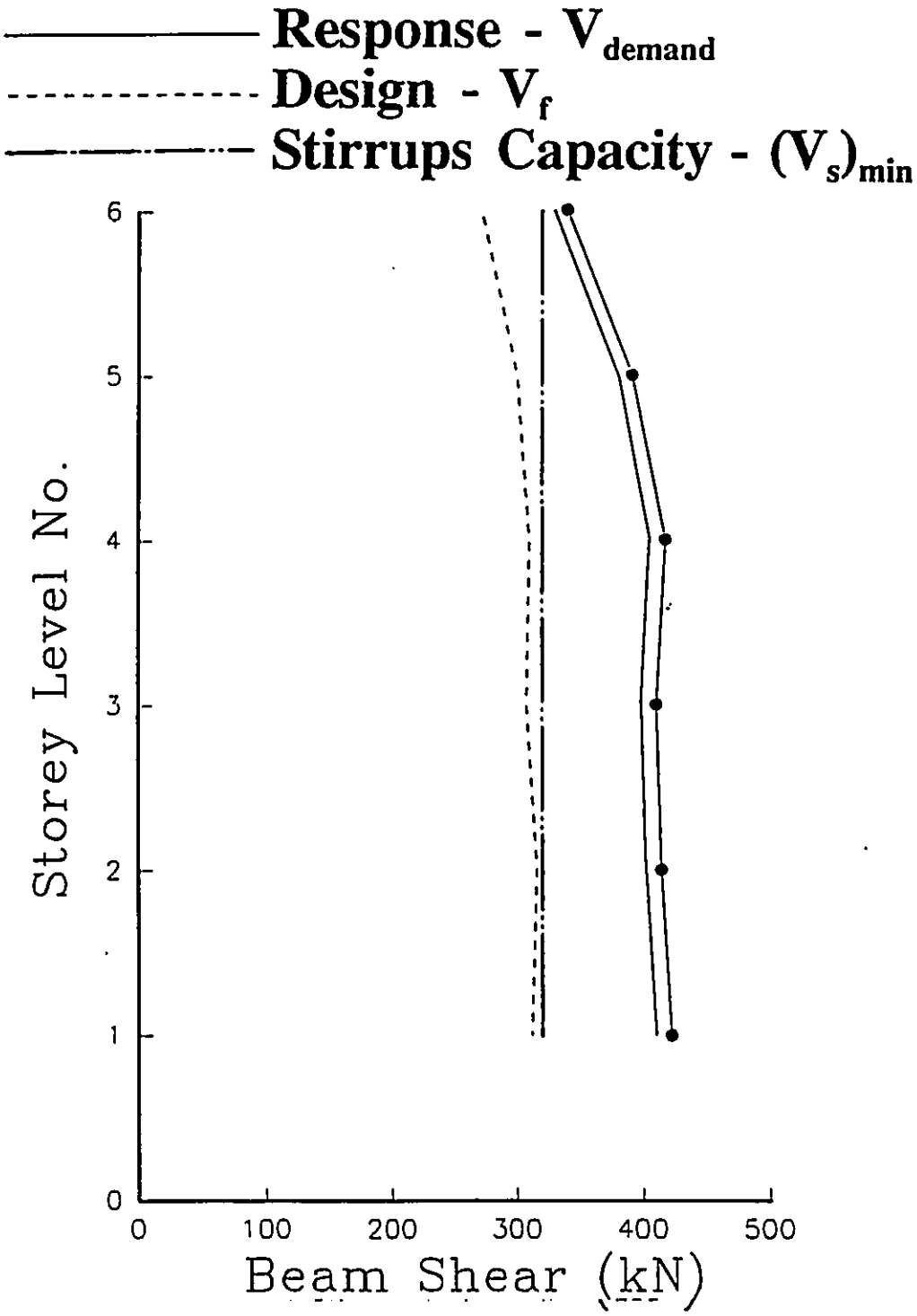

Fig. (3.10) Comparison between the shear demands and shear capacities of the beams of the six storey frame considered in chapter 3 (• = mean + σ).

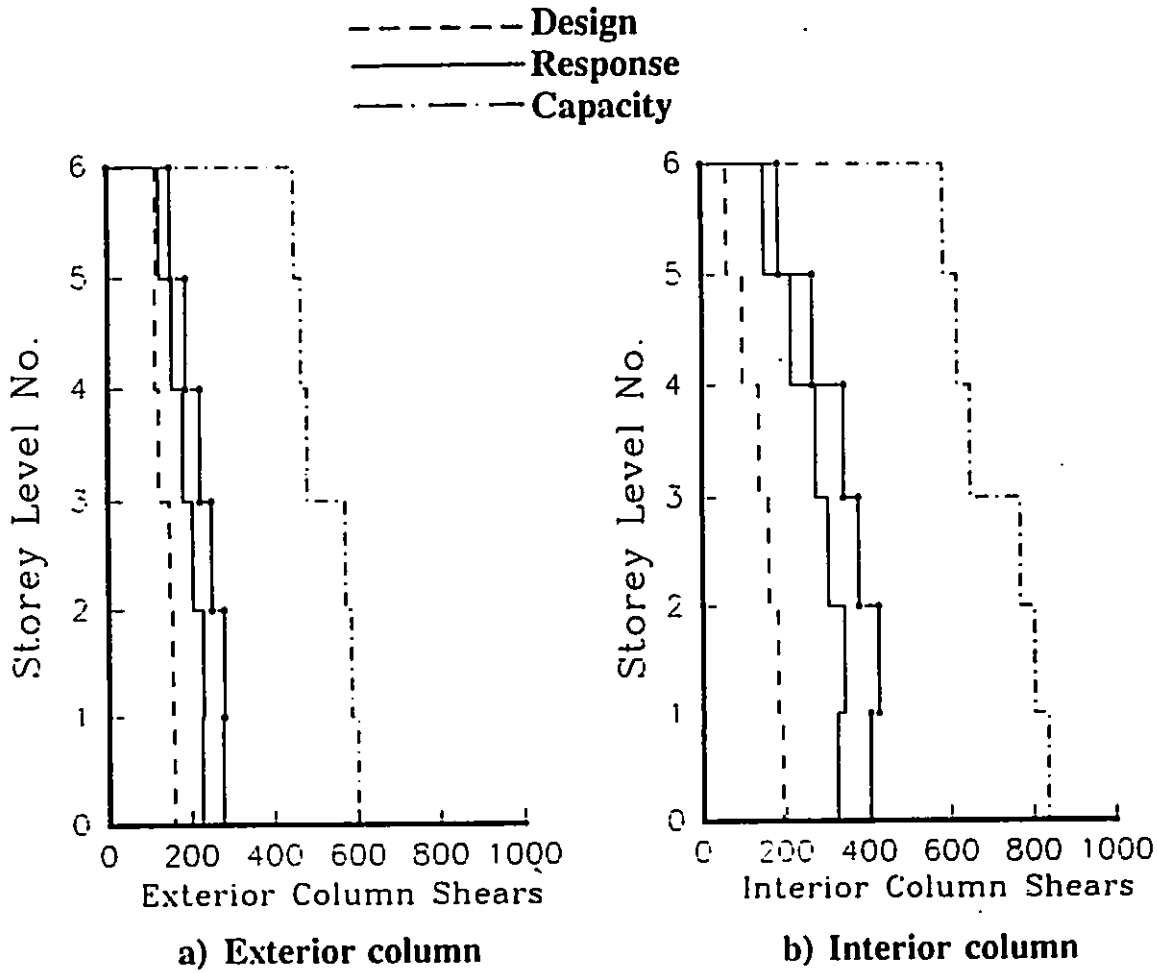

a) Exterior column

b) Interior column

Fig. (3.11) **Comparison between the shear demands and shear capacities of the columns of the six storey frame considered in chapter 3 (• = mean + σ).**

CHAPTER 4

EXPERIMENTAL RESPONSE OF BEAMS IN R/C FRAMES OF NOMINAL DUCTILITY

4.1 INTRODUCTION

An inelastic dynamic analysis of the nominally ductile frame in chapter 3 showed that the beams of that frame experienced shear demands that exceeded the capacity of the provided stirrups. Those beams would not show any distress due to shear if the concrete shear resistance can be counted on, as assumed in the Code for NDMRFs. However, it is debatable whether the concrete shear resistance can be relied upon in this case since the curvature ductility demands in those beams were in the order of 3.0. An experimental investigation is reported herein in order to examine the validity of including the concrete resistance in the design shear resistance calculations of the beams of nominally ductile frames that satisfy the minimum Code requirements. Two specimens were tested in this investigation. They were a scale-model of the beams of the frame described in chapter 3. The design of the specimens was based on the design provisions specified in the Canadian concrete design code (CSA 1984) applicable to nominally ductile frames.

A detailed description of the specimens and the testing procedure is provided in this chapter. The test results are reported, compared and discussed.

4.2 DESCRIPTION OF THE TEST SPECIMENS

The tested specimens were cantilever beams 200 mm wide by 400 mm deep. These cross section dimensions comprise a half-scale model of the beams of the six storey frame described in chapter 3. The dynamic analysis of the frame indicated that the average moment-to-shear ratio (shear span) in the beams is approximately 2.0 metres. For the half-scale specimens tested here, the moment-to-shear ratio (shear span) should be half that of the beams of the full-scale frames. Thus, the shear span of the tested cantilever specimens was selected to be 1086 mm.

The ratios of the longitudinal reinforcement were taken similar to those of a typical beam in the six storey frame described in chapter 3. Specimen I had a main steel ratio, ρ of 1.25 percent and a secondary steel ratio, ρ' of 0.50 percent. Specimen II had $\rho = 1.25$ percent and $\rho' = 0.75$ percent. For both specimens, the main steel consisted of 2 No. 25 bars. The secondary steel was 2 No. 15 bars in specimen I and 2 No. 20 bars in specimen II.

Specimen I was designed to represent a beam in a nominally ductile frame designed according to the current Canadian practice. Both concrete and steel were assumed to resist the applied shear forces and the stirrups were selected to satisfy the minimum requirements of clause 21.9.2.1.2 of the Canadian concrete design code.

The stirrups were spaced at one quarter the member depth, d, for a distance equal to twice the member depth from the face of the enlarged end block. To allow for the half-scale model, the stirrups were taken to be 6 mm diameter bars instead of the No. 10 bars specified in the code for scaling reasons (Krawinkler and Moncraz, 1981). Specimen II was designed to represent a beam in a nominally ductile frame in which the concrete shear resistance is neglected and the provided stirrups are adequate to resist the total applied shear force. The stirrups used in this specimen were also 6 mm diameter bars but placed at a smaller spacing than that of specimen I. The stirrups anchorage for both specimens was according to Code clause 12.13.2. The reinforcement details of the two specimens are shown in figure (4.1).

Both specimens were cast on the same day from the same batch of concrete. High strength ready-mix concrete with a minimum specified compressive strength of 30 MPa was used with a maximum aggregate size of 15 mm and a 75 mm specified slump. Six 150x300 mm cylinders were prepared from the batch. Compression tests on the cylinders at the day of testing resulted in an average compressive strength, f_c', of 32.5 MPa. Tension tests were performed on 300 mm long specimens cut from each of the reinforcing bars. Strains were measured using an extensometer, having a gauge length of 50 mm, clamped to the bar. The average stresses and strains obtained from three samples from each bar size are listed in table (4.1).

The ideal strengths of the two specimens were calculated based on the average properties of steel and concrete. Specimen I had an ideal strength of 122 kN

in the positive direction and 47 kN in the negative direction. The ideal strength of specimen II was 125 kN and 75 kN in the positive and negative directions respectively.

4.3 TEST SETUP

The specimen was held fixed at its enlarged end block while the beam tip was deflected slowly using a hydraulic jack. Figures (4.2) and (4.3) show diagrammatic sketches of the test setup while figure (4.4) shows a photograph of the setup.

To ensure proper fixation of the beam end, the specimens were cast with an enlarged end block. Two WF 310x94 steel beams were placed on top of the end block topped by two hydraulic jacks. The hydraulic jacks were made to react against a steel frame prestressed to the structural floor of the laboratory. The reaction force of the jacks (700 kN each) acted as a clamping force on the enlarged end block. A dial gauge placed to monitor the movement of the end block indicated that the block did not move during all stages of testing.

The load was applied to the tip of the beam using a double acting hydraulic jack. Two 400x200x15 mm plates were placed on the top and bottom of the beam. The plates were tied together using two 19 mm threaded rods. The bottom plate had a vertical plate welded to it. The vertical plate was attached to the end of the loading ram through a greased pinned connection. This will provide the mechanism for transmitting the reversing jack action to the beam. The detail of this connection is shown in figure (4.3).

4.4 INSTRUMENTATION AND DATA ACQUISITION

During testing, data was recorded from three sources :

1) The load applied to the specimen was measured by a load cell on the load ram. Deflection of the load point was measured by an independent LVDT mounted on a tubular frame.

2) Four additional LVDT's were positioned over the beam plastic hinge zone as shown in figure (4.5), to measure the shearing and flexural deformations in this region. The LVDT's were attached to a steel frame mounted on the specimen by four bolts using friction. The plastic hinge zone was assumed to extend into the beam a distance equal to the overall depth of the beam.

3) Two electrical resistance strain gauges attached to the second and fourth stirrup from the face of the end block to measure the strains in the stirrups.

Data from all sources was recorded by a computerized data acquisition system. The movement of the loading ram was stopped at different displacement levels to allow for the recording of the data. The load-displacement loops were plotted on the computer screen to allow the continuous monitoring of the progress of the test.

4.5 LOADING HISTORY

The loading history shown in figure (4.6) was used in testing both specimens. This loading history consists of two phases;

Load Control

Two cycles at 75 percent of the ideal strength of the specimen are applied to determine the initial elastic stiffness and extrapolate the yield displacement (Park, 1989). The yield displacement of specimen I was found to be 9 mm while it was 8 mm for specimen II. The two elastic cycles also help to ensure that all data acquisition channels are functioning properly.

Displacement Control

After determining the yield displacement from the elastic cycles, the specimen was subjected to an increasing displacement controlled loading history. Two cycles were applied at each ductility level starting from $\Delta/\Delta_y = 1.0$. Testing was continued until the specimen lost all ability to resist the applied load.

The main aim of loading was to subject the specimens to the same level of inelastic deformations experienced during earthquake excitation. The inelastic dynamic analysis showed that the beams of NDMRFs underwent mean curvature ductility demands ranging from 2.20 to 3.24. If the tested cantilever specimens were to behave in a purely flexural manner (as assumed in the dynamic analysis), these curvature ductility demands would correspond to displacement ductility demands ranging from to 2.04 to 3.08. Thus, it will be of particular interest to monitor the specimen performance within the above mentioned range of displacement ductility.

4.6 TEST RESULTS

The results recorded during testing and the observations made of each of the specimens behaviour are presented in this section. The main points of interest were the force- displacement loops, the cracking patterns and the measured strains in the stirrups. The objective is to determine the differences in behaviour of specimens I and II, having different hypothesis on the contribution of concrete to the shear resistance.

4.6.1 SPECIMEN I

This specimen had a nominal stirrups capacity, V_s, of 100 kN and a nominal concrete shear resistance, V_c, of 80 kN. The maximum applied shear force was 136 kN which is smaller than the hypothetical beam shear capacity ($V_c + V_s = 180$ kN). The specimen suffered a rapid strength deterioration in the positive direction of loading as shown in figure (4.7). The load-displacement loops show an obvious pinching effect near the zero-displacement portion of the curves. The specimen developed its ideal strength (P_i) in both the positive and negative directions at a ductility of 1.0. In the positive direction, the specimen developed its maximum strength, 136 kN, in the first cycle at a ductility of 3.0. This maximum strength is 12 percent higher than the specimen's ideal strength, 122 kN. In the negative direction, the specimen developed its maximum strength, 65 kN, at a ductility of 4.0. This maximum strength is 40 percent higher than the specimen's ideal strength, 47 kN. The strength deterioration in the positive direction was more rapid than it was in the

negative direction because of the much larger shear forces experienced by the specimen when loading is applied in the positive direction.

Figure (4.8) shows the propagation of cracks in this specimen at different displacement ductility levels. At a ductility of 1.0 (μ=1.0), vertical cracks appeared at the top and bottom of the specimen section. At μ= 2.0, the vertical cracks increased in length and width in addition to two major diagonal cracks which formed under loading in the positive direction. At a ductiiity of +3.0,the number of vertical cracks increased but their width did not increase significantly. However, one of the diagonal cracks has widened significantly as shown in figure (4.8b). At this stage, (second cycle at μ=+3), the strength in the positive direction dropped below 80 percent of the maximum strength attained during the test. This point marks the end of the acceptable behaviour of the specimen (Park, 1989). At μ=4.0, the diagonal cracks increased in width and length in addition to a slight concrete crushing occurred at the top of the section. Failure of the specimen occurred when the top steel was ruptured at μ=-5.0. At this stage, the plastic hinge zone was a mesh of intersecting vertical and diagonal cracks.

The readings of the strain gauges placed on the transverse reinforcement showed that the stirrups started to yield at a ductility of + 3.0. The yielding of the stirrups resulted in the widening of diagonal cracks and increased shear deformations in the plastic hinge zone. For a given beam tip displacement, this increased shear deformations resulted in less straining of the longitudinal reinforcement and

therefore reduced the flexural strength the specimen could develop. This is reflected in the reduction of loads sustainable in the load-displacement plot. The increased shear displacements also resulted in the abrasion and grinding of the concrete along the crack faces during the cyclic loading since flexural cracks no longer close completely at subsequent cycles.

Since the shear capacity of this specimen (concrete+stirrups) is greater than the maximum applied shear forces, the stirrups will yield if (and only if) the concrete shear resistance becomes unattainable at this stage of loading. The displacement ductility level at which the stirrups started to yield and the rapid strength deterioration started is around 3.0.

4.6.2 SPECIMEN II

In this specimen, the nominal capacity of the stirrups (165 kN) was larger than the maximum induced shear force in the specimen (152 kN). The load-displacement curves shown in figure (4.9) indicate that the loops of the specimen were stable. The strength developed in the second cycle at each ductility level was only slightly lower than the strength in the first cycle at the same ductility level. However, when the specimen was displaced to the next ductility level, the strength increased above the strength in the previous cycle. This increase in strength was observed up to a ductility of 5.0 in the positive direction and 6.0 in the negative direction. Afterwards, the strength started to deteriorate. A much reduced pinching effect was observed in the loops. The specimen developed its ideal strength in both the positive and negative

directions at a ductility of 1.0. In the positive direction, the specimen developed its maximum strength, 152 kN, in the first of the two cycles at a ductility of 5.0. This maximum strength is 25 percent higher than the specimen's ideal strength. In the negative direction, the specimen developed its maximum strength, 100 kN, at a ductility of 6.0. This maximum strength is 35 percent higher than the specimen's ideal strength.

Figure (4.10) shows the propagation of cracks at different ductility levels. Essentially, the cracking patterns and crack propagation were similar to those observed in specimen I. However, the diagonal cracks growth was effectively controlled by the stirrups even at ductility levels of 3.0 and 4.0. Spalling of the concrete cover started at a ductility of +5.0 but was not extensive till a ductility of 7.5 was reached. The spalled cover was the main reason for the deterioration of the specimen strength. The strength of the specimen dropped below 80 percent of the maximum strength in the second cycle at a ductility of 7.5 which marks the failure of the specimen.

Comparing the crack patterns of specimens I and II at μ=3.0 (figures 4.8b and 4.10b) shows that the number of diagonal cracks in specimen I was more extensive than that in specimen II. Moreover, the diagonal cracks in specimen I were significantly wider and deeper. Specimen II mainly experienced vertical flexural cracking until this stage of loading.

The better performance of specimen II over specimen I can be attributed to the fact that the stirrups alone were adequate to resist the applied shear forces resulting in controlled diagonal cracking and hence led to smaller inelastic shear deformations. The readings of the strain gauges placed on the transverse reinforcement of specimen II have shown that the stirrups did not yield during the whole test. The controlled shear deformations in turn resulted in less abrasion and grinding on the faces of the diagonal and vertical cracks. The controlled shear deformations allowed the increase of the flexural rotation in proportion to the beam tip displacement. This caused increased straining of the longitudinal steel with the increase of the imposed displacement resulting in developing larger specimen strength.

4.7 FLEXURAL AND SHEAR DEFORMATIONS IN THE PLASTIC HINGE ZONE

Under cyclic loading, a large portion of the deflection of a concrete beam results from inelastic flexural and shear deformations due to cracking in the hinging zones. In such a case, using the conventional methods to estimate the beam tip deflection can result in large errors. For this reason, the measurements of the LVDTs placed in the hinging zone will be used to calculate the distortion occurring in that region.

4.7.1 CALCULATION OF HINGE FLEXURAL AND SHEAR DEFORMATIONS FROM LVDT DATA

Consider the hinging zone of the specimen EABG as shown in figure (4.11) where the zone is assumed to extend into the beam a distance equal to the overall beam depth. Due to both flexural and shear deformations, point A moves to A' and B to B'. The data from the LVDT's placed in the hinging zone can be used to estimate the flexural rotation and shear strain in that region. Referring to figure (4.11), the following notations are used;

L_1 = EA' (4.1a)
L_2 = GB' (4.1b)
L_3 = GA' (4.1c)
L_4 = EB' (4.1d)

From trigonometry;

$$\angle A'EG = \cos^{-1}\left[\frac{L_1^2+H^2-L_3^2}{2HL_1}\right] \tag{4.2a}$$

$$\angle B'GE = \cos^{-1}\left[\frac{L_2^2+H^2-L_4^2}{2HL_2}\right] \tag{4.2b}$$

Assuming an initial right angle between the beam and the face of the end block;

$$\theta_1 = \frac{\pi}{2} - A'EG \tag{4.3a}$$

$$\theta_2 = B'GE - \frac{\pi}{2} \tag{4.3b}$$

Using equations (4.2) and (4.3) it can be shown that,

$$\theta_3 = \tan^{-1}\left[\frac{L_1\sin\theta_1 + L_2\sin\theta_2}{L_1\cos\theta_1 + L_2\cos\theta_2}\right] \tag{4.4a}$$

$$\theta_4 = \sin^{-1}\left[\frac{L_1\cos\theta_1 - L_2\cos\theta_2}{H}\right] \tag{4.4b}$$

The angle θ_3 is taken as the shear strain within the plastic hinge zone while the angle θ_4 is taken as the angle of flexural rotation within the zone.

4.7.2 SHEARING BEHAVIOUR OF THE PLASTIC HINGE ZONE

The relationship between the applied load and the shear strain in the plastic hinge zone for specimens I and II are shown in figure (4.12). It can be seen that the curves are similar in shape for both specimens, even though the magnitude of shear strains for specimen I was much larger than those for specimen II. The curves show an obvious pinch near the zero load portion of the load-shear strain relationship. This pinch can be explained based on the shear resistance mechanisms at various stages of loading. Consider the scenario when the applied load is reduced from its maximum positive value, cracks in the lower part of the beam remain open due to the yielding of the longitudinal steel. When the load is reversed, other cracks open in the upper part of the beam resulting in a vertical crack over the whole depth of the beam. In those cases, the shear is resisted solely by the dowel action in the

longitudinal reinforcement resulting in very low shear stiffness. As the load is increased in the negative direction, cracks in the lower part are closed allowing aggregate interlock, friction and stirrups to start resisting shear resulting in an increase in the shear stiffness. The relatively flexible mechanism of dowel action alone to resist shear is the cause of the pinching in the shape of the load-deformation curves.

The shear strain in the second cycle at any specified beam tip displacement is always larger than the shear strain in the first cycle at the same displacement level as shown in figure (4.12). This happened due to the increase in the crack widths and the abrasion of concrete on the crack faces with the increase in the number of cycles.

4.7.3 FLEXURAL BEHAVIOUR OF THE PLASTIC HINGE ZONE

The relationship between the applied load and the flexural rotation in the plastic hinge zone of specimens I and II are shown in figure (4.13). It can be seen that the load-flexural rotation relationships are more stable than the load-shear strain relationships. There is only slight pinching in the loops of either specimen, because as a vertical crack is open over the entire depth of the beam, the moment is carried primarily by the top and bottom steel. After the cracks close due to local compression, part of the compression force is transferred from the compressed reinforcement to the concrete. The transition of the compression forces from steel to concrete during the process of crack closing does not cause a significant change in the flexural stiffness.

4.7.4 COMPARISON OF MEASURED AND CALCULATED DEFLECTIONS

Four different components of deflection were considered in calculating the beam tip deflection at various load points. Referring to figure (4.14), the beam tip deflection, Δ, can be calculated as follows;

$$\Delta = \Delta_1 + \Delta_2 + \Delta_3 + \Delta_4 \qquad (4.5)$$

where

Δ_1 = Deflection due to flexural rotation within the plastic hinge zone.
Δ_2 = Deflection due to shear strain within the plastic hinge zone.
Δ_3 = Deflection due flexural deformations outside the plastic hinge zone.
Δ_4 = Deflection due shear deformations outside the plastic hinge zone.

The flexural rotation within the hinging zone was monitored using the LVDT measurements as explained in section (4.7.1). The beam tip displacement due to the hinge flexural rotation can be calculated as the product of the angle of rotation times the distance between the hinging zone and the load application point.

The shear strain within the hinging zone was also calculated using the LVDT readings. Elastic methods were considered inappropriate due to the typically nonlinear shear stress-shear strain behaviour of the hinge region. The beam tip displacement due to hinge shear strain is the product of the shear strain angle times the plastic hinge length (assumed equal to the overall beam depth).

The deflection due to the flexural deformation outside the plastic hinge zone can be calculated using elastic methods of deflection calculation based on a cracked section of the specimen. The cracked moment of inertia is assumed as 60 percent of the gross moment of inertia of the beam section neglecting steel. Deflections due to

shear deformations between the hinging zone and the beam end were calculated using elastic analysis as follows;

$$\Delta_4 = \frac{Vl'}{bdG_c} \qquad (4.6)$$

where
V = measured beam shear.
l' = length of beam section between the hinging zone and point of load application.
b = beam width.
d = beam effective depth.
G_c = concrete shear modulus = $0.4\,E_c$
E_c = concrete modulus of elasticity = $5000\sqrt{f'_c}$
f'_c = concrete compressive strength.

Figures (4.15) and (4.16) show the comparison between the measured and calculated deflections at different ductility levels for specimens I and II respectively. There is an excellent agreement between measured and calculated deflections for both specimens. The beam tip deflection results mainly from the inelastic flexural and shear deformations within the plastic hinge zone (Δ_1 and Δ_2). Moreover, the contribution of the hinge shear strain to the total deflection is very large at the low displacement values. This is due to the low shear stiffness values at or near zero displacement levels as explained in section 4.7.2.

The contribution of the different components to the beam tip deflection was calculated as a percentage of the total deflection at the peak displacement at each ductility level up to μ=5.0. The percentages of the different components for specimens I and II are shown in figure (4.17).

In specimen I, the deflection due to the hinge shear strain increased from 25 percent of total deflection at μ=1.0 to 60 percent of total deflection at μ=5.0. In specimen II, the deflection due to the hinge shear strain increased from 25 percent of total deflection at μ=1.0 to only 35 percent of total deflection at μ=5.0. In specimen I, the hinge flexural rotation contributed less to the total deflection as the ductility level increased. This indicates that the strain in the longitudinal steel did not increase in proportion to the beam tip displacement, thus resulting in the beam not able to develop larger flexural strength as the ductility level increased. In specimen II, the contribution of the hinge flexural rotation to the total deflection was almost constant for all ductility levels. This indicates that the strain in the longitudinal reinforcement increased in proportion to the beam tip displacement resulting in increased flexural strength as the ductility level increased.

4.7.5 RELATIONSHIP BETWEEN DISPLACEMENT AND CURVATURE DUCTILITIES

If the tested specimens were to behave in a purely flexural manner (i.e. shear deformations were non-existent), the relationship between displacement ductility, μ_Δ and curvature ductility, μ_ϕ would be a straight line given by the following formula (Park and Paulay, 1975)

$$\mu_\phi = \frac{(\mu_\Delta - 1)\, L/L_p}{3\,(1 - 0.5 L_p/L)} + 1 \qquad (4.7)$$

where
L = specimen length
L_p = plastic hinge length (assumed equal to overall beam depth)

This relationship is depicted by the dotted lines in figures (4.18a) and (4.18b) for specimens I and II respectively.

For the specimens tested here, a large part of the beam tip deflection was due to shear deformations within the plastic hinge zone. Therefore, the relationship between μ_ϕ and μ_Δ will not follow the straight line given by equation (4.7). The flexural deformations of the plastic hinge zone can be used to calculate the curvature ductility at different displacement ductility levels. This relationship is depicted by the solid lines in figure (4.18). In specimen I, the difference between the solid and dotted lines is larger than that for specimen II. The reason is the larger inelastic shear deformations in specimen I due to the stirrups yielding.

In specimen I, the rapid strength deterioration started at a displacement ductility of 3.0. According to figure (4.18a), the corresponding curvature ductility is 2.20. This is in the same order as (or even lower than) the ductility demands experienced during earthquake excitation in the beams of NDMRFs that satisfy the minimum code requirements.

4.8 CALCULATION OF AVAILABLE DUCTILITY

According to Park (1989), the available ductility factor of a specimen is "that ductility level which the specimen can sustain for four cycles with a less than 20

percent drop in strength". To obtain the available ductility of any specimen subjected to a loading history such as the one used in this experiment, Park (1989) suggested the following procedure;

1) Determine the load excursion at which the strength of the specimen drops below 80 percent of the maximum strength attained during the test.

2) Calculate the cumulative ductility factor, $\Sigma\mu$, up to but not including the load excursion determined in step 1.

3) The available ductility factor is calculated as $\mu_a = \Sigma\mu/8$.

The above mentioned procedure assumes that four cycles at a ductility μ_a (eight load excursions) will result in the same reduction in applied load as any arbitrary loading history applied up to $\Sigma\mu = 8\mu_a$.

Application of this procedure to specimen I is shown in figure (4.19). The cumulative ductility is found to be 14 and thus $\mu_a = 1.75$. Similar calculation for specimen II, shows that the cumulative ductility is 92 and μ_a was found to be 11.5. Therefore, the behaviour of specimen II is shown to be more ductile than specimen I.

4.9 ENERGY DISSIPATION CAPACITIES

One of the most important aspects of structural performance under cyclic loading is the ability of the structure to adequately dissipate energy. The energy dissipated by the beams in this study is calculated as the area enclosed by the load-

displacement loops. Specimen I dissipated 22.1 kN.m while specimen II dissipated 121 kN.m. However, comparing specimen behaviour solely on the basis of energy dissipation can lead to misleading results. For example, as a beam size or reinforcement is increased, the energy dissipated under cyclic loading may increase, but the beam may be suffering strength deterioration and pinching due to larger shear forces.

An improved measure of cyclic performance can be obtained using the energy dissipation index, D_i (Darwin and Nmai, 1986), which normalizes the total dissipated energy with respect to the elastic energy at yield.

$$D_i = \frac{E_H}{0.5(P_y^+\Delta_y^+ + P_y^-\Delta_y^-)} \qquad (4.8)$$

where
E_H = Total dissipated hysteretic energy.
P_y^+ = Positive yield load.
Δ_y^+ = Positive yield displacement.

A comparison of the energy index computed at different load cycles for specimens I and II is shown in figure (4.20). It can be seen that D_i for specimen II was larger than that for specimen I for all load cycles. This is an indication that the capacity of energy dissipation of specimen II was superior to that of specimen I.

4.10 SUMMARY OF EXPERIMENTAL RESULTS

The results of the experiments performed on two cantilever beams were reported and discussed in this chapter. Specimen I was designed and detailed to represent a beam in a nominally ductile frame according to the current Canadian practice. Specimen II represented a beam in a nominally ductile frame in which the concrete shear resistance is neglected in the design and the stirrups are designed to resist the total applied shear force. The following remarks summarize the findings of this experimental investigation;

1) Although the shear capacity of specimen I (concrete and stirrups) was larger than the applied shear forces, the stirrups started to yield at a calculated curvature ductility level of 2.20, indicating that the concrete shear resistance can not be relied upon for ductility demand levels larger than that level. Since the same order of ductility demands was obtained in the inelastic dynamic analysis of the nominally ductile frame reported in chapter 3, it is concluded that concrete shear resistance V_c should not be taken into account in evaluating the shear resistance of the beams of NDMRFs that satisfy the minimum code requirements. This is in contrast to the recommendation given in the current Canadian Code, where V_c can be taken into account for beam shear resistance evaluation in NDMRFs.

2) Due to stirrups yielding, specimen I exhibited large diagonal cracks and excessive shear deformations. This resulted in rapid strength deterioration and

significant pinching in the hysteresis loops. In specimen II, the stirrups did not yield and the load-displacement loops were stable with only slight strength deterioration and pinching.

3) In specimen I, the contribution of the hinge shear strains to the total deflection was larger than that in specimen II, especially at higher ductility levels. This indicates that the inelastic shear deformations were uncontrolled due to the stirrups yielding.

4) The available ductility factor (Park, 1989) for specimen II was approximately 7 times larger than that of specimen I. This indicates that specimen II would be able to sustain larger ductility demands than specimen I without a significant loss in strength.

5) The energy dissipation index of specimen II was much larger than that of specimen I. Thus specimen II is superior to specimen I in energy dissipation which makes it (specimen II) more desirable as a member of a structure in a seismically active zone.

Table (4.1) Properties of reinforcing bars used in the experiment.

bar	Area(mm^2)	f_y(MPa)	f_u(MPa)	ϵ_u
6mm	28	440	622	0.14
No. 10	100	480	668	0.20
No. 15	200	472	675	0.16
No. 20	300	458	663	0.17
No. 25	500	451	628	0.15

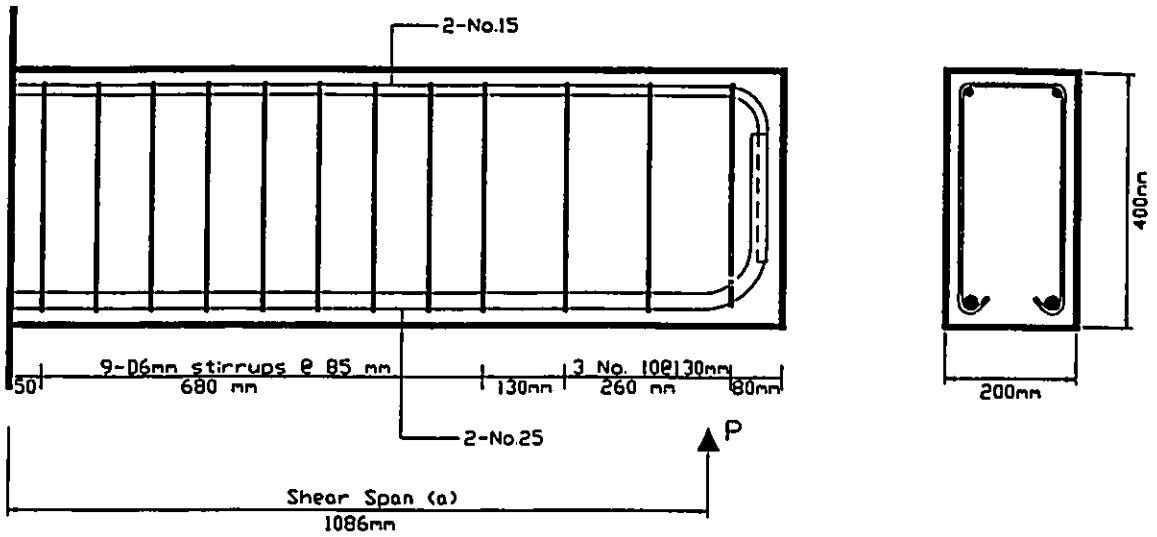

a) Specimen I.

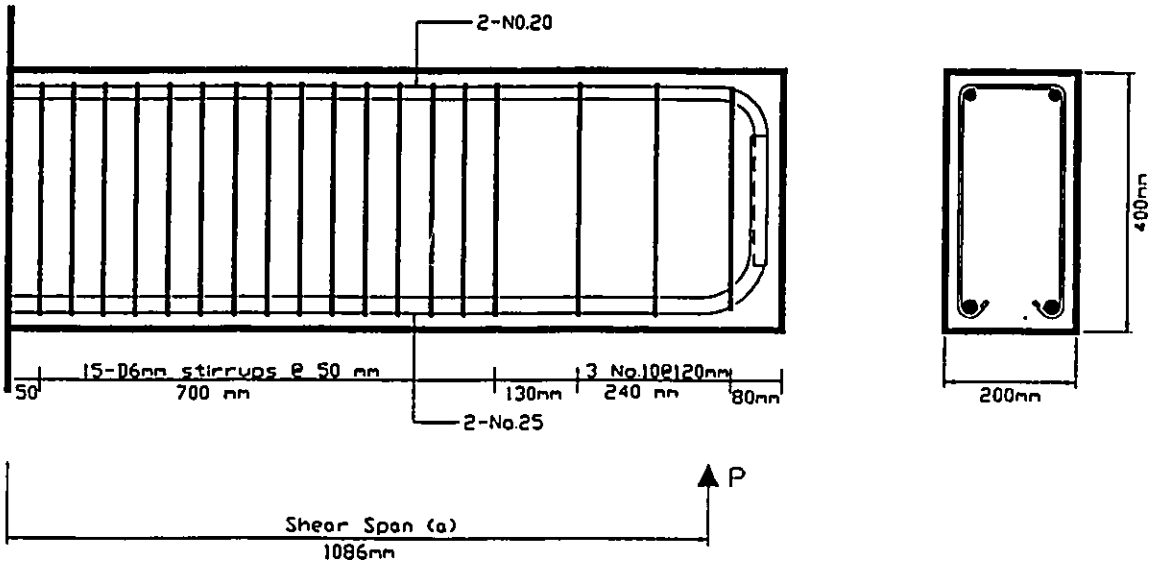

b) Specimen II.

Fig. (4.1) Reinforcement details of the test specimens.

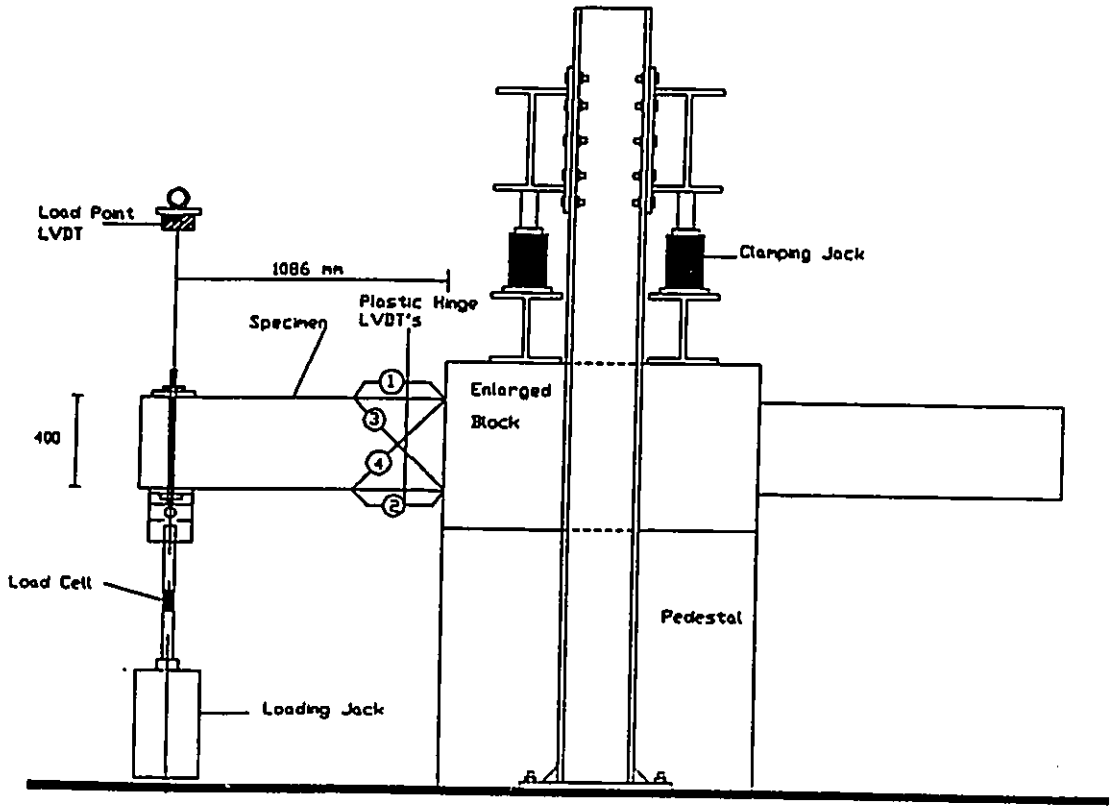

Fig. (4.2) Front view of the test setup.

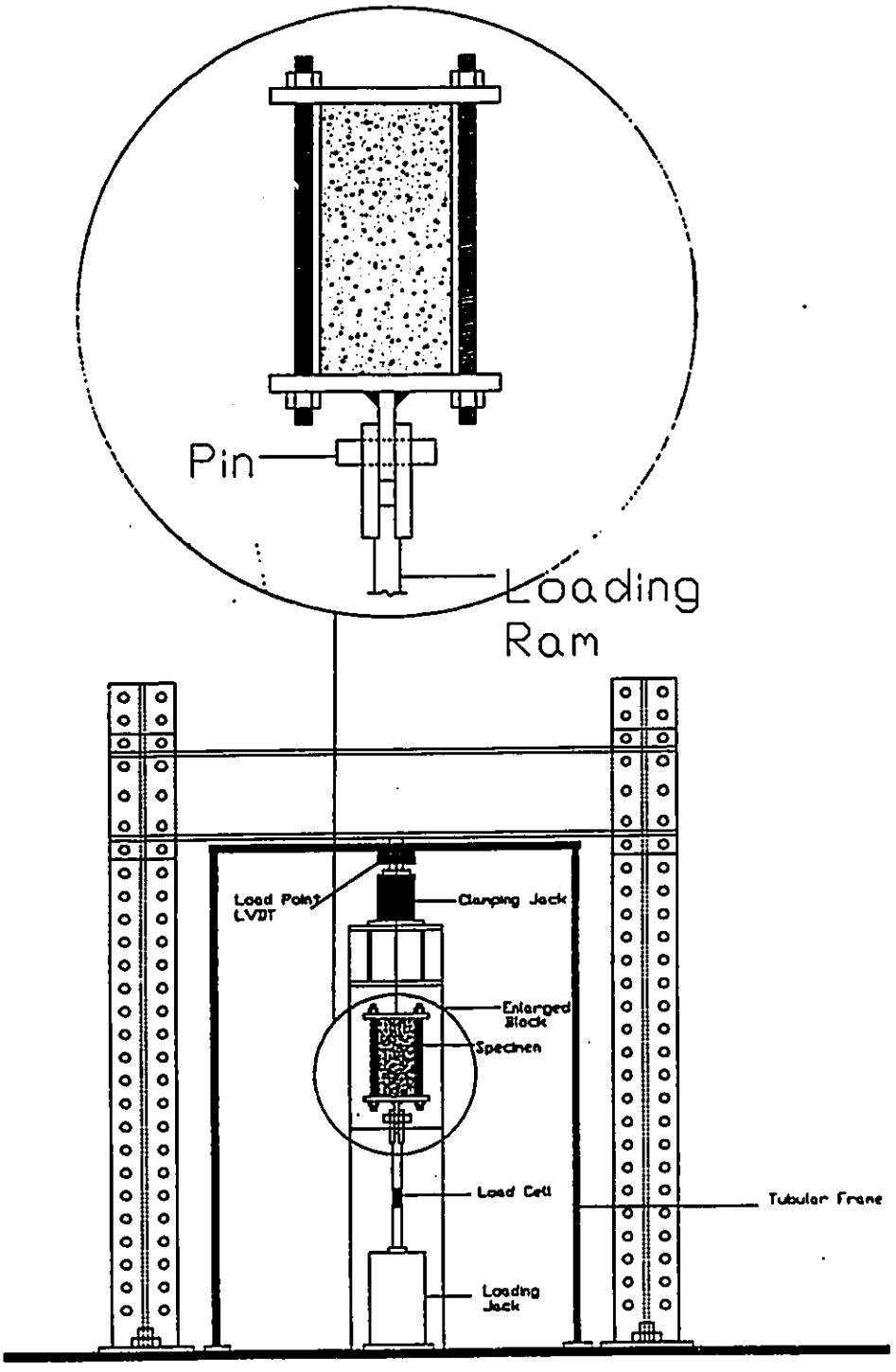

Fig. (4.3) Side view of the test setup.

Fig. (4.4) Photograph of the test setup.

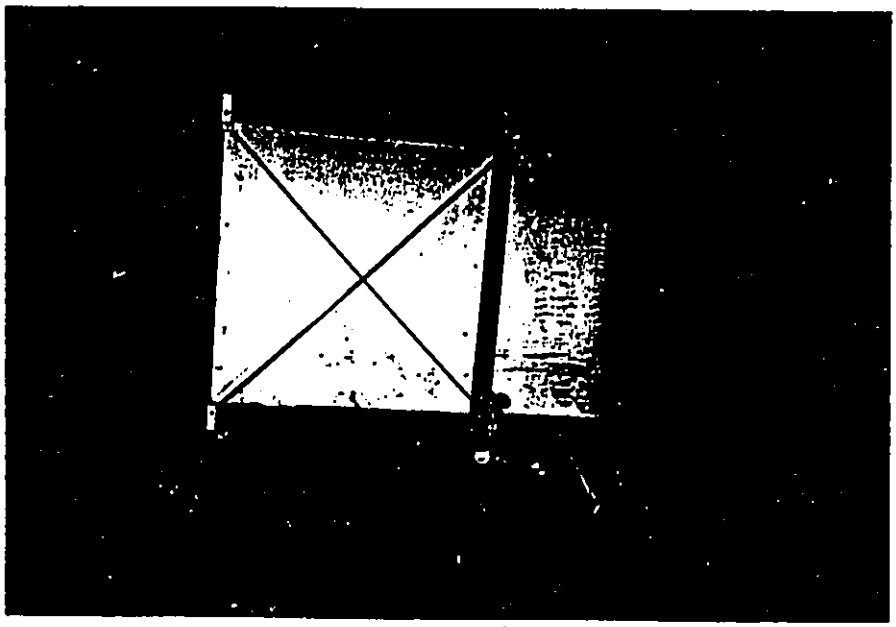

Fig. (4.5) Arrangement of LVDT's in plastic hinge zone.

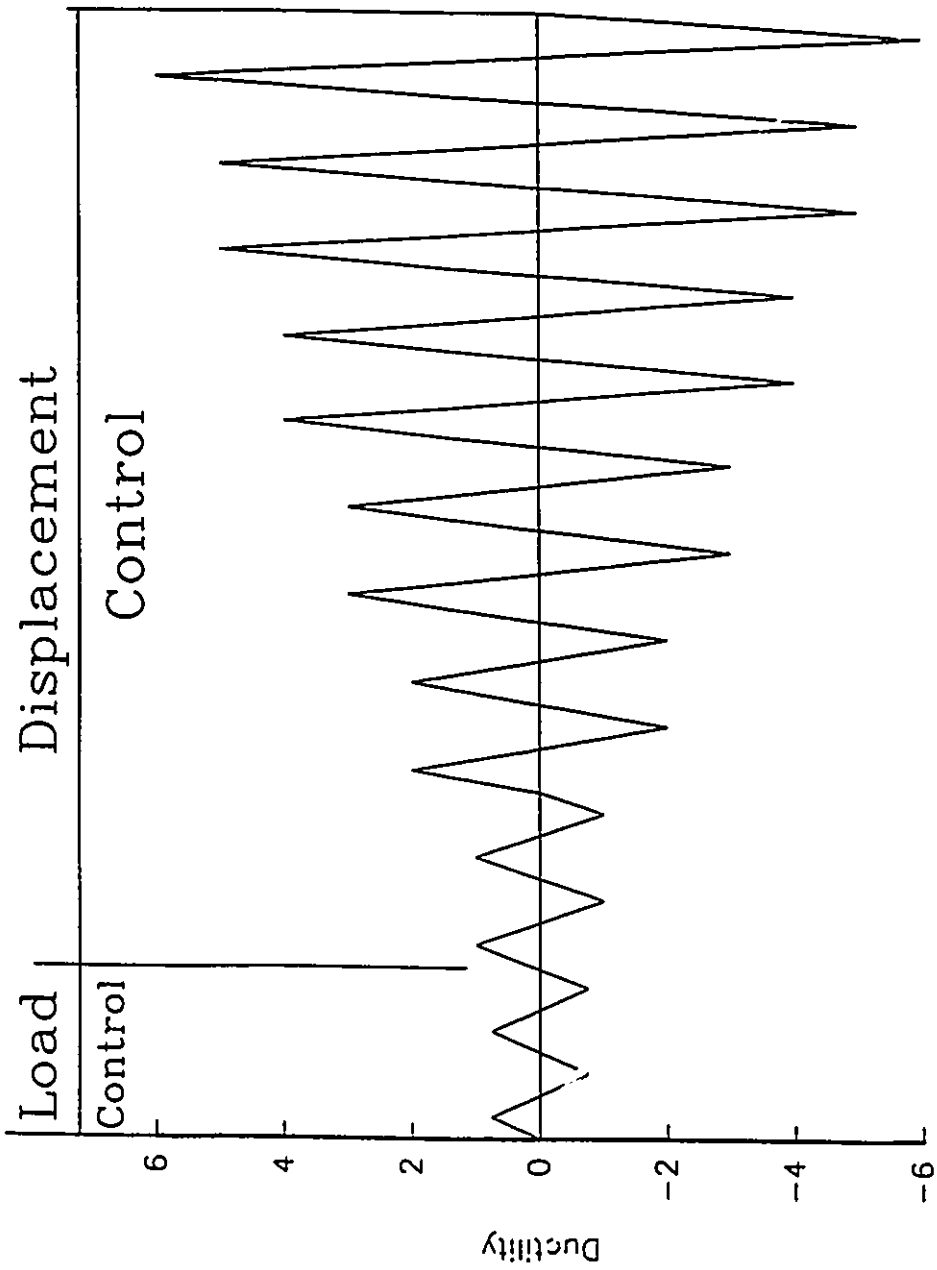

Fig. (4.6) Loading history used in the experiments.

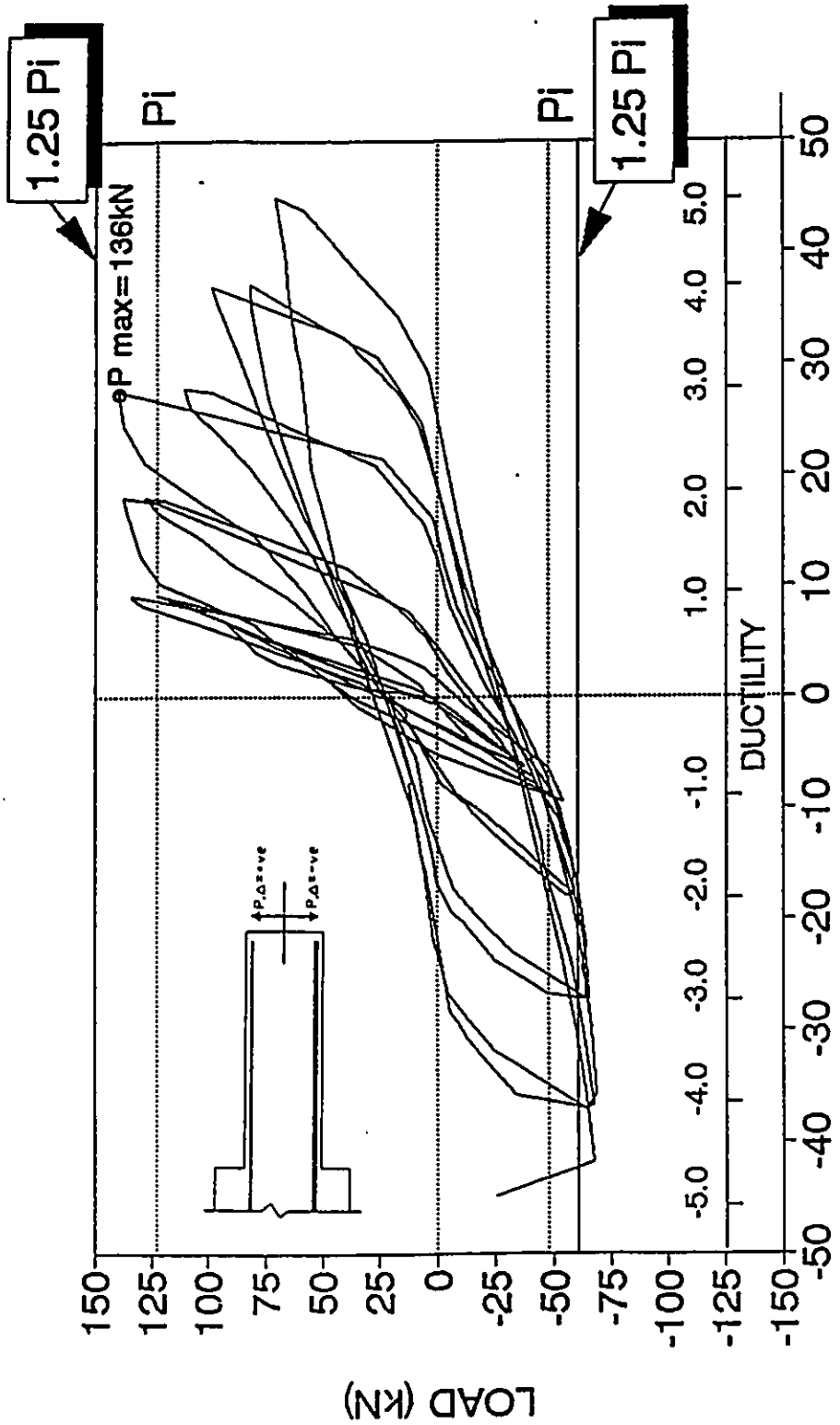

Fig. (4.7) Load-displacement loops of specimen I.

a) $\mu = 2.0$

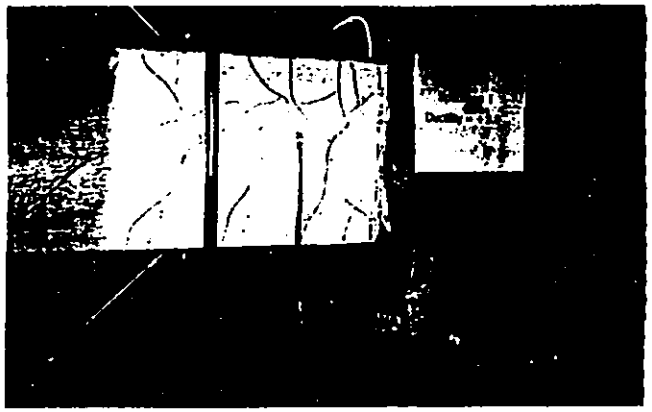

b) $\mu = 3.0$

c) $\mu = 4.0$

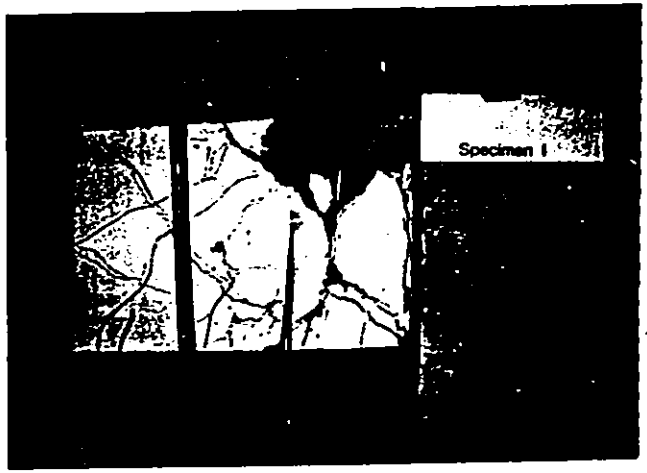

d) failure

Fig. (4.8) Crack propagation in specimen I.

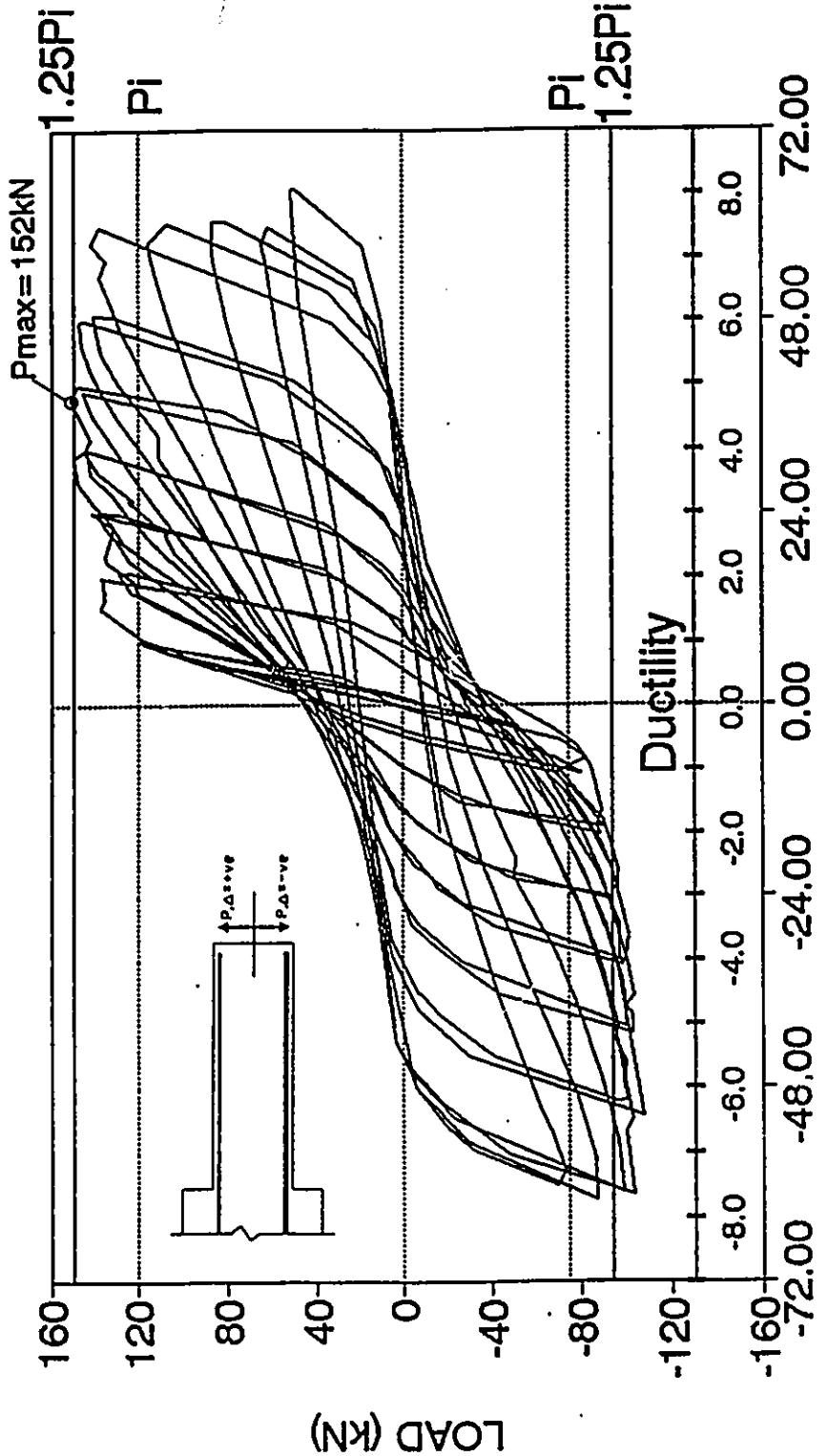

Fig. (4.9) Load-displacement loops of specimen II.

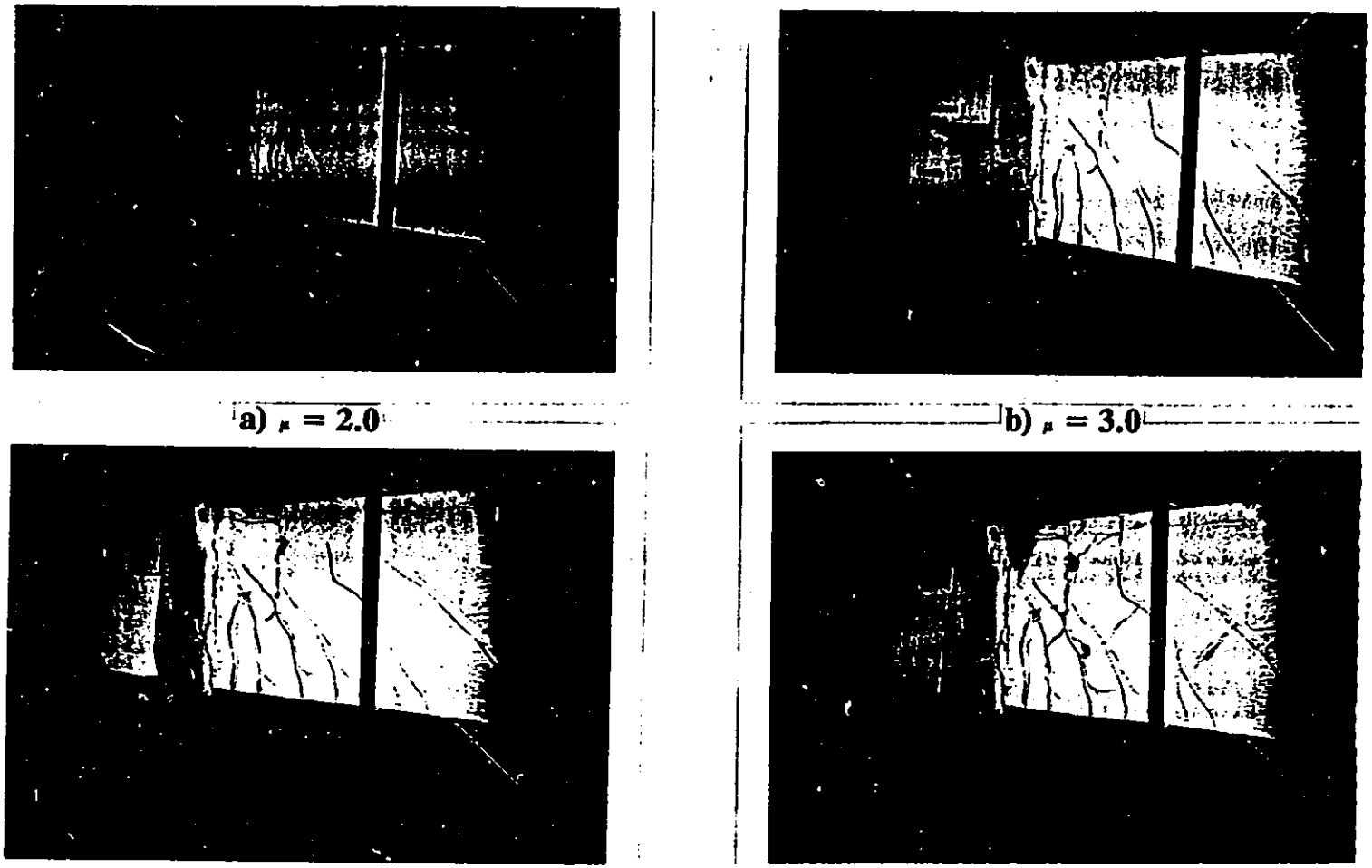

a) $_{\mu}$ = 2.0 b) $_{\mu}$ = 3.0

c) $_{\mu}$ = 4.0 d) $_{\mu}$ = 5.0

Fig. (4.10) Crack propagation in specimen II.

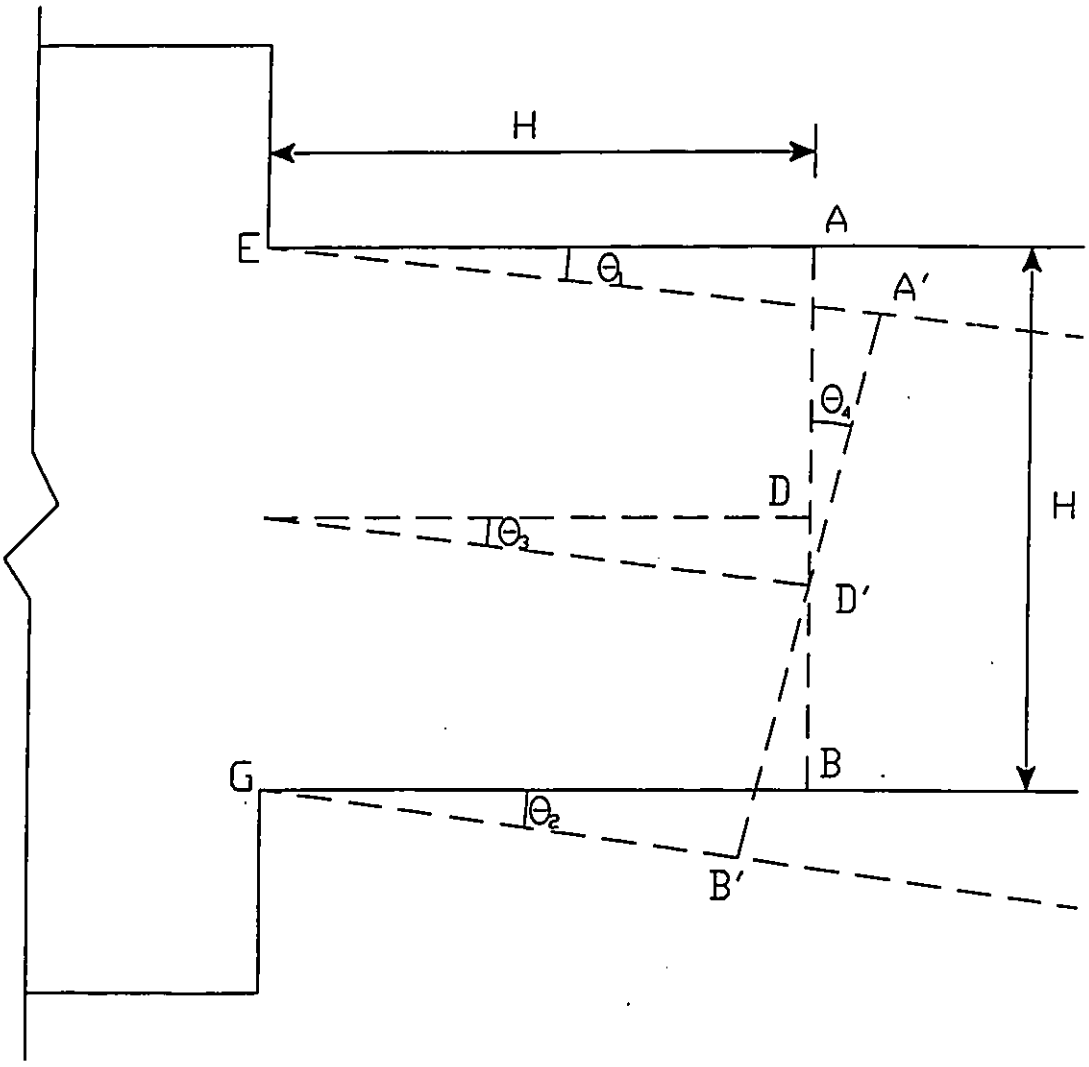

Fig. (4.11) Calculation of flexural and shear deformations in plastic hinge zone.

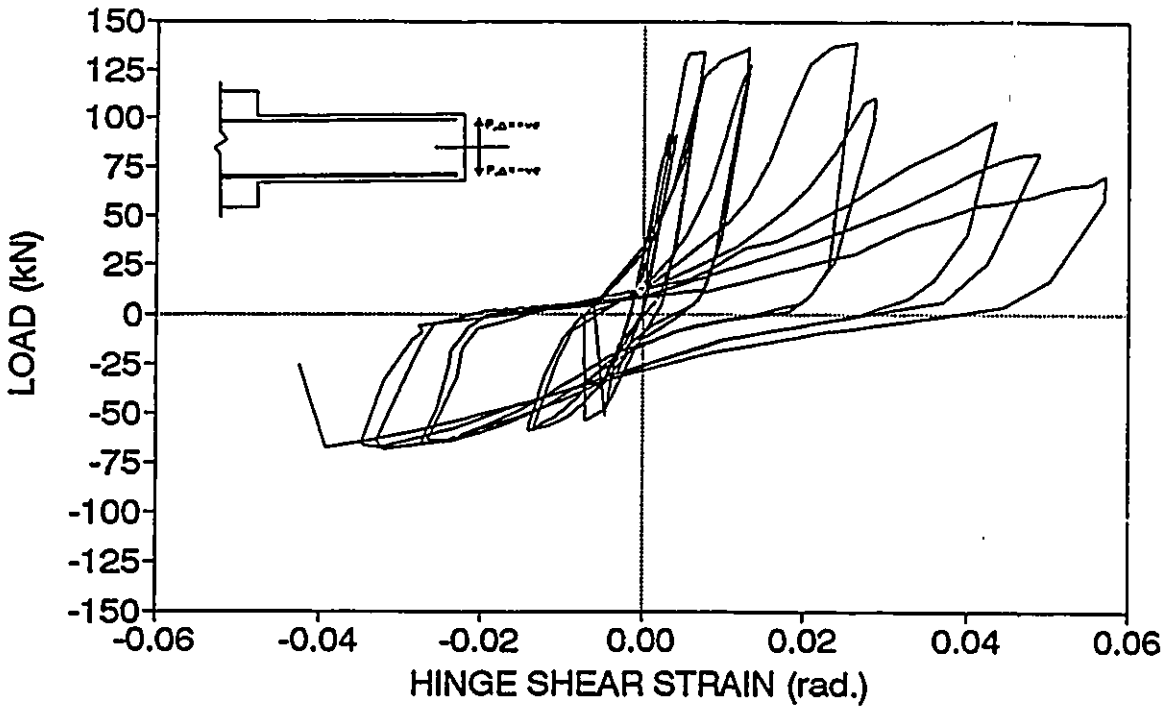

a) Specimen I.

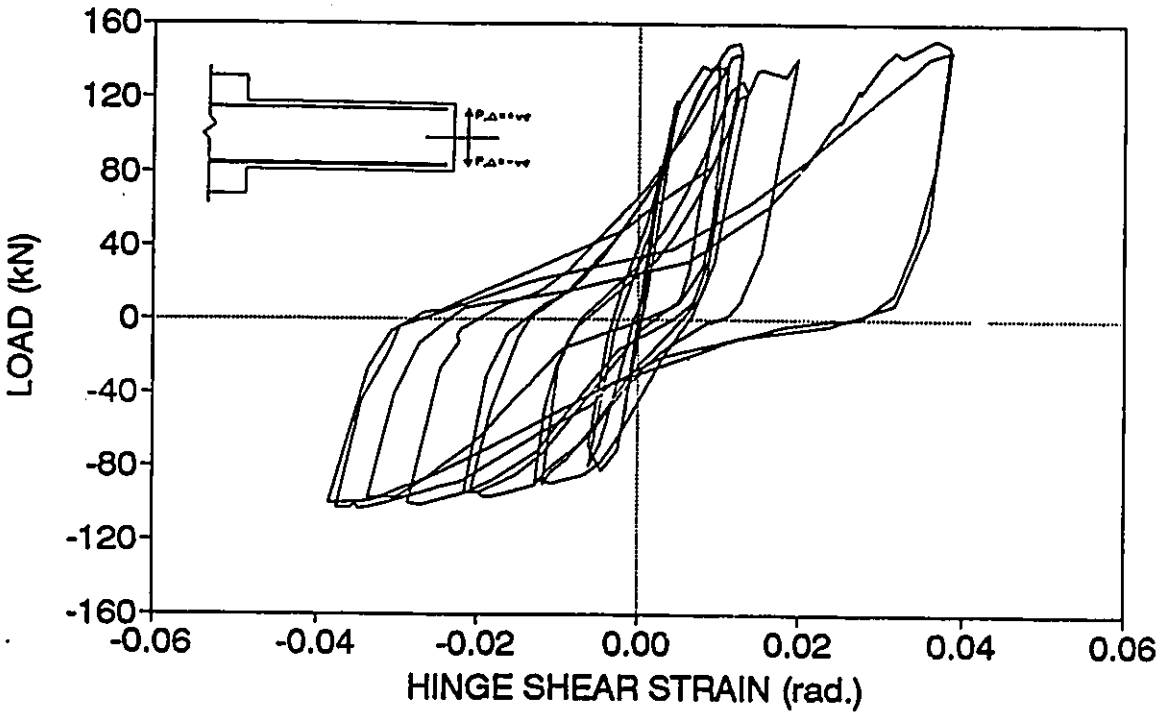

b) Specimen II.

Fig. (4.12) Load-shear strain loops for the tested specimens.

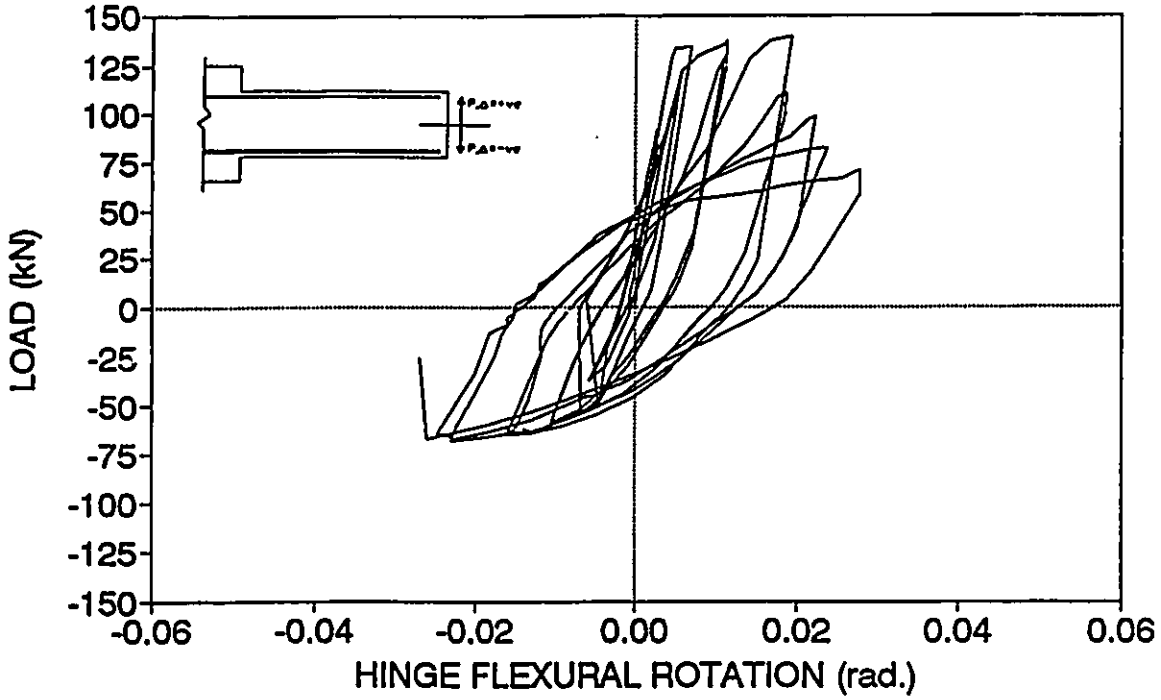

a) Specimen I.

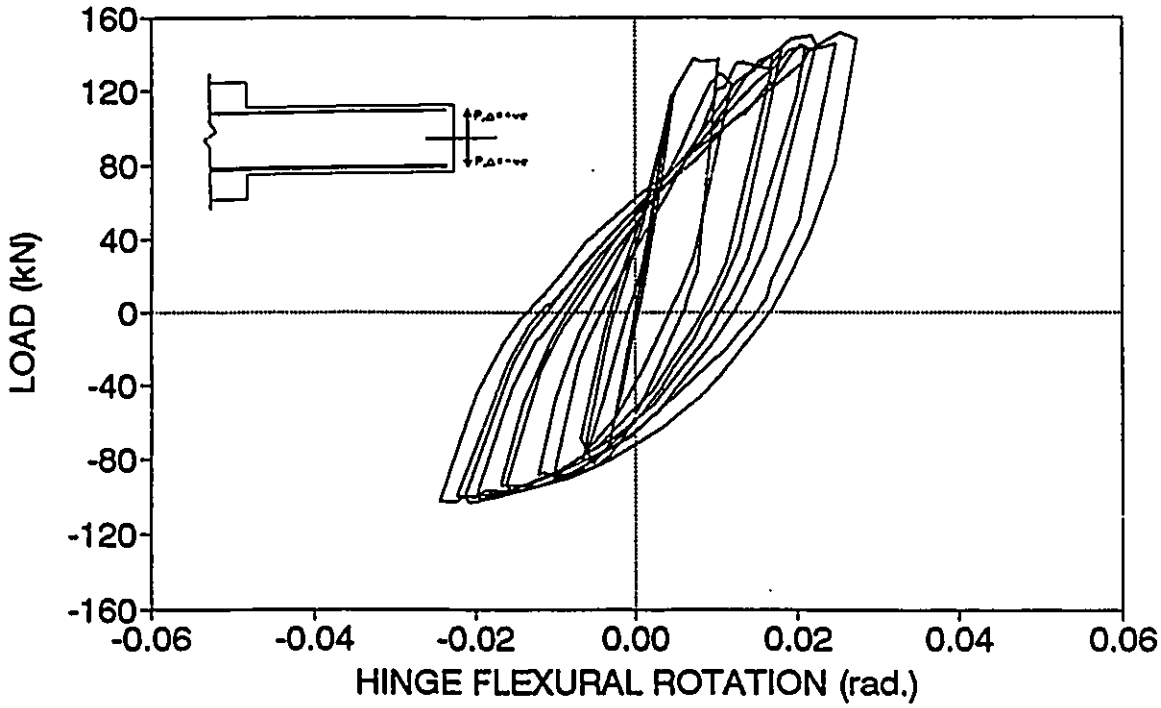

b) Specimen II.

Fig. (4.13) Load-flexural rotation loops for the tested specimens.

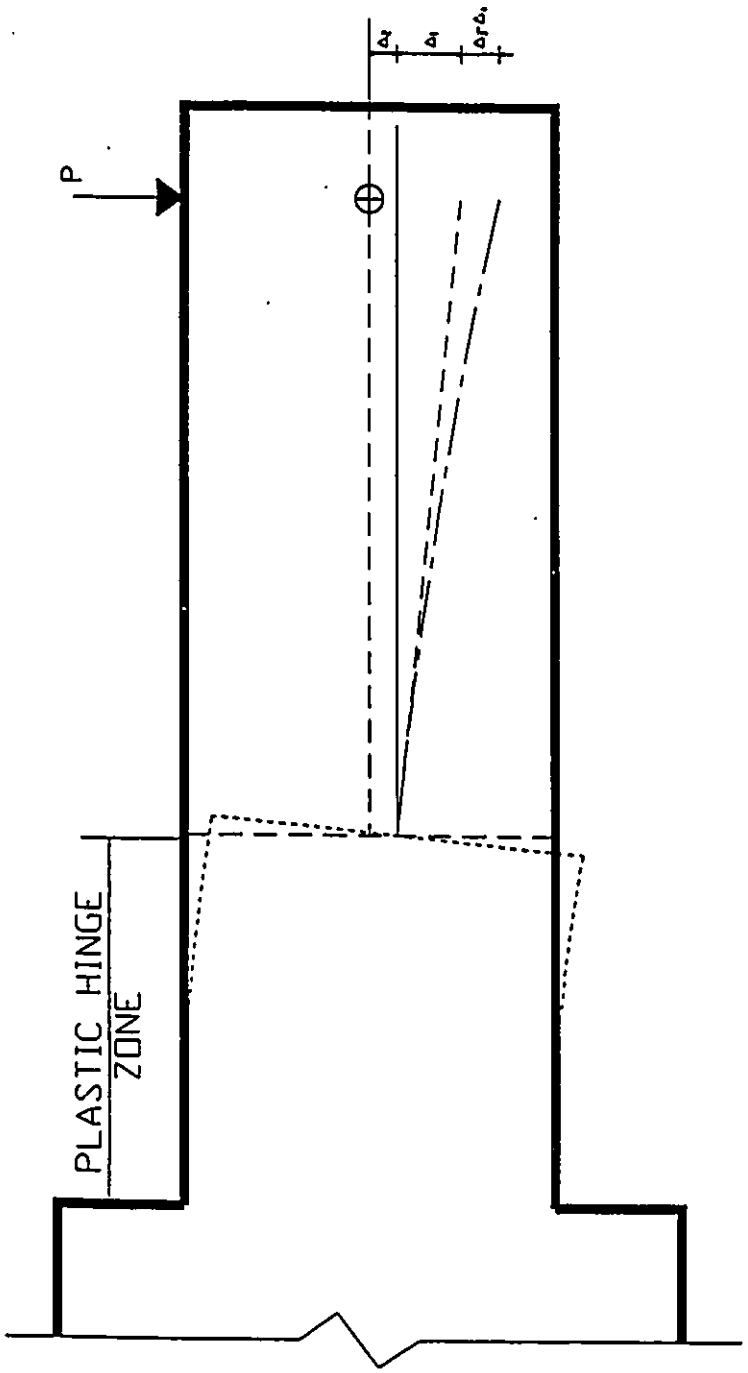

Fig. (4.14) Different components of the beam tip deflection.

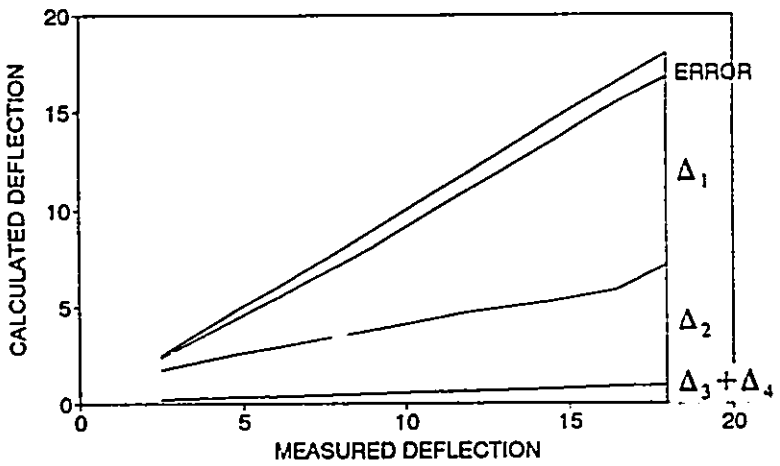

a) $\mu = 2.0$

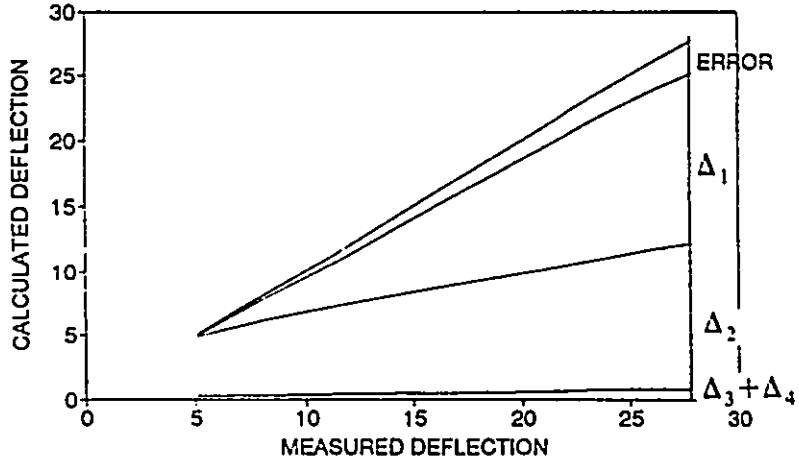

b) $\mu = 3.0$

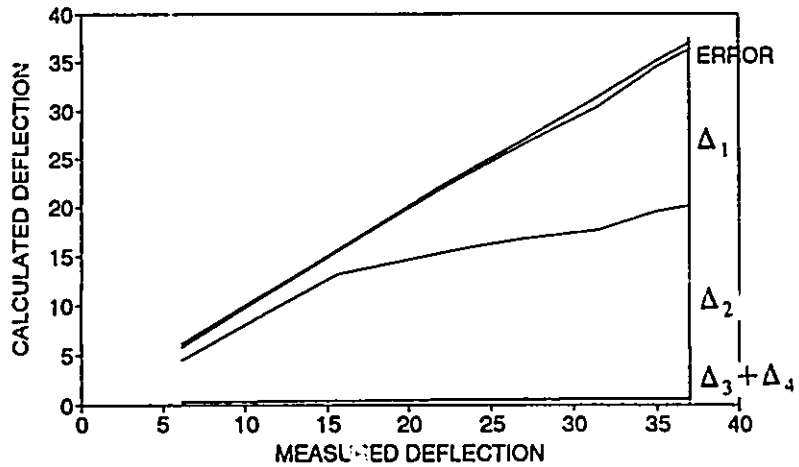

c) $\mu = 4.0$

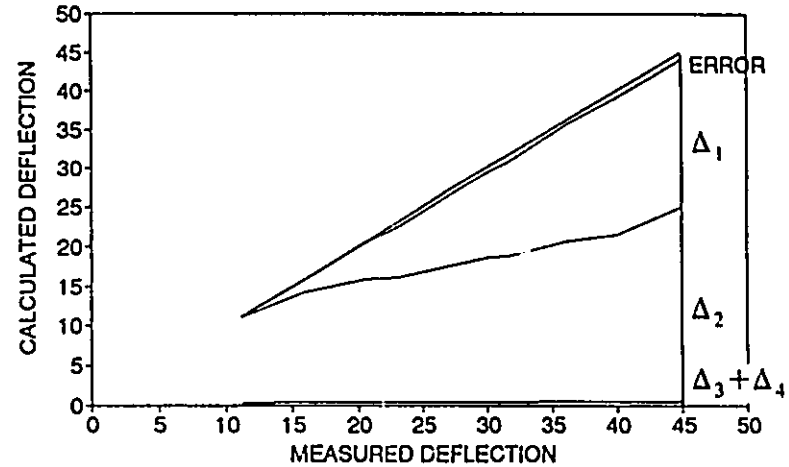

d) $\mu = 5.0$

Fig. (4.15) Comparison between measured and calculated deflections for specimen I. (Deflections in mm).

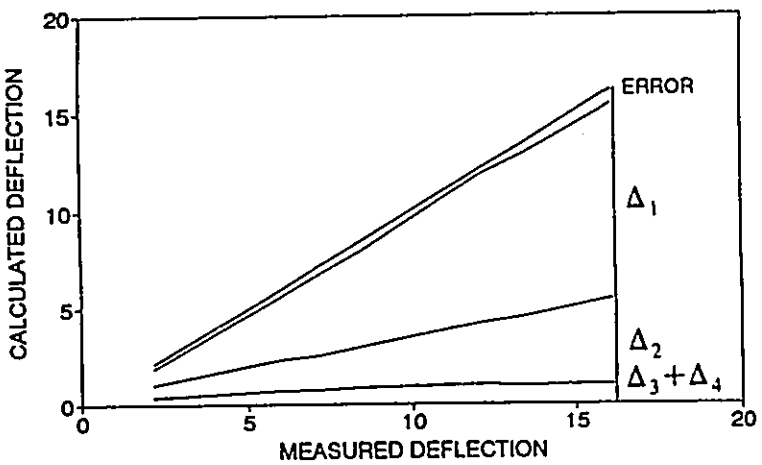

a) $\mu = 2.0$

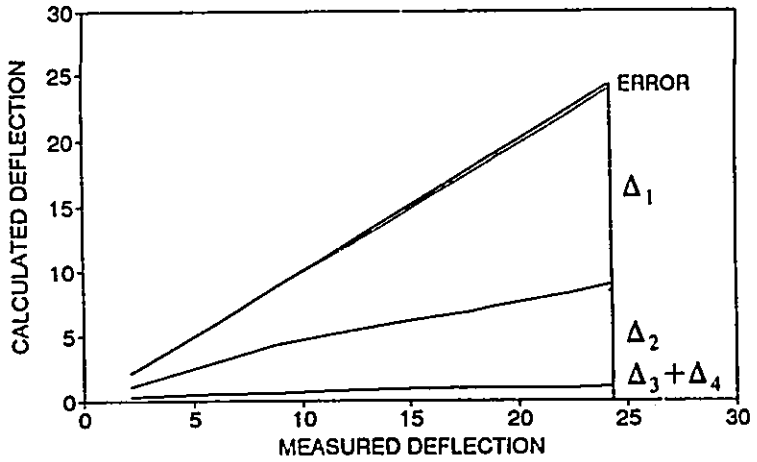

b) $\mu = 3.0$

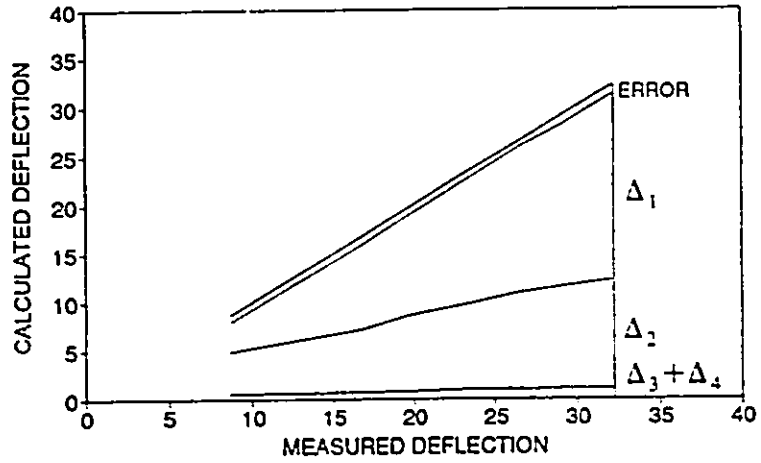

c) $\mu = 4.0$

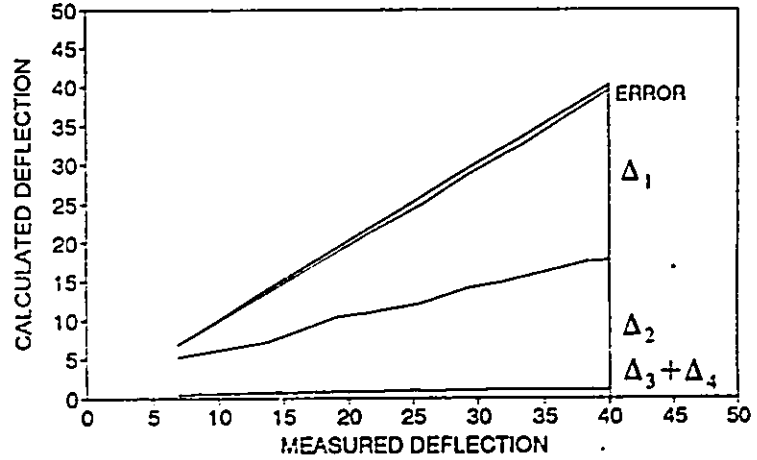

d) $\mu = 5.0$

Fig. (4.16) Comparison between measured and calculated deflections for specimen II. (Deflections in mm).

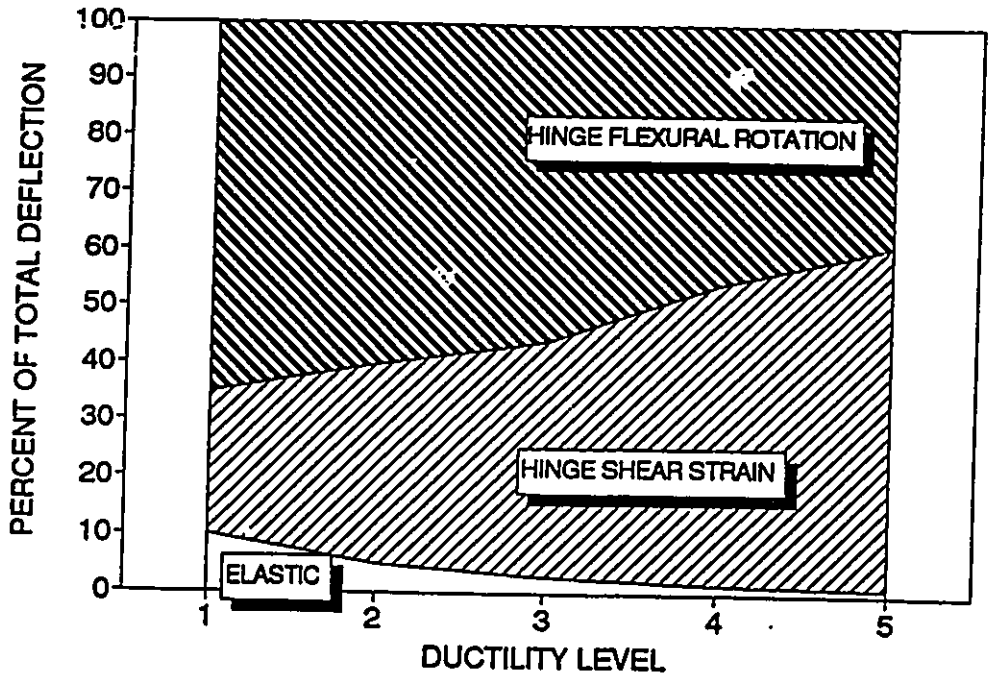

a) Specimen I.

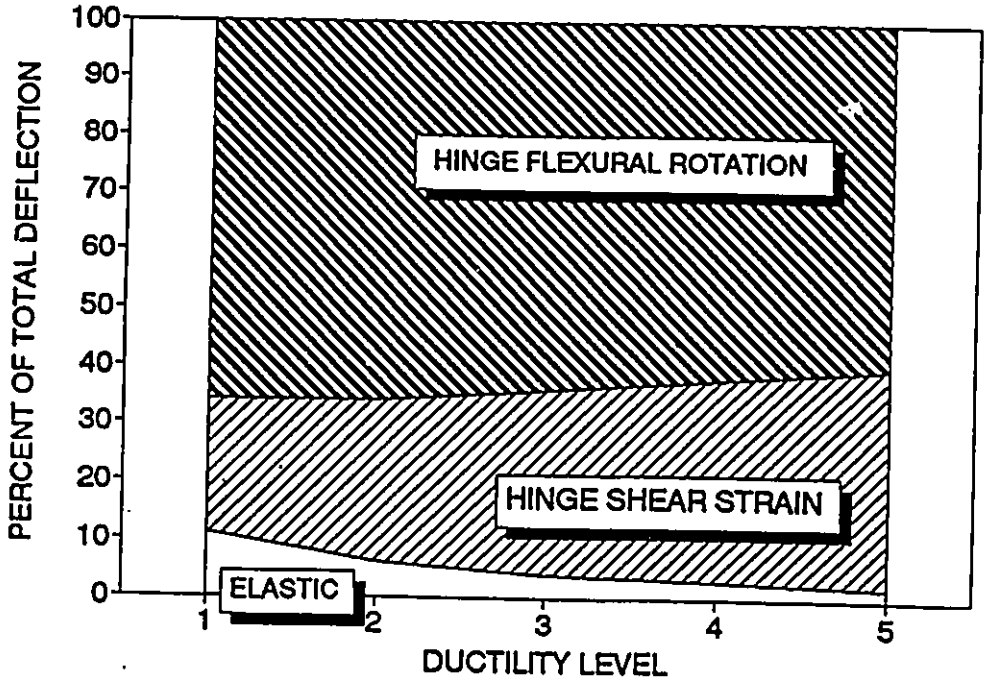

b) Specimen II.

Fig. (4.17) Contribution of the different components to the beam tip deflection.

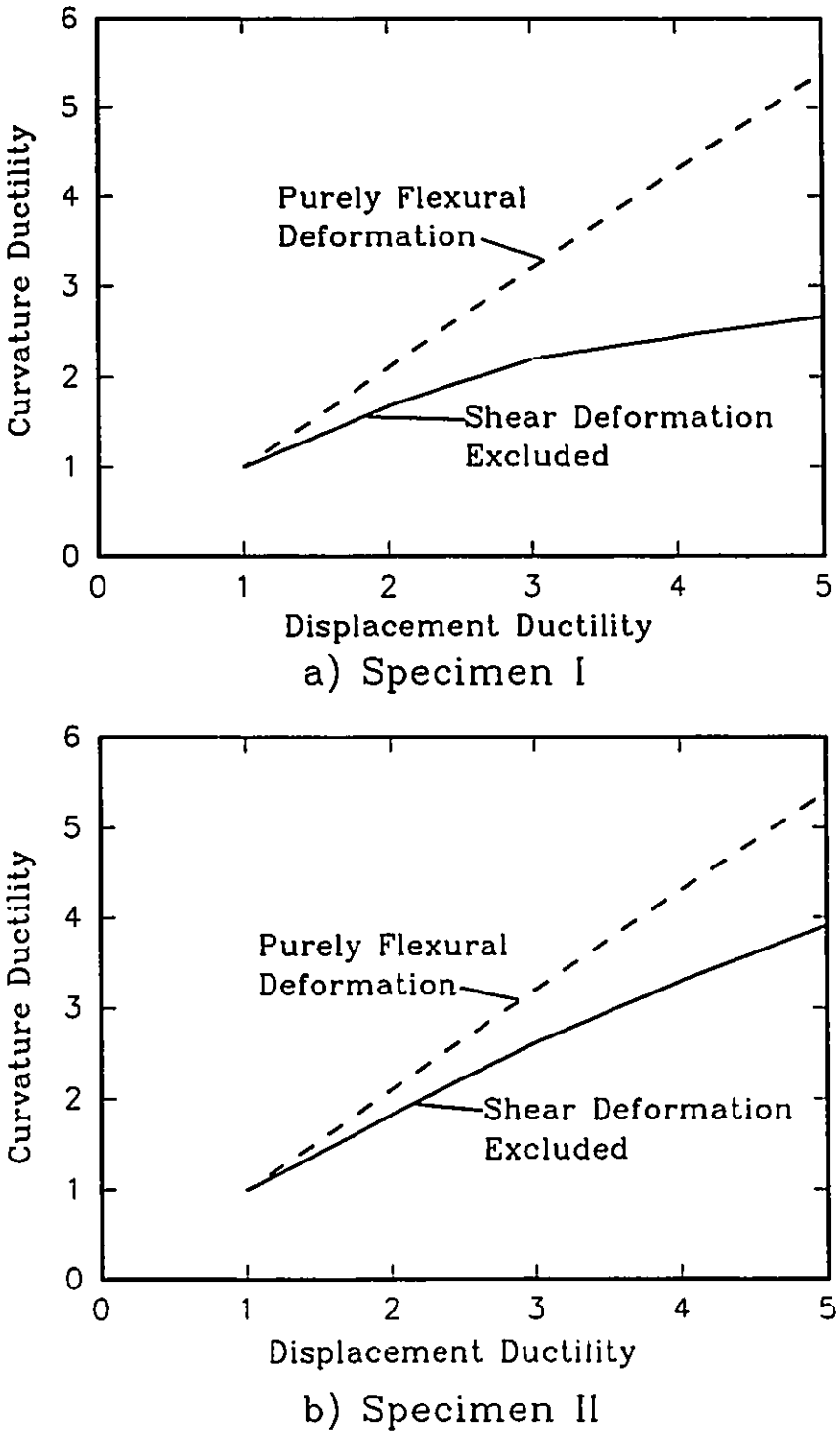

Fig. (4.18) Relationship between displacement and curvature ductilities.

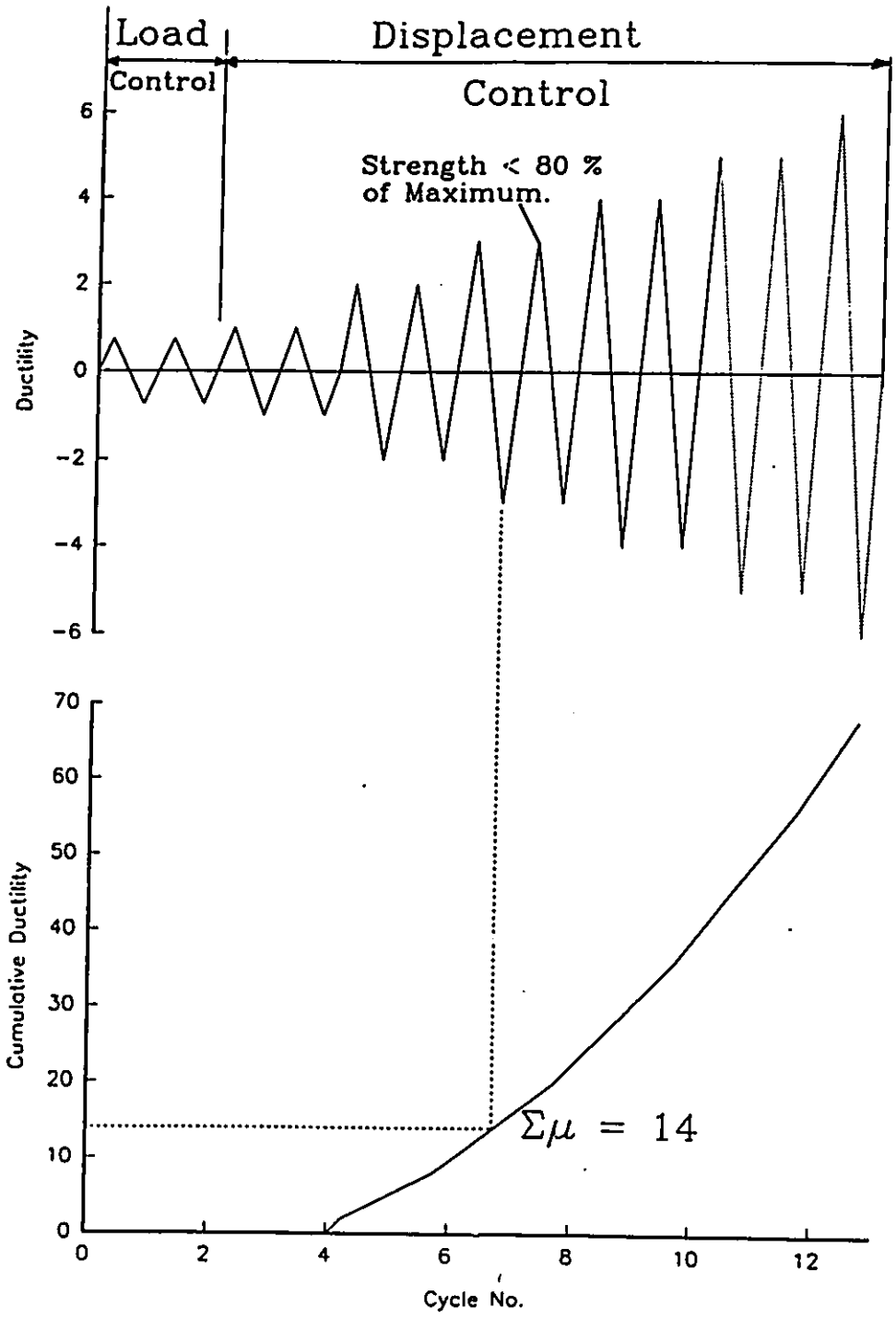

Fig. (4.19) Calculation of available ductility (Park, 1989) for specimen I.

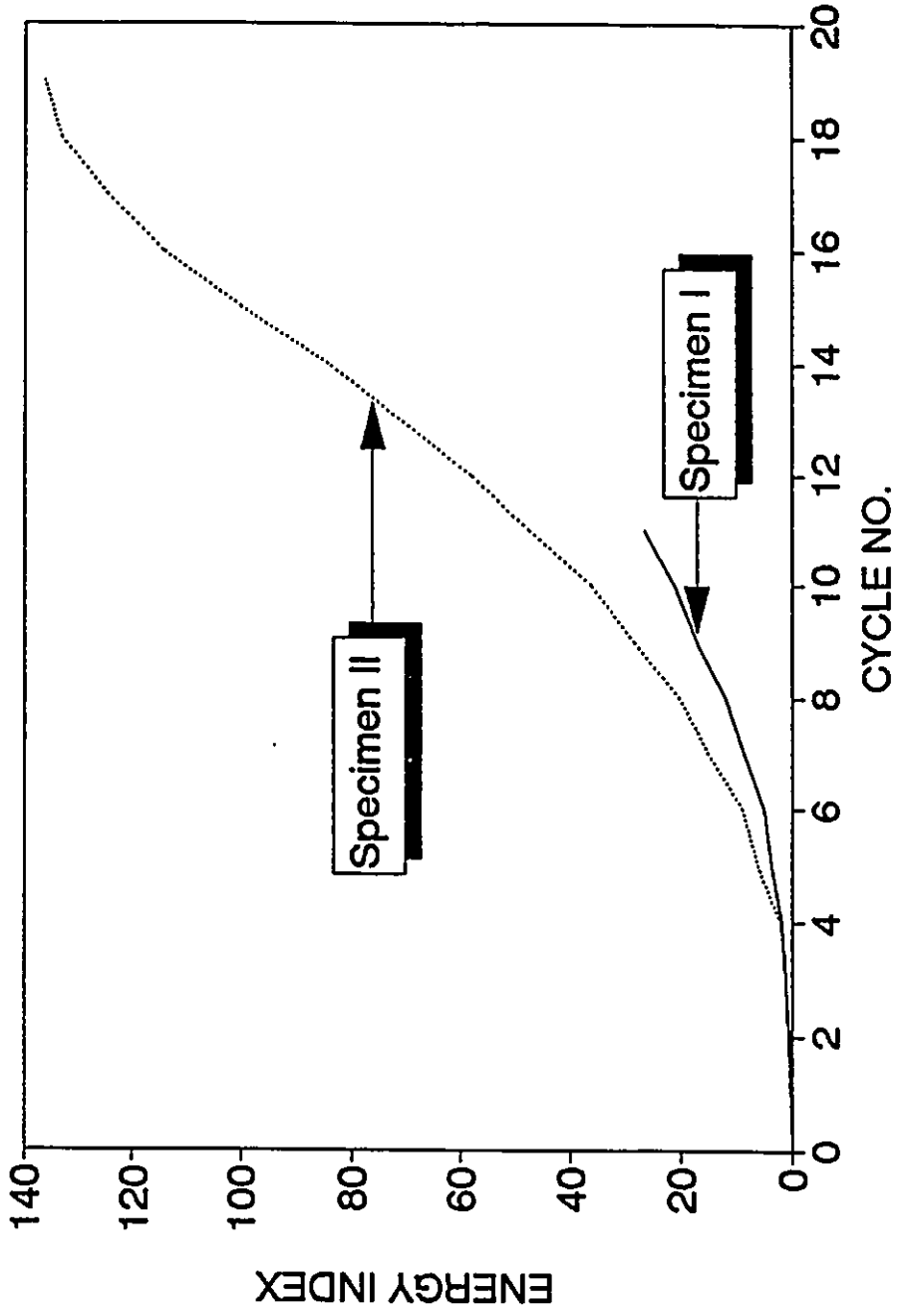

Fig. (4.20) Comparison of the energy dissipation capacities of specimens I and II.

CHAPTER 5

PROPOSED MODIFICATIONS TO THE DESIGN OF NOMINALLY DUCTILE FRAMES

5.1 INTRODUCTION

It was found that the seismic beam shear demands in nominally ductile frames exceed the factored design shears by 30 to 40 percent. Moreover, the ductility demands in the beams of NDMRFs designed strictly following minimum code requirements can be excessive such that it is prudent not to consider the concrete shear resistance effective in shear resistance calculation. Under such a condition, the beam shear capacity will consist only of the resistance of the stirrups. Although, there exists a minimum stirrups requirement specified in the Code for the beams of NDMRFs, the resistance of these minimum stirrups is independent of beam size and/or loading and there is no guarantee that the stirrups resistance will be sufficient to cover the shear demand under all circumstances. Therefore, it is necessary to modify the factored design shears to be more reflective of the demand shears such that adequate stirrups will be provided to avoid shear failure of the beams of NDMRFs.

This chapter provides the description of a procedure for design shear calculations in nominally ductile frames The validity of such a procedure is checked by applying it to the six-storey frames considered in chapters 2 and 3. In addition, a four-storey and a ten-storey nominally ductile frame are created as examples of frames having different heights. The seismic demand shears in the beams of these frames are compared to the design shears calculated using the proposed shear modification procedure to further check its validity.

5.2 REVIEW OF BEAM SHEAR DESIGN PROCEDURE IN DIFFERENT SEISMIC CODES

Since the factored design shears in the beams of nominally ductile frames are consistently smaller than the seismic shear demands, an increase in the design values is required. The increase should apply only to the shear forces due to the seismic lateral loading, while the shear forces due to gravity loads remain unchanged.

The New Zealand concrete design code, NZS 3101 (SANZ, 1982) adopts an approach for magnifying the design shear forces in *structures of limited ductility* (which are equivalent to nominally ductile frames in the Canadian context). A magnification factor is applied to the shear forces due to seismic lateral loading before using the conventional loading combinations. The magnification factor is a function of the structural type factor, S_{NZ}, used in base shear computations in the New Zealand loading code (SANZ, 1984). For structural systems equivalent to NDMRFs, the shear

magnification factor is 2.5. This value is applicable to beams at all storey levels of the structure. The beam stirrups spacing requirements specified for limited ductility structures in the New Zealand code are identical to the stirrups spacing requirements specified for nominally ductile frame in the Canadian code.

A similar shear magnification approach is also used in the ACI-318 (ACI, 1989) concrete design code for *structures in moderate seismic zones*. The constant shear magnification factor is equal to 2.0 for all storey levels. The beam stirrups spacing requirements are also identical to those specified in the Canadian code. However, the minimum stirrups size is #3 (Area = 71 mm^2) instead of the No. 10 bars used in Canada (Area = 100 mm^2).

Figure (5.1) shows a comparison between the demand shears and the design shears calculated using the NBCC 1990, ACI-318 and NZS 3101 approaches for the six storey nominally ductile frames considered in chapter 2, while figure (5.2) shows the same comparison for the six storey frame considered in chapter 3. For all five frames, the ACI and NZS codes underestimated the design shears in the upper storey beams. The constant magnification factor used for all storey levels is the reason behind this discrepancy as explained below.

Table (5.1) lists the design shear forces due to dead, live and seismic loads for the beams of the 6-ND frame considered in chapter 2. Also listed in the table are the design values obtained by using the methodology of the three codes, NBCC, ACI and NZS. The design values due to the equivalent seismic loading are very small at

the upper storey levels. During earthquake excitation, the upper storeys undergo larger deformations than assumed in the Codes due to higher mode effects. These larger deformations produce larger seismic shear forces than those predicted by the Code. Consequently, the difference between the shear demands in the lower and upper storeys is not as wide as the difference predicted using the Code load distribution. Therefore, to arrive at a more realistic design shear distribution, a larger magnification of the Code design shears at the upper storeys becomes necessary.

Another issue to consider here is the effect of the frame height (number of storeys) on the required magnification of the design shear forces. In low-rise frames, the equivalent static seismic loading produces relatively small shear forces in the beams due to the small frame height. Zhu (1989) showed that the beams of low-rise frames undergo larger ductility demands than those of high-rise frames when subjected to the same level of earthquake excitation. The larger ductility demands in the beams of low-rise frames produce larger shear forces when compared to the design shear forces. Therefore, the difference between codified and dynamic shears is larger for low-rise frames than it is for high-rise frames. This implies that a larger magnification factor is required for the beams of low-rise frames.

5.3 PROPOSED BEAM SHEAR MODIFICATION PROCEDURE

The procedure suggested here involves applying a variable magnification factor to the shear forces due to the seismic lateral loading, V_Q. The number of

storeys and the storey level location are considered in calculating the shear magnification factor as given in equation (5.1)

$$(V_Q^*)_i = \begin{cases} \left(2 + \frac{2.5}{N-i}\right)(V_Q)_i & i \neq N \\ 4.5\,(V_Q)_N & i = N \end{cases} \qquad (5.1)$$

where
i = storey level under consideration
N = total number of storeys in the frame
V_Q = beam shear force due to seismic lateral loading
V_Q^* = magnified beam shear force due to seismic lateral loading

The modified factored design shear force, V_f^*, will be the greatest value resulting from the load combinations given in equation (5.2) below

$$V_f^* = \begin{matrix} 1.25\,V_D + 1.5\,V_L \\ 1.25\,V_D + 1.0\,V_Q^* \\ 1.25\,V_D + 0.7\,(1.5\,V_L + 1.0\,V_Q^*) \end{matrix} \qquad (5.2)$$

where
V_D = shear force due to dead load
V_L = shear force due to live load

To get an idea of how the magnification factor varies with the number of storeys and the storey level under consideration, a few examples are given here. For the first storey beam of a four-storey frame (low-rise), the magnification factor is 2.83. In a ten storey frame (high-rise), the magnification factor for the first storey beam would be 2.28. In the top two storeys of both low- and high-rise frames the magnification factor would be 4.5. Although, the magnification factor for the top two storeys is quite large, it does not result in absurd values of the design shears since it

will be multiplied by the shear force due to the equivalent static loading which is quite small for the two upper levels. Table (5.2) shows the calculation of the modified design shear forces for the beams of the 6-ND frame.

5.4 IMPLICATIONS OF THE PROPOSED PROCEDURE ON NDMRFs

The procedure suggested in the previous section will be used to calculate the modified design shears in the beams of NDMRFs of different configurations. Moreover, the required stirrups will be estimated in order to study the effect of the proposed procedure on the amount of provided stirrups. It is prudent to ignore the contribution of concrete to the beam shear resistance in the design in view of the relatively high ductility demands attained in the beams of nominally ductile frames during earthquake excitation. Therefore, the stirrups will be designed to resist the total modified shear force.

5.4.1 APPLICATION TO BUILDINGS WITH 6.0 METRE FRAME SPACING

Figure (5.3) shows a comparison between the demand shears and the modified design shears for the small columns NDMRFs, 6SND and 6SPM, considered in chapter 2. Figure (5.4) shows the same comparison for the large columns NDMRFs, 6-ND and 6-PM. The factored design shears calculated per NBCC 1990 are also shown in the above mentioned figures. The proposed procedure results in excellent agreement between the modified design shears and the demand shears attained

during earthquake excitation. The modified design shears are approximately 30 to 40 percent larger than the NBCC factored shears.

The stirrups required for these frames are calculated using the modified design shears and ignoring the concrete contribution to the beam shear resistance. The beam experiencing the largest design shears requires the 2-legged No. 10 stirrups to be spaced at 1/4 the beam effective depth. Beams with smaller modified design shears will require larger spacing. However, the d/4 stirrups spacing specified for the beams of NDMRFs in the Code will be used for all beams to satisfy the minimum stirrups requirement. Therefore, the suggested procedure will not result in an increase in the amount of stirrups for beams in which the minimum stirrups are already sufficient to resist the demand shears.

5.4.2 APPLICATION TO BUILDINGS WITH 8.0 METRE FRAME SPACING

The six storey building considered in chapter 3 had an eight metre frame spacing. The beams of that frame underwent demand shears that exceeded the factored design shears and the minimum stirrups capacity. The suggested procedure will be used to calculate the design shears for this frame. Moreover, to further verify the proposed approach, two additional NDMRFs, one four storey and the other ten storey, will be considered. They represent typical frames of a four and a ten storey buildings having the same floor plan as the six storey building considered in chapter 3 (i.e. 8.0 metre frame spacing). The buildings are assumed to be located in Quebec City and will be designed accordingly. The design seismic base shears for the frames

are given in table (5.3). The design is carried out following the steps outlined in section (2.3) with the exception that the design shears will be calculated using the shear modification procedure suggested in this chapter. The member dimensions of the four and ten storey frames are shown in figure (5.5) while figure (5.6) shows the longitudinal reinforcement ratios of the two frames. The fundamental natural period of the four and ten storey frames were found to be 0.48 and 1.17 seconds respectively. These values are 20 percent larger than the values assumed in the base shear computations (0.1N).

The four and ten storey frames were analyzed under earthquake excitation. Figure (5.7) shows that there is an excellent agreement between the modified design shears and the demand shears for the beams of the four, six and ten storey frames in buildings having 8.0 metre frame spacing. This emphasizes the ability of the proposed procedure to predict the demand shears in NDMRFs of different heights and configurations.

For the four, six and ten storey frames, the stirrups are calculated based on the modified design shears and ignoring the concrete contribution to the beam shear resistance. Using 2-legged No. 10 stirrups, the required spacing was found to be smaller than the maximum spacing specified by the Code (d/4) and the smaller spacing was adopted. Table (5.4) gives the beam stirrups spacing for the beams of the different storeys of the four, six and ten storey frames. Also listed in the table are the d/4 spacing specified in the Code. The required spacing is approximately 30 percent

smaller than the d/4 spacing due to the larger design shears. Figure (5.7) shows that the nominal capacity of the provided stirrups exceeds the demand shears while the capacity of the minimum stirrups (d/4 spacing) was lower than the demand shears.

5.5 SUMMARY

A shear modification procedure was suggested for the beams of nominally ductile frames. The procedure was used to calculate the design shears in the beams of the six storey nominally ductile frames considered in chapters 2 and 3. It was found that the modified design shears are in good agreement with the demand shears attained during earthquake excitation. To further check the validity of the proposed shear modification procedure, a four storey and a ten storey buildings were designed as nominally ductile frames. The design shears in the beams were calculated using the proposed procedure and they were found to be in good agreement with the demand shears attained during the earthquake response of the frames.

For beams in which the minimum stirrups are already sufficient to resist the demand shears, the suggested procedure did not result in an increase in the amount of provided stirrups (e.g. buildings with 6.0 metre frame spacing). For beams sustaining larger loads, and consequently higher shears, the suggested procedure provided a rational way to arrive at the required stirrups spacing to prevent any shear failure in the beams (e.g. buildings with 8.0 metre frame spacing).

The proposed shear modification procedure is relatively simple for use in the design office and deserves serious consideration for Code adaptation.

Although the suggested shear modification procedure minimizes the possibility of beam shear failure, it will not reduce the large interstorey drifts experienced in NDMRFs designed strictly following minimum code requirements. In this sense, it is a partial solution to improve the performance of NDMRFs. Chapter 6 presents an alternative design approach with the objective of avoiding all the perceived problems in the seismic performance of NDMRFs.

Table (5.1) Comparison of beam design shears (kN) according to different codes

Level	D	L	Q	NBCC 90	ACI	NZS
1	75	58	66	201	247	270
2	75	58	64	200	244	267
3	75	58	57	195	234	254
4	72	58	47	184	217	233
5	72	58	31	177	194	205
6	72	58	13	177	177	177

Table (5.2) Calculation of the modified design shears

Level	D	L	Q	Q^*	NBCC 90	Suggested
1	75	58	66	165	201	270
2	75	58	64	168	200	272
3	75	58	57	162	195	268
4	72	58	47	153	184	258
5	72	58	31	140	177	249
6	72	58	13	59	177	192

Table (5.3) Design seismic base shears

Number of Storeys	Four	Ten
	554 kN 13.2 % W*	728 kN 6.8 % W*

* W = Total weight of building

Table (5.4) Spacing of the provided stirrups in the beams

Storey Level Number	Stirrups spacing (mm)					
	Four Storey		Six Storey		Ten Storey	
	Actual	d/4	Actual	d/4	Actual	d/4
10					135	140
9					106	140
8					110	155
7					110	155
6			136	155	112	165
5			111	155	112	165
4	130	140	113	165	112	165
3	100	140	113	165	114	180
2	104	104	118	180	114	180
1	104	104	118	180	114	180

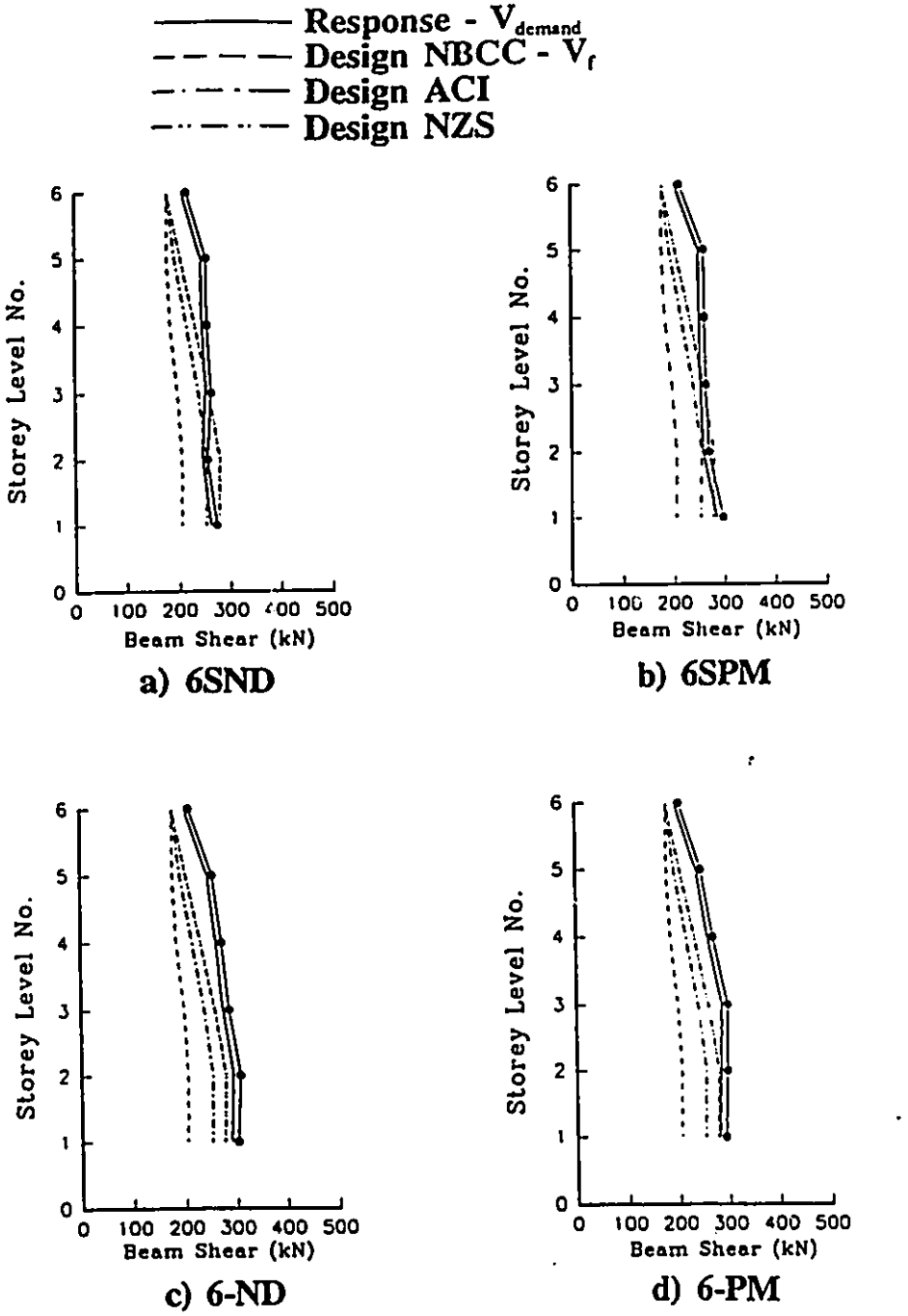

Fig. (5.1) **Application of the New Zealand and ACI shear modification approaches to the six storey frames considered in chapter 2, 6SPM, 6SND, 6-ND and 6-PM (• = mean + σ)**

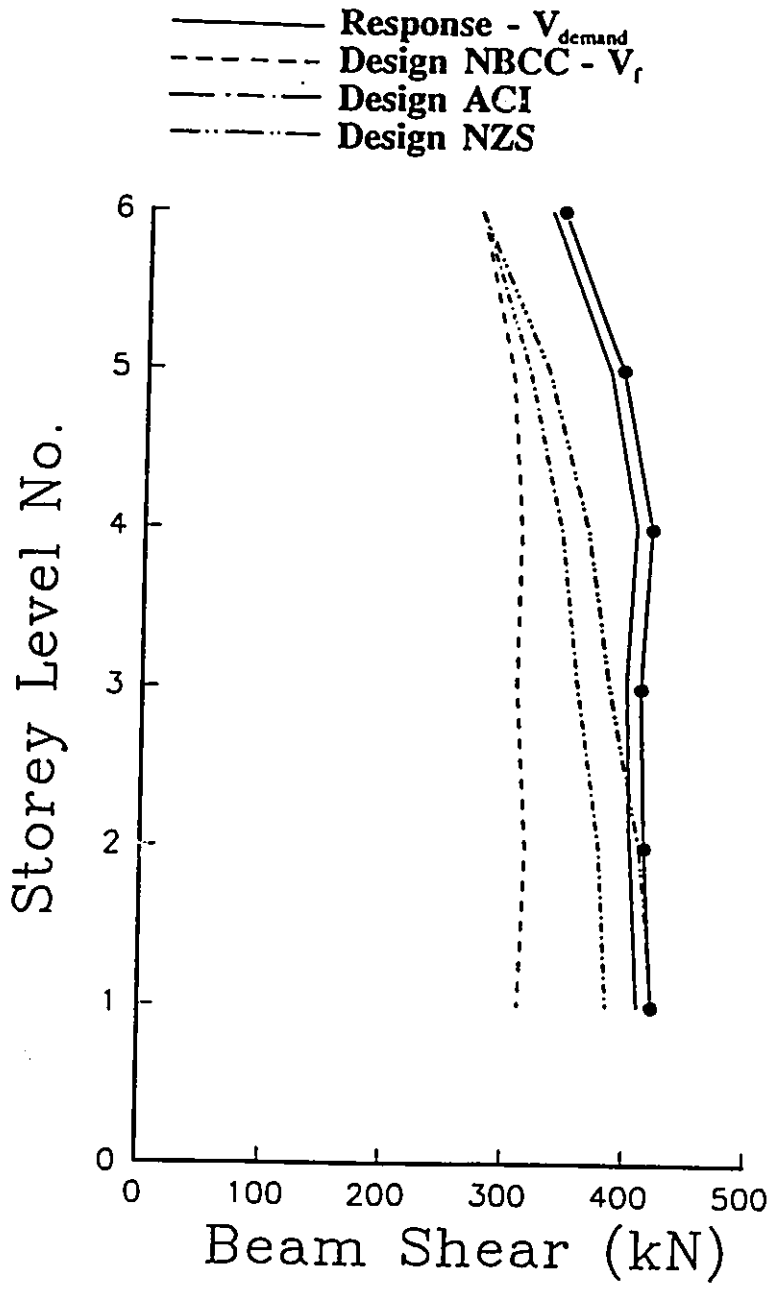

Fig. (5.2) **Application of the New Zealand and ACI shear modification approaches to the six storey frame with 8.0 metre frame spacing (• = mean + σ)**

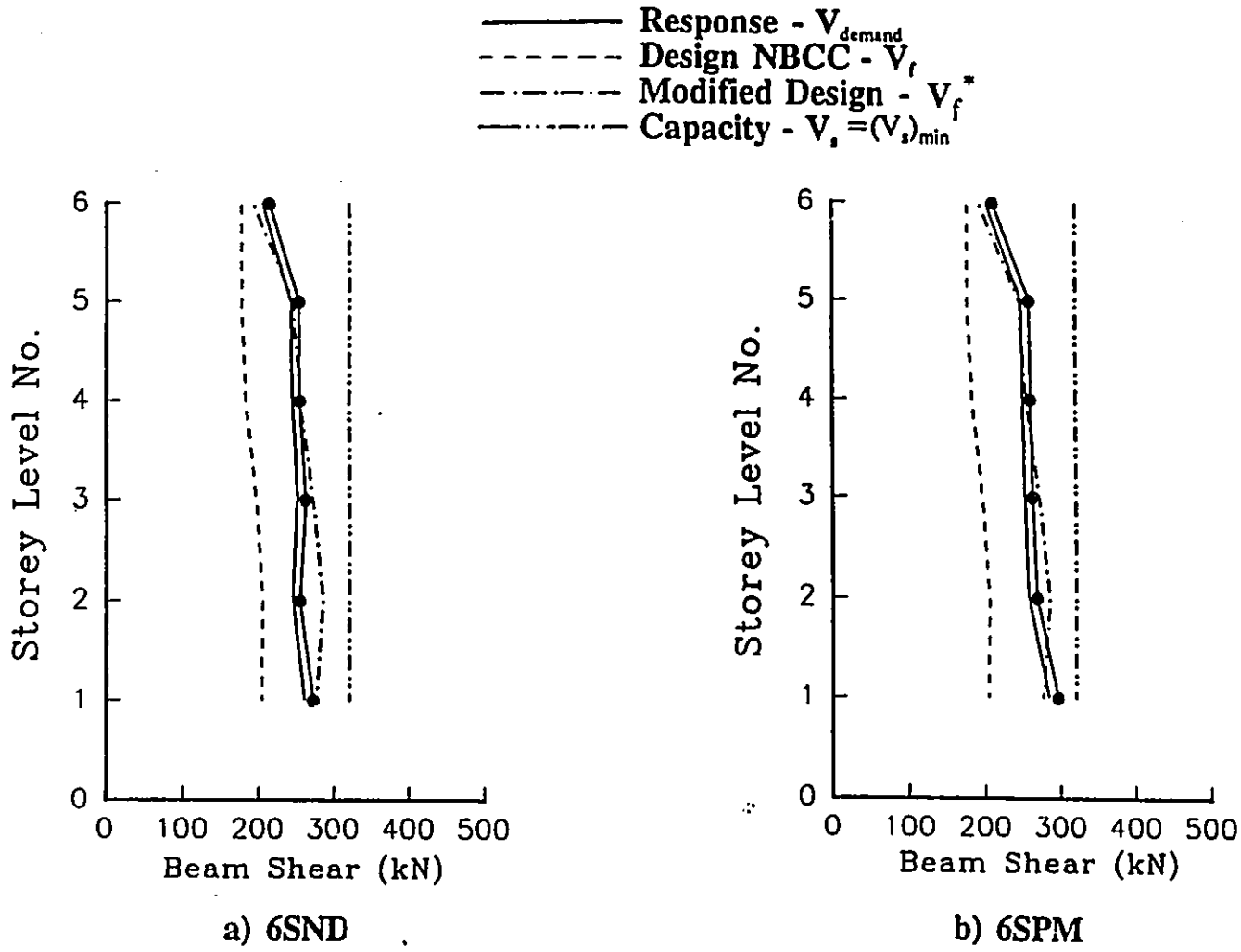

a) 6SND b) 6SPM

Fig. (5.3) Comparison between the shear demands and the modified design shears in the beams of the small columns six storey frames considered in chapter 2, 6SPM and 6SND (• = mean + σ)

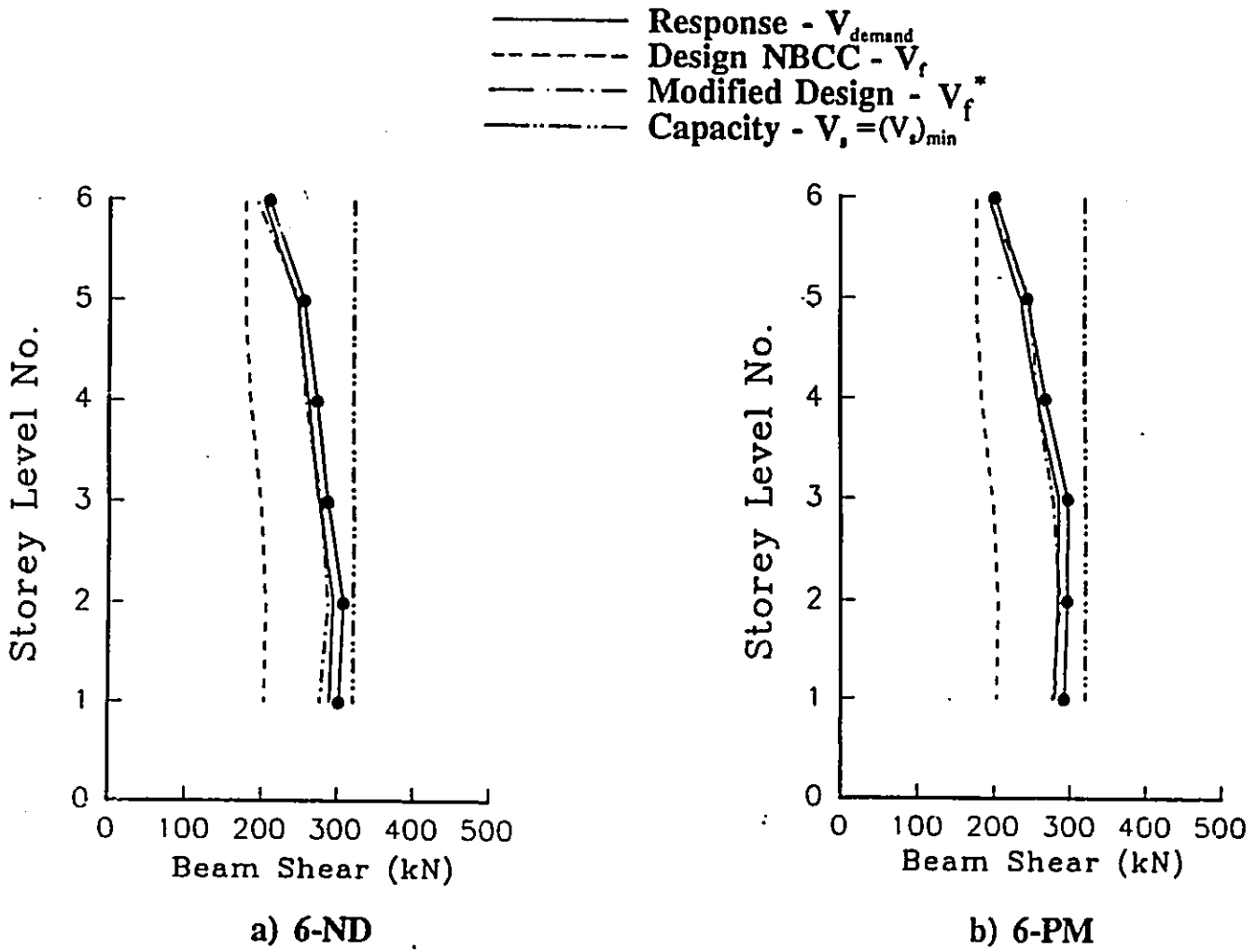

a) 6-ND

b) 6-PM

Fig. (5.4) **Comparison between the shear demands and the modified design shears in the beams of the large columns six storey frames considered in chapter 2, 6SPM and 6SND (• = mean + σ)**

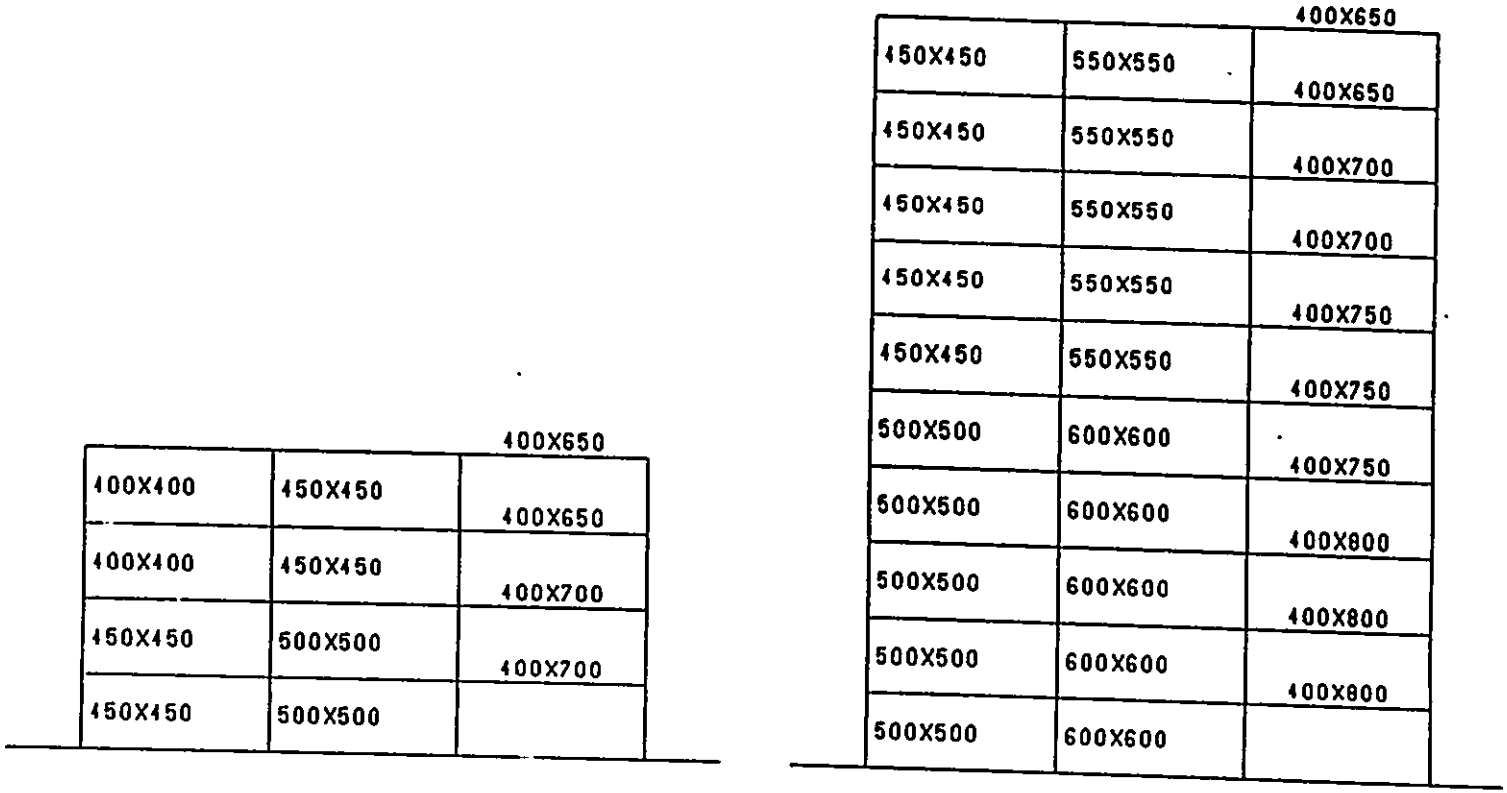

a) Four storey

b) Ten storey

Fig. (5.5) Member dimesions (mm) of the four and ten storey frames

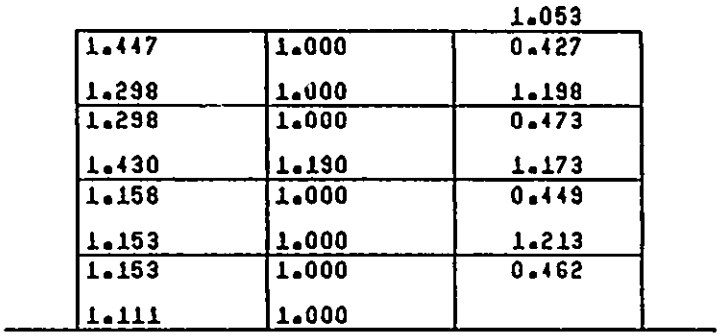

a) Four storey

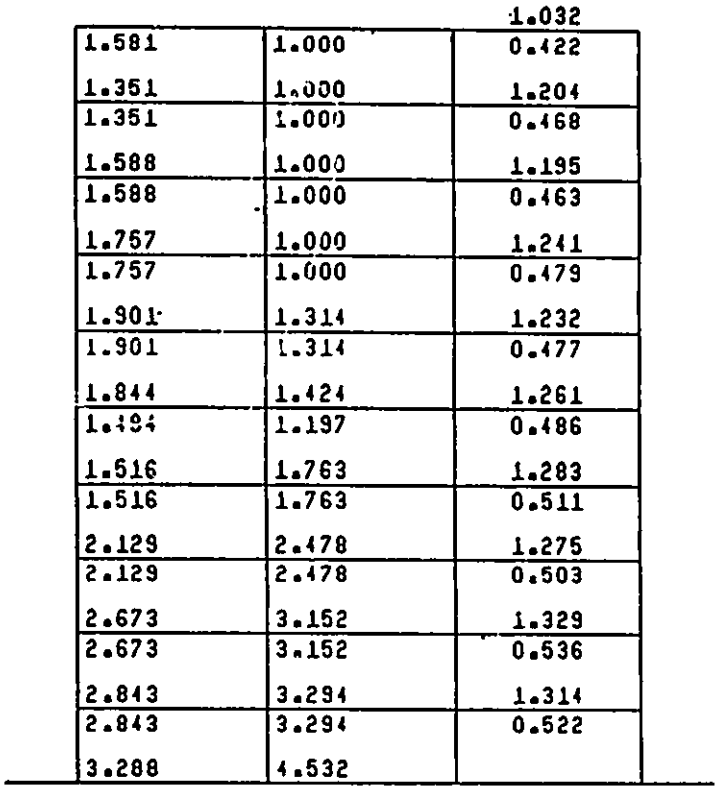

b) Ten storey

Fig. (5.6) Reiforcement ratios (%) of the four and ten storey frames.

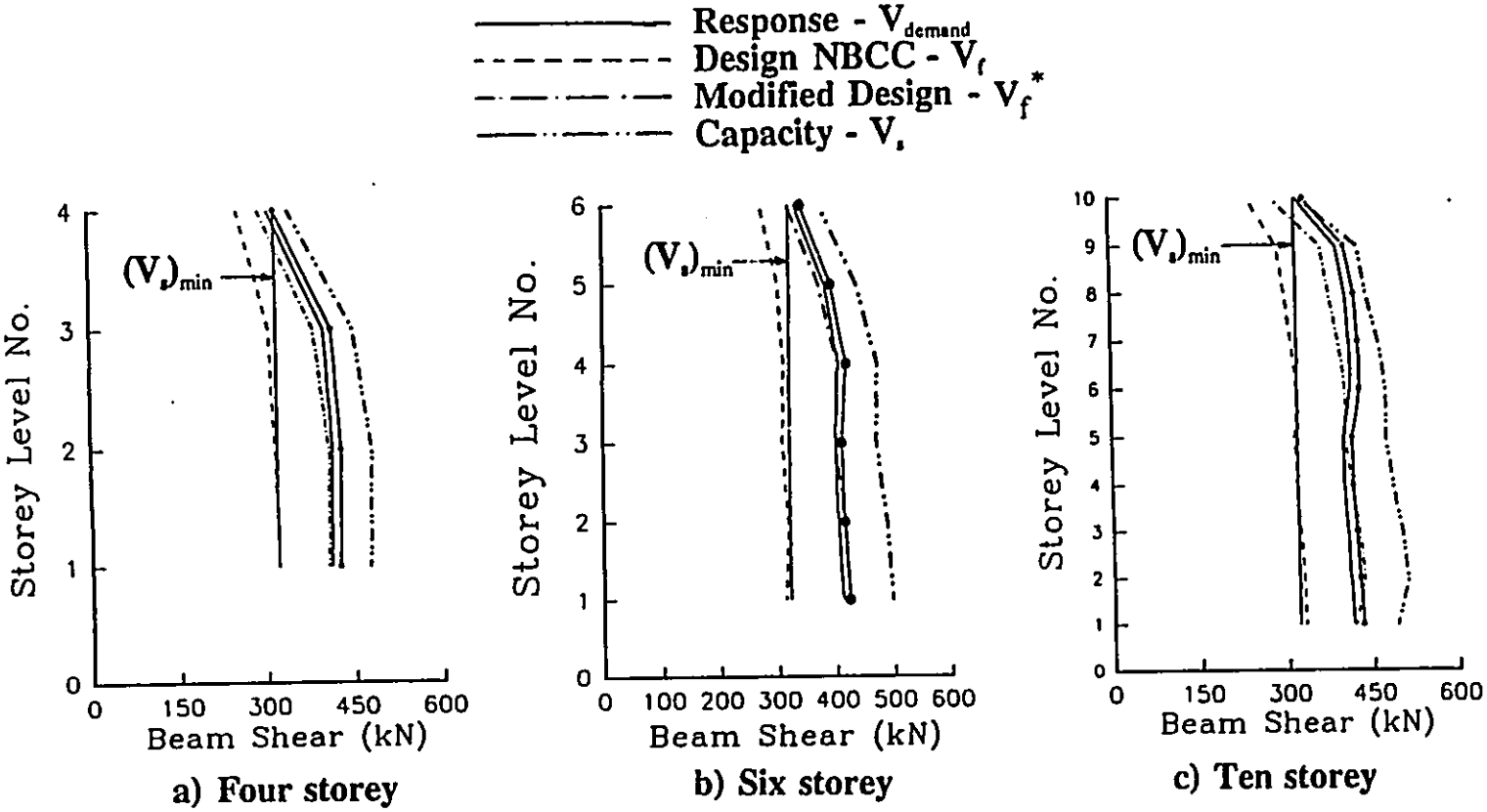

Fig. (5.7) Comparison between the shear demands and the modified design shears in the beams of the frames with the 8.0 metre spacing (• = mean + σ).

CHAPTER 6

ALTERNATIVE DESIGN APPROACH FOR LOW RISE REINFORCED CONCRETE FRAMES

6.1 INTRODUCTION

Current seismic design provisions for ductile frames require designing stronger columns than beams to limit the plastic hinges to the beams and the column bases. The failure mechanism of such a design is shown in figure (6.1a). Such a failure mechanism is desirable for the following reasons; i) plastic hinges in beams have larger ductility capacity than those in columns, ii) the energy dissipation is more evenly distributed over a large number of beam hinges instead of a limited number of column hinges as the case of a storey side-sway mechanism and iii) damaged beams are easier to repair than damaged columns. However, in low rise frames with large beam spans, applying the strong column-weak beam design concept can result in unrealistic conservatism in column design. This occurs because in low rise frames the strength of the beams is usually controlled by the gravity load rather than the seismic load moments. Designing the columns to be stronger than the beams will result in columns which are much stronger than those required. Consequently the

lateral strength of the frame will be much higher than the design base shear. In such a case the designer may choose to disregard the strong column-weak beam concept and prefer to design the frame using the moments obtained from the elastic static analysis (nominally ductile frames in the Canadian practice). It has been shown in chapters 2, 3 and 5 that nominally ductile frames designed strictly following the current Canadian minimum code requirements have several deficiencies. Since the strong column-weak beam requirement need not be followed in the design of nominally ductile frames, such frames may develop the undesirable storey side-sway mechanism as shown in figure (6.1b), leading to excessive drifts. Moreover, it was found that the ductility demands in the beams and columns of nominally ductile frames can be considerably larger than what is implied in the design code. It was also found that nominally ductile frames can undergo beam shear demands that exceed the factored beam shears. Although NDMRFs may be designed beyond the minimum requirements set by the Code to achieve acceptable seismic performance (Paultre and Mitchell, 1991), unfortunately there are no guidelines to arrive at the overdesigned column sizes or reinforcement used in order to obtain desirable seismic behaviour for nominally ductile frames.

Paulay (1989) suggested an alternate design approach for low-rise frames which is essentially a compromise between ductile and nominally ductile frame design. The alternative approach involves designing the exterior columns to be stronger than the beams that frame into them while the interior columns are

designed for the critical combinations of factored gravity and seismic loads only. At the exterior joints, the plastic hinges are expected tc form in the beams rather than the columns. At the interior joints, the plastic hinges will most likely occur in the columns due to the large strength of the beams dictated by gravity load requirements. Such a strength hierarchy will prevent the formation of plastic hinges in the exterior columns thus preventing the occurrence of a storey side-sway mechanism. The failure mechanism of a frame designed using this alternative approach is shown in figure (6.1c).

Figure (6.2) shows the failure mechanism of a frame in which the exterior columns remain virtually elastic. At the onset of yielding, the rotation in the column plastic hinges, θ_y can be expressed as

$$\theta_y = \frac{\Delta_y}{H} \tag{6.1}$$

where Δ_y is the roof displacement at yield and H is the frame height. Since the exterior columns would remain elastic at the maximum deformation of the frame, Δ_u, the deflected shape of the frame would be essentially a straight line. In this case, the maximum rotation in the column hinges, θ_u can be approximated as

$$\theta_u \approx \frac{\Delta_u}{H} \tag{6.2}$$

Thus, the ratio of maximum rotation to yield rotation is approximately the same as the ratio of maximum deformation to yield deformation. This indicates that the rotational ductility demands in the columns will be in the same order as the global displacement ductility demand. The alternate approach will be referred to as the "Strong Exterior Column Design" approach in this thesis.

This chapter explores this design concept in the context of the Canadian design practice and provides a proposed procedure for this design approach. The design of beams, columns and joints for flexure and shear is fully explained. The proposed approach is then used to redesign the six storey frames considered in chapter 2. The designed frames are first analyzed under monotonically increasing static loading to evaluate their overstrength. Then, they are analyzed dynamically under earthquake excitation. The static and dynamic responses of the frames designed in this chapter are compared to those of the nominally ductile frames designed to minimum code requirement and those designed by Paultre and Mitchell (1991) to validate the aim of this "strong exterior column" design methodology.

6.2 DESCRIPTION OF THE STRONG EXTERIOR COLUMN DESIGN APPROACH

This design approach is a compromise between ductile and nominally ductile frame designs. The exterior bay is expected to perform similar to the components of a ductile frame (strong column-weak beam). To achieve such performance, capacity

design principles need to be adopted. In the Canadian practice, these principles are outlined in chapter 21 of the concrete design code (CSA 1984). These capacity design principles, with some modifications, will be used for the design of exterior bays as explained in the following sections. Wherever necessary, reference will be made to the appropriate code clauses. One important feature of the behaviour of gravity dominated frames is that positive plastic hinges may not form at the column face (Meggett and Fenwick, 1989). The gravity load dominance will cause the maximum positive moment to occur some distance away from the column face. This fact will be considered in the design of the exterior bays as explained in a subsequent section.

The interior bays are not expected to perform similar to ductile frames. Therefore, the capacity design principles need not be used for these bays. The design of the interior bays will follow the design principles of nominally ductile moment resisting frames with some modifications to accommodate the ductility demands anticipated in the columns. Since no definite strength hierarchy is implemented in designing the beams and columns framing into the interior joints, plastic hinges may occur in the beams as well as the columns. The designer will have to determine where the hinges will occur in order to provide adequate detailing. Some guidelines will be provided to help the designer to determine the location of plastic hinges.

The frame is to be designed for the critical combinations of gravity and seismic loads. It is assumed that the appropriate design seismic base shear corresponds to a force modification factor $R = 2.0$, the same as NDMRFs.

To obtain the design actions, the frames are to be analyzed statically under the prescribed factored code loads. Appropriate allowance on the beam and column stiffness values must be considered to account for cracking. A T-shape for the beam cross section should be assumed to allow for the contribution of the slab to the beam stiffness. The effective flange width can be calculated according to clause 8.10.2 of the Code. The finite size of the joints should be taken into consideration by using rigid elements from the joint centre lines to the member face.

To obtain the design moments including P-delta effects, it is suggested to use either a second-order analysis involving iterations or a first-order analysis taking the effects of geometric stiffness into consideration (Wilson and Habibullah, 1987). The first-order analysis involves forming a geometric stiffness matrix based on the column axial force due to gravity loading. The geometric stiffness matrix is then subtracted from the element stiffness matrix to obtain the element stiffness including geometric nonlinearities. The solution of the problem is then obtained directly without any iterations. The member slenderness effects are to be considered in designing the columns using the procedure suggested in clause 10.11.6 of the Code.

The approaches used for the dimensioning and detailing of exterior and interior bays are distinctly different. Therefore, the design and detailing of the components of the exterior and interior bays will be described in separate sections. Figure (6.3) shows the different frame components and gives the thesis section in which the design of each component is explained.

6.3 DESIGN OF EXTERIOR BAY MEMBERS

6.3.1 BEAMS

a) Design for flexure

The beam design moments are to be obtained from the results of the elastic static analysis including P-delta effects. It is recommended to redistribute the gravity load moments by reducing the negative moments at the face of the exterior column by up to 20 percent, the maximum value allowed by clause 8.4 of the Code. This redistribution of negative moments is a desirable step as it will result in less reinforcement in the exterior columns which are required to be stronger than the beams framing into them.

In determining the flexural reinforcement for the beams, the contribution of the slab bars to the negative moment resistance of the beam must be considered (clause 21.4.2.2of the concrete design code). A lower bound is to be imposed in determining the positive reinforcement at the beam end sections. This lower bound is intended to recognize the cyclic nature of the seismic loading and also to provide confinement for the compressed concrete in the plastic hinge zones. The lower bound given in code clause 21.9.2.1.1for the beams of nominally ductile frames may be used here. Moreover, the beam reinforcement ratios are to be bound by the lower and upper bounds for flexural members given by code clauses 10.5.1 and 10.3.3 respectively.

Due to gravity load dominance, the plastic hinge under positive moment is likely to occur some distance away from the face of the exterior column. The location of this plastic hinge will be at the point where the increasing bending moment diagram first intersects the capacity diagram as shown in figure (6.4a). This location will coincide with the bar-cut off point (sudden drop in the positive moment capacity). The location of the cut-off point can be readily determined if the positive factored moment resistances at the end and middle of the span are known (figure 6.4b). The positive moment resistance at the beam end is specified to be at least one third of the negative moment resistance and is thus known. The moment resistance at the middle of the span can be determined from the envelope of factored moments. The determination of the location of the plastic hinge is crucial in order to determine the region for which special detailing is to be provided. The detailing requirements are explained in a subsequent section.

b) Design for shear

To prevent shear failure in the beams, the design shears will be based on the probable strength of the potential plastic hinges. At the exterior joint end, the beam plastic hinge will be assumed to develop its negative probable strength. At the interior joint end, the beam moment is obtained by considering the moment input from the columns that frame into the interior joint. The columns above and below the joint are assumed to have developed their probable strength, evaluated taking into account the axial force effect. The sum of the column probable strengths above

and below the joint will be distributed to the beams framing into the interior joint according to their relative stiffness. The moment in the exterior span at the face of the interior column will be taken in the positive direction. This moment, when acting with the negative probable moment resistance at the exterior joint will produce maximum seismic shears in the beams of the exterior bays. Figure (6.5) and equations (6.3) and (6.4) summarize the procedure for calculating the design shear forces in the exterior spans.

$$M_b^{ext} = (M_{pc}^a + M_{pc}^b)\frac{I_{ext}/L_{ext}}{I_{ext}/L_{ext} + I_{int}/L_{int}} \tag{6.3}$$

$$V_f = V_g + \frac{M_p^- + M_b^{ext}}{L_{ext}} \tag{6.4}$$

where

M_p^- = negative probable moment resistance of the beam section at the exterior column

M_b^{ext} = positive beam moment at the face of the interior columns.

M_{pc} = column probable strength, the superscripts *a* and *b* denote the columns above and below the joints respectively.

I, L = moment of inertia and clear length of the beam respectively. The subscripts *ext* and *int* refer to exterior and interior spans respectively.

Due to the expected ductility demands in the beam hinges, the concrete contribution to the beam shear resistance is to be ignored. Therefore, the stirrups will be designed to resist the total factored design shears, V_f. The area and/ or spacing of the required stirrups can be calculated from equation (6.3) below,

$$V_s = \frac{V_f}{\phi_s} = \frac{A_v f_{yv} d}{s} \qquad (6.5)$$

where
ϕ_s = steel resistance factor = 0.85
A_v = area of stirrups
f_{yv} = yield strength of stirrups steel
d = effective beam depth
s = spacing between stirrups

c) Detailing

At both ends of the beam, No. 10 stirrups or larger should be provided over a special region. The extent of the special regions into the span will be different for each end of the beam. For the beam end that frames into the exterior column, the special region will be assumed to extend from the column face to a point twice the beam depth beyond the bar cut-off point towards midspan. For the beam end that frames into the interior column, the special region will be assumed to extend a distance of twice the beam depth from the column face towards midspan. Figure (6.6) shows a diagrammatic sketch of the two special end regions. The spacing of stirrups within the end regions shall not exceed:

a) d/4
b) 8 times the diameter of the smallest longitudinal bar enclosed
c) 24 times the diameter of the stirrup bar or
d) 300 mm

For the remainder of the beam length, the stirrup spacing should not exceed d/2.

6.3.2 COLUMNS

a) Design for flexure

The exterior columns are to be designed to remain elastic in order to prevent the occurrence of a storey side-sway mechanism. Therefore, the exterior columns will be provided with sufficient strength such that, at the exterior joint, the plastic hinges will form in the beams. The strong column weak beam requirement of clause 21.4.2.2 may be adopted here such that

$$\sum M_{rc} \geq 1.1|M^{-}_{nb}| \qquad (6.6)$$

where

M^{-}_{nb} = nominal negative moment resistance of the beam framing into the exterior joint

ΣM_{rc} = sum of the factored design moments of the top and bottom columns framing into the exterior joint.

ΣM_{rc} can be distributed to the columns above and below the joint according to their relative stiffness to obtain the column design moments. The design axial forces are to be obtained from the elastic static analysis. Only the load combinations in which the seismic loads produce negative moments in the beam at the exterior joint needs to be considered.

b) Design for shear

The shear resistance of exterior columns will conform to the requirements of the columns of ductile frame given in code clause 21.7.2.2.The concrete shear resistance may be taken into consideration according to code clauses 21.7.3.1(b)and 11.3.4.3.The hoops should conform to the spacing requirements described below.

c) Detailing

It is suggested that the detailing requirements shall conform to those specified for the columns of nominally ductile frames in clause 21.9.3 of the Code.

6.3.3 JOINTS

The joints should be designed and detailed as those of ductile frames as given by clause 21.6 of the concrete design code.

6.4 DESIGN OF INTERIOR BAYS MEMBERS

6.4.1 BEAMS

a) Design for flexure

The design moments are to be obtained from the elastic static analysis including P-Delta effects. Moment redistribution may be performed if desired. The lower and upper bounds given by Code clauses 10.5.1 and 10.3.3 are to be employed in determining the beam reinforcement.

After the column reinforcement has been determined, the designer must check whether the plastic hinges will form in the beams or the columns framing into the interior joints. This can be determined by comparing the strengths of the beams and columns framing into the joint as given by equation (6.7).

$$\sum M_{rb} \geq 1.1 \sum M_{nc} \qquad (6.7)$$

where

ΣM_{rb} = sum of the factored moment resistance of the beams framing into the interior joint

ΣM_{nc} = sum of the nominal moment resistance of the columns framing into the interior joint. The moment resistance is to correspond to the axial load, consistent with the direction of lateral forces considered, which results in the highest flexural resistance.

If the condition given by equation (6.7) is satisfied, the designer may assume that the plastic hinges will occur only in the columns. No special seismic considerations will be required in the design of the interior bay beams. If, at any interior joints, equation (6.7) is not satisfied, plastic hinges may occur in the beams as well as the columns. In such a case, a lower bound is to be imposed on the positive reinforcement in the beams on either side of the joint. The lower bound given by code clause 21.9.2.1may be employed here. It should be noted that in most cases of gravity dominated frames equation (6.7) will be satisfied because the beams already possess large strength due to gravity load requirements.

b) Design for shear

The design shear forces can be calculated using the shear modification procedure described in chapter 5 of this thesis. In that procedure, the shear forces due to seismic loads, V_Q, are magnified by the beam shear factor to get V^*_Q. V^*_Q will then combine with the gravity loads to obtain the design shear force V^*_f. If equation (6.7) is satisfied (i.e. no plastic hinges in the beams), the concrete contribution to the beam shear resistance may be considered in the design. If, at any interior joint, equation (6.7) is violated, the concrete shear resistance is to be ignored in the design

of the beams framing into that joint. Thus, the stirrups area and/or spacing can be calculated using equations (6.8) and (6.9) below;

$$V_c = \begin{cases} 0.2\sqrt{f'_c}\,bd & \text{if } \sum M_{rb} \geq 1.1 \sum M_{nc} \\ 0 & \text{if } \sum M_{rb} < 1.1 \sum M_{nc} \end{cases} \qquad (6.8)$$

$$V_s = \frac{V_f^* - \phi_c V_c}{\phi_s} = \frac{A_v f_{yv} d}{s} \qquad (6.9)$$

where
ϕ_c = concrete resistance factor = 0.6
f_c' = concrete compressive strength
b = beam width

c) Detailing

If it is found that the beams may develop plastic hinges at any interior joint, the detailing requirements of the beams on either side of the joint should conform to those specified for the interior end of exterior spans. If it is found that the beam will not develop plastic hinges (equation 6.5 is satisfied) the detailing requirements may be relaxed. The following gives the maximum allowed stirrups spacing in this case.

a) d/2
b) 16 times the diameter of the smallest longitudinal bar enclosed
c) 48 times the diameter of the stirrup bar
d) the beam width
e) 300 mm

6.4.2 COLUMNS

a) Design for flexure

The interior columns are to be designed for the moments and axial forces obtained directly from the elastic analysis including P-delta effects. These design moments are to be amplified to account for column slenderness effects according to code clause 10.11.6.The column design charts provided by the Canadian Portland Cement Association (1985) may be used to determine the column reinforcement ratios based on the amplified design moments and the corresponding axial forces.

b) Design for shear

The interior columns should be designed for the shear forces corresponding to the probable strength of the column plastic hinges. This probable strength shall be calculated for the axial load which results in the highest flexural resistance. The factored design shear force in this case will be

$$V_{col} = \frac{M_{pc}^{top} + M_{pc}^{bot}}{h_c} \qquad (6.10)$$

where M_{pc} is the probable resistance of the column plastic hinges and the superscripts *top* and *bot* refer to the top and bottom of the column respectively.

Both concrete and steel can be assumed to offer resistance to the factored shears. The provided hoops shall conform to the detailing requirements described below.

c) Detailing

The interior columns are expected to undergo inelastic deformations. The concrete and steel should be confined properly to ensure that the column section can attain the ductility demands imposed on it. It is suggested here that the ties or hoops provided in the interior columns should conform to the requirements for columns in ductile frames given in code clauses 21.4.4.2through 21.4.4.5(inclusive). The main difference between these requirements and the ones specified for exterior columns is the proper calculation of the amount of confining steel and also the smaller maximum specified tie spacing.

6.4.3 JOINTS

It is suggested here to design and detail the interior joints as those of ductile frames, with one exception : the calculation of the joint shear forces. The difference between the beam moments to the left and right of the joint is what causes shear forces in the joint due to the transfer of bond stresses from the beam longitudinal steel to the concrete in the joint. This difference between the beam moments on either side of the joint can not exceed the sum of the probable resistances of the columns above and below the joint. Referring to figure (6.7) the joint design shear forces, V_j, can be calculated as

$$V_j = \frac{M_{pc}^a + M_{pc}^b}{d-d'} - V_{col} \qquad (6.11)$$

where d-d' is the distance between the top and bottom reinforcement in the beam.

6.5 APPLICATION OF THE PROPOSED DESIGN PROCEDURE TO THE SIX STOREY BUILDING WITH 6.0 METRE FRAME SPACING

The six storey building reported by Paultre and Mitchell (1991) was redesigned using the proposed approach outlined in sections 6.2 to 6.4. The loading, material properties and the member dimensions were kept the same as those used by Paultre and Mitchell. Two frames were designed. The first frame, designated as 6SAD, had the same member dimensions as the small columns frame 6SPM, while the second frame 6-AD had the same member dimensions as 6-PM. The letters AD in the frame designation stand for Alternative Design. The longitudinal and transverse reinforcement in the beams and columns were calculated. Figure (6.8) shows the reinforcement ratios of the two frames designed here. For comparison purposes, the reinforcement ratios of the frames designed by Paultre and Mitchell are also shown in figure (6.8). The following are the main features of the design of 6SAD and 6-AD.

a) The designed frames contained 20 percent more steel than the nominally ductile frames designed to minimum code requirements. However, the frames designed here contained 20 percent less steel than the nominally ductile frames designed by Paultre and Mitchell (1991).

b) At the interior joints, the beams were found to be stronger than the columns (equation 6.5 was satisfied). Therefore, the relaxed detailing requirements will be employed in the interior spans.

c) In the exterior span beams, the maximum factored shear was 270 kN. Using 2-legged No. 10 stirrups and neglecting the concrete shear resistance, the required spacing will be 0.26 d. This is slightly larger than the maximum spacing suggested for the exterior spans (d/4). Therefore, the stirrups provided in the end regions of the exterior spans will be 2-legged No. 10 bars spaced at 1/4 of the beam depth.

d) In the interior spans, maximum factored shear was 280 kN. Taking the concrete shear resistance into consideration, the required spacing of two legged No. 10 stirrups will be 240 mm. This spacing is slightly smaller than the maximum spacing suggested for the interior span (d/2). Therefore, the 2-legged No. 10 stirrups will be spaced at 240 mm in the interior spans.

e) Based on the calculated shear forces, only minimum transverse reinforcement is required for the columns. For the exterior columns of 6-AD, 4-legged No. 10 ties are spaced at 150 and 300 mm for the end zones and central portion of the column respectively. For the interior columns, ties are spaced at 100 and 300 mm for the end zones and central portion respectively. For the exterior columns of 6SAD, ties are spaced at 125 and 250 mm for the end zones and central portion of the column respectively. For the interior

columns, ties are spaced at 100 and 250 mm for the end zones and central portion respectively. For the first storey interior columns of both frames, ties are spaced at 100 mm for the full height of the column.

6.6 LATERAL STRENGTHS OF THE DESIGNED FRAMES

The frames designed in this chapter were analyzed statically under monotonically increasing static loading. The loads were distributed over the frame height according to the distribution suggested by NBCC 1990 for the equivalent static seismic loads. Figure (6.9) shows the base shear-top displacement curve of the small column frame, 6SAD, while figure (6.10) depicts the curve for the large column frame, 6-AD. Also shown on the same figures are the force-deformation curves of the nominally ductile frames designed to minimum code requirements (6SND and 6-ND) and those designed by Paultre and Mitchell (6SPM and 6-PM). The static force deformation response of the frames designed using the proposed approach are only slightly different from the response of the frames designed by Paultre and Mitchell (1991). The difference in ultimate strength is less than 10 percent.

Figure (6.11) shows the sequence of plastic hinge formation in the small columns frame 6SAD while figure (6.12) shows this sequence for the large column frame 6-AD. Also shown in the same figures are the plastic hinge sequence for 6SND, 6SPM, 6-ND and 6-PM. In the frames designed using the "strong exterior column" approach the plastic hinges appeared in the exterior span beams and the

interior columns as they were expected. The nominally ductile frames designed to meet minimum code requirements (6SND and 6-ND) developed plastic hinges in both exterior and interior beams and columns. Moreover, both 6SND and 6-ND developed storey side sway mechanisms in the first storey. This behaviour stems from the fact that the design of nominally ductile frames does not follow a definite strength hierarchy as to the relationship between beam and column strengths. In the frames designed by Paultre and Mitchell (1991), 6SPM and 6-PM, the number of hinges was smaller than that observed in 6SND and 6-ND. However, the hinges appeared in both beams and columns with no definite pattern. Moreover, the small columns-frame, 6SPM, developed the undesirable storey side sway mechanism.

It was of interest to study the bending moments in the beams at different stages of loading. The first storey beam of 6-AD was considered. Figure (6.13a) shows the factored moment envelopes from which the bar cut-off points could be determined. Figure (6.13b) shows the beam bending moment diagram at the design base shear level ($V=V_{code}$) while figure (6.13c) shows the moments at the end of the nonlinear static analysis ($V=2.5V_{code}$). At the design base shear level no plastic hinges occurred. At the end of the analysis, plastic hinges occurred only in the exterior spans. In the right exterior span, a negative moment plastic hinge occurred at the face of the exterior column. In the left exterior span, the positive moment plastic hinge would occur at the bar cut-off point as expected.

The advantage of the proposed design approach is evident because it provides a predictable response of the frame by ensuring the plastic hinges occur as conceived in the design. Another advantage is that this desirable and predictable performance is achieved without an excessive overdesign of the columns as the case of DMRF design. In the proposed design approach, only the exterior columns are required to be stronger than the beams framing into them. There is only one beam per floor that frames into the exterior column as compared to two beams framing into each individual interior columns. Thus, this alternative design requires the sum of strengths of the exterior columns above and below a joint to be greater than the strength of only one beam. This is a substantial reduction in column strength requirement from DMRF design.

The inelastic static analysis allowed the determination of the overall yield displacements of the frames which were found to be 102 mm for 6SAD and 99 mm for 6-AD. These yield displacements will be used as the normalizing displacement in calculating the global frame ductility demands under dynamic loading.

6.7 DYNAMIC ANALYSIS RESULTS

The frames designed here were analyzed dynamically under earthquake excitation. The dynamic analysis procedures described in chapter 2 were used in the analysis. The dual component bilinear model was used for the columns while the single component stiffness degrading model was used for the beams. The response

parameters used in the investigation are the overall displacements , drifts and ductility demands, the beam and column ductility demands and the beam and column shear demands. The fifteen earthquake records listed in table (2.4) were used as the ground motion input. The results discussed below are based on a statistical analysis of the individual frame responses to each ground motion record.

6.7.1 OVERALL DISPLACEMENTS AND DUCTILITY DEMANDS

Figure (6.14) shows the envelope of mean lateral displacements and mean drift indices for the small columns frame, 6SAD, while figure (6.15) depicts the corresponding results for the large columns frame, 6-AD. Also shown in the same figures are the results for the nominally ductile frames designed to minimum code requirements (6SND and 6-ND) and those designed by Paultre and Mitchell (6SPM and 6-PM). The deformations in 6SAD and 6-AD are only slightly larger than the deformations in 6SPM and 6-PM (designed by Paultre and Mitchell, 1991). This confirms that the overall responses of the frames designed using the proposed approach are similar to the responses of the frames designed by Paultre and Mitchell as shown in the static lateral load analysis. This means that similar seismic performance could be obtained with 20 percent less reinforcing steel, when the definitive design rules proposed here are used. The deformations of 6SAD and 6-AD are smaller than those attained in the nominally ductile frames designed to meet minimum code requirements. This improvement is expected due to the larger amount of steel in the exterior columns.

The mean global ductility demand of 6SAD was 1.46 while it was 1.28 for 6-AD. Once again, these values are only slightly larger than the ductility demands obtained for the frames designed by Paultre and Mitchell.

6.7.2 MEMBER DUCTILITY DEMANDS

6.7.2.1 Beam Ductility Demands

The curvature ductility demands in the beams of the small columns frame, 6SAD are shown in figure (6.16) while figure (6.17) depicts the beam ductility demands in the large columns frame, 6-AD. Also shown in the same figures are the beam ductility demands for the nominally ductile frames designed to minimum code requirements (6SND and 6-ND) and those designed by Paultre and Mitchell (6SPM and 6-PM). By monitoring the positive moment values at different points along the exterior spans of 6SAD and 6-AD, it was found that the demand moments never exceeded the nominal positive moment capacity of the beam. The reason is that the earthquake did not impose sufficient displacement for the beam to develop positive moments large enough to cause yielding. Thus, the ductility demands recorded for the exterior spans were all due to the negative moment plastic hinges at the exterior column faces.

The maximum ductility demands attained in the exterior span beams of 6SAD and 6-AD are in the same order as those observed in the nominally ductile frames designed to meet minimum code requirements, 6SND and 6-ND. However, the interior span beams of the frames 6SAD and 6-AD hardly underwent any inelastic

deformations as conceived by the design approach. In this respect, the performance of 6SAD and 6-AD is superior to that of 6SND and 6-ND.

The ductility demands in the exterior spans of 6SAD and 6-AD are larger than those attained in the beams of the frames designed by Paultre and Mitchell, 6SPM and 6-PM. This fact does not imply that the performance of 6SAD and 6-AD is inferior to that of 6SPM and 6-PM because the ductility demands occurred in the exterior spans where they were expected and where careful detailing was provided to ensure that the ductility demands can be attained without excessive damage.

The large ductility demands in the exterior spans justify the decision to disregard the concrete shear resistance in the design of the exterior span beams. The small ductility demands in the interior spans imply that the concrete shear resistance can be relied upon in the shear design of those spans.

6.7.2.2 Column Ductility Demands

Figure (6.18) shows the curvature ductility demands in the columns of the small columns frames, 6SND, 6SPM and 6SAD, while figure (6.19) shows those ductility demands for the large column frames 6-ND, 6-PM and 6-AD. For the frames designed using the strong exterior column approach 6SAD and 6-AD, the exterior columns remained virtually elastic while the interior columns underwent inelastic deformations. This distribution of inelastic deformations is a direct result of the definite strength hierarchy used in the design of the frames. The ductility demands in the interior columns of 6SAD and 6-AD are in the same order as those observed

in the columns of 6SND and 6-ND. However, the fact that the exterior columns of 6SAD and 6-AD remained virtually elastic implies that a storey side-sway mechanism did not occur. This confirms that the performance of frames designed using the "strong exterior column" approach is better than the performance of nominally ductile frames in which a storey side-sway mechanism may occur.

The ductility demands in the columns of the frames designed by Paultre and Mitchell, 6SPM and 6-PM, are smaller than those attained in the interior columns of the frames designed in this chapter. However, since sufficient detailing is provided in the interior columns and no storey side-sway mechanism has developed, such large ductility demands would not cause excessive damage or collapse of the frame.

6.7.3 BEAM SHEAR DEMANDS vs BEAM SHEAR CAPACITY

Figure (6.20) shows a comparison between the shear demands, the design shears and the shear capacity for the *exterior* span beams of 6SAD and 6-AD. There is a good agreement between the demand shears and the design shears calculated using the procedure suggested in this chapter. As mentioned in the previous section, the ductility demands in the exterior span beams are quite large which implies that the concrete shear resistance can not be relied upon. Figure (6.20) shows that the capacity of the provided stirrups exceeds the shear demand which would prevent any premature shear failure in the beams even if the concrete shear resistance were non existent.

Figure (6.21) shows a comparison between the shear demands, the design shears and the shear capacity for the *interior* span beams of 6SAD and 6-AD. Similar to the case of exterior spans, there is a good agreement between the demand shears and the design shears calculated according to the procedure described in chapter 5. This emphasizes the validity of the proposed shear modification procedure. Since the interior span beams hardly undergo any inelastic deformations, the concrete may be assumed to contribute fully to the beam shear resistance. Figure (6.21) shows that the beam shear capacity (concrete and steel) exceeds the beam shear demands by a large margin thus preventing the possibility of shear failure.

In summary, the proposed procedures for shear design in the exterior and interior span beams are adequate to prevent any shear problems in the beams. This again mainly stems from the deterministic approach used in the design of the entire frame.

6.7.4 COLUMN SHEAR DEMANDS vs COLUMN SHEAR CAPACITY

Figures (6.22) and (6.23) show a comparison between the shear demands, the design shears and the shear capacity of the columns of 6SAD and 6-AD respectively. The shear demands are in good agreement with the design shears for both exterior and interior columns. This confirms the validity of the procedures proposed for calculating the design shear forces in the columns. Figures (6.22) and (6.23) also show that the column shear capacity always exceeded the demand shears thus preventing shear failure in the columns.

6.8 SUMMARY

An alternative approach was proposed for the design of low-rise reinforced concrete frames in seismic regions. The proposed approach avoids the very large conservatism arising from adopting the strong column-weak beam requirements of ductile frames. It also avoids the shortcomings found in the performance of nominally ductile frames designed to meet minimum code requirements. The proposed approach involves designing the exterior columns to be stronger than the exterior bay beams while the interior columns are designed for the factored forces and moments. The proposed approach was used to design the six storey building used by Paultre and Mitchell. The static and dynamic responses of the designed frames were compared to the responses of the nominally ductile frames designed by Paultre and Mitchell (1991) and those designed to meet the minimum code requirements. The following remarks could be drawn from the results of the analyses performed in this chapter;

1) The overall deformations and ductility demands for the frames designed using the alternative approach were smaller than those for the frames designed to meet the minimum code requirements. Moreover, the distribution of inelastic deformations within the frame when subjected to seismic excitation was as conceived by the design approach. Therefore, the proposed design approach had the advantage of providing a predictable behaviour such that careful detailing can be provided at the locations of plastic hinges.

2) The deformations and ductility demands of the frames designed using the proposed approach were found to be larger than those attained in the frames designed by Paultre and Mitchell (1991). However, since the ductility demands in the frames designed in this chapter were concentrated where adequate detailing was provided, they do not constitute a shortcoming in the frame performance since they will not cause excessive damage due to the quality of detailing. The predictable distribution of inelastic deformations was a result of the definite design rules employed in the "strong exterior column" approach.

   The "strong exterior column" design approach produces an acceptable seismic performance of the designed frames with smaller amounts of steel than the frames designed by Paultre and Mitchell (20 percent savings in steel weight). Moreover, the proposed design approach can be carried out under definite design rules. On the other hand, the rules of the Paultre and Mitchell design are not explicitly available.

3) The proposed beam shear design procedures resulted in design shears that were in good agreement with the demand shears. The beam shear capacity (stirrup's shear capacity only allowed in exterior spans, stirrups and concrete shear capacity allowed in the interior spans) always exceeded the shear demands preventing any premature shear failure in the beams. The proposed column shear design procedures also produce good agreement between the

demand and design shears. The column shear capacity exceeded the shear demands which would prevent shear failure in the columns.

4) The amount of reinforcement in the strong exterior column frames was 20 percent more than the amount required for the nominally ductile frames designed to meet minimum code requirements. The increase is mainly due to reinforcement in the exterior columns. It should be pointed out that the frames considered here had three bays with two exterior columns and two interior columns. If the frame had more bays, the ratio of the number of exterior columns to interior columns will decrease. This will result in decreasing the percentage of additional reinforcement acquired due to adopting the alternative design procedure. Figure (6.24) shows a schematic relationship between the number of bays and the increase in steel due to using the proposed approach as compared to the nominally ductile frame design. It is evident that the alternative design approach is most suited for low-rise frames having a large number of bays. In such a case, the proposed approach will provide a better performance than nominally ductile frames with a minimal increase in the provided reinforcement.

5) The shear forces in the joints were not monitored in the dynamic analysis. Further research is required to examine the adequacy of the procedures suggested here for the shear design of joints.

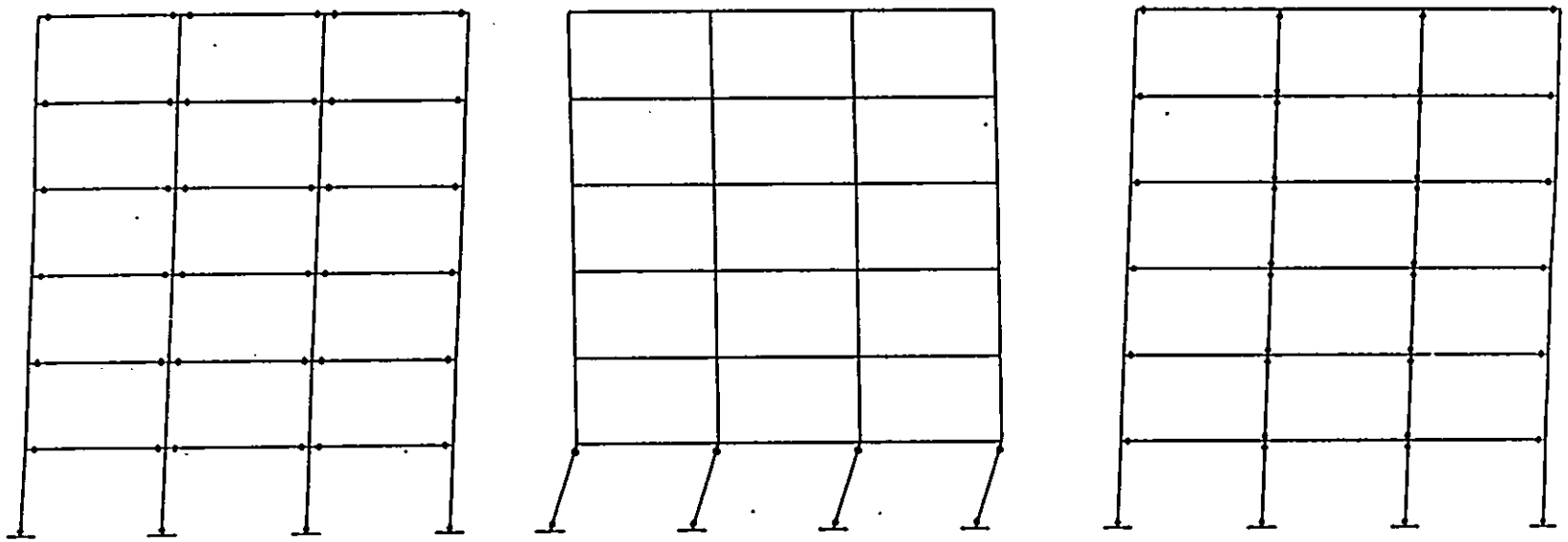

a) Desirable mechanism
(strong column-weak beam)

b) Undesirable mechanism
(Strong beam-weak column)

c) Alternate desirable mechanism
(strong exterior column)

Fig. (6.1) Different failure mechanisms of a multi-storey frame.

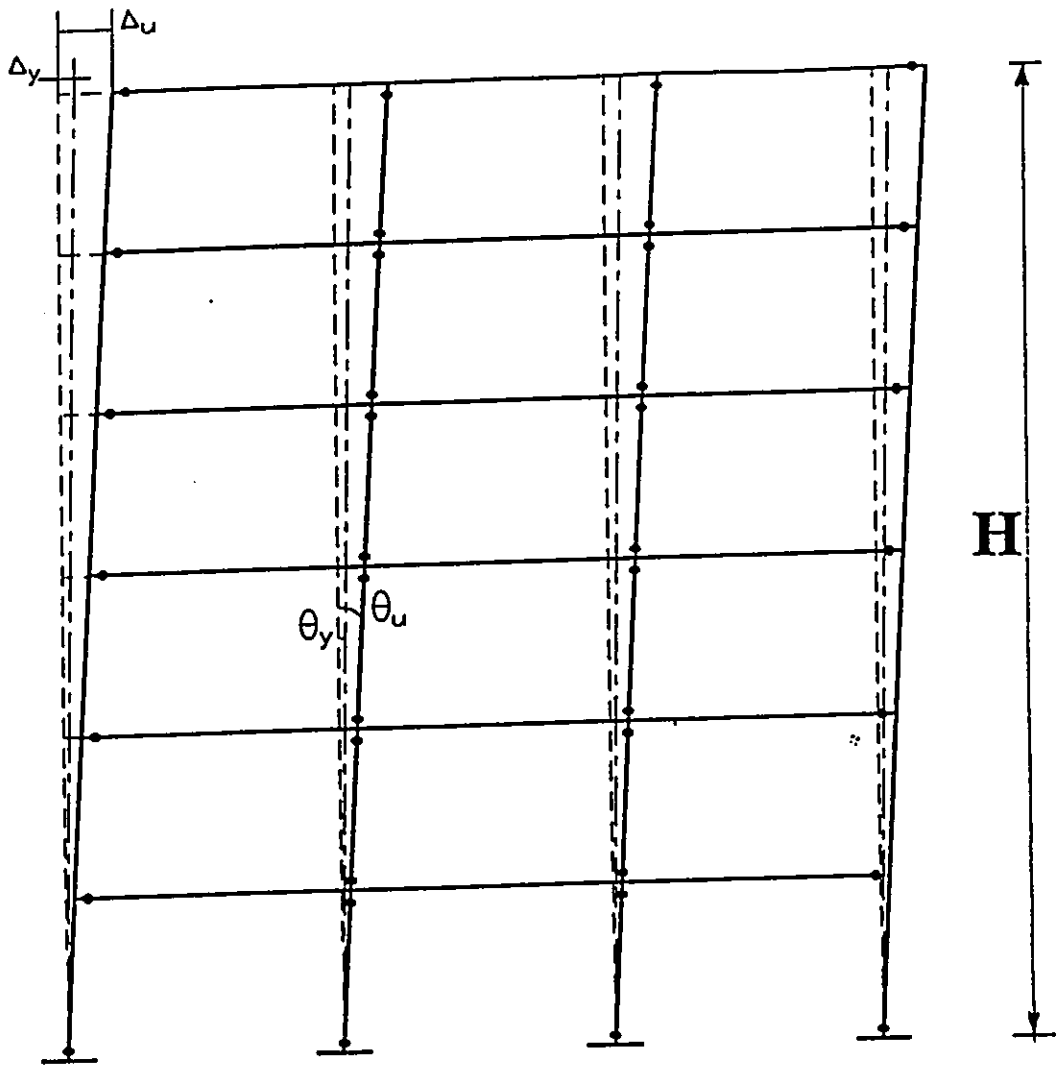

$$\mu_\Delta = \frac{\Delta_u}{\Delta_y} \qquad \mu_\theta = \frac{\theta_u}{\theta_y} \qquad \theta_y = \frac{\Delta_y}{H} \qquad \theta_u = \frac{\Delta_u}{H}$$

$$\therefore \ \mu_\theta = \frac{\theta_u}{\theta_y} \approx \frac{\Delta_u}{\Delta_y} \approx \mu_\Delta$$

Fig. (6.2) Relationship between local and global ductility demands.

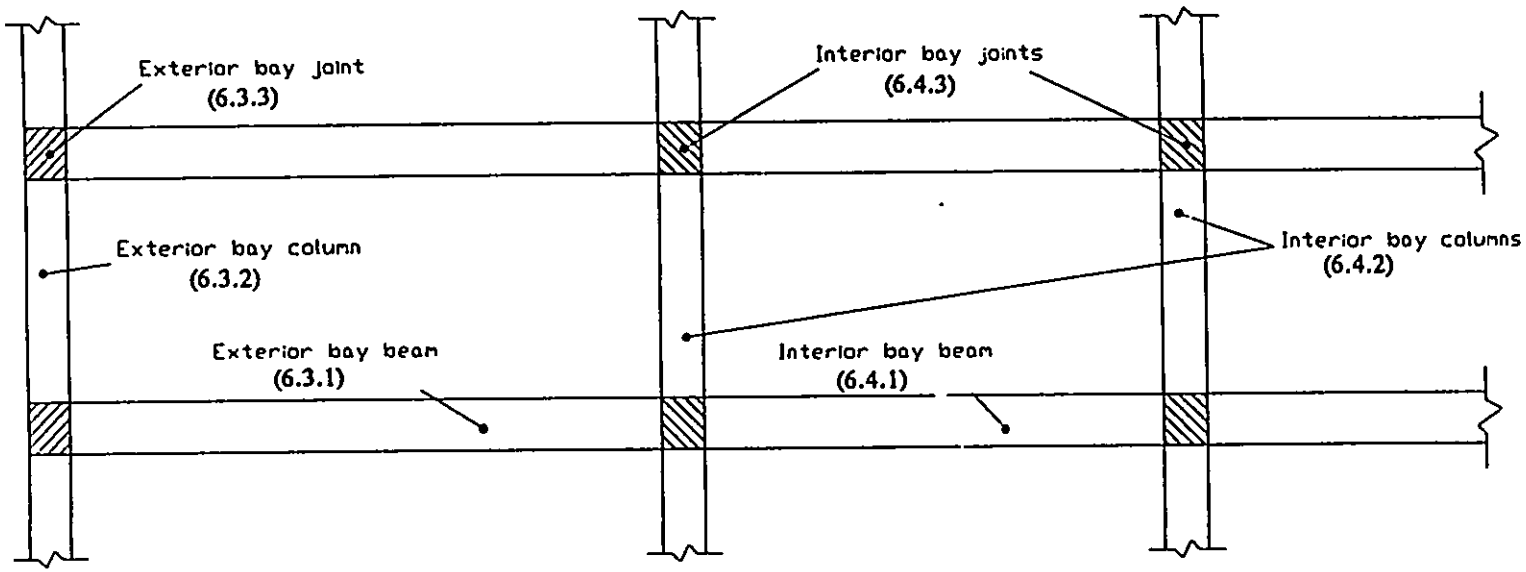

Fig. (6.3) **Different components of the designed frame (numbers in parentheses refer to the section in which the design of the component is explained).**

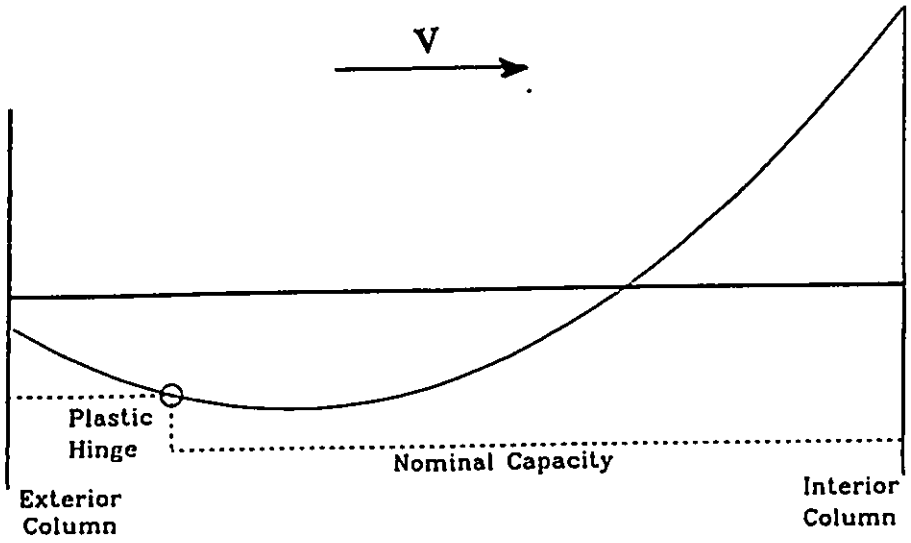

a) Increasing Bending moment diagram

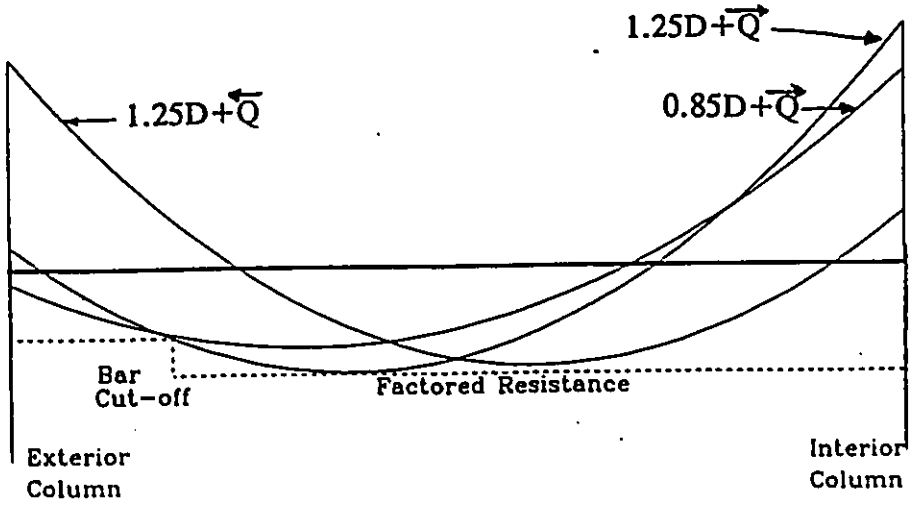

b) Factored moments envelope.

Fig. (6.4) Location of positive moment plastic hinge in the exterior span.

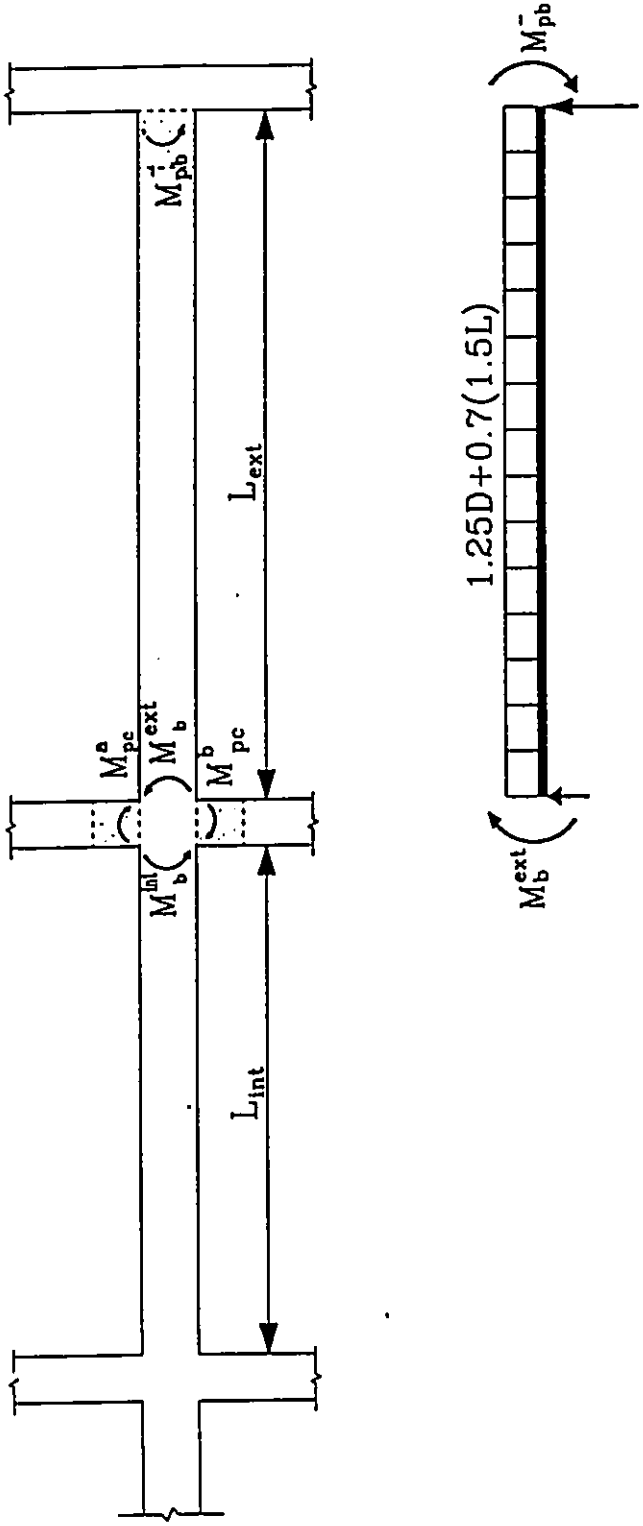

Fig. (6.5) Calculation of design shear forces in exterior span beams.

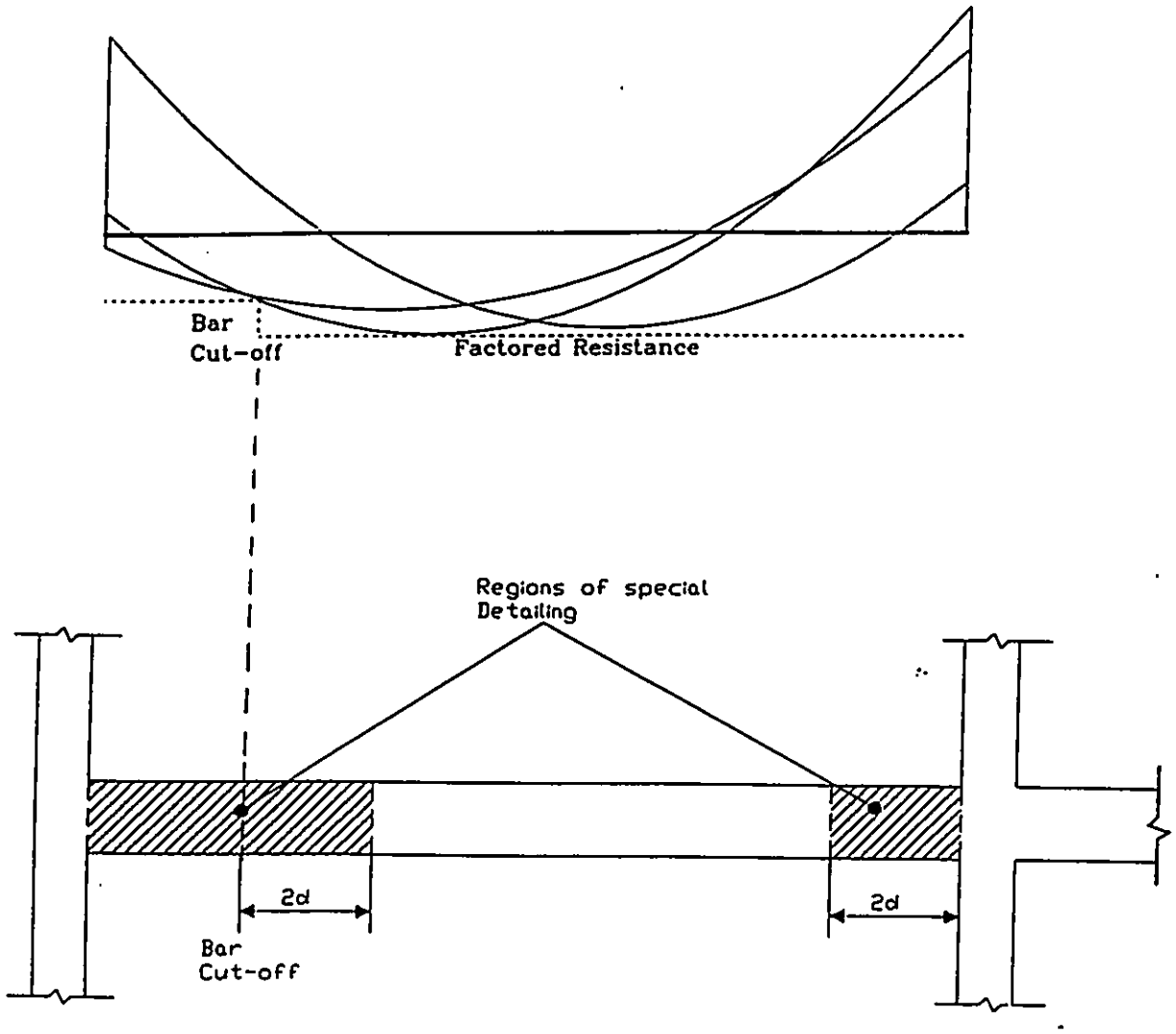

Fig. (6.6) Regions of special detailing in the exterior span.

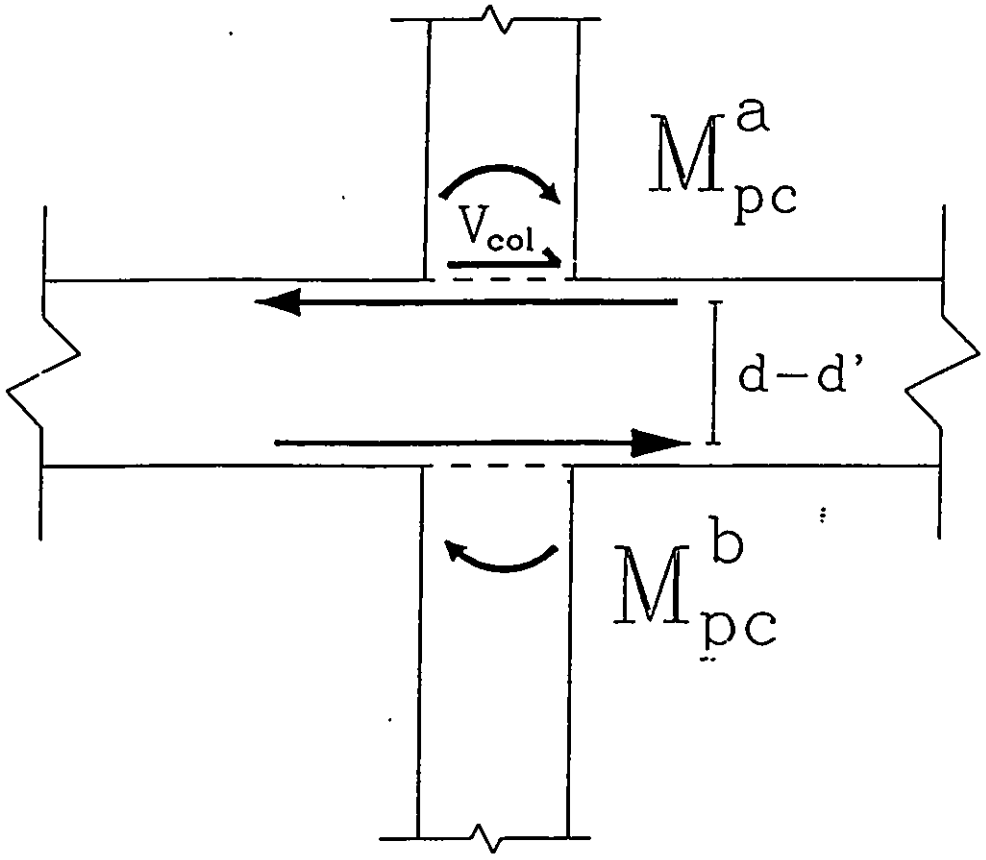

Fig. (6.7) Calculation of design shear forces in the interior joints.

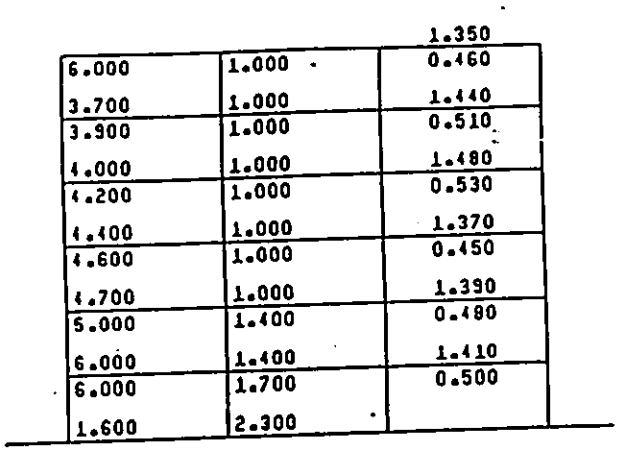

a) 6SAD

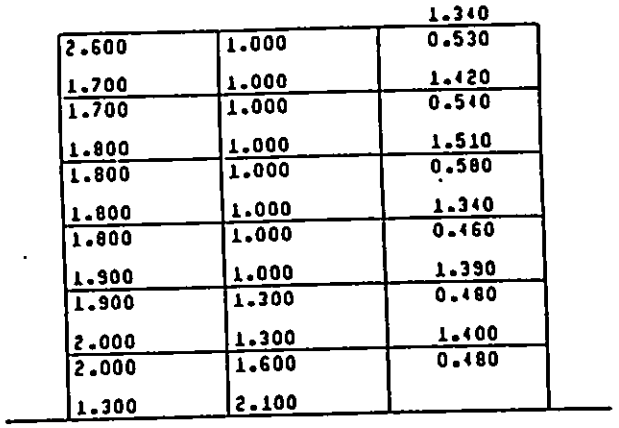

b) 6-AD

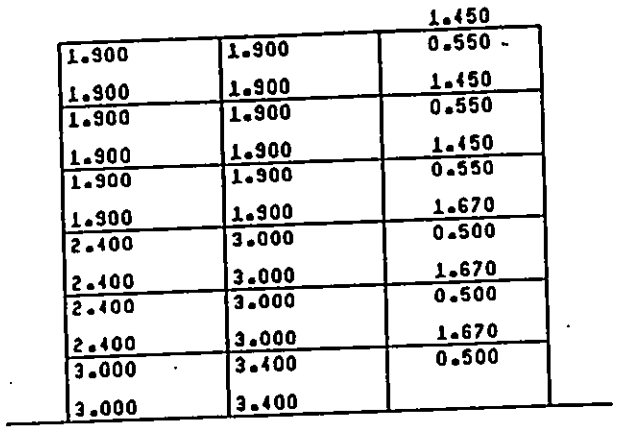

c) 6SPM

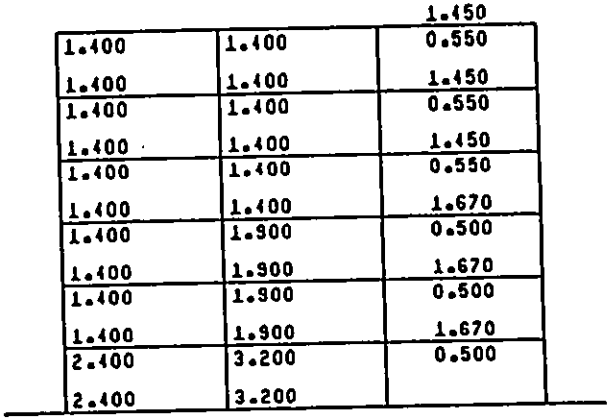

d) 6-PM

Fig. (6.8) **Reinforcement ratios in the frames designed using the proposed design approach and the frames designed by Paultre and Mitchell (1991).**

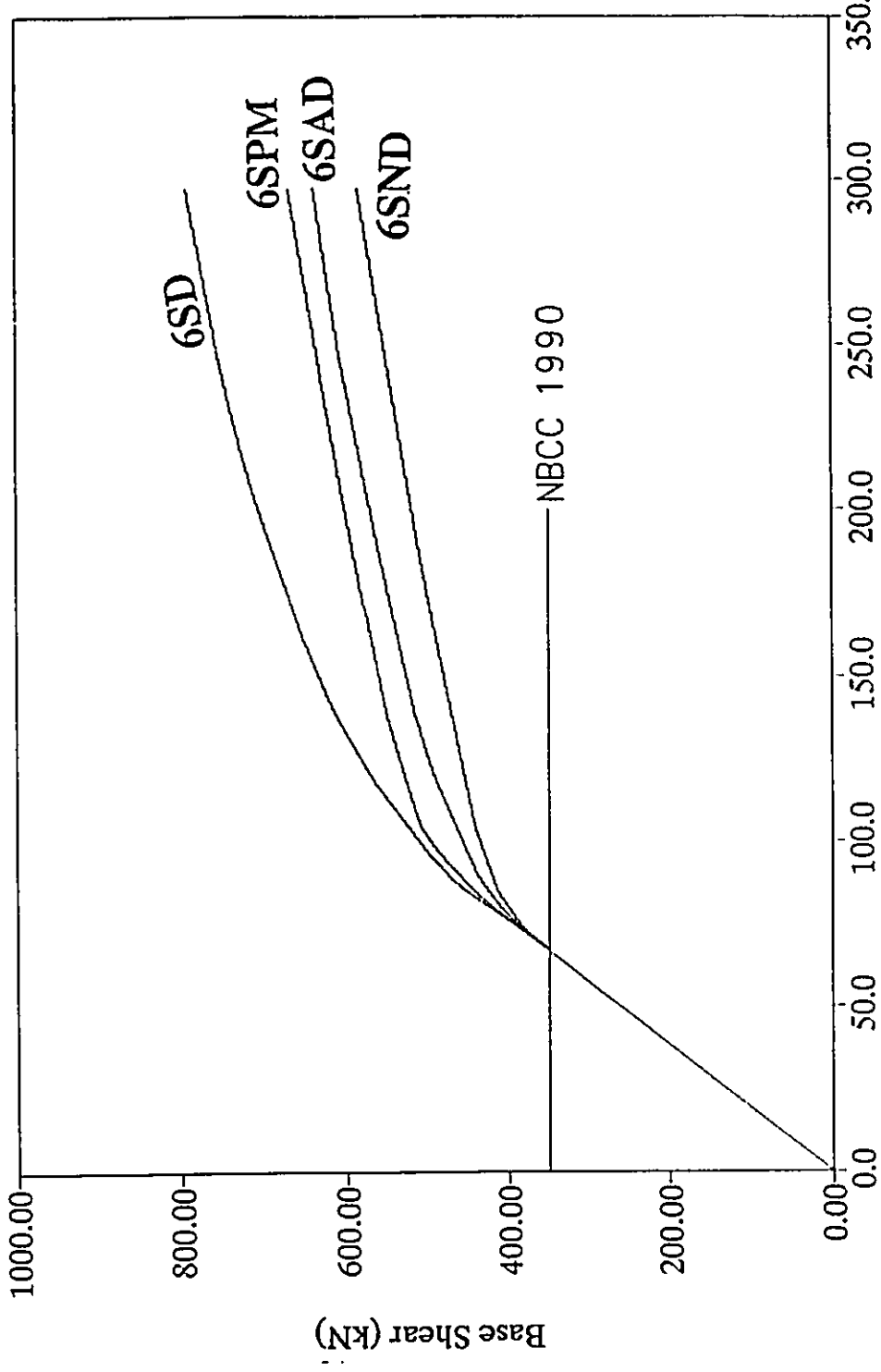

Fig. (6.9) Base shear-top displacement curves of the six storey frames with the small columns.

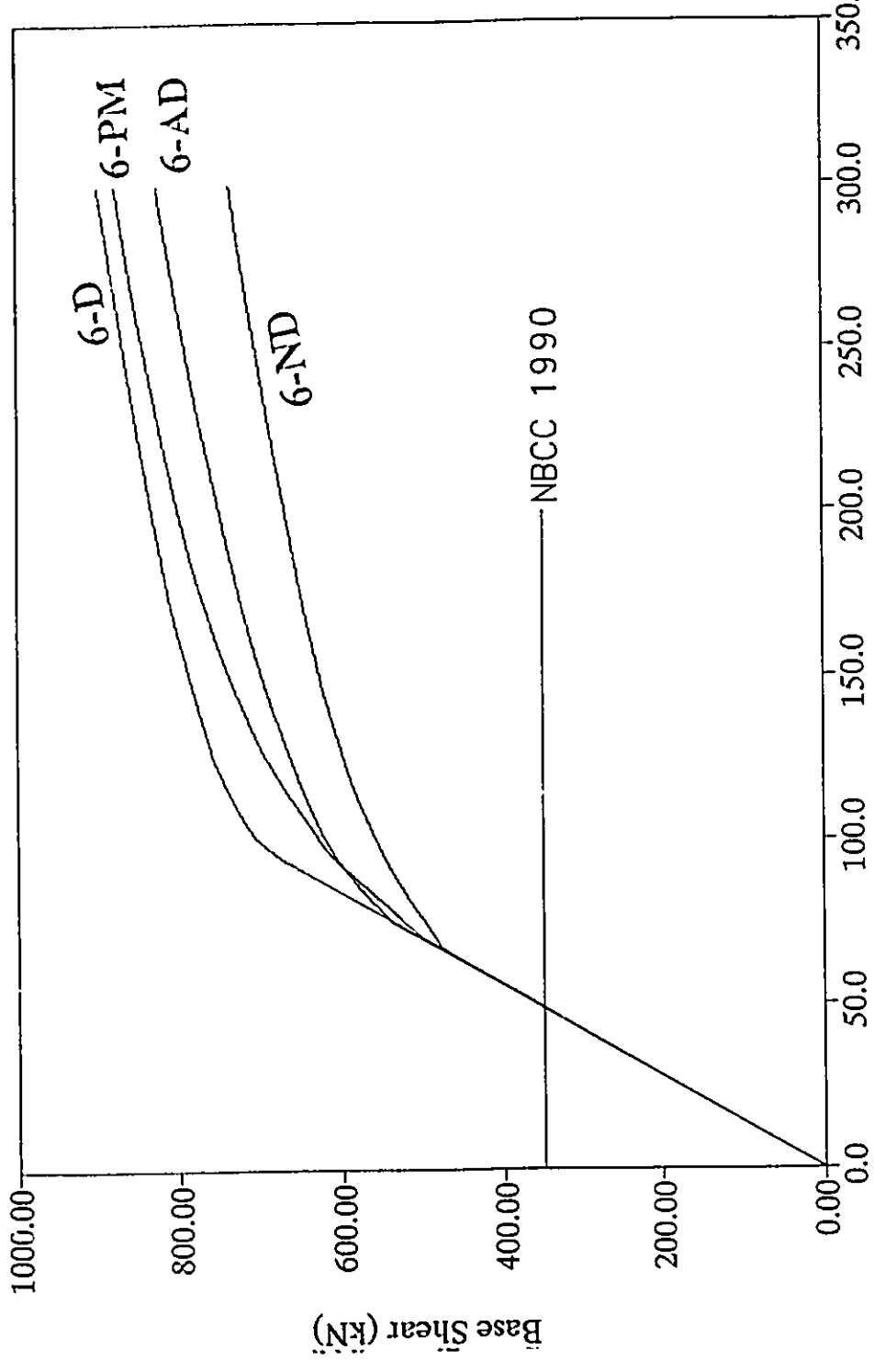

Fig. (6.10) Base shear-top displacement curves of the six storey frames with the large columns.

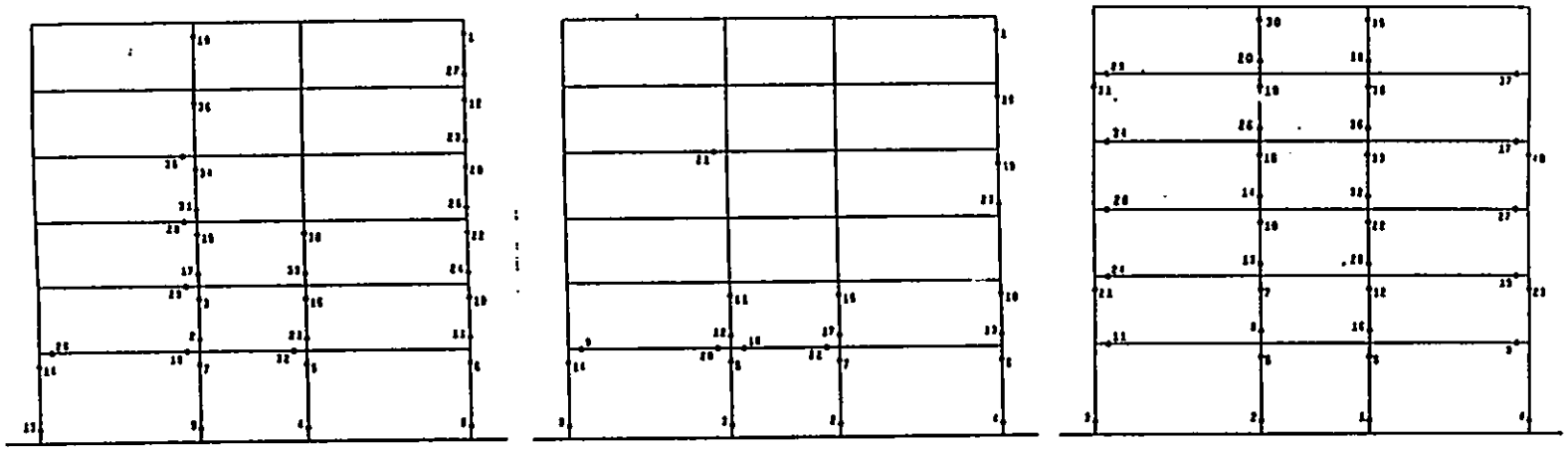

a) 6SND b) 6SPM c) 6SAD

Fig. (6.11) Sequence of plastic hinge formation in the small columns-six storey frames.

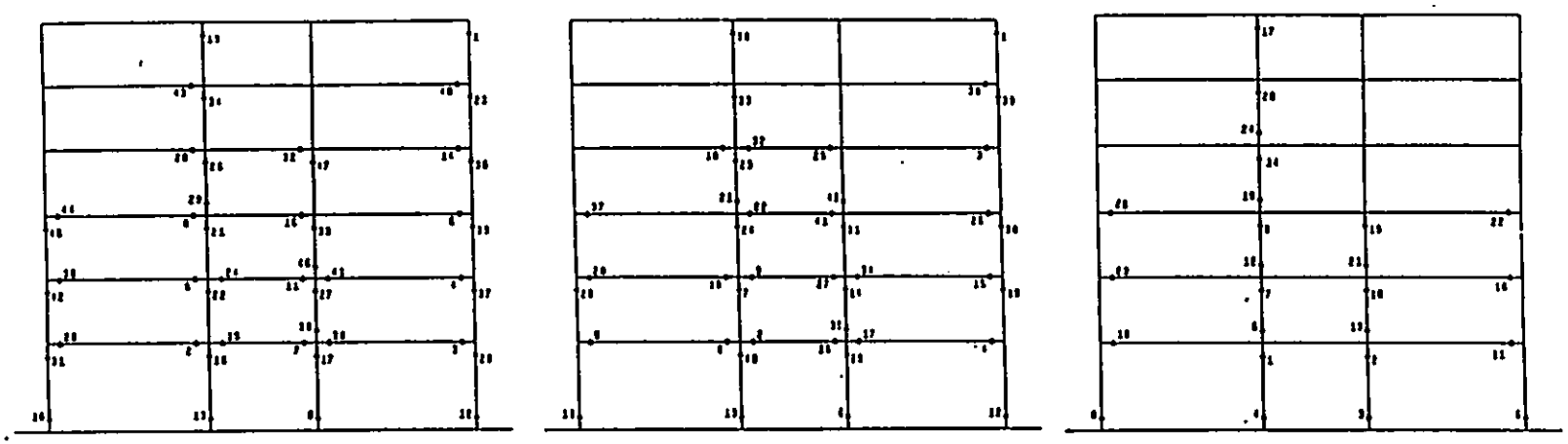

a) 6-ND b) 6-PM c) 6-AD

Fig. (6.12) Sequence of plastic hinge formation in the large columns-six storey frames.

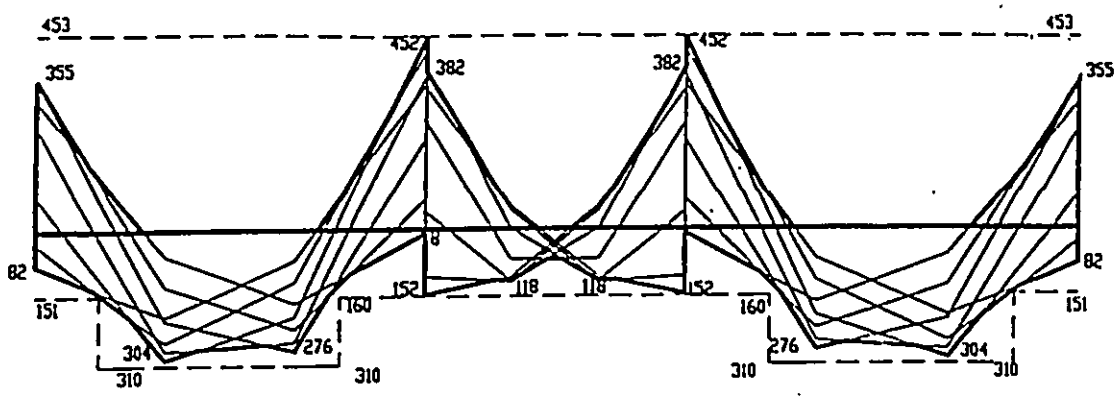

a) Factored moments envelope.

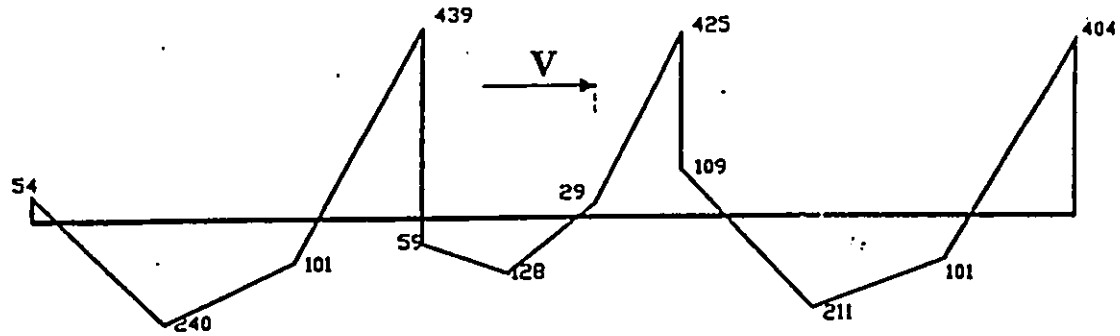

b) Bending moments at Design base shear level (V_{code}).

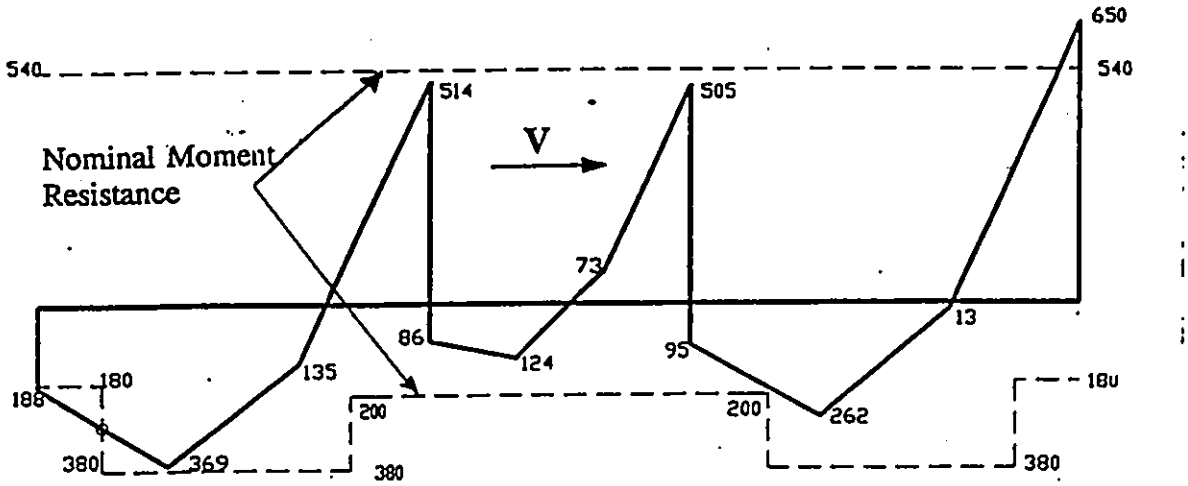

c) Bending moments at 2.5 V_{code}.

Fig. (6.13) Bending moment diagrams in the first storey beam of 6-AD.

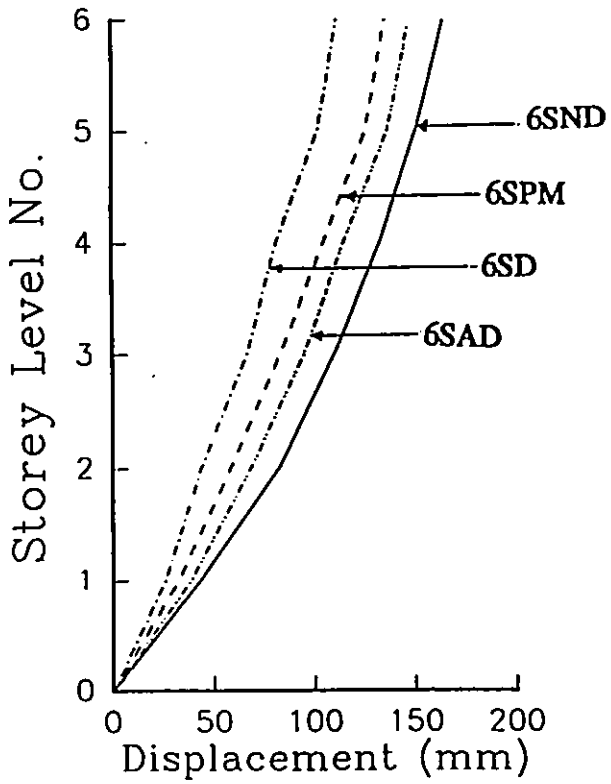

a) Lateral displacements

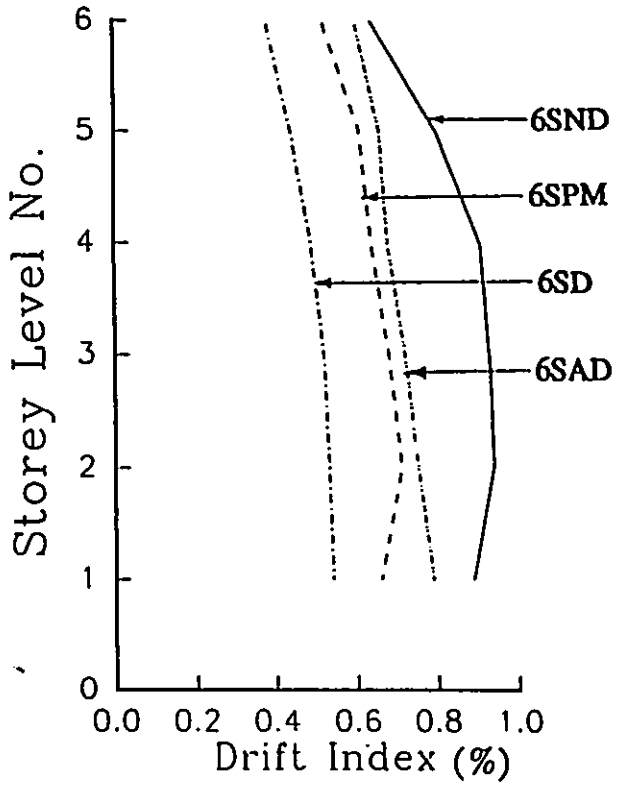

b) Drift indices

Fig. (6.14) **Mean lateral displacements and drift indices of the small column frames.**

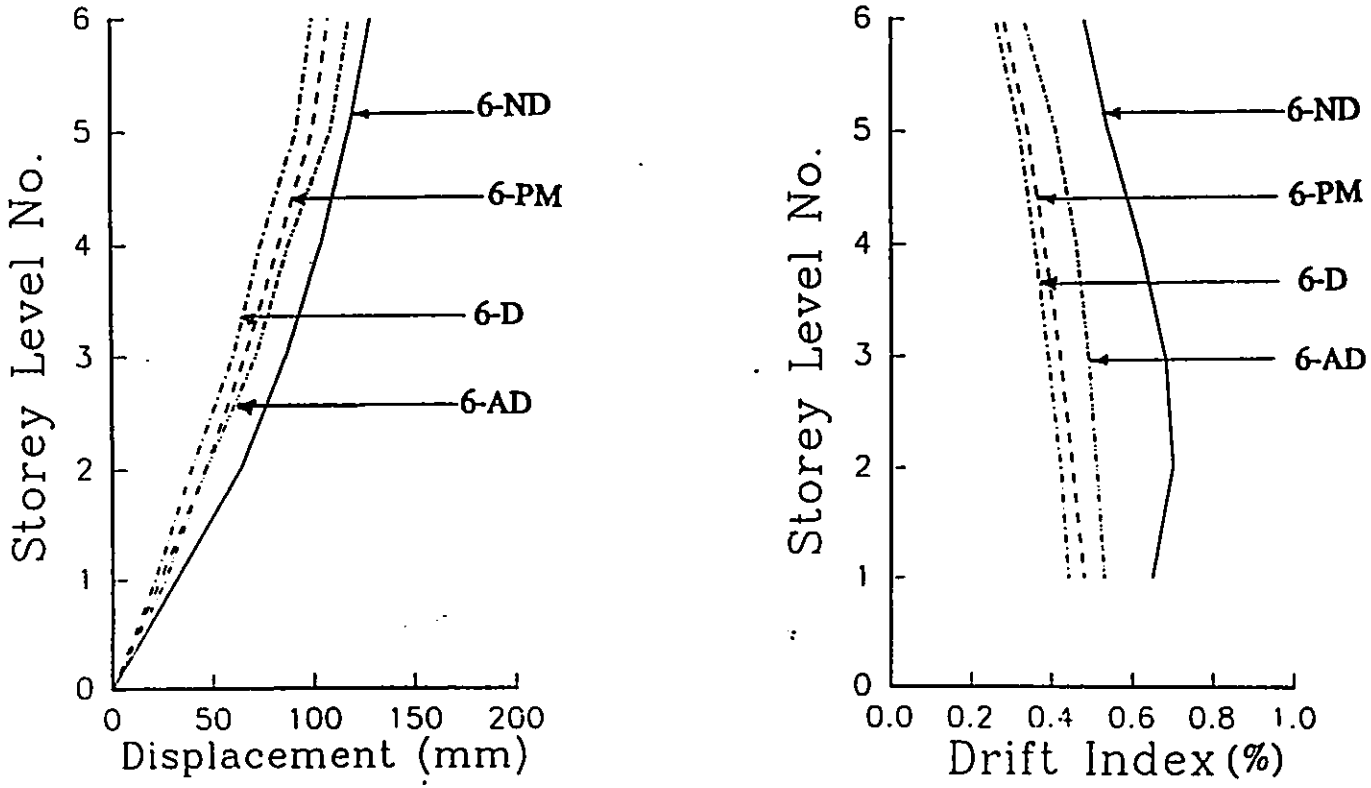

a) Lateral displacements

b) Drift indices

Fig. (6.15) **Mean lateral displacements and drift indices of the large column frames.**

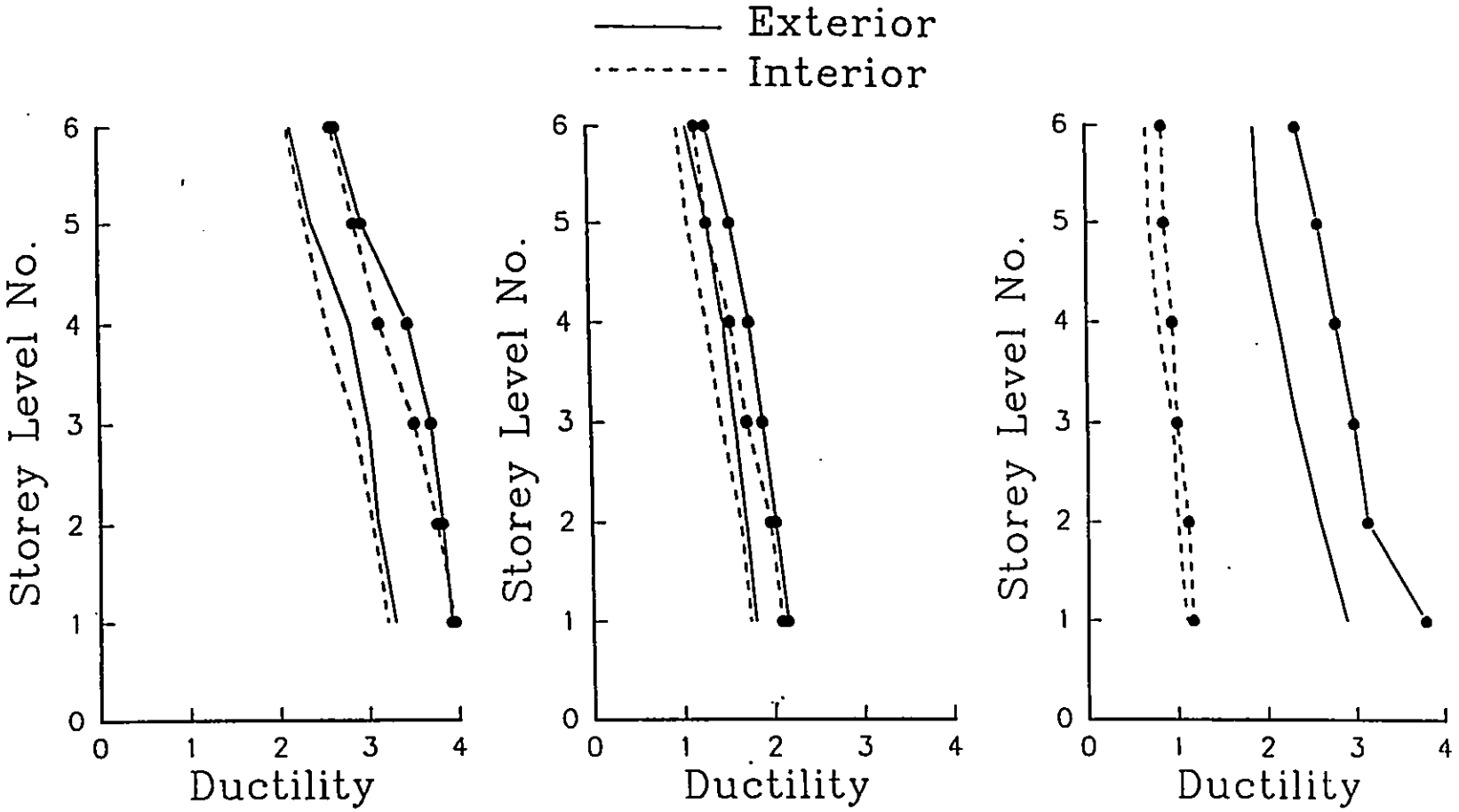

a) 6SND b) 6SPM c) 6SAD

Fig. (6.16) Curvature ductility demands in the beams of the six storey frames with the small columns (• = mean + σ).

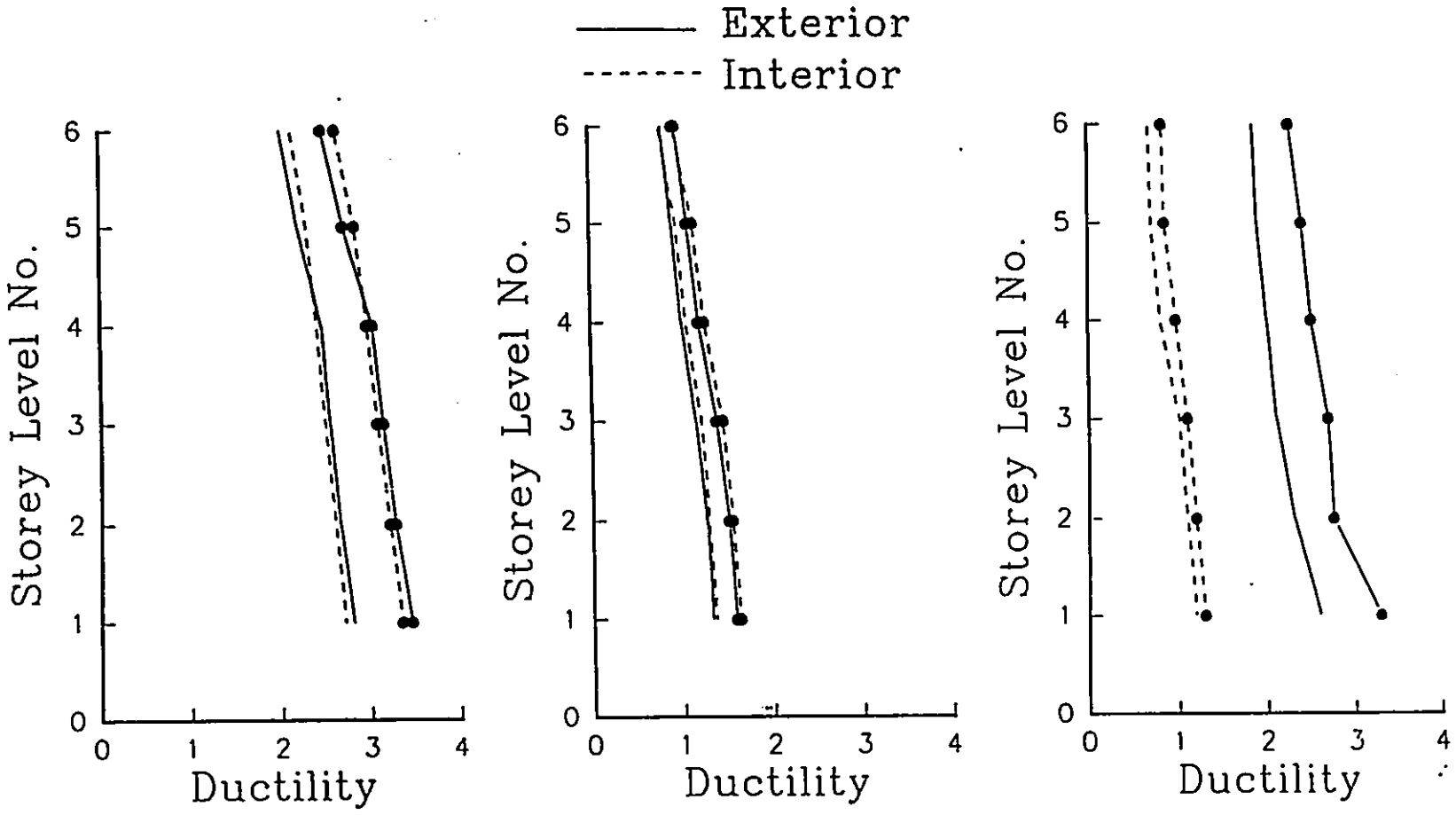

Fig. (6.17) Curvature ductility demands in the beams of the six storey frames with the large columns (• = mean + σ).

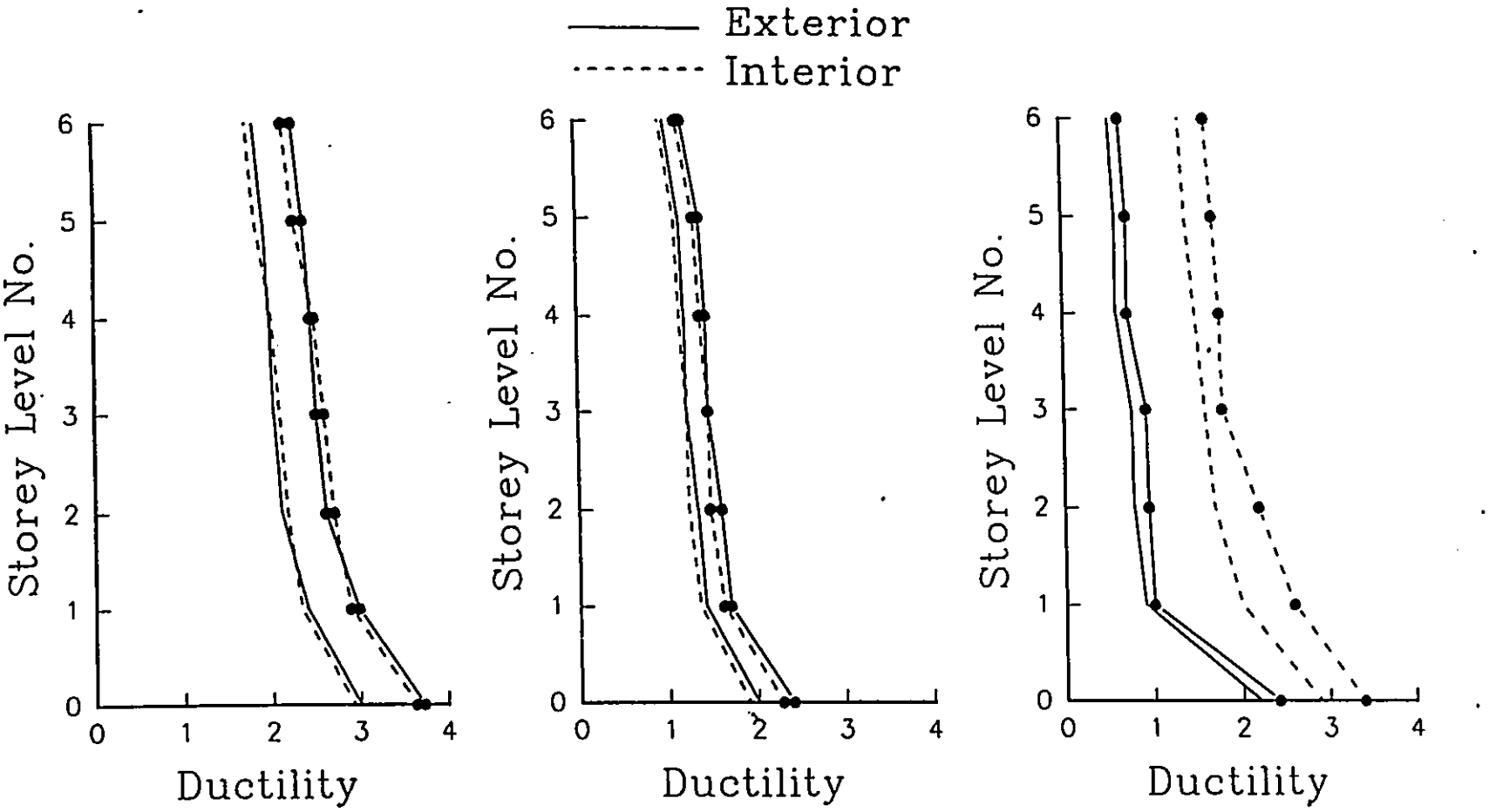

a) 6SND b) 6SPM c) 6SAD

Fig. (6.18) Curvature ductility demands in the columns of the six storey frames with the small columns (• = mean + σ).

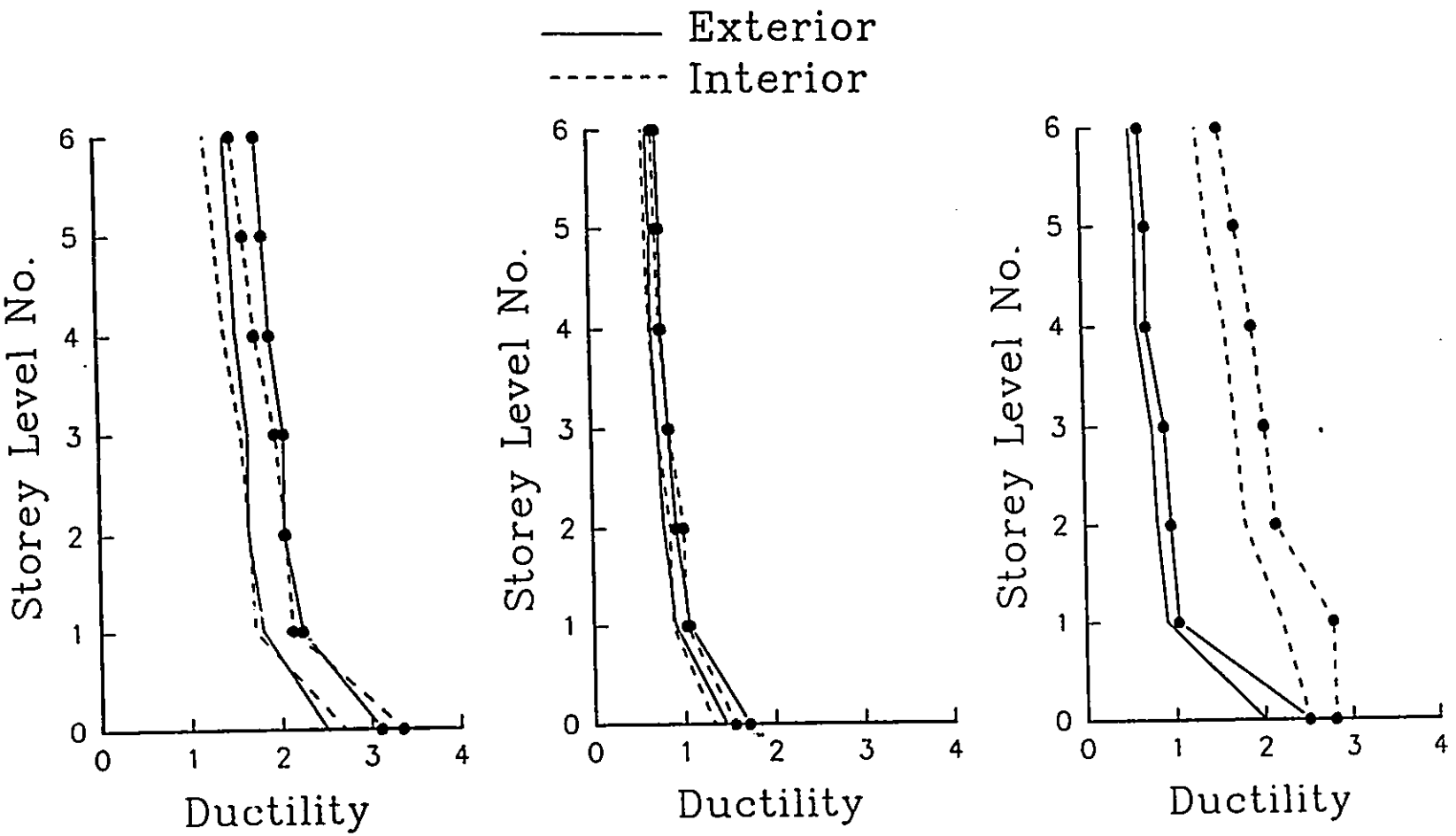

a) 6-ND b) 6-PM c) 6-AD

Fig. (6.19) Curvature ductility demands in the columns of the six storey frames with the large columns (• = mean + σ).

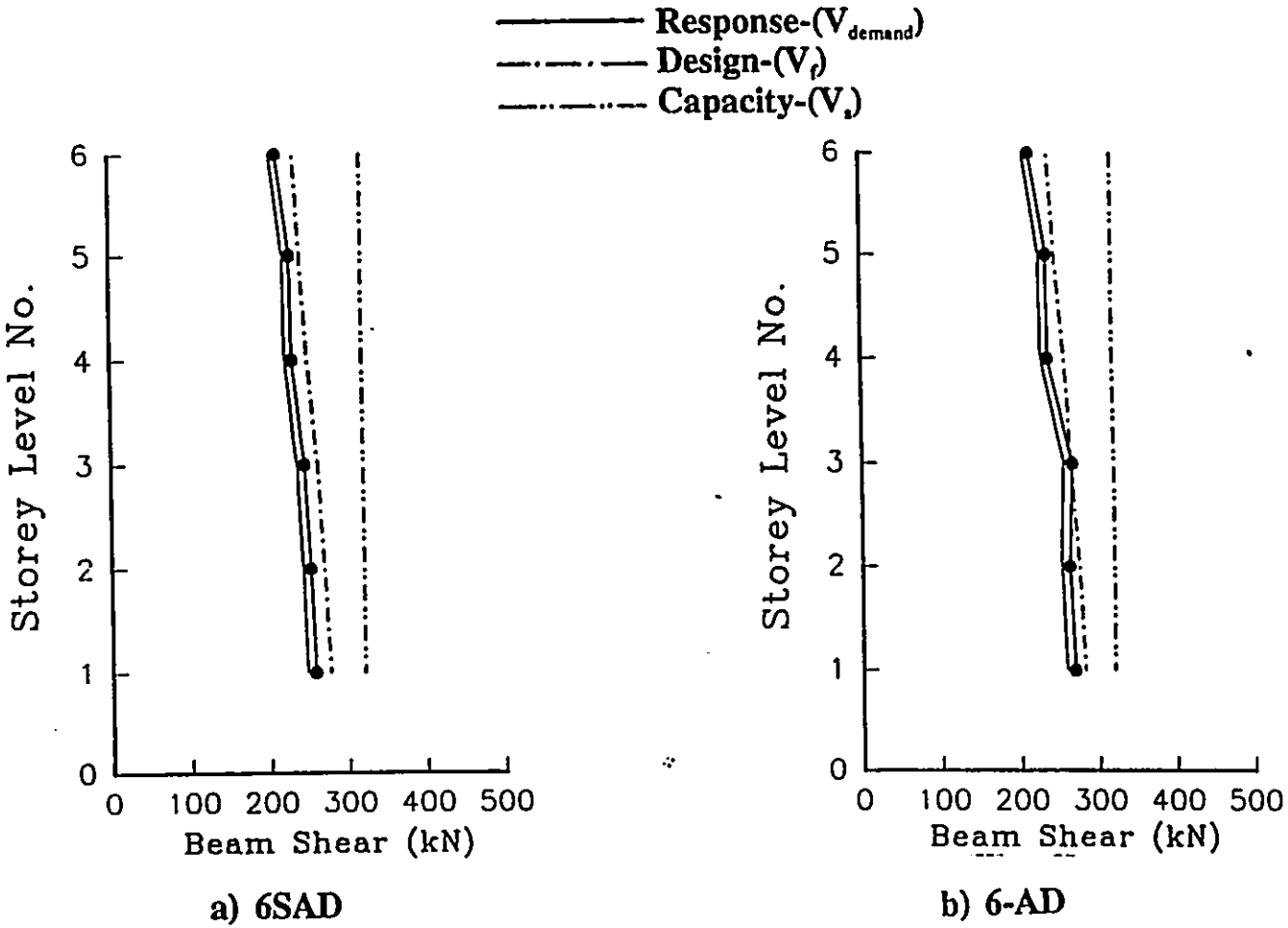

a) 6SAD

b) 6-AD

Fig. (6.20) Comparison between the shear demands and shear capacities of the exterior span beams of the frames designed using the alternative approach (• = mean + σ).

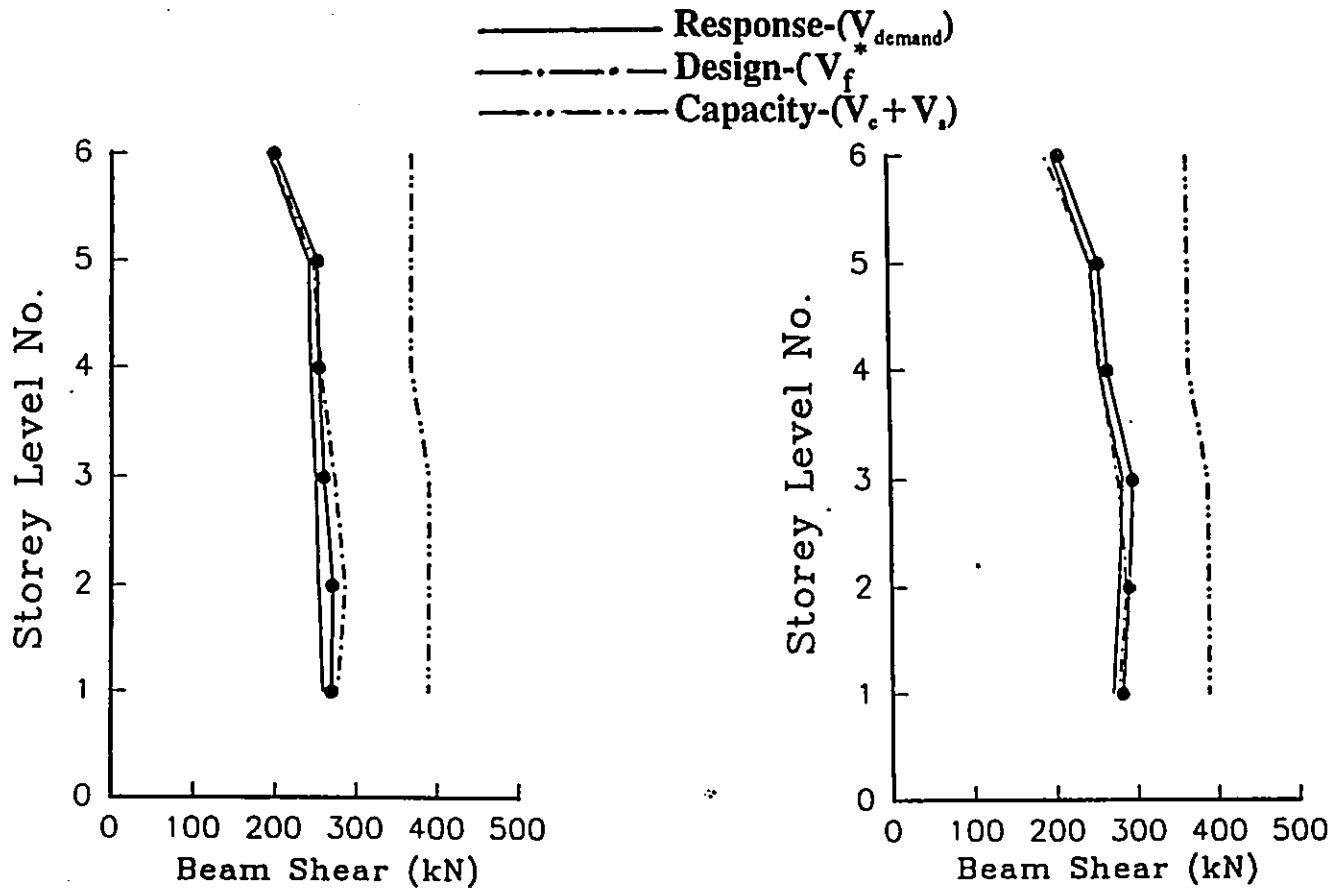

a) 6SAD

b) 6-AD

Fig. (6.21) Comparison between the shear demands and shear capacities of the interior span beams of the frames designed using the alternative approach (• = mean + σ).

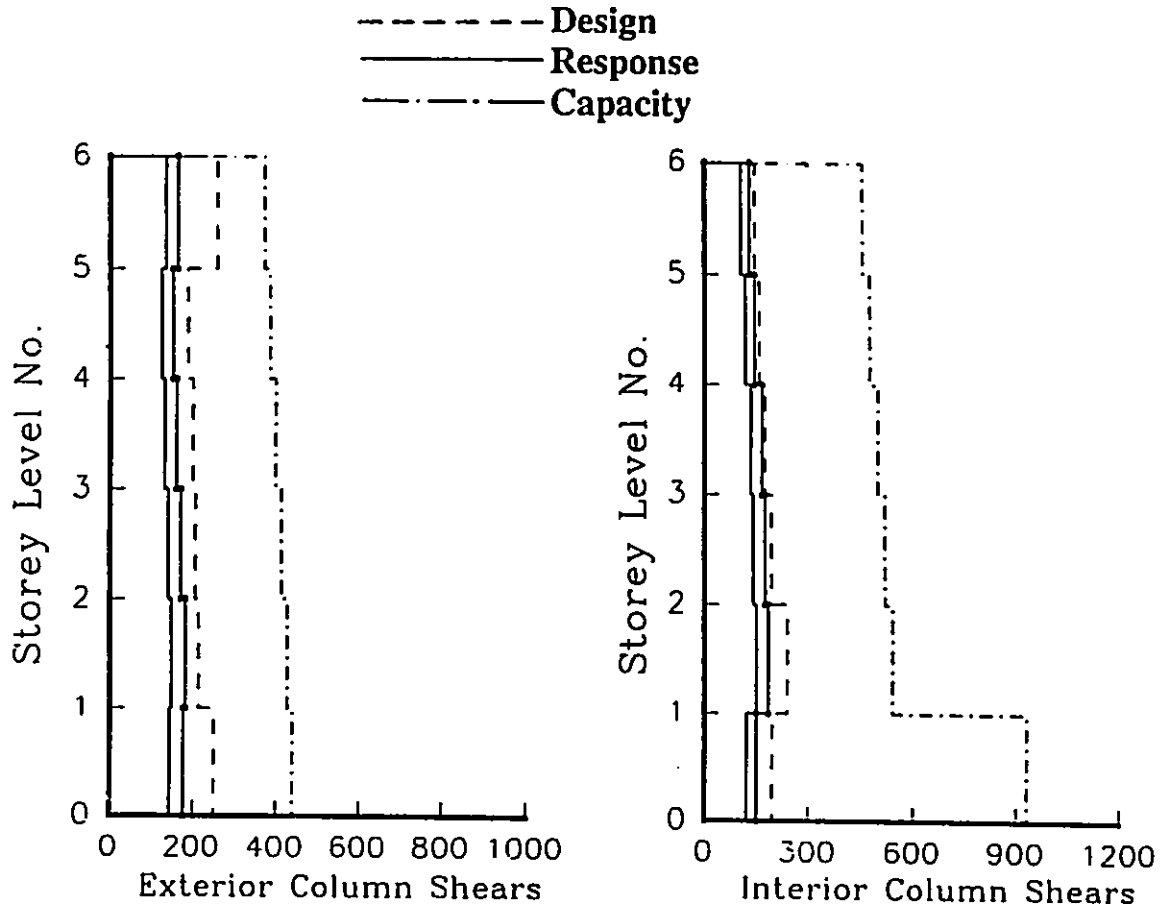

a) Exterior column

b) Interior column

Fig. (6.22) Comparison between the shear demands and shear capacities of the columns of the small columns frame designed using the alternative approach (• = mean + σ).

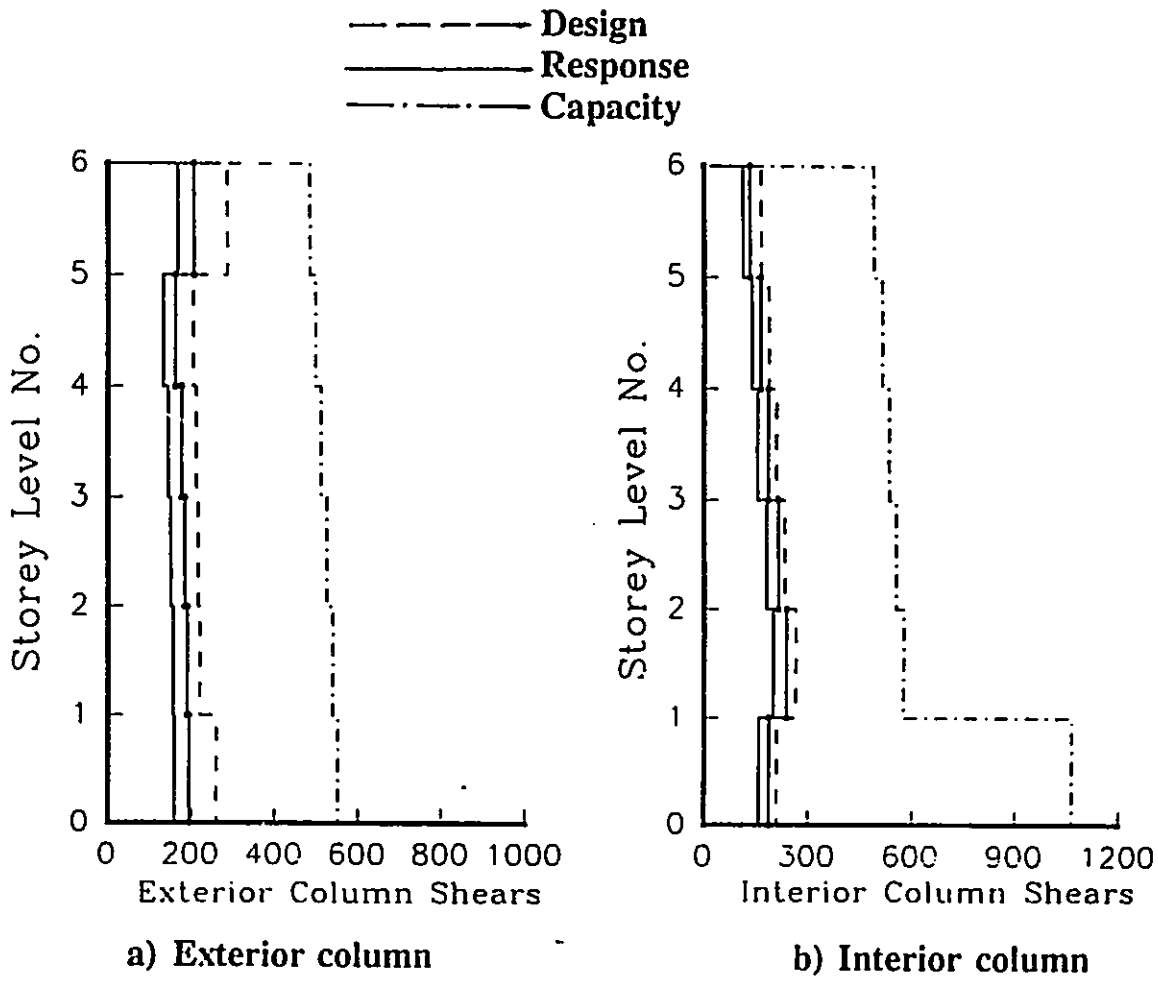

Fig. (6.23) Comparison between the shear demands and shear capacities of the columns of the large columns frame designed using the alternative approach (• = mean + σ).

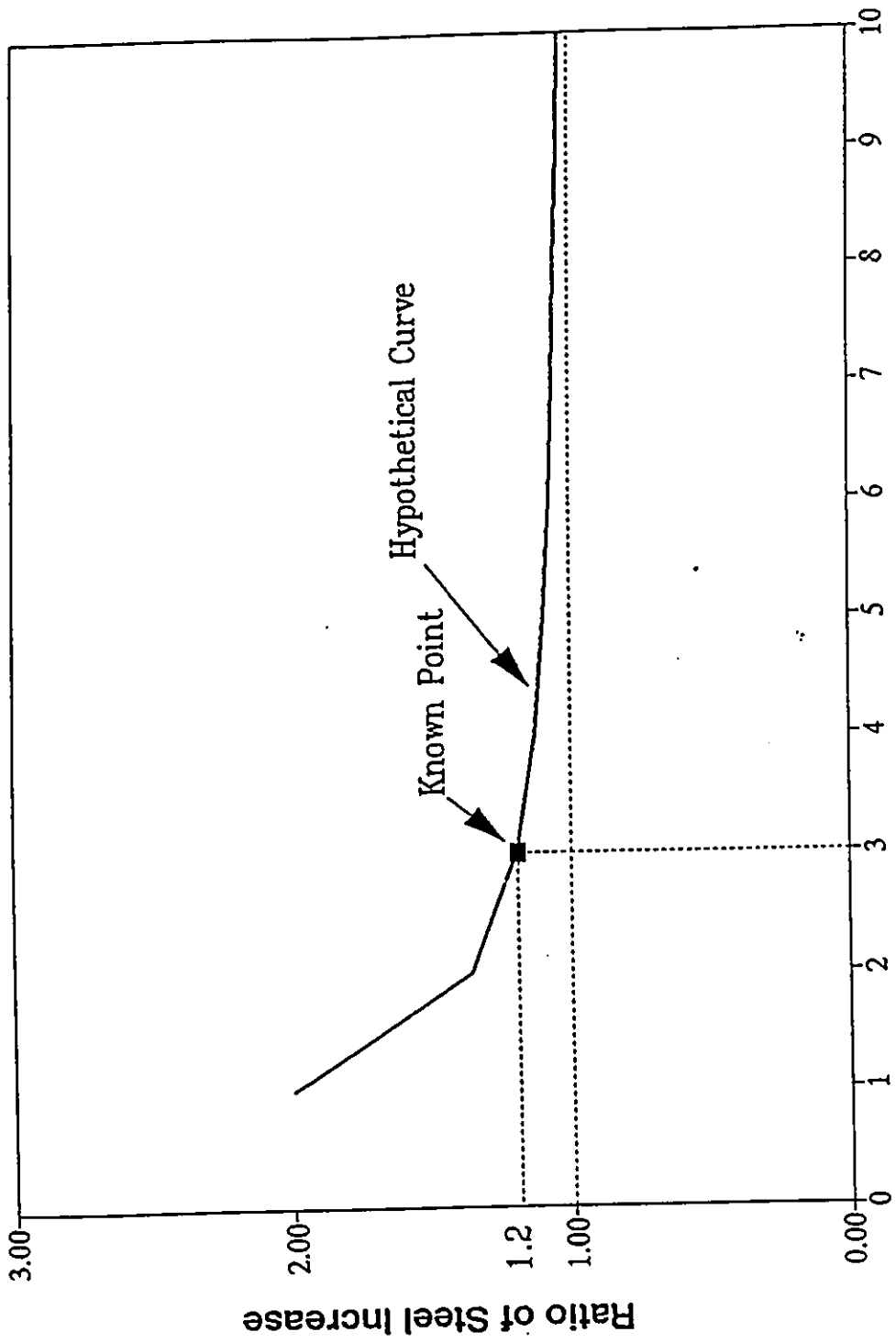

Fig. (6.24) Relationship between the number of bays and the increase in reinforcement due to using the alternative design approach.

CHAPTER 7

SUMMARY AND CONCLUSIONS

7.1 SUMMARY

The objectives of the present study were a) to evaluate the seismic performance of nominally ductile reinforced concrete frames designed according to the current Canadian practice, b) to suggest remedies for some of the shortcomings in the seismic behaviour of nominally ductile frames and c) to propose an alternative design approach to modify the design procedure for low-rise gravity-dominated reinforced concrete frames which are likely to be designed as nominally ductile frames. To achieve these objectives, buildings of different heights were designed as nominally ductile frame structures. The designed frames were analyzed under a monotonically increasing static loading to study their inelastic force deformation characteristics. The designed frames were also analyzed dynamically under earthquake excitation using DRAIN-2D and fifteen ground motion records normalized to the design zonal velocity. The response parameters investigated were the overall displacements, drifts and ductility demands, the local member ductility demands and the beam and column shear demands. An experimental investigation

was carried out to determine the reliability of the concrete shear resistance in the beams of nominally ductile frames when subjected to ductility demands similar to those attained during earthquake excitation. Based on the results of the analytical and experimental analyses, a beam shear modification procedure was proposed in order to increase the design shears to be more representative of the seismic shear demands. Finally, a new design approach for low-rise gravity-dominated was proposed. A brief summary of the different phases of this study is given below;

First, the six storey building previously used by Paultre and Mitchell (1991) was redesigned as a nominally ductile frame structure that satisfies the minimum Code requirements. The static and dynamic responses of the designed frames were compared to those of the frames designed by Paultre and Mitchell (1991) to provide a better understanding of the performance of nominally ductile frames.

Next, the seismic response of a six storey building with wider frame spacing (8.0 metres) was evaluated to show that the larger frame spacing caused an increase in the beam shear demands beyond the capacity of the minimum stirrups required by the Code.

Two beam specimens were tested under reversed cyclic loading. The specimens were a half scale model of the beams of the six storey frame with the 8.0 metre frame spacing. Specimen I was designed and detailed to represent a beam in a nominally ductile frame according to the current Canadian practice. Specimen II represented a beam in a nominally ductile frame in which the provided stirrups are

adequate to resist the maximum applied shear forces. The experimental measurements, including the applied load, the beam tip deflection, the stirrups strains and the flexural and shear deformations in the plastic hinge zone were used to compare the experimental performance of the two specimens.

A shear modification procedure was proposed for the beams of nominally ductile frames. The procedure involves applying a magnification factor to the design shear forces due to seismic lateral loading with the gravity load shears remaining unchanged. The modified design shears were compared to the demand shears in the beams of a four storey, a six storey and a ten storey nominally ductile frames to evaluate the proposed shear modification procedure.

Finally, an alternative design approach was proposed for low-rise gravity dominated frames. In the proposed approach, the exterior columns are designed to be stronger than the beams while the interior columns are designed for the factored combinations of moments and axial forces. The "strong exterior column" design approach was fully explained in the Canadian design context. The proposed approach was used to redesign the frames reported by Paultre and Mitchell (1991). The static and dynamic responses of the designed frames were evaluated in order to validate the aim of the proposed "strong exterior column" design method.

7.2 CONCLUSIONS

The following are the major conclusions that could be drawn from the results of this study;

1) The term nominal ductility as described in the current Canadian codes (NBCC 1990 and CAN3-A23.3-M84) covers a wide variety of frame designs which can be distinctly different in terms of their seismic performance. Since, there are no definite design rules regarding the relationship between beam and column strengths in nominally ductile frames, a designer is allowed to provide any column strength as long as the columns can resist the factored axial forces and moments. Due to this wide variety of frame designs, the conclusions of a particular study may only be applicable to the particular frames considered in that study. The frames designed by Paultre and Mitchell are examples of such a case. Paultre and Mitchell overdesigned the columns of their frame to enhance its seismic performance. The performance of their frame was superior to that of the frame designed strictly following the minimum Code requirements. Therefore, the frame they considered is not representative of NDMRFs and their conclusions may not be generalized to all NDMRFs.

2) NDMRFs designed to meet the minimum Code requirements were found to have several deficiencies in their seismic performance. First, the interstorey drifts can be quite large implying excessive non-structural damage. Second, the

ductility demands in the beams are in the order of 3.0, which can cause the concrete shear resistance to diminish. And finally, the demand shears attained in the beams during earthquake excitation exceed the factored design values by 30 to 40 percent. In some cases, the demand shears also exceed the capacity of the minimum stirrups specified for the beams in the concrete design Code. With large ductility demands and the concrete shear resistance being unreliable, the demand shears that exceed the stirrups capacity can result in an undesirable shear failure. To avoid such a problem, the factored design shears need to be modified in order to be more representative of the demand shears.

3) The specimen representing a beam in a nominally ductile frame (specimen I) had a total shear capacity (concrete and stirrups) that exceeded the maximum applied shear force. In this specimen, the stirrups yielded at a ductility level similar to the ductility demands attained during earthquake excitation. Since the shear capacity of this specimen (concrete+stirrups) is greater than the maximum applied shear forces, the stirrups will yield if (and only if) the concrete shear resistance was unreliable. The yielding of the stirrups in specimen I resulted in large diagonal cracking and excessive inelastic shear deformations and hence led to a rapid strength deterioration and severe pinching in the hysteresis loops. In the specimen which had sufficient stirrups to resist the maximum applied shear forces (specimen II), the stirrups did not

yield resulting in controlled diagonal cracking and shear deformations. This led to stable load-displacement loops with slight strength deterioration and pinching. The results of the experiments showed that the beams in which the shear demands exceed the stirrups capacity would perform poorly when subjected to cyclic loading of ductility demands similar to those attained in nominally ductile frames during earthquake excitation. Therefore, it would be prudent to ignore the concrete contribution to the beam shear resistance in the beams of NDMRFs designed to meet the minimum Code requirements.

4) A procedure was proposed for design shear calculations in the beams of nominally ductile frames. The procedure involves modifying the factored design shears to be more representative of the demand shear and discounting the concrete contribution to the beam shear resistance. A variable magnification factor is to be applied to the design shear forces due to seismic lateral loading in the beams of different storeys. The magnification factor is a function of the total number of storeys and the storey level under considerations. The proposed procedure was shown to give modified design shears that are in close agreement with the shear demands for nominally ductile frames of different heights and configurations.

5) An alternative approach was proposed for the design of low-rise gravity-dominated frames in which the strength of the beams would be controlled by gravity rather than lateral load requirements. The proposed "strong exterior

column" design approach is a compromise between ductile and nominally ductile frame designs. This approach aims at avoiding the unrealistic conservatism resulting from adopting the strong column-weak beam strength hierarchy for all columns (ductile frame design). It also aims at avoiding the deficiencies observed in the performance of NDMRFs designed to meet the minimum Code requirements. Only the exterior columns are designed to be stronger than the beams framing into them while the interior columns are designed for the factored moments and axial forces. Capacity design principles are to be used in the design of the exterior bays while the interior bays are to be designed as those of nominally ductile frames with some modifications. The deterministic approach used in the "strong exterior column" design resulted in a predictable distribution of the inelastic deformations. The plastic hinges occurred where they were expected and where adequate detailing was provided to promote those ductility demands. The stronger exterior columns prevented the occurrence of a storey side sway mechanism under static loading and resulted in smaller drift values under earthquake loading.

6) The desirable performance of the strong exterior column frames was achieved with only a 20 percent increase in reinforcement beyond that required for nominally ductile frames designed to minimum code requirements. This increase in reinforcement is mainly due to the additional reinforcement in the strong exterior columns. If the number of bays is increased, the percentage of

additional reinforcement acquired due to adopting the strong exterior column approach would decrease. The percentage of additional reinforcement also depends on the number of storeys in the frame. A parametric study is required in order to determine the range for which the strong exterior column approach will be most economical.

7) Further research is needed in order to test the validity of the procedures suggested for the shear design of joints in the strong exterior column approach.

REFERENCES

Adeli, H., Gere, J.M. and Weaver, E., 1978. Algorithms for nonlinear structural dynamics. Journal of the Structural Division, ASCE, vol. 104, No. ST-2, p.p. 263-280.

American Concrete Institute (ACI) committee 318, 1989. Building code requirements for reinforced concrete, ACI 318-89., Detroit, Michigan, U.S.A.

Associate Committee on National Building Code, 1990. National Building Code of Canada, NBCC 1990., Ottawa, Canada.

Bertero, V. V. and Popov, E. P., 1975. Seismic behaviour of ductile moment-resisting reinforced concrete frames. American Concrete Institute, Special Publication SP53, Detroit, Michigan, p.p. 247-291.

Blondet, J. M., Clough, R. W. and Mahin, S. A., 1980. Evaluation of a shaking table test program on response behaviour of a two-storey reinforced concrete frame. Report No. EERC 80-42, Earthquake Engineering Research Center, University of California, Berkeley, U.S.A.

Canadian Portland Cement Association (CPCA), 1985. Concrete Design Handbook. Rexdale, Ontario.

Canadian Standards Association (CSA), 1984. Design of concrete structures for buildings, CAN3-A23.3-M84, Rexdale, Ontario.

Chung, Y.S., Meyer, C. and Shinozuka, M., 1987. Seismic damage assessment of reinforced concrete members. Report No. NCEER-87-0022, National center for earthquake engineering research, Buffalo, N.Y., U.S.A.

Chung, Y. S., Shinozuka, M. and Meyer, C., 1988. SARCF User's Guide : Seismic Analysis of Reinforced Concrete Frames. Report No. NCEER-88-0044, National center for earthquake engineering research, Buffalo, N.Y., U.S.A.

_____, 1989. Modelling of concrete damage. ACI Structural Journal, vol. 86, No. 3, p.p. 259-271.

Clough, R. W., Benuska, K.L. and Wilson, E.L. 1965. Inelastic earthquake response of tall buildings. Proceedings, third world conference on earthquake engineering, New Zealand, vol. II, p.p. 68-84.

Clough, R. W. and Benuska, K. L., 1967. Nonlinear earthquake behaviour of tall buildings. Journal of the Egineering Mechanics Division, ASCE, vol. 93, No. EM-3, p.p. 129-146.

Clough, R. W. and Penzien, J., 1975. Dynamics of structures. McGraw-Hill book company, New York, p.p. 634.

Clough, R. W. and Gidwani, J., 1976. Reinforced concrete frame 2 : Seismic testing and analytical correlation. Report No. EERC 76-15, Earthquake Engineering Research Center, University of California, Berkeley, U.S.A.

Dally, J. W. and Riley, W. F., 1978. Experimental stress analysis. McGraw-Hill book company, New York, p.p. 571.

Darwin, D. and Nmai, C. K., 1986. Energy dissipation in RC beams under cyclic load. Journal of Structural Engineering, ASCE, vol. 112, No. 8, p.p. 1829-1846.

El-Hafez, M. B. and Powell, G. H., 1973. Computer-aided ultimate load design of unbraced multi-storey steel frames. Report No. EERC 73-3, Earthquake Engineering Research Center, University of California, Berkeley, U.S.A.

Furlong, R. W., 1971. Column slenderness and charts for design. Journal of the American Concrete Institute (ACI), vol. 68, No. 1, p.p. 9-17.

Gosain, N. K., Brown, R. H. and Jirsa, J. O., 1977. Shear requirements for load reversals on RC members. Journal of the Structural Division, ASCE, vol. 103, No. ST-7, p.p. 1461-1476.

Hamdy, K.A., Ghobarah, A. and Tso, W.K., 1990. Additional seismic response index for evaluating damage potential to structures. Proceedings, Canadian Society for Civil Engineering (CSCE) Annual Conference, Hamilton, Ontario, vol. IV, p.p. 15-26.

Hamdy, K.A., Tso, W.K. and Ghobarah, A., 1991. Seismic damage potential to ductile and nominally ductile concrete frames. Proceedings, Sixth Canadian Conference on Earthquake Engineering, Toronto, Ontario, p.p. 261-268.

_____, 1992a. An evaluation of the current Canadian practice for the seismic design of R/C frames. Proceedings, ESE (Egyptian Society of Engineers)/CSCE International Colloquium on Structural Engineering, Egypt, vol. II, p.p. 957-968.

_____,1992b. Experimental study on the seismic response of beams in R/C frames of nominal ductility. Proceedings, CSCE Annual Conference, Quebec City, Canada, vol. IV, p.p. 275-284.

_____, 1992c. Seismic design of R/C frames - a Canadian code perspective. Accepted for presentation and publication in the proceedings of the 10th World Conference on Earthquake Engineering, Madrid, Spain.

Healey, T. and Sozen, M., 1978. Experimental study of the dynamic response of a ten-storey reinforced concrete frame with a tall first storey. Structural Research Series No. 450, University of Illinois at Urbana-Champaign, Illinois, U.S.A.

Hwang, T.-H., 1982. Effects of variation in loading history on cyclic response of concrete flexural members. Ph.D. thesis, University of Illinois at Urbana-Champaign, U. S. A., p.p. 231.

Hwang, T.-H., and Scribner, C. F., 1984. R/C members cyclic response during various loadings., Journal of Structural Engineering, ASCE, Vol. 110, p.p. 477-489.

International Conference of Building Officials, 1988. Uniform Building Code, UBC 88. U.S.A.

Jennings, P. C., 1965. Earthquake response of a yielding structure. Journal of the Engineering Mechanics Division, ASCE, vol. 91, No. EM-4, p.p. 41-68.

Kanaan, A., and Powell, G. H., 1973. DRAIN-2D, a general purpose computer program for inelastic dynamic response of plane structures., Report No. EERC 73-6, Earthquake Engineering Research Centre, University of California, Berkeley, U.S.A.

Krawinkler, H. and Moncarz, P.D., 1981. Theory and application of experimental model analysis in earthquake engineering. John A. Blume Earthquake Center, Stanford University, California, U. S. A., p.p. 274.

Lai, S. A. and MacGregor, J. G., 1983. Geometric nonlinearities in unbraced multi-storey frames. Journal of Structural Engineering, ASCE, vol. 109, No. 11, p.p. 2528-2545.

Meggett, L. M. and Fenwick, R. C., 1989. Seismic behaviour of a reinforced concrete frame sustaining gravity loads. Bulletin of the New Zealand National Society for Earthquake Engineering, vol. 22, No. 1, p.p. 39-49.

Meyer, C., Roufaiel, M. S. L. and Arzoumanidis, S. C., 1983. Analysis of damaged concrete frames for cyclic loads. Earthquake Engineering and Structural Dynamics, vol. 11, p.p. 207-228.

Moehle, J. P. and Sozen, M. A., 1978. Earthquake simulation tests of a ten-storey reinforced concrete frame with a discontinued first-level beam. Structural Research Series No. 451, University of Illinois at Urbana-Champaign, Illinois, U.S.A.

Naumoski, N., Tso, W. K. and Heidebrecht, A. C. 1988. A selection of strong motion earthquake records having different a/v ratios., Report No. EERG 88-01, Earthquake Engineering Research Group, McMaster university, Hamilton, Ontario.

Newmark, N. M., 1962. A method of computation for structural dynamics. Transactions, American Society of Civil Engineers (ASCE), vol. 127, p.p. 1406.1435.

Newmark, N.M. and Hall, W.J., 1982. Earthquake spectra and design. Earthquake Engineering Research Institute (EERI), Berkeley, California, U.S.A.

Nmai, C. K. and Darwin, D., 1986. Lightly reinforced concrete beams under cyclic load. Journal of the American Concrete Institute, vol. 83, No. 5, p.p. 777-783.

Otani, S., 1974. SAKE: A computer program for inelastic response of R/C frames to earthquakes. Structural Research Series No. 413, University of Illinois at Urbana-Champaign, Illinois, U.S.A.

Park, R., Kent, D. C. and Sampson, R. A., 1972. Reinforced concrete members with cyclic loading. Journal of the Structural Division, ASCE, vol. 98, No. ST-7, p.p. 1341-1360.

Park, R., 1989. Evaluation of ductility for structures and structural assemblages from laboratory testing. Bulletin of the New Zealand National Society for Earthquake Engineering, vol. 22, No. 3, p.p. 155-166.

Park, R. and Paulay, T., 1975. Reinforced concrete structures. John Wiley and Sons, New York, 769 p.p.

Park, Y. J., Reinhorn, A. M. and Kunnath, S. K., 1987. IDARC : Inelastic Damage Analysis of Reinforced Concrete frame shear-wall structures. Report No. NCEER-87-0008, National center for earthquake engineering research, Buffalo, N.Y., U.S.A.

Paulay, T., 1980. Deterministic design procedure for ductile frames in seismic areas. American Concrete Institute, Special Publication SP63, Detroit, Michigan, p.p. 357-381.

_____, 1981. Developments in the seismic design of reinforced concrete frames in New Zealand. Canadian Journal of Civil Engineering, vol. 8, p.p. 91-113.

_____, 1989. Private communications from Dr. Thomas Paulay.

Paulay, T. and Priestly, M. J. N., 1992. Seismic design of reinforced concrete and masonry buildings. John Woley and Sons, New York, 744 p.p.

Paultre, P. and Mitchell, D., 1987a. Evaluation of seismic performance of concrete frame structures in Canada. Structural Engineering Series, Report No. 87-4, McGill university, Montreal, Canada, p.p. 188.

_____, 1987b. Investigation of Canadian seismic code requirements for reinforced concrete frames. Proceedings, Fifth Canadian Conference on Earthquake Engineering, Ottawa, Canada, p.p. 241-249.

Paultre, P., Castele, D., Rattnay, S. and Mitchell, D., 1989. Seismic response of reinforced concrete subassemblages-a Canadian code perspective. Canadian Journal of Civil Engineering, vol. 16, No. 5, p.p. 627-649.

Paultre, P. and Mitchell, D., 1991. Assessment of some Canadian seismic code requirements for concrete frame structures. Canadian Journal of Civil Engineering, Vol. 18, No. 3, p.p. 343-357.

Powell, G.H., 1975. Supplement to computer program DRAIN-2D. Report No. EERC 73-22,Earthquake Engineering Research Center, University of California, Berkeley, U.S.A.

Rainer, J. H., 1987. Force reduction factors for the seismic provisions of the national building code of Canada. Canadian Journal of Civil Engineering, vol.14,p.p. 447-454.

Robinson, L. M., 1980. Shear walls of limited ductility. Bulletin of the New Zealand National Society for Earthquake Engineering, vol. 13, No. 2, p.p. 144-161.

Roufaiel, M. S. L. and Meyer, C., 1987. Analytical modelling of hysteretic behaviour of R/C frames. Journal of Structural Engineering, ASCE, vol. 113, No. 3, p.p. 429-444.

Rutenberg, A., 1982. Simplified P-Delta analysis for asymmetric structures. Journal of the Structural Division, ASCE, vol. 108, No. 9, p.p. 1995-2013.

Scribner, C. F. and Wight, J. K., 1978. Delaying shear strength decay in reinforced concrete flexural members under cyclic load reversals. Report No. UMEE-78R2, Department of Civil Engineering, University of Michigan, Ann Arbor, Michigan.

_____, 1980. Strength decay in R/C beams under load reversals. Journal of the Structural Division, ASCE, vol. 106, No. ST-4, p.p. 861-876.

Standard Association of New Zealand (SANZ), 1982. Code of practice for the design of concrete structures, NZS 3101, Wellington, New Zealand.

Standard Association of New Zealand (SANZ), 1984. Code of practice for general structural design and design loadings for buildings, NZS 4203, Wellington, New Zealand.

Takeda, T., Sozen, M. A. and Neilson, N. M., 1970. Reinforced concrete response to simulated earthquakes. Journal of the Structural Division, ASCE, vol. 96, No. ST-12, p.p. 2557-2573.

Tso, W.K. 1991. Overview of seismic provision changes in national building code of Canada, 1990. Proceedings, Sixth Canadian Conference on Earthquake Engineering, Toronto, Ontario, p.p. 743-750.

Viawathanatepa, S., Popov, E. P. and Bertero, V. V., 1979. Seismic behaviour of reinforced concrete interior beam-column subassemblages. Report No. EERC 79-14, Earthquake Engineering Research Center, University of California, Berkeley, U.S.A.

Wilson, E. L., Hollings, J. P. and Dovey, H. H., 1975. Three dimensional analysis of building systems (extended version)., Report No. EERC 75-13, Earthquake Engineering Research Center, University of California, Berkeley, U.S.A.

Wilson, E.L. and Habibullah, A., 1987. Static and dynamic analysis of multi-storey buildings including P-Delta effects. Earthquake spectra, EERI, vol.3, No.2, p.p. 289-298.

Zhu, T. J., 1989. Inelastic response of reinforced concrete frames to seismic ground motions having different characteristics., Ph.D. thesis, McMaster university, Hamilton, Canada, 296 pages.

Zhu, T. J., Tso, W. K. and Heidebrecht, A. C., 1991. Seismic performance of high-rise reinforced concrete frame buildings located in different seismic regions. Proceedings, Sixth Canadian Conference on Earthquake Engineering, Toronto, Ontario, p.p 551-558.

APPENDIX A

After the completion of this thesis, it was drawn to my attention (Mitchell, 1992) that the series of structures that were in figure (2) of Paultre and Mitchell (1991) were actually designed for locations in Vancouver not for Montreal. Since Vancouver is in a higher seismic zone than Montreal, this may explain the higher reinforcement of the 6SPM and 6-PM frames.

Mitchell, D., 1992. Private Communication.